Oklahoma Department of Transportation
200 NE 21st Street, Oklahoma City, OK 73105-3204

FINAL REPORT ~ FHWA-OK-15-06

SELECTION OF LONG LASTING REHABILITATION TREATMENT USING LIFE CYCLE COST ANALYSIS AND PRESENT SERVICEABILITY RATING

Maryam S. Sakhaeifar, Ph.D.
Mona Nobakht, Ph.D. Candidate
Zachry Department of Civil Engineering
College of Engineering
Texas A&M University
College Station, Texas

David Newcomb, Ph.D. P.E.
Material and Pavement Division
Texas A&M Transportation Institute
College Station, Texas

B. Shane Underwood, Ph.D.
Padmini P. Gudipudi, Ph.D.
Jeff Stempihar, Ph.D.
School of Sustainability and the Built Environment
Ira A. Fulton Schools of Engineering
Arizona State University
Tempe, Arizona

October 2015

SELECTION OF LONG LASTING REHABILITATION TREATMENT USING LIFE CYCLE COST ANALYSIS AND PRESENT SERVICEABILITY RATING

FINAL REPORT ~ FHWA-OK-15-06

ODOT SP&R ITEM NUMBER 2261

Submitted to:

John R. Bowman, P.E.
Director of Capital Programs
Oklahoma Department of Transportation

Submitted by:

Maryam S. Sakhaeifar, Ph.D.
Mona Nobakht, Ph.D. Candidate
Zachry Department of Civil Engineering
Texas A&M University

David Newcomb, Ph.D. P.E.
Material and Pavement Division
Texas A&M Transportation Institute

B. Shane Underwood, Ph.D.
Padmini P. Gudipudi, Ph.D. Candidate
Jeff Stempihar, Ph.D.
School of Sustainability and the Built Environment
Arizona State University

October 2015

TECHNICAL REPORT DOCUMENTATION PAGE

1. REPORT NO.	2. GOVERNMENT ACCESSION NO.	3. RECIPIENTS CATALOG NO.
FHWA-OK-15-06		

4. TITLE AND SUBTITLE	5. REPORT DATE
Selection of Long Lasting Rehabilitation Treatment Using Life Cycle Cost Analysis and Present Serviceability Rating	October 2015
	6. PERFORMING ORGANIZATION CODE
7. AUTHOR(S)	8. PERFORMING ORGANIZATION REPORT
Maryam S. Sakhaeifar, David Newcomb, Mona Nobakht, B. Shane Underwood, Padmini P. Gudipudi, Jeff Stempihar	
9. PERFORMING ORGANIZATION NAME AND ADDRESS	10. WORK UNIT NO.
Texas A&M University, Zachry Department of Civil Engineering, 3136 TAMU, College Station, TX 77843-3136	
	11. CONTRACT OR GRANT NO.
	ODOT SP&R Item Number 2261
12. SPONSORING AGENCY NAME AND ADDRESS	13. TYPE OF REPORT AND PERIOD COVERED
Oklahoma Department of Transportation Materials and Research Division 200 N.E. 21st Street, Room 3A7 Oklahoma City, OK 73105	Final Report "November 2013" – "October 2015"
	14. SPONSORING AGENCY CODE

15. SUPPLEMENTARY NOTES

16 . ABSTRACT

A wide range of variables influence the selection strategy for rehabilitation and maintenance of pavements. The focus of this study is to conduct a project-level evaluation of high traffic volume asphalt-surfaced pavements located in the state of Oklahoma and develop a performance based rehabilitation strategy. In order to develop feasible rehabilitation strategies, a systematic collection of relevant pavement-related data was provided by ODOT. The collected data includes performance measurements, traffic, climate and structural integrity of existing pavements obtained by falling weight deflectometer (FWD) analysis. These various data sets are supplemented with laboratory testing to determine the material characterization and damage characterization of different surface rehabilitation mixtures. The national highways located in the state of Oklahoma are divided in several pavement family groups. The representative pavement sections for family groups are identified and the required data for analysis are either extracted from existing sources or measured in the laboratory. Three levels of rehabilitation activities including light, medium and heavy rehabilitation are considered for each of the pavement family groups and a mechanistic-empirical methodology is employed to obtain an estimate of the performance of potential rehabilitation activities and their extended service life. A combination of local material properties, structural integrity and environmental condition are used for structural analysis and development of an evaluation output matrix. At the end of this study a series of time-based renewal solutions are recommended for pavement family groups with a similar existing condition and the most cost effective methodology is determined by performing life cycle cost analysis using RealCost software.

17. KEY WORDS	18. DISTRIBUTION STATEMENT
Rehabilitation strategy, mechanistic-empirical analysis, pavement performance, life cycle cost analysis	No restrictions. This publication is available from the Materials & Research Div., Oklahoma DOT.

19. SECURITY CLASSIF. (OF THIS REPORT)	20. SECURITY CLASSIF. (OF THIS PAGE)	21. NO. OF PAGES	22. PRICE
Unclassified	Unclassified	264	N/A

SI* (MODERN METRIC) CONVERSION FACTORS

APPROXIMATE CONVERSIONS TO SI UNITS				
SYMBOL	**WHEN YOU KNOW**	**MULTIPLY BY**	**TO FIND**	**SYMBOL**
LENGTH				
in	inches	25.4	millimeters	mm
ft	feet	0.305	meters	m
yd	yards	0.914	meters	m
mi	miles	1.61	kilometers	km
AREA				
in^2	square inches	645.2	square millimeters	mm^2
ft^2	square feet	0.093	square meters	m^2
yd^2	square yard	0.836	square meters	m^2
ac	acres	0.405	hectares	ha
mi^2	square miles	2.59	square kilometers	km^2
VOLUME				
fl oz	fluid ounces	29.57	milliliters	mL
gal	gallons	3.785	liters	L
ft^3	cubic feet	0.028	cubic meters	m^3
yd^3	cubic yards	0.765	cubic meters	m^3
NOTE: volumes greater than 1000 L shall be shown in m^3				
MASS				
oz	ounces	28.35	grams	g
lb	pounds	0.454	kilograms	kg
T	short tons (2000 lb)	0.907	megagrams (or "metric ton")	Mg (or "t")
TEMPERATURE (exact degrees)				
^oF	Fahrenheit	5 (F-32)/9 or (F-32)/1.8	Celsius	^oC
ILLUMINATION				
fc	foot-candles	10.76	lux	lx
fl	foot-Lamberts	3.426	candela/m^2	cd/m^2
FORCE and PRESSURE or STRESS				
lbf	poundforce	4.45	newtons	N
lbf/in^2	poundforce per square inch	6.89	kilopascals	kPa

APPROXIMATE CONVERSIONS FROM SI UNITS				
SYMBOL	**WHEN YOU KNOW**	**MULTIPLY BY**	**TO FIND**	**SYMBOL**
LENGTH				
mm	millimeters	0.039	inches	in
m	meters	3.28	feet	ft
m	meters	1.09	yards	yd
km	kilometers	0.621	miles	mi
AREA				
mm^2	square millimeters	0.0016	square inches	in^2
m^2	square meters	10.764	square feet	ft^2
m^2	square meters	1.195	square yards	yd^2
ha	hectares	2.47	acres	ac
km^2	square kilometers	0.386	square miles	mi^2
VOLUME				
mL	milliliters	0.034	fluid ounces	fl oz
L	liters	0.264	gallons	gal
m^3	cubic meters	35.314	cubic feet	ft^3
m^3	cubic meters	1.307	cubic yards	yd^3
MASS				
g	grams	0.035	ounces	oz
kg	kilograms	2.202	pounds	lb
Mg (or "t")	megagrams (or "metric ton")	1.103	short tons (2000 lb)	T
TEMPERATURE (exact degrees)				
ºC	Celsius	1.8C+32	Fahrenheit	ºF
ILLUMINATION				
lx	lux	0.0929	foot-candles	fc
cd/m^2	candela/m^2	0.2919	foot-Lamberts	fl
FORCE and PRESSURE or STRESS				
N	newtons	0.225	poundforce	lbf
kPa	kilopascals	0.145	poundforce per square inch	lbf/in^2

*SI is the symbol for the International System of Units. Appropriate rounding should be made to comply with Section 4 of ASTM E380.

TABLE OF CONTENTS

Executive Summary 1
Chapter 1. Introduction 2
1.1. Background 2
1.2. Objective 3
1.3. Literature Review of Existing Pavement Management System Data of ODOT 4
1.3.1. Overview of National Highway System (NHS) in Oklahoma 4
1.3.2. Current Pavement Preservation Approach 5
Chapter 2. Categorization of Pavement Sections 10
2.1. Development of Pavement Families for The Present Study 10
2.2. Identification of Representative Pavement Sections for The Study 11
2.3. Review of Pavement Management System Database for Representative Pavement Sections 12
2.3.1. Summary of Treatment History of Representative Pavement Sections 12
2.3.2. Field Performance Measures 22
Chapter 3. Experimental Test Plan 27
3.1. Mixture Database 27
3.1.1. Mixture Fabrication Procedure 28
3.1.2. Sample Preparation 30
3. 2. Material Characterization Testing 32
3.2.1. Dynamic Modulus (|*E**|) Testing 32
3.2.2. Hamburg Wheel-Track Testing 42
3.2.3. Direct Tension Cyclic Fatigue Test 48
3.2.4. Indirect Tension (IDT) Creep Compliance and Strength Test 53
Chapter 4. Falling Weight Deflectometer (FWD) Data Analysis 61
4.1. FWD/GPR Database Review 61
4.2. Backcalculation Using AASHTO 1993 Design Guidance 65
4.2.1. Flexible Pavement Sections 65
4.2.2. Composite Pavement Sections 69
4.3. Backcalculation for MEPDG Analysis 74
4.3.1. Flexible Pavement Sections 76
4.3.2. Composite Pavement Sections 83
4.4. FWD Data Analysis Summary 88
Chapter 5. Mechanistic-Empirical Pavement Analysis 89
5.1. MEPDG Overview 89
5.1.1.Traffic 89
5.1.2. Climate Data 89
5.1.3. Pavement Structure and Material Data 90
5.2. MEPDG Analysis 91
Chapter 6. Development of Time-Based Rehabilitation Stretegies 95
6.1. Definition of Typical Flexible and Composite Pavement Sections 95
6.2. Time-Based Rehabilitation Strategies 96
Chapter 7. Life Cycle Cost Analysis 101
7.1. LCCA Inputs and Assumptions 101
7.2. LIfe Cycle Cost Results and Discussion 102

Chapter 8. Summary and Recommendation 109
8.1. Dynamic Modulus Test 109
8.2. Hamburg Wheel Tracking Test 109
8.3. Direct Tension Cyclic Fatigue Test 110
8.4. Indirect Tension (IDT) Creep Compliance and Strength Test 110
8.5. Falling Weight Deflectometer (FWD) Data Analysis 110
8.6. Mechanistic-Empirical Pavement Analysis 110
8.7. Development of Time-Based Rehabilitation Strategies and Life Cycle Cost 111
8.8. Recommendation for Future Research 111
References 112
Appendix A. Aggregate Proportion and JMF of Tested Mixtures 116
Appendix B. Dynamic Modulus Data 121
Appendix C. Uniaxial Fatigue TesT Results 123
Appendix D. Indirect Tension (IDT) Creep Compliance and Strength Test 125
Appendix E. Verification Data for FWD Analysis 135
Appendix G. Project Information of Representative Sections 231

LIST OF FIGIURES

Figure 1 Representative Pavement Family Groups Investigated in This Study 11
Figure 2 Structure Profile of Control Section 68-22 MP 13.0-17.6 14
Figure 3 Structure Profile of Control Section 44-05 MP 10.78-12.04 14
Figure 4 Structure Profile of Control Section 44-05 MP 13.85-16.5 15
Figure 5 Structure Profile of Control Section 14-06 MP 3.35-7.0 15
Figure 6 Structure Profile of Control Section 09-05 MP 4.18-10.8 16
Figure 7 Structure Profile of Control Section 55-68 MP 6.55-11.9 16
Figure 8 Structure Profile of Control Section 20-04 MP 0.0-6.0 17
Figure 9 Structure Profile of Control Section 25-46 MP 17.0-20.3 17
Figure 10 Structure Profile of Control Section 42-30 MP 7.09-12.7 18
Figure 11 Structure Profile of Control Section 55-09 MP 8.54-13.0 18
Figure 12 Structure Profile of Control Section 16-49 MP 0.0-3.0 19
Figure 13 Structure Profile of Control Section 50-32 MP 0.0-6.54 19
Figure 14 Structure Profile of Control Section 25-46 MP 0.0-4.06 20
Figure 15 Structure Profile of Control Section 72-09 MP 9.0-11.0 20
Figure 16 Pavement Quality Index (PQI) and Ride Index Evaluation for Flexible Representative Pavement Sections in Control Sections: (a) 68-22, milepost 13 to 17.6, (b) 44-05, milepost 10.78 to 12.04, (c) 09-05, milepost 4.18 to 10.8, (d) 20-04, milepost 0 to 6, (e) 44-05, milepost 13.85 to 16.5, (f) 55-68, milepost 6.55 to 11.9; and (g) 14-06, milepost 3.35 to 7.0. 24
Figure 17 Pavement Quality Index (PQI) and Ride Index Evaluation for Composite Representative Pavement Sections in Control Sections: (a) 25-46, milepost 17 to 20.3, (b) 16-49, milepost 0 to 3, (c) 42-30, milepost 7.09 to 12.7, (d) 55-09, milepost 8.54 to 13, (e) 50-32, milepost 0 to 6.54, (f) 25-46, milepost 0 to 4.06; and (g) 25-46, milepost 0 to 4.06. 25
Figure 18 Dynamic Modulus Master-curve for S4 PG 70-28 Specimens in Logarithmic Scale 35
Figure 19 Dynamic Modulus Master-curve for S4 PG 76-28 Specimens in Logarithmic Scale 36
Figure 20 Dynamic Modulus Master-curve for S3 PG 64-22 Specimens in Logarithmic Scale 36
Figure 21 Dynamic Modulus Master-curve for S4 PG 64-22 Specimens in Logarithmic Scale 37
Figure 22 Dynamic Modulus Master-curve for S5 PG 76-28 Specimens in Logarithmic Scale 37
Figure 23 Dynamic Modulus Mastercurve for S4 PG 70-28 Specimens in Arithmetic Scale 38
Figure 24 Dynamic Modulus Mastercurve for S4 PG 76-28 Specimens in Arithmetic Scale 38
Figure 25 Dynamic Modulus Mastercurve for S3 PG 64-22 Specimens in Arithmetic Scale 39
Figure 26 Dynamic Modulus Mastercurve for S4 PG 64-22 Specimens in Arithmetic Scale 39
Figure 27 Dynamic Modulus Mastercurve for S5 PG 76-28 Specimens in Arithmetic Scale 40

Figure 28 Average Dynamic Modulus Master-curves for Mixtures in Arithmetic Scale . 40
Figure 29 Average Dynamic Modulus Master-curves for Mixtures in Logarithmic Scale41
Figure 30 Hamburg Test Results for S3 PG 64-22 Mixture 44
Figure 31 Hamburg Test Results for S4 PG 64-22 Mixture 45
Figure 32 Hamburg Test Results for S4 PG 70-28 Mixture 45
Figure 33 Hamburg Test Results for S4 PG 76-28 Mixtures 46
Figure 34 Hamburg Test Results for S5 PG 76-28 Mixtures 46
Figure 35 Hamburg Curve for the Average of Two Replicates for Tested Mixtures 47
Figure 36 Uniaxial Fatigue Test Sample Gluing Process (left) and sample Setup inside Testing Chamber (right). 48
Figure 37 Typical Cycle-Wise Test Results from The Axial Fatigue Test (a) Apparent Dynamic Modulus and (b) Phase Angle. 49
Figure 38 Experimental Fatigue Lives Plot for All Five Mixtures. 50
Figure 39 C-S Model Fit Curves for S3 and S4 Asphalt Concrete Mixtures 52
Figure 40 Fatigue Lives Plots for All Five Mixtures Using Simulated Data 53
Figure 41 Creep Compliance Test Setup with Fixture inside the Testing Chamber 54
Figure 42 Creep Compliance Test Data (a) before Shifting (b) after Shifting. 57
Figure 43 Creep Compliance Master Curves for S3 64-22 Mix (Average of 3 Replicates). 58
Figure 44 Average Tensile Strength of Study Mixtures (psi) 59
Figure 45 Applied Load over Versus Pavement Length, AC Control Section 66-18..... 63
Figure 46 Applied load versus Di/Di_Analysis Relationships: (a) Section 56-04; (b) Section 03-02; (c) Section 54-22; (d) Section 42-30; (e) Section 20-04; (f) Section 47-06; (g) Section 25-46; and (h) Section 66-18. 65
Figure 47 AASHTO 1993 Temperature Adjustment Factor for Pavement with Granular or Asphalt-Treated Base (3). 67
Figure 48 AASHTO 1993 M_r versus Chainage of Control Section 09-05 (a) before Deletion of Outliers; and (b) after Deletion of Outliers. 68
Figure 49 AASHTO 1993 M_r versus Chainage of Control Section 42-30 (a) before Deletion of Outliers; and (b) after Deletion of Outliers. 72
Figure 50 Structural Configuration and Treatment History for; (a) Control Section 68-22 and (b) Control Section 54-22. 75
Figure 51 Raw Backcalculated AC Modulus for Primary Direction of Section 68-22 (Horizontal Lines Represent the Average and 95% Confidence Interval)..... 76
Figure 52 Temperature Prediction for Section 68-22; (a) Primary Direction and (b) Secondary Direction. 78
Figure 53 Comparison of Raw Backcalculated AC Modulus and Temperature Corrected AC Modulus (68°F). 79
Figure 54 Temperature Corrected Modulus (a) before Deletion of Outliers and (b) after Deletion of Outliers. 80
Figure 55 Three Typical Flexible Pavement Sections 95
Figure 56 Two Typical Composite Pavement Sections 96
Figure 57 Two Suggested Rehabilitation Strategies, Alternatives (a) and (b), for Flexible Pavements with Structural Index>80 97
Figure 58 Two Suggested Rehabilitation Strategies, Alternatives a and b, for Flexible Pavements with 60≤ Structural Index ≤80 98

Figure 59 Two Suggested Rehabilitation Strategies, Alternatives a and b, for Flexible Pavements with Structural Index <60 98
Figure 60 Two Suggested Rehabilitation Strategies for Composite Pavements with Structural index>80 99
Figure 61 Two Suggested Rehabilitation Strategies for Composite Pavements with 60≤ Structural Index ≤80 99
Figure 62 Two Suggested Rehabilitation Strategies, Alternatives a and b, for Composite Pavements with Structural index <60 100
Figure 63 Comparison of Net Present Value (NPV) in Terms of (I) User, (II) Agency and (III) Total (Agency and User) Life-Cycle Cost for Rehabilitation Alternatives of Typical Flexible Pavement Sections. 104
Figure 64 Comparison of Net Present Value (NPV) in Terms of (I) User, (II) Agency and (III) Total (Agency and User) Life Cycle Cost for Rehabilitation Alternatives of Typical Composite Pavement Sections. 106
Figure 65 Cost-effective Time-based Rehabilitation Strategies for Flexible Pavements Sections with (I) Structural Index>80, (II) 60≤ Structural Index ≤80, (III) Structural Index<60 107
Figure 66 Cost-effective Time-based Rehabilitation Strategies for Composite Pavements Sections with (I) Structural Index>80, (II) 60≤ Structural Index ≤80, (III) Structural Index<60 108
Figure 67 Collapse of C-S Curve for: (a) S4_64-22 Mix (b) S3 _64-22 Mix (c) S4_70-28 Mix (d) S4_76-28 Mix and (e) S5_76-28 Mix. 124
Figure 68 Creep Compliance Master Curves for S3 64-22 Mix Replicates; (a) Compacted Sample 1 Bottom Slice, (b) Compacted Sample 1 Top Slice, (c) Compacted Sample 2 Bottom Slice, and (d) Compacted Sample 2 Top Slice. 125
Figure 69 Creep Compliance Master Curves Fit for S3 64-22 Mix (Average of 3 Replicates) 126
Figure 70 Creep Compliance Master Curves for S4 64-22 Mix Replicates; (a) Compacted Sample 1 Top Slice, (b) Compacted Sample 1 Bottom Slice, and (c) Compacted Sample 2 Top Slice. 127
Figure 71 Creep Compliance Master Curve Fit for S4 64-22 Mix (Average of 3 Replicates). 127
Figure 72 Creep Compliance Master Curves for S4 70-28 Mix Replicates; (a) Compacted Sample 1 Top Slice, (b) Compacted Sample 1 Bottom Slice, and (c) Compacted Sample 2 Top Slice. 129
Figure 73 Creep Compliance Master Curves Fit for S4 70-28 Mix (Average of 3 Replicates) 129
Figure 74 Creep Compliance Master Curves for S4 76-28 Mix Replicates; (a) Compacted Sample 1 Bottom Slice, (b) Compacted Sample 2 Bottom Slice, and (c) Compacted Sample 2 Top Slice. 131
Figure 75 Creep Compliance Master Curve Fit for S4 76-28 Mix (Average of 3 Replicates) 131
Figure 76 Creep Compliance Master Curves for S5 76-28 Mix Replicates; (a) Compacted Sample 2 Bottom Slice, (b) Compacted Sample 1 Top Slice, and (c) Compacted sample 2 Top Slice. 133

Figure 77 Creep Compliance Master Curve Fit for S5 76-28 Mix (Average of 3 Replicates). 133
Figure 78 Comparison of 2010 Reported and AASHTO 1993 Verified values of (a) Mr Based on GPR and (b) Mr Based on Core, (c) Ep Based on GPR and (d) Ep based on Core for Control Section 68-22..... 135
Figure 79 Comparison of 2010 Reported and AASHTO 1993 Verified Values of (a) Mr Based on GPR and (b) Mr Based on Core, (c) Ep Based on GPR and (d) Ep based on Core for Control Section 54-22..... 136
Figure 80 Comparison of 2004 Reported and AASHTO 1993 Verified Values of (a) Mr Based on GPR and (b) Mr Based on Core, (c) Ep Based on GPR and (d) Ep based on Core for Control Section 54-22..... 137
Figure 81 Comparison of 2010 Reported and AASHTO 1993 Verified Values of (a) Mr Based on GPR and (b) Mr Based on Core, (c) Ep Based on GPR and (d) Ep based on Core for Control Section 44-05..... 138
Figure 82 Comparison of 2004 Reported and AASHTO 1993 Verified Values of (a) Mr Based on GPR and (b) Mr Based on Core, (c) Ep Based on GPR and (d) Ep Based on Core for Control Section 44-05..... 139
Figure 83 Comparison of 2010 Reported and AASHTO 1993 Verified Values of (a) Mr Based on GPR and (b) Mr Based on Core, (c) Ep Based on GPR and (d) Ep Based on Core for Control Section 09-05..... 140
Figure 84 Comparison of 2004 Reported and AASHTO 1993 Verified Values of (a) Mr Based on GPR and (b) Mr Based on Core, (c) Ep Based on GPR and (d) Ep Based on Core for Control Section 09-05..... 141
Figure 85 Comparison of 2010 Reported and AASHTO 1993 Verified Values of (a) Mr Based on GPR and (b) Mr Based on Core, (c) Ep Based on GPR and (d) Ep Based on Core for Control Section 55-68..... 142
Figure 86 Comparison of 2004 Reported and AASHTO 1993 Verified Values of (a) Mr Based on GPR and (b) Mr Based on Core, (c) Ep Based on GPR and (d) Ep Based on Core for Control Section 55-68..... 143
Figure 87 Comparison of 2010 Reported and AASHTO 1993 Verified Values of (a) Mr Based on GPR and (b) Mr Based on Core, (c) Ep Based on GPR and (d) Ep Based on Core for Control Section 20-04..... 144
Figure 88 Comparison of 2004 Reported and AASHTO 1993 Verified Values of (a) Mr Based on GPR and (b) Mr Based on Core, (c) Ep Based on GPR and (d) Ep Based on Core for Control Section 20-04..... 145
Figure 89 Comparison of 2010 Reported and AASHTO 1993 Verified Values of (a) Mr Based on GPR and (b) Mr Based on Core, (c) Ep Based on GPR and (d) Ep Based on Core for Control Section 72-78..... 146
Figure 90 Comparison of 2004 Reported and AASHTO 1993 Verified Values of (a) Mr Based on GPR and (b) Mr Based on Core, (c) Ep Based on GPR and (d) Ep Based on Core for Control Section 72-78..... 147
Figure 91 AASHTO 1993 Verified Mr Values Versus Distance in (a) Direction 5 and (b) Direction 6 for Control Section 68-22. 147
Figure 92 AASHTO 1993 Verified M_r Values Versus Distance for (a) 2010 data in Direction 5, (b) 2010 Data in Direction 6, (c) 2004 Data in Direction 5, and (d) 2004 Data in Direction 6 for Control Section 54-22..... 148

Figure 93 AASHTO 1993 Verified M_r Values Versus Distance for (a) 2010 data in Direction 5, (b) 2010 Data in Direction 6, (c) 2004 Data in Direction 5, and (d) 2004 Data in Direction 6 for Control Section 44-05..... 149
Figure 94 AASHTO 1993 Verified M_r Values Versus Distance for (a) 2010 data in Direction 5, (b) 2010 Data in Direction 6, (c) 2004 Data in Direction 5, and (d) 2004 Data in Direction 6 for Control Section 09-05..... 150
Figure 95 AASHTO 1993 Verified M_r Values Versus Distance for (a) 2010 Data in Direction 5, (b) 2010 Data in Direction 6, (c) 2004 Data in Direction 5, and (d) 2004 Data in Direction 6 for Control Section 55-68..... 151
Figure 96 AASHTO 1993 Verified M_r Values Versus Distance for (a) 2010 Data in Direction 5, (b) 2010 Data in Direction 6, (c) 2004 Data in Direction 5, and (d) 2004 Data in Direction 6 for Control Section 20-04..... 152
Figure 97 AASHTO 1993 Verified M_r Values Versus Distance for (a) 2010 Data in Direction 5, (b) 2004 Data in Direction 6 for Control Section 72-78..... 152
Figure 98 GPR and Core AASHTO 1993 Verified E_p Values Versus Distance for (a) 2010 Data in Direction 5, (b) 2010 Data in Direction 6 for Control Section 68-22. 153
Figure 99 GPR and Core AASHTO 1993 Verified E_p Values Versus Distance for (a) 2010 Data in Direction 5, (b) 2010 Data in Direction 6, (c) 2004 Data in Direction 5, and (d) 2004 Data in Direction 6 for Control Section 54-22..... 153
Figure 100 GPR and Core AASHTO 1993 Verified E_p Values Versus Distance for (a) 2010 Data in Direction 5, (b) 2010 Data in Direction 6, (c) 2004 Data in Direction 5, and (d) 2004 Data in Direction 6 for Control Section 44-05..... 154
Figure 101 GPR and Core AASHTO 1993 Verified E_p Values Versus Distance for (a) 2010 Data in Direction 5, (b) 2010 Data in Direction 6, (c) 2004 Data in Direction 5, and (d) 2004 Data in Direction 6 for Control Section 09-05..... 155
Figure 102 GPR and Core AASHTO 1993 Verified E_p Values Versus Distance for (a) 2010 Data in Direction 5, (b) 2010 Data in Direction 6, (c) 2004 Data in Direction 5, and (d) 2004 Data in Direction 6 for Control Section 55-68..... 156
Figure 103 GPR and Core AASHTO 1993 Verified E_p Values Versus Distance for (a) 2010 Data in Direction 5, (b) 2010 Data in Direction 6, (c) 2004 Data in Direction 5, and (d) 2004 Data in Direction 6 for Control Section 20-04..... 157
Figure 104 GPR and Core AASHTO 1993 Verified E_p Values Versus Distance for (a) 2010 Data in Direction 6, and (b) 2004 Data in Direction 6 for Control Section 72-78. 157
Figure 105 Comparison of 2010 Reported and AASHTO 1993 Verified Values of (a) Mr Based on GPR and (b) Mr Based on Core, (c) Ep Based on GPR and (d) Ep Based on Core for Control Section 25-46..... 158
Figure 106 Comparison of 2004 Reported and AASHTO 1993 Verified Values of (a) Mr Based on GPR and (b) Mr Based on Core, (c) Ep Based on GPR and (d) Ep Based on Core for Control Section 25-46..... 159
Figure 107 Comparison of 2010 Reported and AASHTO 1993 Verified Values of (a) Mr Based on GPR and (b) Mr Based on Core, (c) Ep Based on GPR and (d) Ep Based on Core for Control Section 42-30..... 160
Figure 108 Comparison of 2004 Reported and AASHTO 1993 Verified Values of (a) Mr Based on GPR and (b) Mr Based on Core, (c) Ep Based on GPR and (d) Ep Based on Core for Control Section 42-30..... 161

Figure 109 Comparison of 2010 Reported and AASHTO 1993 Verified Values of (a) Mr Based on GPR and (b) Mr Based on Core, (c) Ep Based on GPR and (d) Ep Based on Core for Control Section 65-09.... 162
Figure 110 Comparison of 2010 Reported and AASHTO 1993 Verified Values of (a) Mr Based on GPR and (b) Mr Based on Core, (c) Ep Based on GPR for Control Section 16-49 (Note: the GPR data for this section did not include thickness of PCC layer so E_p could not be calculated from the GPR values). 163
Figure 111 Comparison of 2004 reported and AASHTO 1993 Verified Values of (a) Mr Based on GPR and (b) Mr Based on Core, (c) Ep Based on GPR and (d) Ep Based on Core for Control Section 16-49.... 164
Figure 112 Comparison of 2010 reported and AASHTO 1993 Verified Values of (a) Mr Based on GPR and (b) Mr Based on Core, (c) Ep Based on GPR and (d) Ep Based on Core for Control Section 50-32.... 165
Figure 113 Comparison of 2010 reported and AASHTO 1993 Verified Values of (a) Mr Based on GPR and (b) Mr Based on Core, (c) Ep Based on GPR and (d) Ep Based on Core for Control Section 25-46.... 166
Figure 114 Comparison of 2004 reported and AASHTO 1993 Verified Values of (a) Mr Based on GPR and (b) Mr Based on Core, (c) Ep Based on GPR and (d) Ep Based on Core for Control Section 25-46.... 167
Figure 115 Comparison of 2010 reported and AASHTO 1993 Verified Values of (a) Mr Based on GPR and (b) Mr Based on Core, (c) Ep Based on GPR and (d) Ep Based on Core for Control Section 72-09.... 168
Figure 116 Comparison of 2004 reported and AASHTO 1993 Verified Values of (a) Mr Based on GPR and (b) Mr Based on Core, (c) Ep Based on GPR and (d) Ep Based on Core for Control Section 72-09.... 169
Figure 117 Comparison of 2004 reported and AASHTO 1993 Verified Values of (a) k Based on GPR and (b) k Based on Core, (c) k_{eff_static} Based on GPR and (d) k_{eff_static} Based on Core for Control Section 25-46.... 170
Figure 118 Comparison of 2004 reported and AASHTO 1993 Verified Values of (a) k Based on GPR and (b) k Based on Core, (c) k_{eff_static} Based on GPR and (d) k_{eff_static} Based on Core for Control Section 42-30.... 171
Figure 119 Comparison of 2004 reported and AASHTO 1993 Verified Values of (a) k Based on GPR and (b) k Based on Core, (c) k_{eff_static} Based on GPR and (d) k_{eff_static} Based on Core for Control Section 16-49.... 172
Figure 120 Comparison of 2004 Reported and AASHTO 1993 Verified Values of (a) k Based on GPR and (b) k Based on Core, (c) k_{eff_static} Based on GPR and (d) k_{eff_static} Based on Core for Control Section 25-46.... 173
Figure 121 Comparison of 2004 reported and AASHTO 1993 Verified Values of (a) k Based on GPR and (b) k Based on Core, (c) k_{eff_static} Based on GPR and (d) k_{eff_static} Based on Core for Control Section 72-09.... 174
Figure 122 AASHTO 1993 Verified M_r Values Versus Distance for (a) 2010 Data in Direction 5, (b) 2010 Data in Direction 6, (c) 2004 Data in Direction 5, and (d) 2004 Data in Direction 6 for Control Section 25-46.... 175
Figure 123 AASHTO 1993 Verified M_r Values Versus Distance for (a) 2010 Data in Direction 5, (b) 2010 Data in Direction 6, (c) 2004 Data in Direction 5, and (d) 2004 Data in Direction 6 for Control Section 42-30.... 176

Figure 124 AASHTO 1993 Verified M_r Values Versus Distance for (a) 2010 Data in Direction 5, and (b) 2010 Data in Direction 6 for Control Section 65-09..... 177
Figure 125 AASHTO 1993 Verified M_r Values Versus Distance for (a) 2010 Data in Direction 5, (b) 2010 Data in Direction 6, (c) 2004 Data in Direction 5, and (d) 2004 Data in Direction 6 for Control Section 16-49..... 177
Figure 126 AASHTO 1993 Verified M_r Values Versus Distance for (a) 2010 Data in Direction 5, and (b) 2010 Data in Direction 6 for Control Section 50-32..... 178
Figure 127 AASHTO 1993 Verified M_r Values Versus Distance for (a) 2010 Data in Direction 5, (b) 2010 Data in Direction 6, (c) 2004 Data in Direction 5 and (d) 2004 Data in Direction 6 for Control Section 25-46..... 178
Figure 128 AASHTO 1993 Verified M_r Values Versus Distance for (a) 2010 Data in Direction 5, (b) 2010 Data in Direction 6, (c) 2004 Data in Direction 5, and (d) 2004 Data in Direction 6 for Control Section 72-09..... 179
Figure 129 GPR and Core AASHTO 1993 Verified E_p Values Versus Distance for (a) 2010 Data in Direction 5, (b) 2010 Data in Direction 6, (c) 2004 Data in Direction 5, and (d) 2004 Data in Direction 6 for Control Section 25-46..... 180
Figure 130 GPR and Core AASHTO 1993 Verified E_p Values Versus Distance for (a) 2010 Data in Direction 5, (b) 2010 Data in Direction 6, (c) 2004 Data in Direction 5, and (d) 2004 Data in Direction 6 for Control Section 42-30..... 181
Figure 131 GPR and Core AASHTO 1993 Verified E_p Values Versus Distance for (a) 2010 Data in Direction 5 and (b) 2010 Data in Direction 6 for Control Section 65-09. 181
Figure 132 GPR and Core AASHTO 1993 Verified E_p Values Versus Distance for (a) 2010 Data in Direction 5, (b) 2010 Data in Direction 6, (c) 2004 Data in Direction 5, and (d) 2004 Data in Direction 6 for Control Section16-49..... 182
Figure 133 GPR and Core AASHTO 1993 Verified E_p Values Versus Distance for (a) 2010 Data in Direction 5, (b) 2010 Data in Direction 6 for Control Section 50-32. 183
Figure 134 GPR and Core AASHTO 1993 Verified E_p Values Versus Distance for (a) 2010 Data in Direction 5, (b) 2010 Data in Direction 6, (c) 2004 Data in Direction 5, and (d) 2004 Data in Direction 6 for Control Section 25-46..... 183
Figure 135 GPR and Core AASHTO 1993 Verified E_p Values Versus Distance for (a) 2010 Data in Direction 5, (b) 2010 Data in Direction 6, (c) 2004 Data in Direction 5, and (d) 2004 Data in Direction 6 for Control Section 72-09..... 184
Figure 136 2010 GPR AASHTO 1993 Verified Values of (a) k in Direction 5, (b) k in Direction 6, (c) k_{eff_static} in Direction 5 and (d) k_{eff_static} in Direction 6 Versus Distance for Control Section 25-46..... 185
Figure 137 2004 GPR AASHTO 1993 Verified Values of (a) k in Direction 5, (b) k in Direction 6, (c) k_{eff_static} in Direction 5 and (d) k_{eff_static} in Direction 6 Versus Distance for Control Section 25-46..... 186
Figure 138 2010 core AASHTO 1993 Verified Values of (a) k in Direction 5, (b) k in Direction 6, (c) k_{eff_static} in Direction 5 and (d) k_{eff_static} in Direction 6 Versus Distance for Control Section 25-46..... 187
Figure 139 2004 core AASHTO 1993 Verified Values of (a) k in Direction 5, (b) k in Direction 6, (c) k_{eff_static} in Direction 5 and (d) k_{eff_static} in Direction 6 Versus Distance for Control Section 25-46..... 188

Figure 140 2010 GPR AASHTO 1993 Verified Values of (a) *k* in Direction 5, (b) *k* in Direction 6, (c) k_{eff_static} in Direction 5 and (d) k_{eff_static} in Direction 6 Versus Distance for Control Section 42-30 189
Figure 141 2004 GPR AASHTO 1993 Verified Values of (a) *k* in Direction 5, (b) *k* in Direction 6, (c) k_{eff_static} in Direction 5 and (d) k_{eff_static} in Direction 6 Versus Distance for Control Section 42-30 190
Figure 142 2010 Core AASHTO 1993 Verified Values of (a) *k* in Direction 5, (b) *k* in Direction 6, (c) k_{eff_static} in Direction 5 and (d) k_{eff_static} in Direction 6 Versus Distance for Control Section 42-30 191
Figure 143 2004 Core AASHTO 1993 Verified Values of (a) *k* in Direction 5, (b) *k* in Direction 6, (c) k_{eff_static} in Direction 5 and (d) k_{eff_static} in Direction 6 Versus Distance for Control Section 42-30 192
Figure 144 2010 GPR AASHTO 1993 Verified Values of (a) *k* in Direction 5, (b) *k* in Direction 6, (c) k_{eff_static} in Direction 5 and (d) k_{eff_static} in Direction 6 Versus Distance for Control Section 65-09 193
Figure 145 2010 Core AASHTO 1993 Verified Values of (a) *k* in Direction 5, (b) *k* in Direction 6, (c) k_{eff_static} in Direction 5 and (d) k_{eff_static} in Direction 6 Versus Distance for Control Section 65-09 194
Figure 146 2010 GPR AASHTO 1993 Verified Values of (a) k in Direction 5, and (b) k in Direction 6 Versus Distance for Control Section 16-49. 194
Figure 147 2004 GPR AASHTO 1993 Verified Values of (a) *k* in Direction 5, (b) *k* in Direction 6, (c) k_{eff_static} in Direction 5 and (d) k_{eff_static} in Direction 6 Versus Distance for Control Section 16-49 195
Figure 148 2010 Core AASHTO 1993 Verified Values of (a) *k* in Direction 5, (b) *k* in Direction 6 Versus Distance for Control Section 16-49 195
Figure 149 2010 Core AASHTO 1993 Verified Values of (a) *k* in Direction 5, (b) *k* in Direction 6, (c) k_{eff_static} in Direction 5 and (d) k_{eff_static} in Direction 6 Versus Distance for Control Section 16-49 196
Figure 150 2010 GPR AASHTO 1993 Verified Values of (a) *k* in Direction 5, (b) *k* in Direction 6, (c) k_{eff_static} in Direction 5 and (d) k_{eff_static} in Direction 6 Versus Distance for Control Section 50-32 197
Figure 151 2010 Core AASHTO 1993 Verified Values of (a) *k* in Direction 5, (b) *k* in Direction 6, (c) k_{eff_static} in Direction 5 and (d) k_{eff_static} in Direction 6 Versus Distance for Control Section 50-32 198
Figure 152 2010 GPR AASHTO 1993 Verified Values of (a) *k* in Direction 5, (b) *k* in Direction 6, (c) k_{eff_static} in Direction 5 and (d) k_{eff_static} in Direction 6 Versus Distance for Control Section 25-46 199
Figure 153 2004 GPR AASHTO 1993 Verified Values of (a) *k* in Direction 5, (b) *k* in Direction 6, (c) k_{eff_static} in Direction 5 and (d) k_{eff_static} in Direction 6 Versus Distance for Control Section 25-46 200
Figure 154 2010 Core AASHTO 1993 Verified Values of (a) *k* in Direction 5, (b) *k* in Direction 6, (c) k_{eff_static} in Direction 5 and (d) k_{eff_static} in Direction 6 Versus Distance for Control Section 25-46 201
Figure 155 2004 Core AASHTO 1993 Verified Values of (a) *k* in Direction 5, (b) *k* in Direction 6, (c) k_{eff_static} in Direction 5 and (d) k_{eff_static} in Direction 6 Versus Distance for Control Section 25-46 202

Figure 156 2010 GPR AASHTO 1993 Verified Values of (a) *k* in Direction 5, (b) *k* in Direction 6, (c) k_{eff_static} in Direction 5 and (d) k_{eff_static} in Direction 6 Versus Distance for Control Section 72-09 203
Figure 157 2004 GPR AASHTO 1993 Verified Values of (a) *k* in Direction 5, (b) *k* in Direction 6, (c) k_{eff_static} in Direction 5 and (d) k_{eff_static} in Direction 6 Versus Distance for Control Section 72-09 204
Figure 158 2010 Core AASHTO 1993 Verified Values of (a) *k* in Direction 5, (b) *k* in Direction 6, (c) k_{eff_static} in Direction 5 and (d) k_{eff_static} in Direction 6 Versus Distance for Control Section 72-09 205
Figure 159 2004 Core AASHTO 1993 Verified Values of (a) *k* in Direction 5, (b) *k* in Direction 6, (c) k_{eff_static} in Direction 5 and (d) k_{eff_static} in Direction 6 Versus Distance for Control Section 72-09 206
Figure 160 2010 Backcalculated (a) AC Layer, (b) Layer 2, (c) Layer 3 and (d) Layer 4 Moduli for Control Section 68-22, Direction 5. 207
Figure 161 2010 Backcalculated (a) AC Layer, (b) Layer 2, (c) Layer 3 and (d) Layer 4 Moduli for Control Section 68-22, Direction 6. 208
Figure 162 2010 Backcalculated (a) AC Layer, (b) Layer 2, (c) Layer 3 and (d) Layer 4 Moduli for Control Section 54-22, Direction 5. 209
Figure 163 2010 Backcalculated (a) AC Layer, (b) Layer 2, (c) Layer 3 and (d) Layer 4 Moduli for Control Section 54-22, Direction 6. 210
Figure 164 2010 Backcalculated (a) AC Layer, (b) Layer 2, and (c) Layer 3 Moduli for Control Section 44-05 MP 10.8, Direction 5. 211
Figure 165 2010 Backcalculated (a) AC Layer, (b) Layer 2, and (c) Layer 3 Moduli for Control Section 44-05 MP 10.8, Direction 6. 212
Figure 166 2010 Backcalculated (a) AC Layer, (b) Layer 2, (c) Layer 3 and (d) Layer 4 Moduli for Control Section 09-05, Direction 5. 213
Figure 167 2010 Backcalculated (a) AC Layer, (b) Layer 2, (c) Layer 3 and (d) Layer 4 Moduli for Control Section 09-05, Direction 6. 214
Figure 168 2010 Backcalculated (a) AC Layer, (b) Layer 2, and (c) Layer 3 Moduli for Control Section 55-68, Direction 5. 215
Figure 169 2010 Backcalculated (a) AC Layer, (b) Layer 2, and (c) Layer 3 Moduli for Control Section 55-68, Direction 6. 216
Figure 170 2004 Backcalculated (a) AC Layer, (b) Layer 2, (c) Layer 3 and (d) Layer 4 Moduli for Control Section 20-04, Direction 5. 217
Figure 171 2004 Backcalculated (a) AC Layer, (b) Layer 2, (c) Layer 3 and (d) Layer 4 Moduli for Control Section 20-04, Direction 6. 218
Figure 172 2010 Backcalculated (a) AC Layer, (b) Layer 2, and (c) Layer 3 Moduli for Control Section 44-05 MP 13.85, Direction 5. 219
Figure 173 2010 Backcalculated (a) AC Layer, (b) Layer 2, and (c) Layer 3 Moduli for Control Section 44-05 MP 13.85, Direction 6. 220
Figure 174 2010 Backcalculated (a) AC Layer, (b) Layer 2, (c) Layer 3 and (d) Layer 4 Moduli for Control Section 14-06, Direction 5. 221
Figure 175 2010 Backcalculated (a) AC Layer, (b) Layer 2, (c) Layer 3 and (d) Layer 4 Moduli for Control Section 14-06, Direction 6. 222
Figure 176 2010 Backcalculated (a) AC Layer, (b) Layer 2, and (c) Layer 3 Moduli for Control Section 25-46 MP 17, Direction 5. 223

Figure 177 2004 Backcalculated (a) AC Layer, (b) Layer 2, and (c) Layer 3 Moduli for Control Section 42-30, Direction 6. 224
Figure 178 Backcalculated (a) AC Layer, (b) Layer 2, (c) Layer 3 and (d) Layer 4 Moduli for Control Section 55-09, Direction 5. 225
Figure 179 2010 Backcalculated (a) AC Layer, (b) Layer 2, (c) Layer 3 and (d) Layer 4 Moduli for Control Section 55-09, Direction 6. 226
Figure 180 2010 Backcalculated (a) AC Layer, (b) Layer 2, and (c) Layer 3 Moduli for Control Section 16-49, Direction 6. 227
Figure 181 2010 Backcalculated (a) AC Layer, (b) Layer 2, and (c) Layer 3 Moduli for Control Section 50-32, Direction 6. 228
Figure 182 2010 Backcalculated (a) AC Layer, (b) Layer 2, and (c) Layer 3 Moduli for Control Section 25-46 MP 0, Direction 5. 229
Figure 183 2010 Backcalculated (a) PCC Layer, and (b) Layer 4 Moduli for Control Section 72-09, Direction 5. 230
Figure 184 2010 Backcalculated (a) PCC Layer, and (b) Layer 4 Moduli for Control Section 72-09, Direction 6. 230

LIST OF TABLES

Table 1 A Summary of the Pavement Performance Programming for Interstate Roads in Oklahoma National Highway System (NHS) 6
Table 2 Summary of the Trigger Values Used in Pavement Preservation Decision Tree for AC or Composite Pavements in ODOT 6
Table 3 Pavement Preservation Decision Tree for Roads with <2,000 AADT in ODOT .. 7
Table 4 Pavement Preservation Decision Tree for Roads with 2,000<AADT<10,000 in ODOT 8
Table 5 Pavement Preservation Decision Tree for Roads with 10,001<AADT<30,000 in ODOT 9
Table 6 Pavement Preservation Decision Tree for Roads with 30,001<AADT<40,000 in ODOT 9
Table 7 Classification of Traffic Levels in ODOT Decision Tree 12
Table 8 Summary of Representative Pavement Sections 13
Table 9 A summary of Treatment History of Representative Pavement Sections (i) 21
Table 10 A summary of Treatment History of Representative Pavement Sections (ii) .. 22
Table 11 Data Sets to Be Collected from Existing Records/Database on Rehab/ Preservations Sites 26
Table 12 Mixture Usage Report by Mix and Binder Type for Year 2012 28
Table 13 Selected Mixtures Information 28
Table 14 Combined Aggregate Gradation in JMF 30
Table 15 Maximum Theoretical Specific Gravity 30
Table 16 Summary of Information Required for Performance Testing 31
Table 17 Bulk Specific Gravity, Air Void Content and Asphalt Binder Content of Specimens Used for Dynamic Modulus Test 33
Table 18 Data Quality Statistics Requirements 34
Table 19 Optimized Value of Fitting Parameters 41
Table 20 Bulk Specific Gravity, Air Void Content and Asphalt Binder Content of Specimens Used for Hamburg Tracking Test 43
Table 21 Oklahoma Hamburg Rut Test Requirements 44
Table 22 Summary of Hamburg Tracking Test 47
Table 23 C-S Curve Model Fit Parameters for Five Mixtures 51
Table 24 Air Voids of IDT Test Specimens 54
Table 25 Creep Compliance Coefficients for Mastercurves 58
Table 26 Predicted Creep Compliance for Study Mixtures 60
Table 27 A Summary of Data Elements in FWD/GPR Database 62
Table 28 Summary of Representative Average Design Mr and Ep Values of Asphalt Pavement Control Sections 68
Table 29 Summary of Representative Average Design Mr and Ep, k and keff_stat Values of Composite Sections 72
Table 30 Example Backcalculation Input 74
Table 31 Backcalculated Layer Moduli Values for Flexible Pavement Sections (Direction 5) 84
Table 32 Backcalculated Layer Moduli Values for Flexible Pavement Sections (Direction 6) 85
Table 33 Example of Assumed AC Layer Moduli Used for Composite Sections 86

Table 34 Backcalculated Layer Moduli Values for Composite Pavement Sections 87
Table 35 Database Catalog Collection for Rehabilitation Selection 89
Table 36 Calibration Coefficient Applied for MEPDG Analysis 91
Table 37 Threshold Values Used in This Study for Interstate Highways 92
Table 38 Evaluation Matrix for Identification of Rehabilitation Treatments for Composite Pavement Sections 93
Table 39 Evaluation Matrix for Identification of Rehabilitation Treatments for Flexible Pavement Sections 94
Table 40 Major LCCA Components Used in This Study 102
Table 41 Life Cycle Cost Associated with Alternatives 106
Table 42 Aggregate Proportion and JMF of Tested Mixture: S3 PG 64-22 116
Table 43 Aggregate Proportion and JMF of Tested Mixture: S4 PG 64-22 117
Table 44 Aggregate Proportion and JMF of Tested Mixture: S4 PG 70-28 118
Table 45 Aggregate Proportion and JMF of Tested Mixture: S4 PG 76-28 119
Table 46 Aggregate Proportion and JMF of Tested Mixture: S5 PG 76-28 120
Table 47 Summary of Dynamic Modulus Data for Mixtures Tested by October 2014 . 121
Table 48 Summary of Fatigue Test Results 123
Table 49 Creep Compliance of S3 64-22 Mix Replicates 126
Table 50 Tensile Strength Test Summary of S3 64-22 Mix Replicates 126
Table 51 Creep Compliance of S4 64-22 Mix Replicates 128
Table 52 Tensile Strength Test Summary of S4 64-22 Mix Replicates 128
Table 53 Creep Compliance of S4 70-28 Mix Replicates 130
Table 54 Tensile Strength Test Summary of S4 70-28 Mix Replicates 130
Table 55 Creep Compliance of S4 76-28 Mix Replicates 132
Table 56 Tensile Strength Test Summary of S4 76-28 Mix Replicates 132
Table 57 Creep Compliance of S5 76-28 Mix Replicates 134
Table 58 Tensile Strength Test Summary of S5 76-28 Mix Replicates 134
Table 59 Project information of Control Section 68-22 Milepost 13 231
Table 60 Project information of Control Section 44-05 Milepost 10.78 232
Table 61 Project information of Control Section 09-05 Milepost 4.18 233
Table 62 Project information of Control Section 55-68 Milepost 6.55 234
Table 63 Project information of Control Section 20-04 Milepost 0.0 235
Table 64 Project information of Control Section 44-05 Milepost 13.85 236
Table 65 Project information of Control Section 14-06 Milepost 3.35 237
Table 66 Project information of Control Section 25-46 Milepost 17 238
Table 67 Project information of Control Section 42-30 Milepost 7.09 239
Table 68 Project information of Control Section 55-09 Milepost 8.54 240
Table 69 Project information of Control Section 16.49 Milepost 0.0 241
Table 70 Project information of Control Section 50-32 Milepost 0.0 242
Table 71 Project information of Control Section 25-46 Milepost 0.0 243
Table 72 Project information of Control Section 72-09 Milepost 9.0 244

EXECUTIVE SUMMARY

A well-planned rehabilitation approach helps agencies to optimize the allocation of annual investments in pavement rehabilitation programs. A wide range of variables influence the selection strategy for rehabilitation and maintenance of each pavement. Currently, many agencies are struggling with the selection of an optimal time-based and cost-effective rehabilitation strategy to address the long-term needs of pavements. The focus of this study is to conduct a project-level evaluation of high traffic volume asphalt-surfaced pavements located in the state of Oklahoma and develop a performance based rehabilitation strategy for selecting a long lasting and cost-effective solution. In order to develop feasible rehabilitation strategies, a systematic collection of relevant pavement-related data was provided by ODOT. The collected data includes performance measurements, traffic, climate and structural integrity of existing pavements obtained by falling weight deflectometer (FWD) analysis. These various data sets are supplemented with laboratory testing to determine the material properties and damage characteristics of different surface rehabilitation mixtures. The national highways located in the state of Oklahoma are divided in several pavement family groups. The representative pavement sections for each family group are identified and the required laboratory and field data are either extracted from existing sources or measured in the lab to evaluate the condition of existing pavements and material characterization of mixtures used in overlay.

A mechanistic-empirical methodology is employed to obtain an estimate of the performance of potential rehabilitation activities and their extended service life. Three levels of rehabilitation activities including light, medium and heavy rehabilitation are considered for each pavement family group and a combination of local material properties, structural integrity and environmental condition are used for structural analysis and the development of an evaluation output matrix. The output matrix can be used as a supplemental tool to help engineers at ODOT with the rehabilitation related decision making process. At the end of this study a series of time-based renewal solutions are recommended for pavement family groups with similar existing condition and the most cost effective methodology is determined by performing the life cycle cost analysis using RealCost software.

CHAPTER 1. INTRODUCTION

1.1. BACKGROUND

Preserving the current pavement network has become one of the top priorities for many highway agencies. There are many pavements on important routes that have exceeded their design lives and are in need of cost effective and sustainable rehabilitation. A viable rehabilitation treatment restores distressed pavements and improves the pavement performance. Furthermore, a well-planned rehabilitation strategy helps agencies to determine the needs for enhancement of the system's functional ability with multi-year maintenance and rehabilitation (M&R) treatment programs. It also helps the agency optimize the allocations of annual investment in pavement rehabilitation programs at network and project levels.

The pavement rehabilitation design procedure employed by different agencies across the United State are mostly based on either the AASHTO design guide of pavement structures (*1*) or the mechanistic-empirical pavement design guide (MEPDG)(*2*). Large improvements have been achieved from the use of the MEPDG through a more theoretically grounded approach rather than just empirical relationships from the AASHTO guide. However, the MEPDG still needs enhancement particularly for rehabilitation design since performance models were calibrated using only new LTPP pavement sections rather than rehabilitated pavements. Several studies have been conducted by researchers on Long-Term pavement Performance (LTPP) Specific Pavement Study (SPS) experiment data to evaluate the impact of different design, construction and rehabilitation features such as climate, traffic, existing pavement condition, surface preparation, overlay thickness and overlay materials on the performance of rehabilitated flexible pavements for specific site conditions (*3*, *4*, *5*, *6*). The findings of such studies, which in many cases are driven from national LTPP database provide helpful information for selecting rehabilitation alternatives and predicting the performance of renewed pavements. This information warrant detailed validation to account for local conditions because of potential differences between the national and local conditions. Therefore, it is essential to consider local material properties, traffic patterns, environmental conditions, construction, and rehabilitation activities in order to ascertain the appropriate rehabilitation strategy for each state across the country.

The characterization of existing pavement conditions is a crucial aspect in any rehabilitation methodology. This process necessitates the collection of a variety of different data to identify the causes of distress, structural adequacy of a pavement and consequently feasible rehabilitation alternatives. Unfortunately, despite significant improvements in pavement design through MEPDG, most transportation agencies still employ old rehabilitation design methods. In most cases these traditional methods are based on an empirical rehabilitation guideline, which are mainly based on empirical relationship or engineering judgment. In most cases, state agencies refrain from using MEPDG for two reasons. The first reason is the lack of required historical pavement performance data such as nondestructive testing and surface distress data (required

input for overlay design) to evaluate the condition of existing pavement sections in need of rehabilitation prior to repair activity. Second, the lack of accuracy in MEPDG rehabilitation design prevents the agencies from adopting it for finding renewal solutions. Carvalho et al. (*7*) evaluated rehabilitated flexible pavements sections from the LTPP SPS-5 experiments using MEPDG and compared the predicted performance with actual distress measurement from the LTPP survey. The findings of this study reveal that the cracking models for fatigue, longitudinal and transverse cracking for HMA overlays are not capable of predicting comparable performance to field measured values. Also, the rutting model needed further enhancement to accurately predict the performance. While extensive efforts has been made by different agencies to locally calibrate the design tool for new pavement design, very little local calibration has been conducted for the purpose of rehabilitation design.

However, several research studies have attempted to develop empirical guidelines for preservation treatment. As part of the second strategic highway research program, Peshkin et al (2011) (*8*) developed a guideline to improve the preservation practices on high-traffic volume roadways. This guideline is based on agency experiences and has been developed from a detailed survey of common practices. Key factors that affect preservation treatment decisions such as traffic levels, existing pavement conditions, climate, work zone duration restrictions, expected treatment performance and costs are taken into consideration in this guideline. In a similar work by Wu et al. (2010) (*9*) the performance of pavement preservation treatments including preventive maintenance, minor rehabilitation and major rehabilitation was examined by collecting data through the detailed questionnaires that were sent to six state DOTs with a well-developed pavement management system. The treatment performance in both Peshkin's and Zheng's studies is defined as the extension in service life of existing pavement resulting from applying the recommended treatment. The reported treatment performance is derived based on a survey from different transportation agencies and expected performance is mostly based on visual observation and engineering judgment instead of a well-developed design. Consequently, the development of a well-established guideline emphasizing evaluation of existing pavement condition, consideration of local material properties, mechanistic analysis and cost-effectiveness analysis can help to develop feasible solutions for pavements in need of rehabilitations. Once such a guideline is developed for a network of pavement sections, the established solutions can be offered for other pavements in similar condition without the need for repeating the whole analysis.

1.2. OBJECTIVE

The objective of this study is to develop a performance based guideline reinforced by the emphasis on cost for pavement rehabilitation strategies to be adopted for high-traffic volume roadways in the state of Oklahoma. In this regard, high volume interstate flexible and composite (asphalt surface over concrete pavements) roads from eight different field divisions are evaluated in terms of their need for rehabilitation. The condition of 14 interstate pavement sections representing 14 different pavement family groups in the state has been investigated using historical data. Also, the MEPDG analysis tool has been adopted for the structural design and performance prediction.

The results of MEPDG analysis are then modified based on the filed observations to properly account for local conditions in Oklahoma. The results are then used to develop an evaluation output matrix and series of time based rehabilitation strategies, which address pavement needs for the next 35 years. The life cycle cost analysis is also conducted to quantify the benefits of selecting each renewal solution. Several major aspects considered in developing the output matrix are as follows:

- The historical pavement conditions are evaluated thoroughly by investigating the pavement management database, nondestructive tests and a series of performance measures.
- Rehabilitation performance are determined by a mechanistic-empirical method rather than engineering judgments.
- Local material properties, traffic pattern, environmental condition, construction and rehabilitation activities are assessed in detail.

More specifically, the objectives of this project intend to respond to the following questions:

- What is the structural and functional condition of interstate pavement network in Oklahoma in terms of their needs for rehabilitation?
- What is the performance of potential rehabilitation alternatives on pavements with different conditions in terms of extension in service life of pavements?
- What rehabilitation strategies are appropriate for each pavement family and how do they address the long and short term needs of pavements?
- What is the cost associated with each recommended strategy?

Finding from this study can help ODOT engineers determine interstate pavement network needs and make the enhanced rehabilitation decisions for the next 35 years.

1.3. LITERATURE REVIEW OF EXISTING PAVEMENT MANAGEMENT SYSTEM DATA OF ODOT

A literature review of existing pavement management system data of ODOT was conducted for the purpose of the project. This effort has been summarized briefly in the following.

1.3.1. Overview of National Highway System (NHS) in Oklahoma

The National Highway System (NHS) in Oklahoma includes those roads that are “most important to interstate travel, economic expansion, and national defense”, according to the Federal Highway Administrative. The non-toll portion of the NHS in Oklahoma is comprised of approximately 2,799 centerline miles. It consists of the primary commercial, defense, and personal mobility highways in the state, including the interstates. This infrastructure plays a critical role in the state’s economy and the daily lives of its citizens. These routes carry 63 percent of the total traffic on the state highway system although they include 30 percent of the state’s total highway lane miles

(*5*). The fundamental elements of the pavement management process for these highways include:

- Establishing strategic goals, objectives, and performance measures.
- Conducting periodic system condition inventories.
- Forecasting system conditions based upon projected rates of deterioration.
- Predicting the impact of various treatment scenarios.
- Evaluating different investment scenarios based upon benefit cost analysis.
- Developing a multi-year investment program.
- Monitoring the performance of system investments.

The ODOT's NHS database has been investigated thoroughly and representative pavement sections from each division have been identified based on the availability of the needed datasets in this project.

1.3.2. Current Pavement Preservation Approach

A key concept adopted in this project from pavement management system of ODOT is the maintenance of pavements in a "good" condition for the longest time at the lowest possible total cost. Therefore, it is necessary to treat deteriorating pavements early and while they are still in relatively good condition, rather than waiting until they need costly and major renewal solution. By applying minor and less expensive renewal solutions early in a pavement's life, the need for more expensive rehabilitation or eventual reconstruction can be delayed. By employing this concept, an agency can postpone costly reconstruction and reduce the overall budget needed to preserve the network. This strategy results in the lowest overall cost and the best overall condition. Table 1 summarizes the pavement performance programming for National Highway System (NHS) in the state of Oklahoma (*10*).
A summary of the trigger values and pavement preservation decision trees are extracted from the Pavement Management System (PMS) database (*10*) and the resulting 3P flowchart information is presented in Table 2 through Table 6 for conducting the future tasks.

Table 1 A Summary of the Pavement Performance Programming for Interstate Roads in Oklahoma National Highway System (NHS)

Conditions and Performance	**Investment Analysis Level**	
Performance Measures	PL-1: 86<IRI<100	Smooth and exhibit few surface defects
Performance Measures	PL-2: 76<IRI<85	Roughness or mild to moderate surface defects
Performance Measures	PL-3: IRI<76	In need of rehabilitation or reconstruction
Benefit Cost Analysis	Incremental benefit cost (IBC)	
Investment Scenarios	Do nothing Scenario	
	Maintain Current Condition Scenario	
	Improve Condition by Five Percent	
Improvement Types	Preservation	
	Rehabilitation	
	Reconstruction	
Analysis Strategy	Network Optimization Model: seeks to achieve the desired performance goal for the entire network at the lowest cost[1]	

[1] This is opposed to a project optimization model that would seek the lowest life cycle cost for each individual pavement section.

Table 2 Summary of the Trigger Values Used in Pavement Preservation Decision Tree for AC or Composite Pavements in ODOT

Traffic volume (AADT)	**Index Type**	**Index Min Values for 3P**	**Treatment Definitions for 3P**
<2,000	Structural	70	Thin overlay 1”-2” Medium overlay 2”-3” Hot in-place recycle w/cap
	Rut	40	
	Functional	45	
2,000-10,000	Structural	75	Thin overlay 1”-2” Medium overlay 2”-3” UTBWC Hot in-place recycle w/cap
	Rut	40	
	Functional	60	
10,001-30,00	Structural	80	Thin overlay 1”-2” Medium overlay 2”-3” UTBWC Hot in-place recycle w/cap
	Rut	65	
	Functional	70	
30,001-40,000	Structural	87	Thin overlay 1”-2” Medium overlay 2”-3” UTBWC Hot in-place recycle w/cap
	Rut	70	
	Functional	N/A	

Table 3 Pavement Preservation Decision Tree for Roads with <2,000 AADT in ODOT

Structural Index (SI)		Rut Index (RI)		Functional Index (FI)		Selected Treatment
Range	**Description**	**Range**	**Description**	**Range**	**Description**	**Description**
90<SI<100	Little or no fatigue or wheel path cracking	80<RI<100	Not much rutting	85<FI<100	Not much transverse or block cracking	Microsurface
				70<FI<85	Some transverse or block cracking	Thin overlay
				45<FI<70	Lots of transverse or block cracking	Medium overlay or HIR
		60<RI<80	Some rutting	70<FI<100	Bad transverse or block cracking	Thin overlay
				45<FI<70	Lots of transverse or block cracking	Medium overlay or HIR
		40<RI<60	Significant rutting	0<FI<100	N/A	Medium overlay or HIR
80<SI<90	Some fatigue or wheel path cracking	60<RI<100	Not bad rutting	70<FI<100	Not bad transverse or block cracking	Thin overlay
				45<FI<70	Lots of transverse, or block cracking	Medium overlay or HIR
		40<RI<60	Significant rutting	0<FI<100	N/A	Medium Overlay or HIR
70<SI<80	More fatigue or wheel path cracking	0<RI<100	N/A	0<FI<100	N/A	Medium Overlay or HIR

Table 4 Pavement Preservation Decision Tree for Roads with 2,000<AADT<10,000 in ODOT

Structural Index (SI)		Rut Index (RI)		Functional Index (FI)		Selected Treatment
Range	**Description**	**Range**	**Description**	**Range**	**Description**	**Description**
92<SI<100	Little or no fatigue cracking	85<RI<100	Not much rutting	85<FI<100	Not much transverse or block cracking	Microsurface
				70<FI<85	Some transverse or block cracking	Thin overlay or UTBWC
				60<FI<70	Lots of transverse or block cracking	Medium overlay or HIR
		60<RI<85	Some rutting	70<FI<100	Not bad transverse or block cracking	Thin Overlay or UTBWC
				60<FI<70	Lots of transverse or block cracking	Medium overlay or HIR
		45<RI<60	Significant rutting	0<FI<100	N/A	Medium overlay or HIR
		40<RI<45	Bad rutting	0<FI<100	N/A	3” overlay or HIR
85<SI<92	Some fatigue cracking	70<RI<100	Not bad rutting	70<FI<100	Not bad transverse or block cracking	Thin overlay or UTBWC
				60<FI<70	Lots of transverse or block cracking	Medium Overlay or HIR
		45<RI<70	Significant rutting	0<FI<100	N/A	Medium Overlay or HIR
		40<RI<45	Bad rutting	0<FI<100	N/A	3” overlay or HIR
75<SI<85	More fatigue cracking	0<RI<100	N/A	0<FI<100	N/A	Medium overlay or HIR

Table 5 Pavement Preservation Decision Tree for Roads with 10,001<AADT<30,000 in ODOT

Structural Index (SI)		Rut Index (RI)		Functional Index (FI)		Selected Treatment
Range	**Description**	**Range**	**Description**	**Range**	**Description**	**Description**
92<SI< 100	Little or no fatigue cracking	85<RI<100	Not much rutting	85<FI<100	Not much transverse or block cracking	Microsurface
				70<FI<85	Some transverse or block cracking	Thin overlay or UTBWC
		75<RI<85	It's got rutting	0<FI<100	N/A	Mill & thin overlay or HIR
		65<RI<75	Worse rutting	0<FI<100	N/A	Mill & medium overlay or HIR
80<SI<92	Some fatigue cracking	80<RI<100	No bad rutting	0<FI<100	N/A	Medium overlay or HIR
		65<RI<80	Worse rutting	0<FI<100	N/A	Mill & medium overlay or HIR

Table 6 Pavement Preservation Decision Tree for Roads with 30,001<AADT<40,000 in ODOT

Structural Index (SI)		Rut Index (RI)		Functional Index (FI)		Selected Treatment
Range	**Description**	**Range**	**Description**	**Range**	**Description**	**Description**
93<SI<100	Little or no fatigue cracking	85<RI<100	Not much rutting	0<FI<100	N/A	Thin overlay or UTBWC
		70<RI<85	It's got rutting	0<FI<100	N/A	Mill & thin overlay or UTBWC
87<SI<93	Some fatigue cracking	85<RI<100	Not much rutting	0<FI<100	N/A	Medium overlay or HIR
		70<RI<85	It's got rutting	0<FI<100	N/A	Mill & medium overlay or HIR

CHAPTER 2. CATEGORIZATION OF PAVEMENT SECTIONS

The available ODOT PMS database is used in the current study to group the pavements routes and identify test sections. Since investigation of the entire Oklahoma pavement network was not possible within the project constraints, a grouping approach was adopted. Group is a practical approach to take into consideration the whole range of contributing factors in rehabilitation selection process such as pavement type, structural composition, functional classification and performance issues.

2.1. DEVELOPMENT OF PAVEMENT FAMILIES FOR THE PRESENT STUDY

The historical database used in this study comes from the National Highway System (NHS) routes in Oklahoma. NHS consists of the primary commercial, defense and personal mobility highways in the state and plays a critical role in the state economy and the daily lives of citizens. Although this highway system contains only 30 percent of the state's total highway lane miles, these routes carry 63 percent of the total traffic and include eight field divisions in the state highway system. It also covers all the traffic levels and climate conditions. Therefore, pavement groups and representative test sections have been identified through NHS routes. The pavement management system (PMS) data provided by ODOT includes only information for interstate routes and the research team did not have access to the information related to profile section of non-interstate highways. Therefore, the focus of this study is on asphalt surfaced interstate routes on high-volume highways. For this purpose, six flexible and composite pavement family groups are identified based on the structure composition. The structural profiles for the pavement family groups assessed in this study are presented in Figure 1.

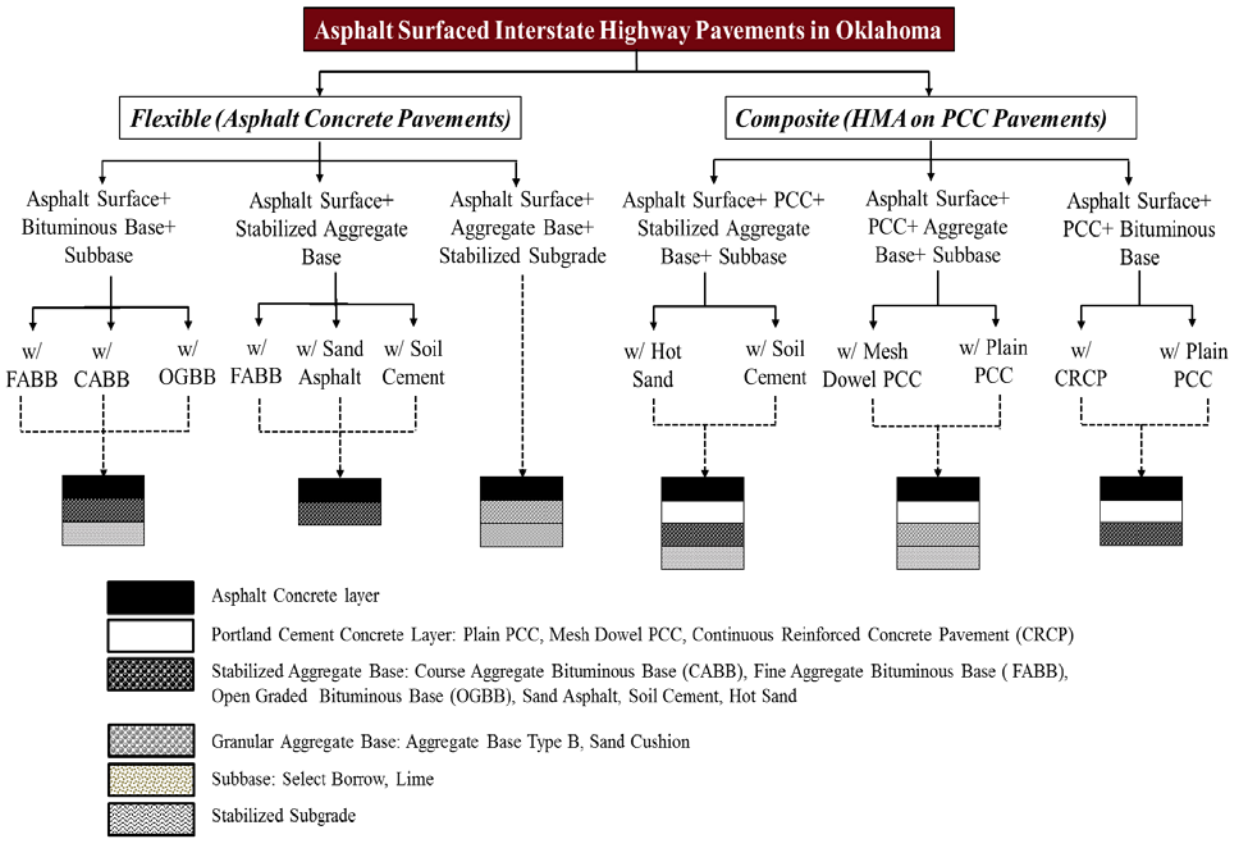

Figure 1 Representative Pavement Family Groups Investigated in This Study

2.2. IDENTIFICATION OF REPRESENTATIVE PAVEMENT SECTIONS FOR THE STUDY

Representative test sections of each family group have been identified based on the traffic level and availability of FWD data. According to the ODOT pavement preservation decision tree, traffic volume is categorized in four levels. Table 7 shows the different levels used in ODOT 3P flowchart. Based on the available information, traffic volume between 30,000 and 40,000 AADT was found to be the highest traffic level used in ODOT decision tree. However, based on the PMS database found in the National Highway System in Oklahoma, there are some interstate roads with AADT much more than 40,000. Also, there are only a few cases with the low and medium traffic volume level on the Oklahoma interstate highways. Therefore, two levels of high to very high traffic levels were used to identify the representative test sections in this study. Based on NHS report (2012) (*10*) interstate highways include mostly high and very high volume traffic and non-interstate highways including US and State highways mainly include low and medium volume traffic.

Table 7 Classification of Traffic Levels in ODOT Decision Tree

Traffic volume (AADT)	Description
<2,000	Low
2,000_ 10,000	Medium
10,001_ 30,000	High
30,001_ 40,000	Very high

Two pavement structure types have been considered in the selection of representative test sections, which include asphalt concrete pavement and composite pavements (asphalt layer over concrete). The 2010 and 2011 FWD data were used in this project to identify the representative pavement sections. Since FWD data was not available for the entire pavement network and as this data provide significant information to assess the condition of existing pavement, only sections with available FWD data are taken into account for the selection of representative pavement sections. For each pavement family group, the control section with the highest traffic among all divisions has been selected as a representative pavement section. Also, the beginning and ending mile post of each section have been selected such that the structure composition and renewal activities performed on section during the service life are not changed over the identified section length. A summary of identified representative sections with the length of each section have been presented in Table 8. The basis to select these sections is to present few sections with available FWD data from each division to include different pavement structure, and traffic levels.

2.3. REVIEW OF PAVEMENT MANAGEMENT SYSTEM DATABASE FOR REPRESENTATIVE PAVEMENT SECTIONS

A pavement management system (PMS) summarizes pavement information and uses the data for selecting the cost-effective treatment strategies for a network (*10*). PMS data used in this study includes pavement profiles, treatment activities history, performance measurements and falling weight deflectometer data. These data along with data obtained from lab testing provide required sources for conducting the rehabilitation design analysis.

2.3.1. Summary of Treatment History of Representative Pavement Sections

The structure profile and treatment history of each section are extracted from PMS database. When associated with performance measurements and non-destructive test data, these data can describe the current condition of pavements. Figure 2 through Figure 15 show the structure profiles of representative sections over time. As it can be seen, most of the flexible interstate sections have been upgraded to structures that could be considered as perpetual pavements since their original construction. These profiles also illustrate the frequency of rehabilitation practices applied on sections and provide a general review of the rehabilitation activities by ODOT over time. It should be

noted that according to ODOT engineers, every overlay placed after 1980 is associated with 1-2” milling even if it is not recorded in the pavement profile database.

Table 8 Summary of Representative Pavement Sections

Field Division	Pavement Structure	Control Section*	Route	Beg. Milepost	End Milepost	2015 AADT
1	Asphalt Concrete	68-22	I040	13.00	17.60	19995
3	Asphalt Concrete	44-05	I035	13.85	16.5	41015
		44-05	I035	10.78	12.04	35399
		14-06	I035	3.35	7.00	103477
	AC Over PCC	25-46	I035	17.00	20.30	33179
4	Asphalt Concrete	09-05	I040	4.18	10.80	29394
		55-68	I040	6.55	11.90	44910
	AC Over PCC	55-09	I035	8.54	13.00	51461
		42-30	I035	7.09	12.70	27523
5	Asphalt Concrete	20-04	I040	0.00	6.00	25706
7	AC Over PCC	16-49	I044	0.00	3.00	8115
		50-32	I035	0.00	6.54	34668
		25-46	I035	0.00	4.06	33688
8	AC Over PCC	72-09	I244	9.00	11.00	62913

*ODOT supplied, 2-digit county, dash, 2-digit control section

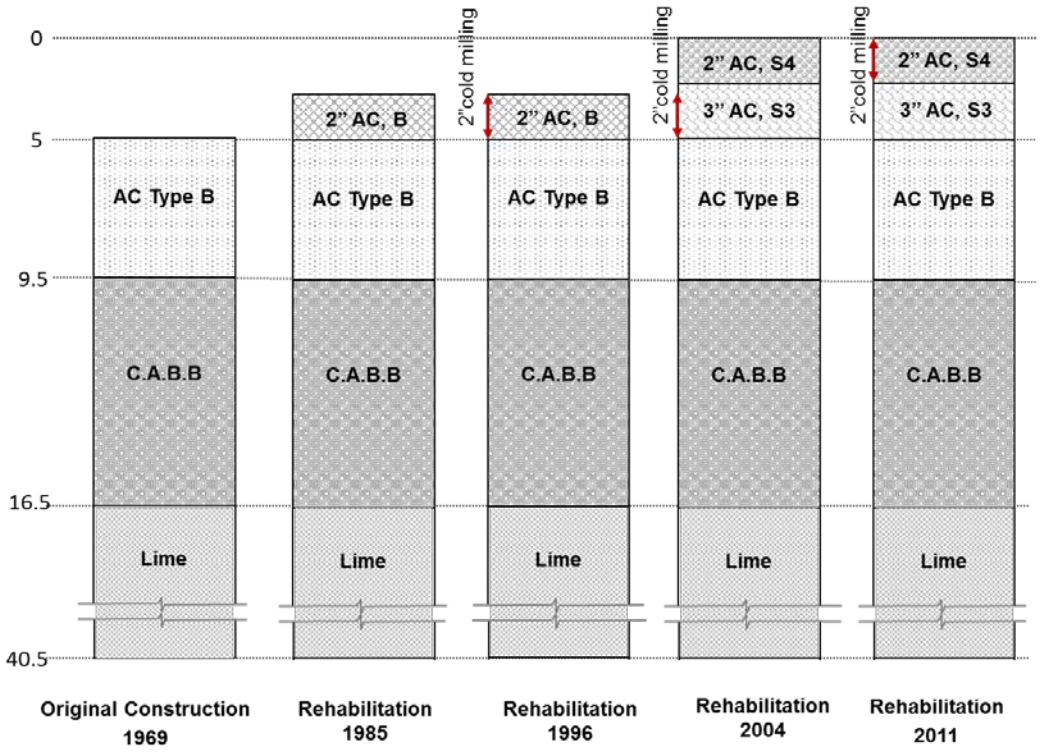

Figure 2 Structure Profile of Control Section 68-22 MP 13.0-17.6

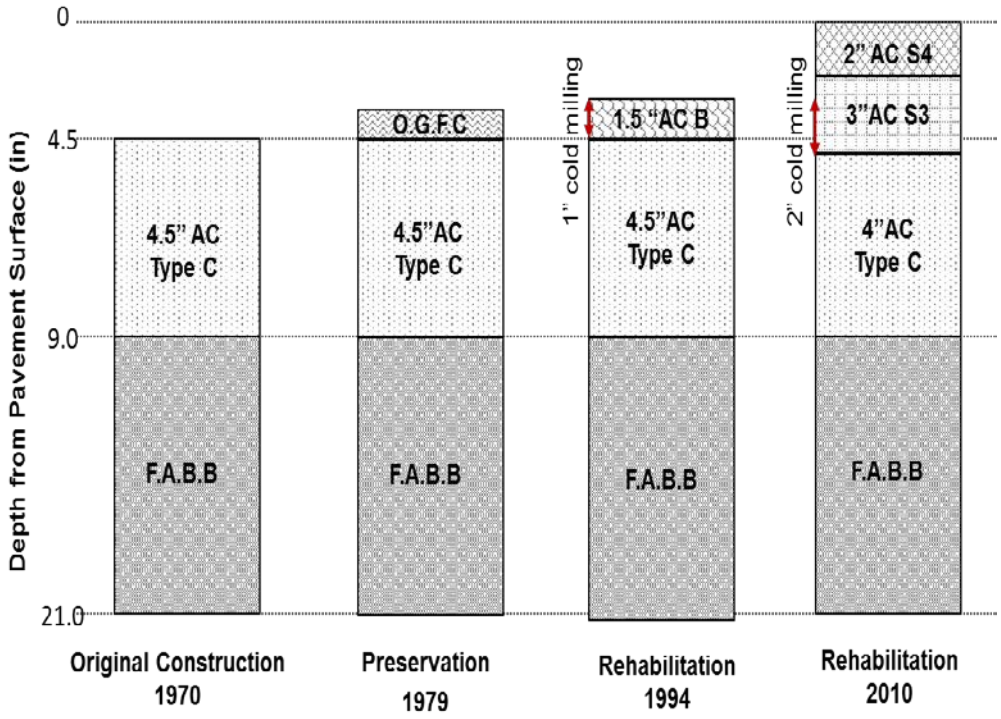

Figure 3 Structure Profile of Control Section 44-05 MP 10.78-12.04

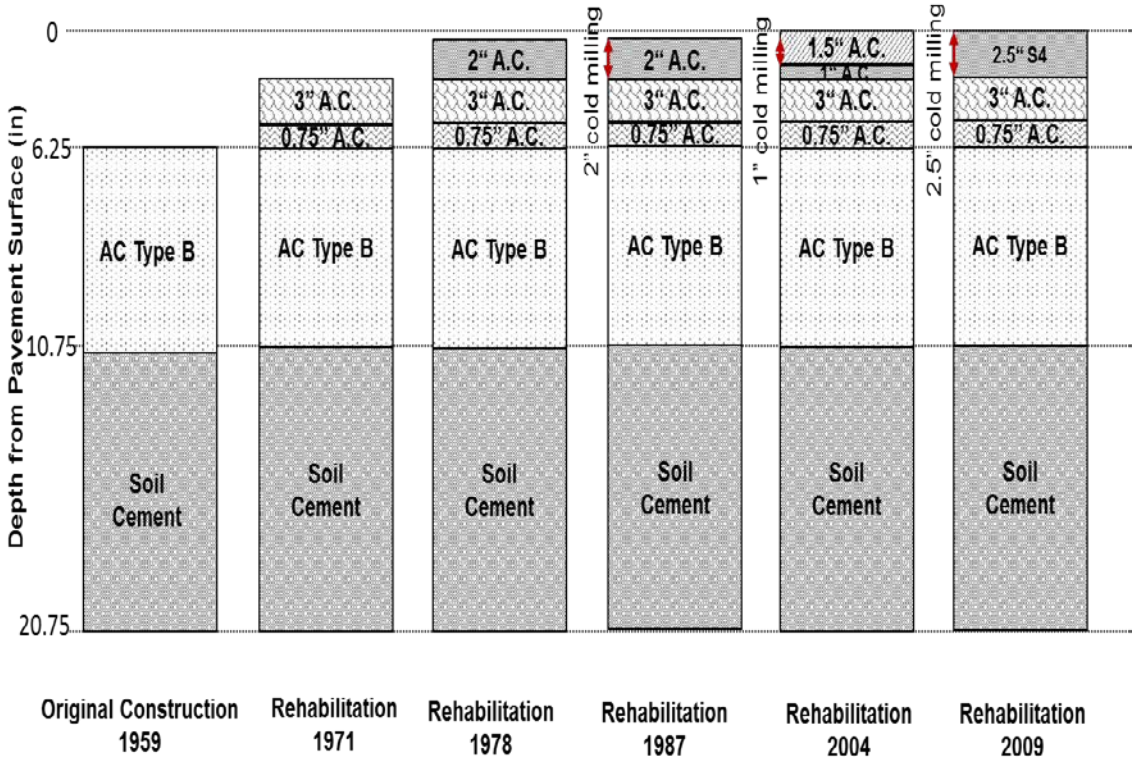

Figure 4 Structure Profile of Control Section 44-05 MP 13.85-16.5

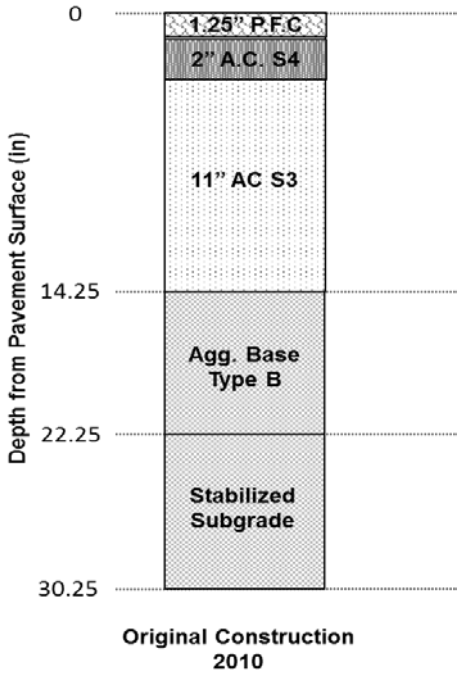

Figure 5 Structure Profile of Control Section 14-06 MP 3.35-7.0

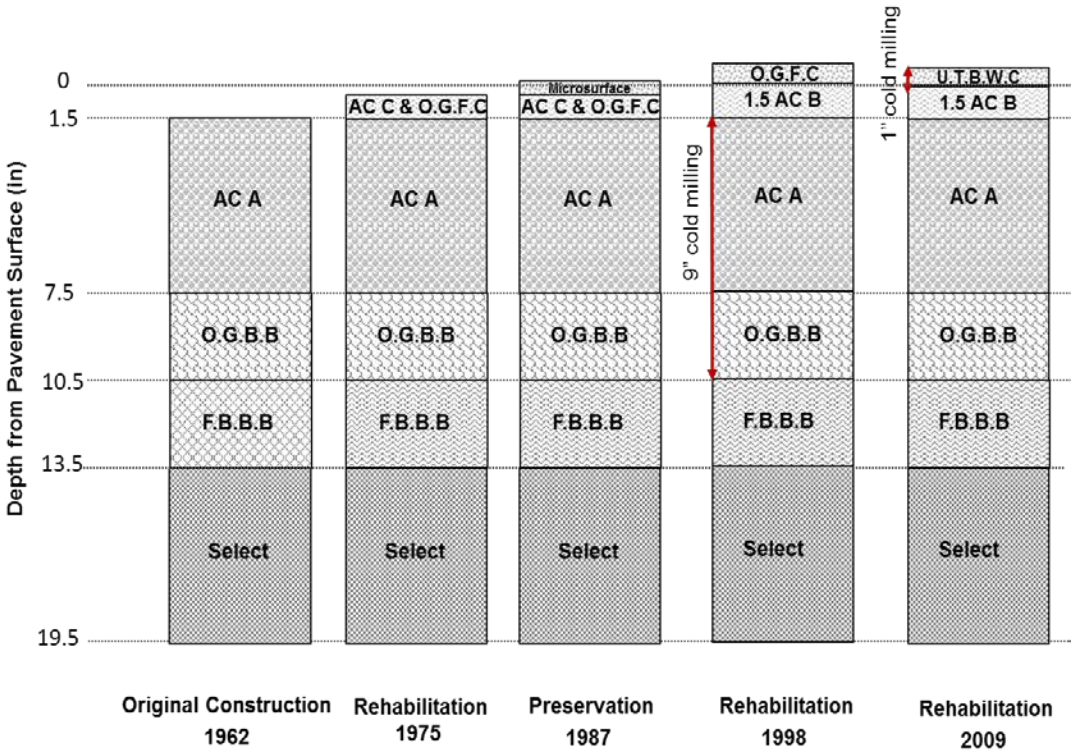

Figure 6 Structure Profile of Control Section 09-05 MP 4.18-10.8

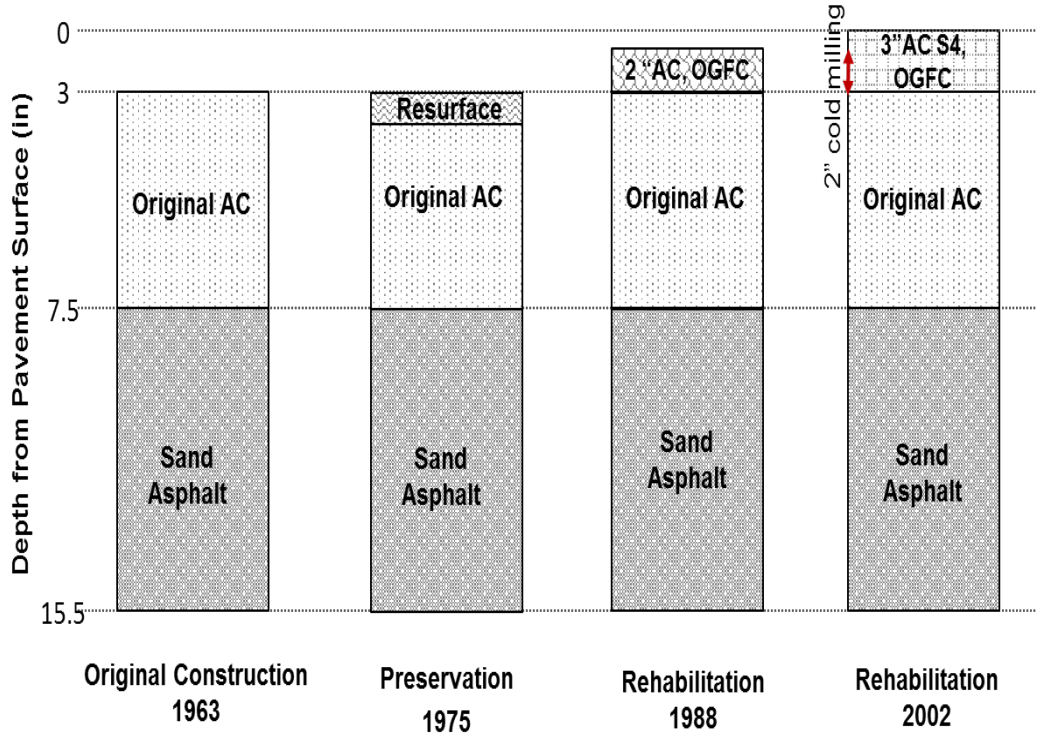

Figure 7 Structure Profile of Control Section 55-68 MP 6.55-11.9

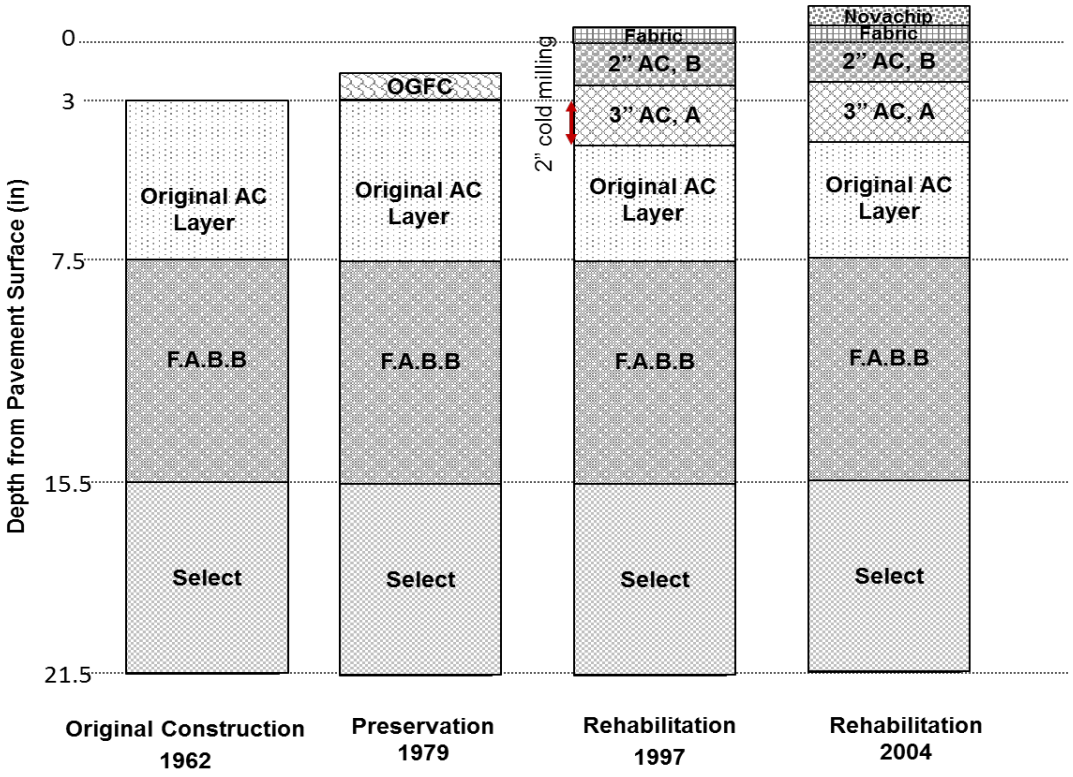

Figure 8 Structure Profile of Control Section 20-04 MP 0.0-6.0

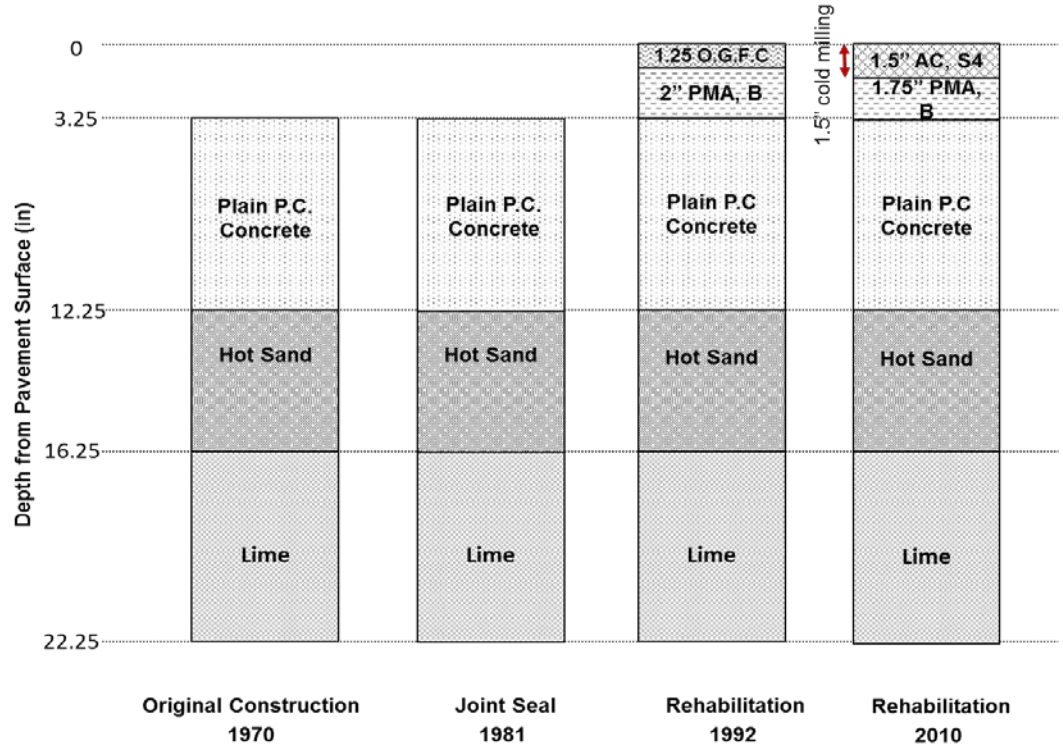

Figure 9 Structure Profile of Control Section 25-46 MP 17.0-20.3

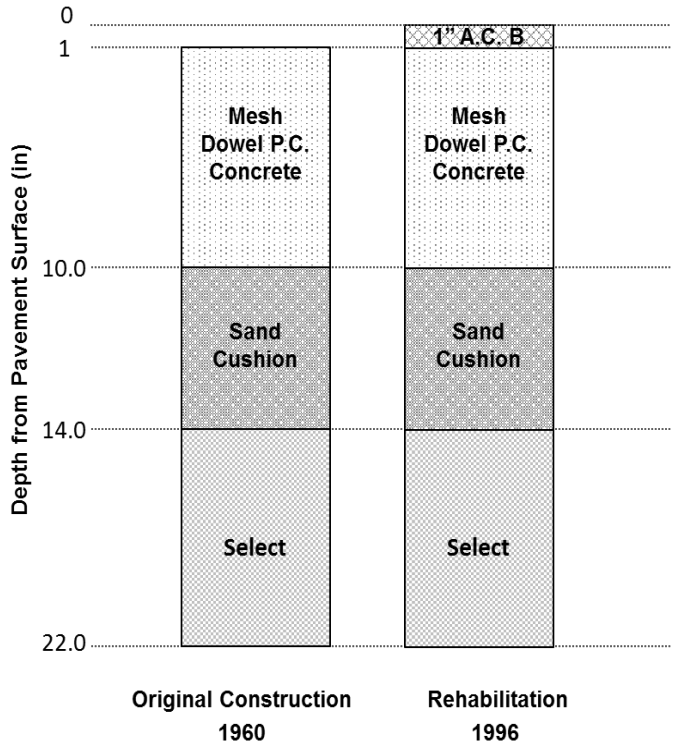

Figure 10 Structure Profile of Control Section 42-30 MP 7.09-12.7

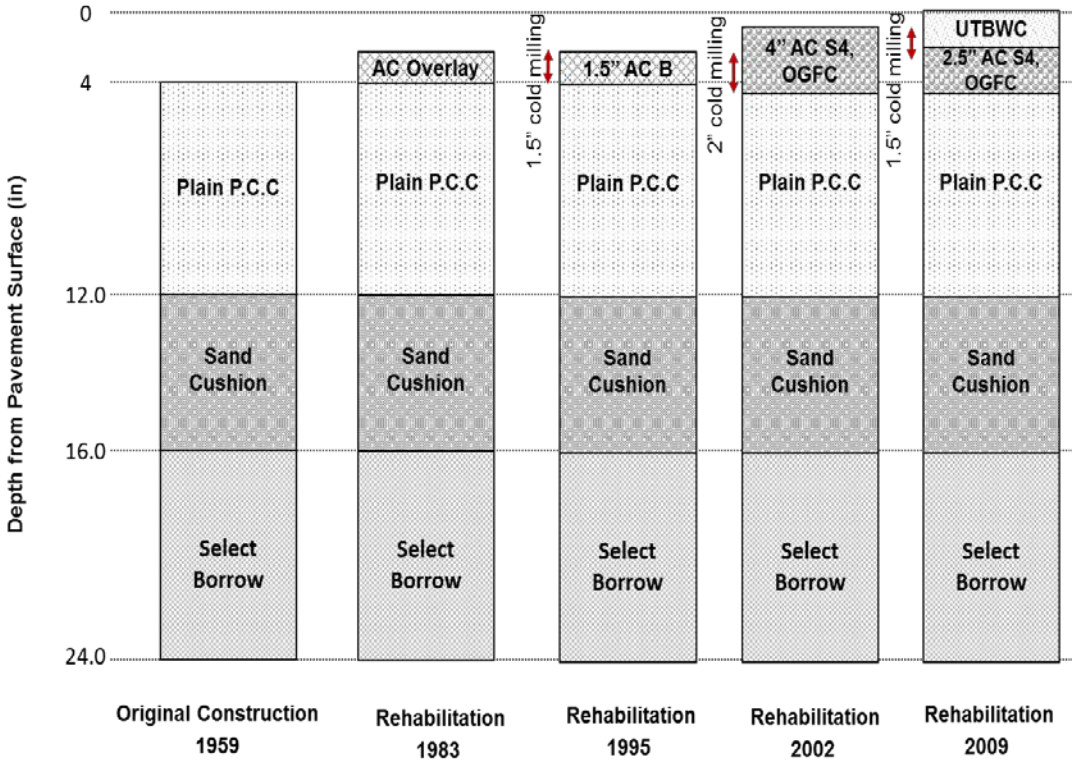

Figure 11 Structure Profile of Control Section 55-09 MP 8.54-13.0

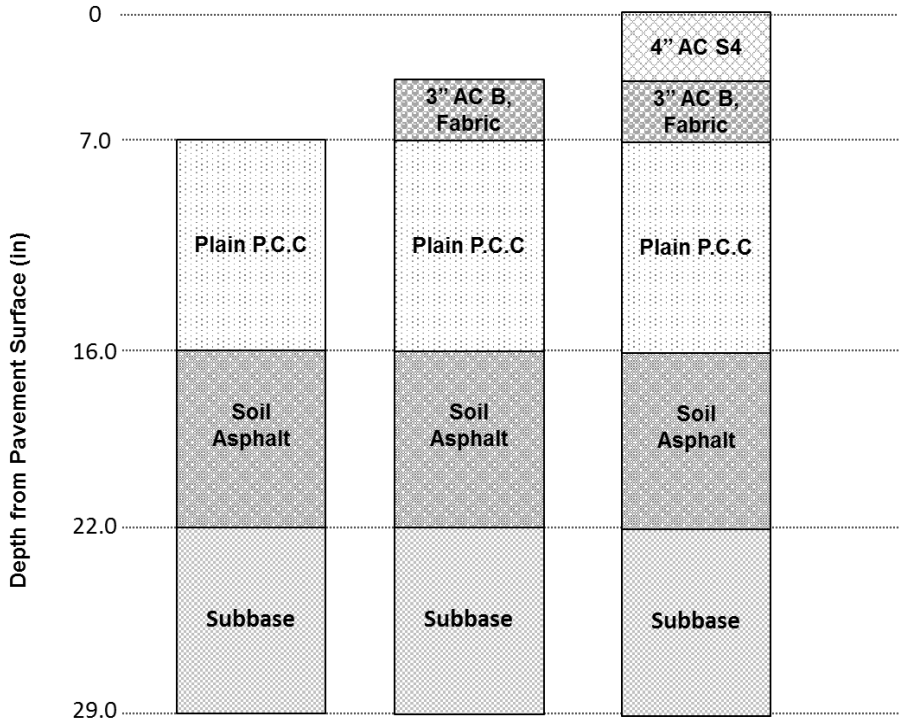

Figure 12 Structure Profile of Control Section 16-49 MP 0.0-3.0

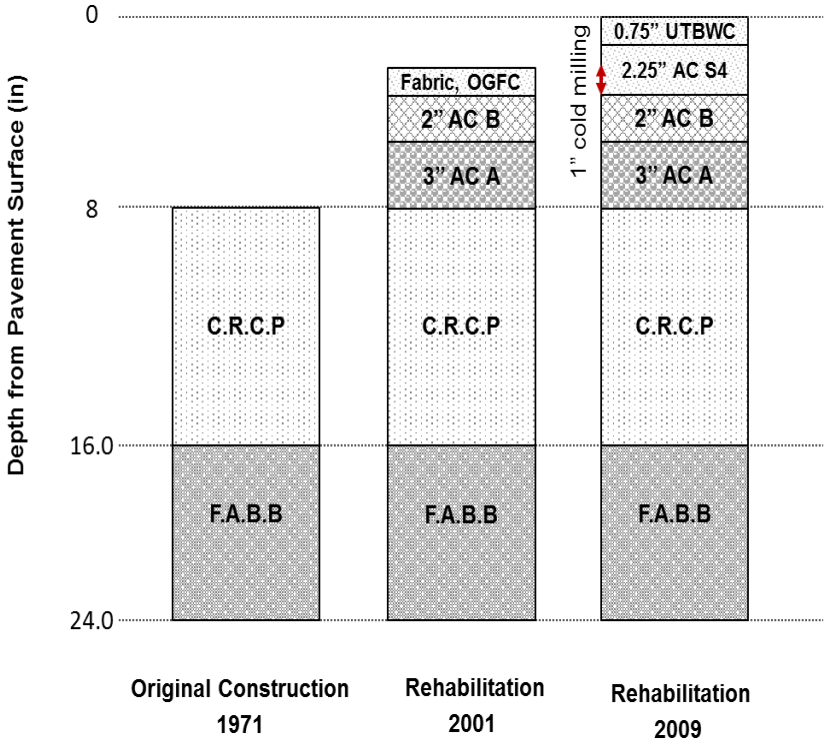

Figure 13 Structure Profile of Control Section 50-32 MP 0.0-6.54

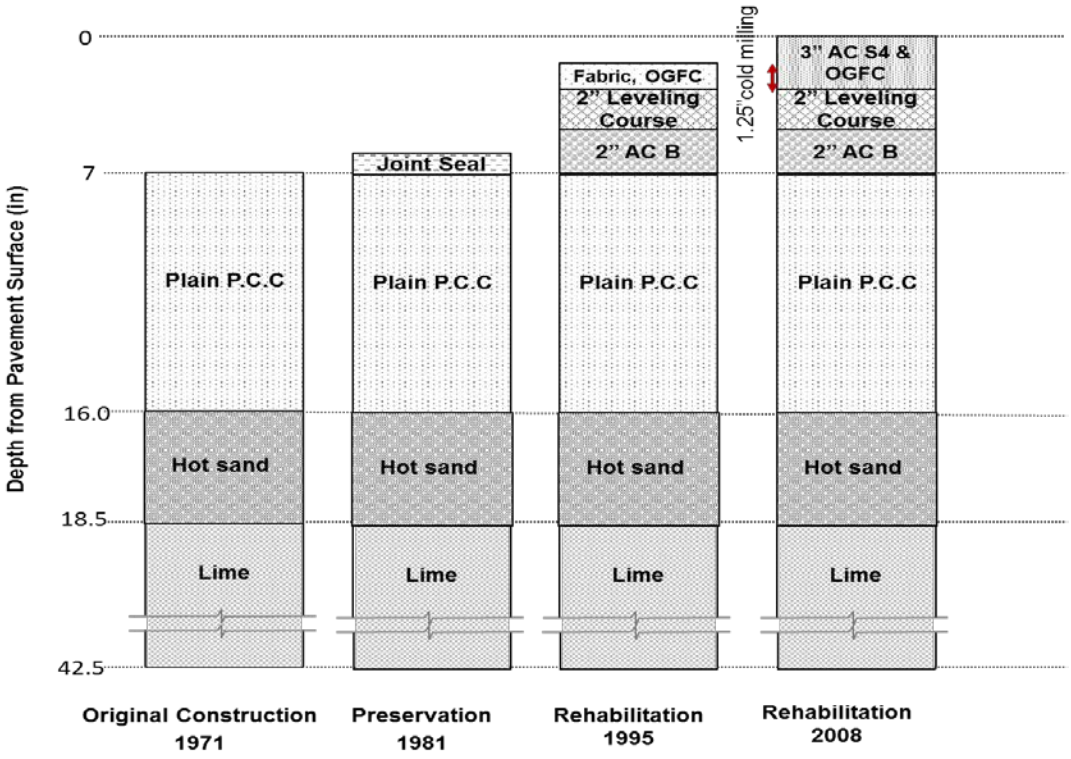

Figure 14 Structure Profile of Control Section 25-46 MP 0.0-4.06

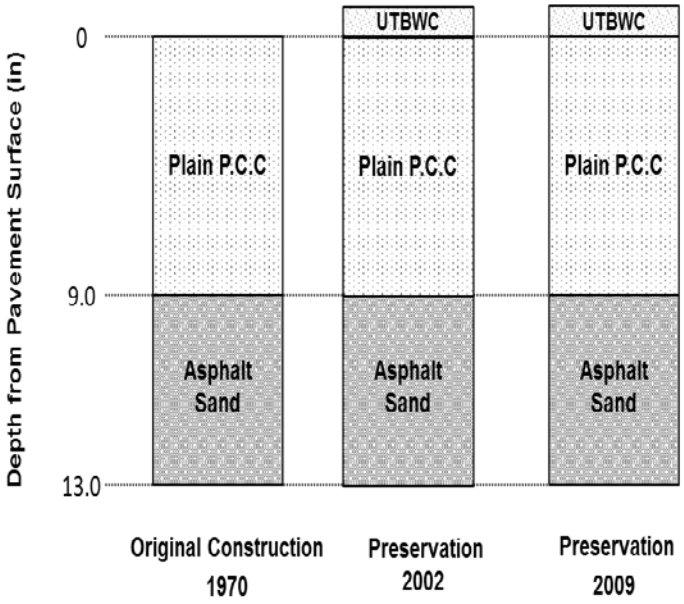

Figure 15 Structure Profile of Control Section 72-09 MP 9.0-11.0

The list of treatment activities on the selected interstate highways identified for each field division is presented in Table 9 and Table 10.

Table 9 A summary of Treatment History of Representative Pavement Sections (i)

Field Division	Pavement Section	Treatment History	
		Year	Activity
1	Control Section: 68-22 Route: 1040 Milepost: 13 to 17.6 Direction: 5&6	1969	Original Construction
		1976	AC overlay
		1985	2" AC Type B
		1996	2" AC Type B
		2004	3" S3, 2" S4 W/2" Coldmilling
		2011	2" AC S4
3	Control Section: 44-05 Route: 1035 Milepost: 10.78 to 12.04 Direction: 5&6	1970	Original Construction
		1979	Leveling Course, OGFSC.[1]
		1994	1 1/2" AC Type B W/ 1" Coldmilling
		2010	3" S3, 2" S4 W/2" Coldmilling
3	Control Section: 44-05 Route: 1035 Milepost: 13.85 to 16.5 Direction: 5&6	1959	Original Construction
		1964	3/4" AC Type B
		1971	3" AC Type B
		1978	2" AC Type B
		1987	2" AC Type B W/2" Coldmilling
		2004	1.5" S4 W/1" Coldmilling
		2009	2.5" S4 W/ 2.5" Coldmilling
3	Control Section: 14-06 Route: I035 Milepost: 3.35 to 7.0 Direction: 5&6	2010	Original Construction
3	Control Section: 25-46 Route: I035 Milepost: 17 to 20.3 Direction: 5&6	1970	Original Construction
		1981	Joint Seal
		1992	2" Polymer Modified AC Type B, 1.25" Leveling Course, OGFSC and Fabric
		2010	1.5" S4 W/ 1.5"Coldmilling
4	Control Section: 09-05 Route: 1040 Milepost: 4.18 to 10.8 Direction: 5&6	1962	Original Construction
		1975	AC Type C, Leveling Course, OGFSC
		1987	Microsurface
		1998	6" AC Type A, 1 1/2 AC Type B, 3" OGFSC w/ 9" Coldmilling
		2009	U.T.B.W.C.[2] W/ 1" Coldmilling
4	Control Section: 42-30 Route: 1035 Milepost: 7.09 to 12.7 Direction: 5&6	1960	Original Construction
		1996	1" AC Type B w/ Fabric
4	Control Section: 55-68 Route: 1040 Milepost: 6.55 to 11.9 Direction: 5&6	1963	Original Construction
		1975	AC Resurface
		1988	2" AC Overlay, OGFSC
		2002	3" AC. S4, OGFSC w/ 2" Coldmilling

[1] Open-Graded Friction Surface Course
[2] Ultra-Thin Bonded Wearing Course

Table 10 A summary of Treatment History of Representative Pavement Sections (ii)

Filed Division	Pavement Section	Treatment History	
		Year	Activity
4	Control Section: 55-09 Route: 1035 Milepost: 8.54 to 13 Direction: 5&6	1959	Original Construction
		1983	AC. Overlay, OGFSC
		1995	1 1/2" AC Type B w/1 1/2" Coldmilling
		2002	4" AC Tpe S4, O.G.F.C w/ 2" Coldmilling
		2009	U.T.B.W.C W/ 1 1/2" Coldmilling
5	Control Section: 20-04 Route: 1040 Milepost: 0 to 6 Direction: 5&6	1962	Original Construction
		1979	O.G.F.C
		1997	2" AC Type B, 3" AC Type A w/ 2" Coldmilling
		2004	Navachip
7	Control Section: 16-49 Route: 1044 Milepost: 0 to 3 Direction: 5&6	1964	Original Construction
		1994	3" AC Type B w/ Fabric
		2011	4" AC type S4
7	Control Section: 50-32 Route: 1035 Milepost: 0 to 6.54 Direction: 5&6	1971	Original Construction
		2001	3" AC Type A, 2" AC Type B, OGFSC
		2009	2 1/4" AC Type S4, 3/4" U.T.B.W.C W/ 1" Coldmilling
7	Control Section: 25-46 Route: 1035 Milepost: 0 to 4.06 Direction: 5&6	1971	Original Construction
		1981	Joint Seal
		1995	2" AC Type B, 2" Leveling Course, OGFSC
		2008	3" AC Tpe S4 w/ 1 1/4" Coldmilling
8	Control Section: 72-09 Route: 1244 Milepost: 9 to 11 Direction: 5&6	1970	Original Construction
		2002	U.T.B.W.C
		2009	U.T.B.W.C

2.3.2. Field Performance Measures

The ODOT PMS relies on pavement distresses collected using a semi-automated collection method every two years starting from 2008. Four performance measures including ride, rut, structural and functional indices are defined in ODOT PMS to describe the pavement condition. Ride, rut, and functional indices are determined based on the pavement roughness, rut depth and non-load related distress respectively, while the structural index is defined based on the fatigue, patch and pothole distresses. The value of these indices ranges from 0 to 100. High value of each index implies a good pavement condition regarding related distress. For example, the higher ride index is, the smoother pavement would be. These four indices are combined in pavement quality

index (*PQI*) to show the overall pavement condition. PQI is calculated by using Equation (1) and Equation (2) for flexible and composite pavements respectively:

$$PQI = 0.4\times(\text{Ride Index}) + 0.3\times(\text{Rut Index}) + 0.15\times(\text{Functional Index}) + 0.15\times(\text{Structural Index}) \quad (1)$$

$$PQI = 0.4\times(\text{Ride Index}) + 0.15\times(\text{Rut Index}) + 0.3\times(\text{Functional Index}) + 0.15\times(\text{Structural Index}) \quad (2)$$

Performance measures including pavement quality index (PQI) and ride index have been extracted from ODOT PMS data collected in 2008, 2010 and 2012 for representative test sections. Figure 16 and Figure 17 show the changes of PQI and ride index versus the pavement age for flexible and composite pavement family groups respectively. In these figures blue line shows the time of applied treatment according to the PMS pavement treatment history record. The performance curves show that in general interstate highways are in good condition as they have experienced frequent maintenance and rehabilitation activities. The findings of these performance curves can be used to estimate a rough estimation of the extended service life of pavements after each renewal solution. For each representative pavement section the historical database presented in Table 11 have been extracted from the available PMS database. This table further details different types of data that have been collected over years in ODOT.

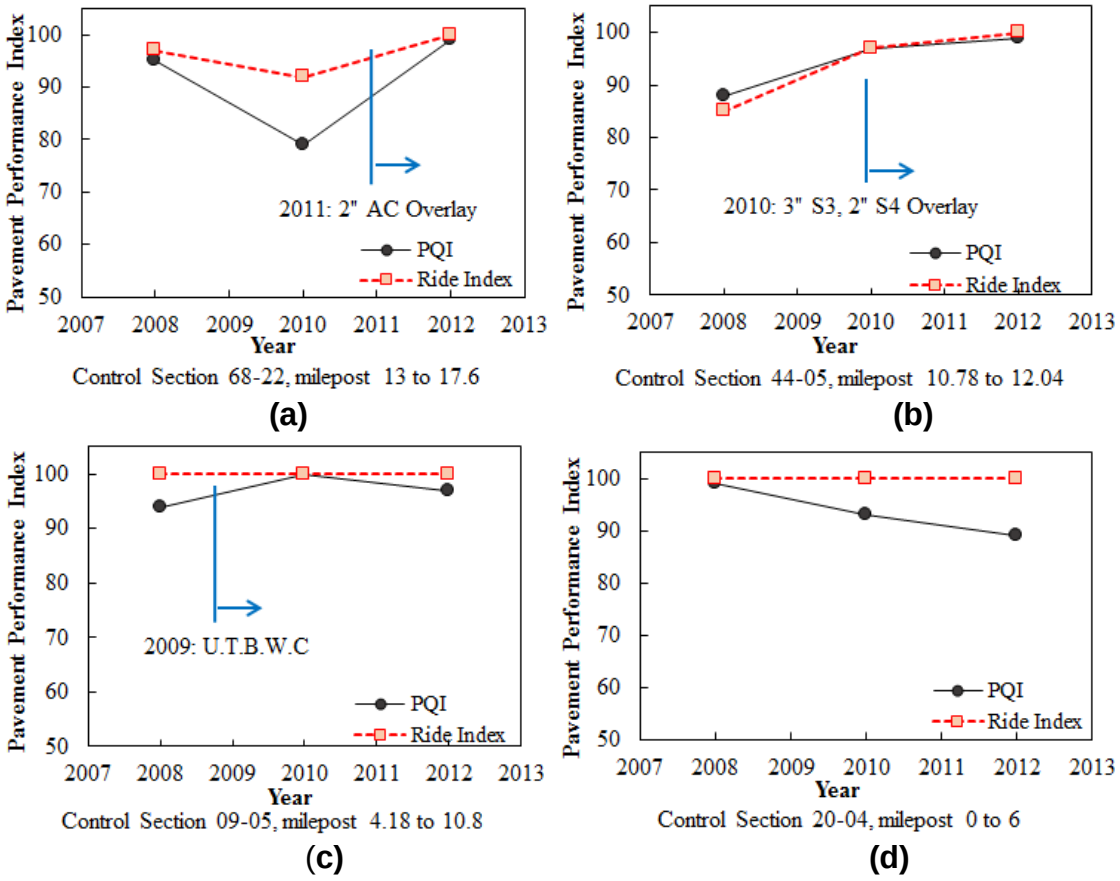

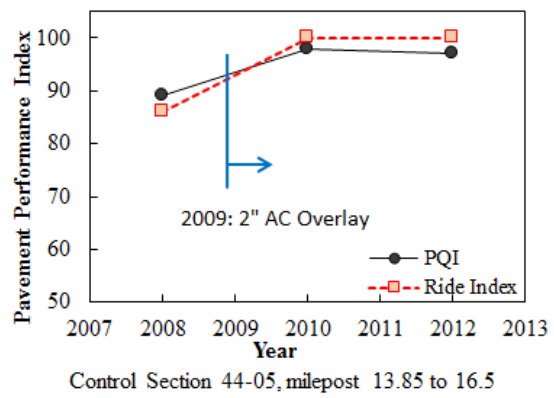

Control Section 44-05, milepost 13.85 to 16.5

(e)

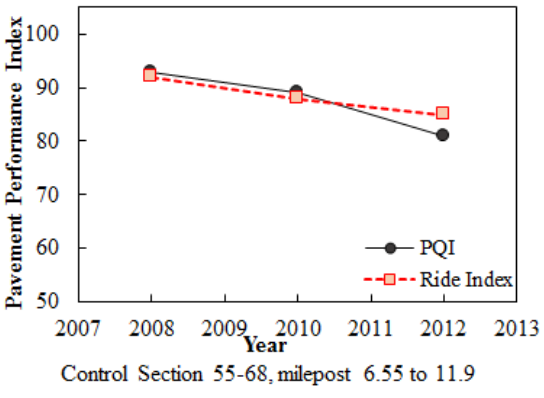

Control Section 55-68, milepost 6.55 to 11.9

(f)

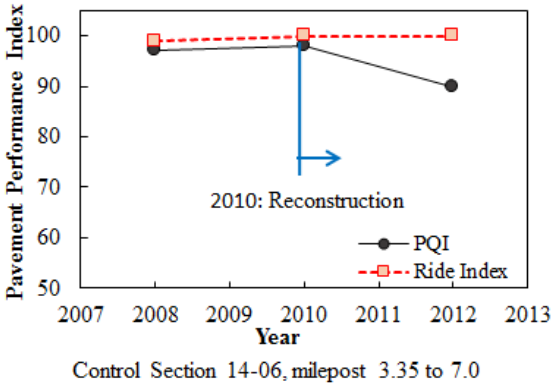

Control Section 14-06, milepost 3.35 to 7.0

(g)

Figure 16 Pavement Quality Index (PQI) and Ride Index Evaluation for Flexible Representative Pavement Sections in Control Sections: (a) 68-22, milepost 13 to 17.6, (b) 44-05, milepost 10.78 to 12.04, (c) 09-05, milepost 4.18 to 10.8, (d) 20-04, milepost 0 to 6, (e) 44-05, milepost 13.85 to 16.5, (f) 55-68, milepost 6.55 to 11.9; and (g) 14-06, milepost 3.35 to 7.0.

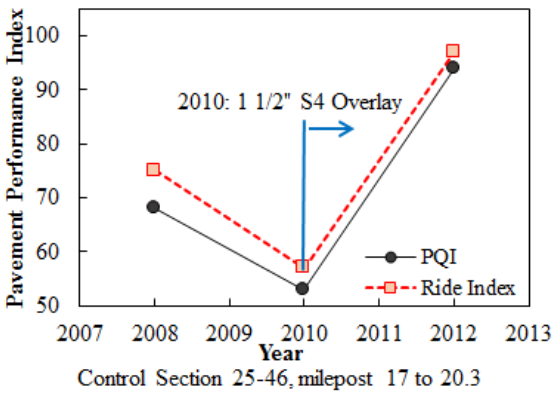

Control Section 25-46, milepost 17 to 20.3

(a)

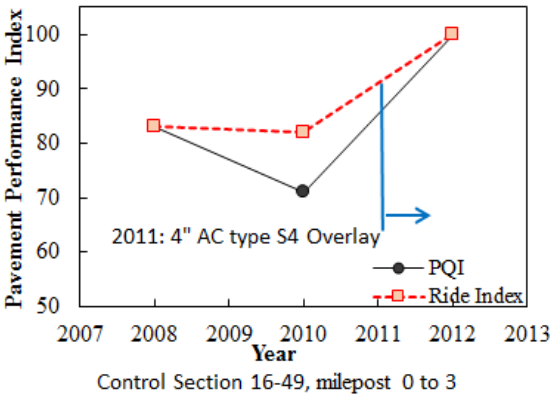

Control Section 16-49, milepost 0 to 3

(b)

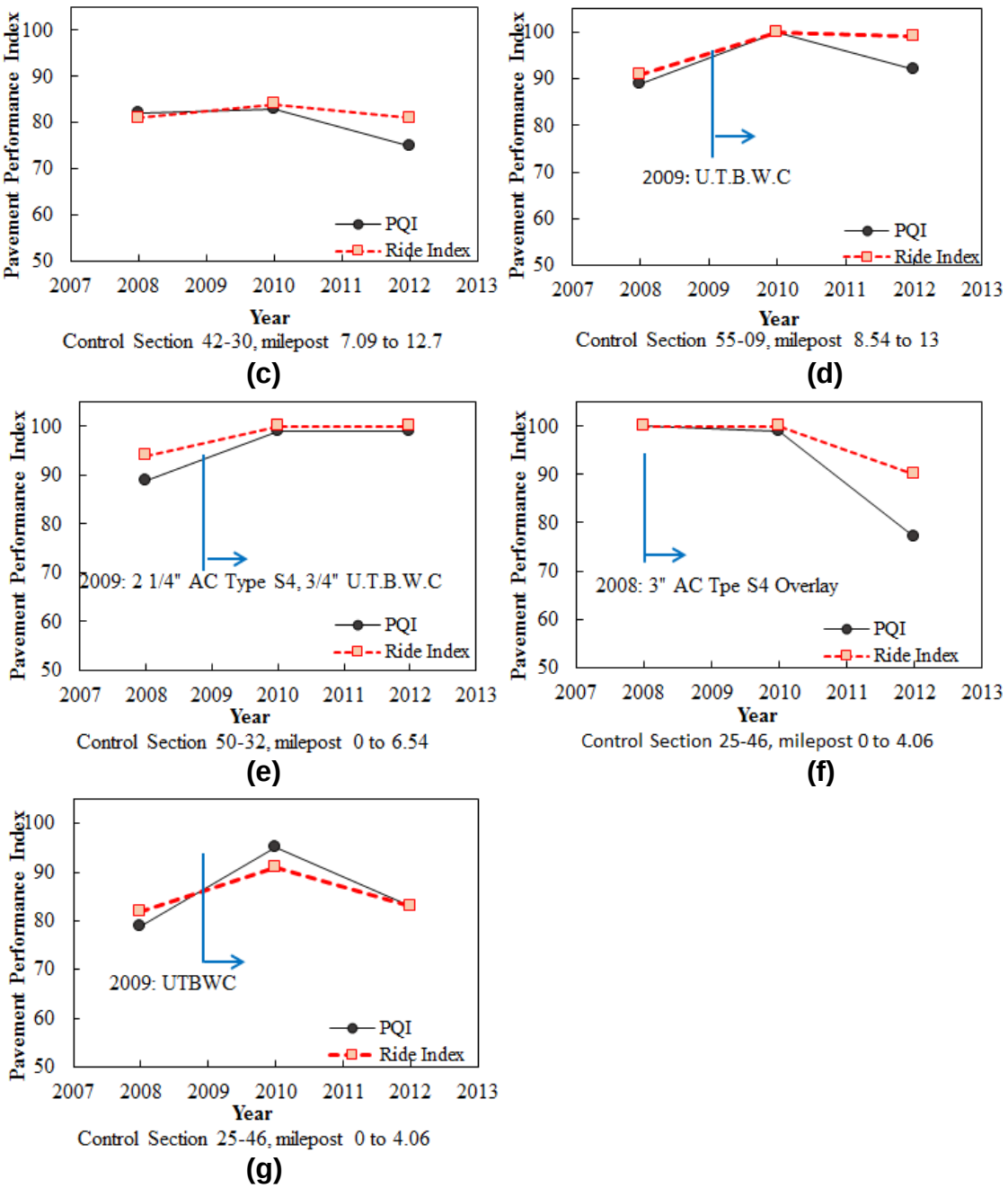

Figure 17 Pavement Quality Index (PQI) and Ride Index Evaluation for Composite Representative Pavement Sections in Control Sections: (a) 25-46, milepost 17 to 20.3, (b) 16-49, milepost 0 to 3, (c) 42-30, milepost 7.09 to 12.7, (d) 55-09, milepost 8.54 to 13, (e) 50-32, milepost 0 to 6.54, (f) 25-46, milepost 0 to 4.06; and (g) 25-46, milepost 0 to 4.06.

Table 11 Data Sets to Be Collected from Existing Records/Database on Rehab/ Preservations Sites

Data Type	Data Source	Description
Existing Pavement Structure	Records/Databases	Layer types
		Layer thicknesses
		Layer designs
Historical Pavement Performance	Pavement Management System (PMS)	Overall condition (aggregate/composite index)
		Roughness (index, profile)
		Surface distress (type, severity, and extent)
		Falling weight deflectometer (FWD)
		Material Integrity and Damage Characterization
		Other (e.g., cost/lane-mile)
Preservation Work	DOT Records/Databases	Treatment type (preservation, rehabilitation or reconstruction)
		Treatment design
		Construction notes
Traffic	Records/Databases (National Highway System (NHS))	Annual average daily traffic (AADT)
		Percent trucks
Climate	Records and/or NOAA Database	Average # days above 35°C/below 0°C
		Average annual precipitation

CHAPTER 3. EXPERIMENTAL TEST PLAN

Material characterization and performance properties of mixtures used in rehabilitation treatments are major inputs for mechanistic-empirical rehabilitation design analysis. Therefore, most commonly mixtures used in rehabilitation projects have been identified and tested under a comprehensive laboratory test plan.

3.1. MIXTURE DATABASE

The Superpave mixtures used in Oklahoma are categorized in three major groups based on their nominal maximum aggregate size (NMAS). Mixtures with NMAS of 19.0 mm, 12.5 mm and 9.5 mm are named as S3 (or AC type A), S4 (or AC type B) and S5 (or AC type C) respectively. Mixtures designated as S3 are used in the base coarse, and S4 and S5 are applied for surface layers. Also, some other mixtures such as course aggregate bituminous base (CABB) and fine aggregate bituminous base (FABB) have been extensively employed in base and subbase layers. These mixtures have been designed based on a modified Hveem mix method that is quite different from the Superpave mix design. A list of asphalt mixes approved for use in the contracts with ODOT has been investigated. Table 12 is taken from ODOT's database and shows the mixture usage report by mix and binder type in year 2012 at Oklahoma. This table shows that S3 PG 64-22 mixture constitutes 25% of total mixtures used in 2012 for different ODOT's projects. The next most widely used mixtures are S4 PG 64-22, S4 PG 70-28 and S4 PG 76-28. In the early stages of this research work, the research team identified some of the most commonly used Superpave asphalt concrete mixtures that are typically used and paved in Oklahoma as surface and base mixtures.

Therefore, mixtures types of S3-PG 64-22, S4-PG 64-22, S4-PG 70-28, S4-PG 76-28 and S5-PG 76-28 have been chosen as the representative mixture types for conducting performance tests in the lab. Among all mix designs placed in categories of S3, S4 and S5 mix types, the final mixtures are selected to represent different field division's, pavement structure (pavement configuration), traffic levels and the use of different amounts of RAP material in the mix design. The job mix formula (JMF) and mix design (MD) sheets for these mixtures have been gathered from the bituminous materials laboratory at the ODOT. The material characterization and performance testing of Superpave mixtures commonly used in Oklahoma resulted in a large database that can be used for various purposes in future. It should also be noted that the use of PG 70-28 and PG 76-28 binders is mostly limited to the top 5 inches whereas PG 64-22 is used when there is more than 5 inches of AC mixture below the pavement surface.

Table 12 Mixture Usage Report by Mix and Binder Type for Year 2012

Mixture Type	Binder Type	Mix Tons	%
PFC	PG 76-28 OK	8,378	0
OGFSC	PG 76-28 OK	2,481	0
UTBWC	PG 70-28 OK	14,831	1
S6	PG 64-22 OK	8,244	0
S5	PG 76-28 E	5,662	0
S5	PG 76-28 OK	21,687	1
S5	PG 70-28 OK	-7,098	0
S5	PG 64-22 OK	77,357	3
S4	PG 76-28	276,570	12
S4	PG 70-28 OK	209,754	9
S4	PG 64-22 OK	566,254	25
S3	PG 76-28 E	18,872	1
S3	PG 76-28 OK	94,587	4
S3	PG 70-28 OK	99,172	4
S3	PG 64-22 OK	829,437	37
S2	PG 64-22 OK	6,572	0
OGBB	PG 64-22 OK	28,856	1
RIL	PG 76-28 E	5,081	0
	TOTALS:	2,266,697	100

Table 13 summarizes some information related to selected mixtures for this project. Mix ID in this table is taken from the mixture design sheets available in the ODOT database. More detailed descriptions of the aggregate combination and JMF of the selected mixtures are included in Appendix A.

Table 13 Selected Mixtures Information

Mix. Type	Mix ID	NMAS (mm)	%AC	%RAP
S3 PG 64-22	S3c00931100102	19	4.4	15
S4 PG 64-22	S4pv0261201600	12.5	4.8	25
S4 PG 70-28	S4qc0131304600	12.5	5.0	15
S4 PG 76-28	S4qc0131304900	12.5	4.9	15
S5 PG 76-28	S5qc0131402500	9.5	5.3	15

3.1.1. Mixture Fabrication Procedure

The following section describes the fabrication process adopted for all the mixtures investigated in this study.

3.1.1.1. RAP Handling

All mixtures selected for this project contain some RAP content. Fine RAPs used in these mixtures are provided from three different suppliers. For each type of RAP, two representative samples are burned in accordance to National Center for Asphalt Technology (NCAT) ignition method (*11*) to determine the percentage of recycled asphalt binder. The average value is then compared with the corresponding number in the job mix formula to determine the appropriate amount of additional binder necessary to achieve the optimal binder content.

In the mixtures containing RAP, it is important to heat up RAP materials enough to have a well-blended zone between RAP and virgin binders. Typically, there are two critical issues when working with RAP material during the heating process in the lab; heating time and temperature. The research team has reviewed different methods that are available for heating process of RAP material. Some researchers suggest preheating RAP at the target mixing temperature for a specific period of time before mixing with virgin aggregates. Others suggest superheat the virgin aggregate and mix the RAP in at room temperature. NCHRP report 452 recommends a preheating temperature of 110°C for RAP and the 10°C above mixing temperature for virgin aggregates (12). Kvasnak (*13*) investigated different approaches for handling RAP in the laboratory and recommended preheating the RAP material at the same target mixing temperature as virgin aggregate between 30 min and 3 hours depending on the RAP content. Typically, one target mixing temperature for both RAP and virgin is more practical. Zhou (*14*) also recommends a single temperature approach and a two-step preheating process as follows:

1. Warming up the RAP overnight (12-15 hours) at 60°C and;
2. Preheating the RAP material at the mixing target temperature for 2 hours which is often the required time for preheating the virgin binder.

For this project, the process recommended by Zhou (*14*) is used for handling RAP.

3.1.1.2. Sieving and Batching

For each mixture, aggregates are proportioned and combined according to the stockpile percentages available in the JMF. The combined aggregates are then sieved and the retained aggregates on each sieve size are stored individually. The washed sieve analysis are performed on two replicates of batched aggregates according to AASHTO T27-14 (*15*) in order to verify the gradation of combined aggregate and assure that it follows the JMF gradation. For each replicate, a total mass of 1,500 grams are batched from the combined sieved aggregates. Furthermore, an adjustment factor is made for batching from each size such that the final gradation of washed combined aggregate is the same as JMF. Table 14 shows the JMF for five selected mixtures.

Table 14 Combined Aggregate Gradation in JMF

Sieve Size	S3 64-22	S4 64-22	S4 70-28	S4 76-28	S5 76-28
3/4"	100	100	100	100	100
1/2"	90	98	94	93	100
3/8"	79	89	85	83	98
#4	57	67	65	64	52
#8	41	50	48	44	37
#16	28	36	35	31	26
#30	19	28	27	24	22
#50	12	20	18	16	18
#100	7	10	7	7	9
#200	5.1	5.6	3	3.7	5

3.1.1.3. Maximum Theoretical Specific Gravity

The maximum theoretical specific gravity, G_{mm}, is determined for mixtures in accordance with AASHTO T 209 (*16*). Two replicates are prepared for each mixture and the average values of G_{mm} are determined. The G_{mm} values of each mixture are summarized in Table 15.

Table 15 Maximum Theoretical Specific Gravity

Mix Type	S3 64-22	S4 64-22	S4 70-28	S4 76-28	S5 76-28
G_{mm}	2.470	2.499	2.463	2.513	2.496

3.1.1.4. Selection of a Target Air Void Percentage for Performance Test Specimens

The air voids of test specimens used in an experimental program must be a representative value of the HMA layers used in future construction. A literature review was conducted to search for field mixture densification data (*17*). This data helped the research team to identify an air void level that is both representative of the initial stage after the construction and appropriate for a successful specimen fabrication in the laboratory. The research team decided to adopt a target air void as it is shown in Table 16 for fabricating performance specimens for all mixtures throughout this project.

3.1.2. Sample Preparation

The required mass for each test specimen is calculated such that specimens achieve the target air void content specified for each test. Table 16 shows the specified target air void content for each test method as well as the number of replicates and dimension of test specimens. An estimate of the mixture's required mass is made using the G_{mm} and the volume of the gyratory specimens. The mass of mixture required for a gyratory specimen with target height, H, is calculated by using Equation (3). A trial gyratory

specimen is compacted to the target height and the test specimen is sawed and cored using the gyratory compacted specimen. The bulk specific gravity of the trial test specimen is measured and air void content of the trial specimen is calculated.

$$Mass = \left[\frac{100-(V_{at}+F)}{100}\right] \times G_{mm} \times 176.7147 \times H \quad (3)$$

where:

Mass = estimated mass of mixture to prepare a test specimen to the target air voids;
V_{at} = target air void content for the test specimen, percent by volume;
G_{mm} = maximum specific gravity of the mixture;
H = height of the gyratory specimen, cm; and
F = air void adjustment factor: 1.0 for fine-graded; 2 for coarse-graded.

An adjusted mass is estimated using Equation (4) if the air void content of the trial test specimen is not within the air void tolerance specified in Table 16. Using the adjusted mass, a second trial gyratory specimen is prepared and air void content of the second trial test specimen is calculated. Additional trial test specimens are prepared and the adjustment is made until the air void tolerance is satisfied.

$$Mass_{adj} = \left[\frac{(100-V_{at})}{(100-V_{am}}\right] \times Mass \quad (4)$$

where:

$Mass_{adj}$ = adjusted gyratory specimen mass, gram;
V_{at} = target air void content for the test specimen, percent by volume;
V_{am} = measured trial test specimen air void content, percent by volume; and
Mass = mass used to prepare the gyratory specimen for the trial test specimen, gram.

Table 16 Summary of Information Required for Performance Testing

Performance Test		Dynamic Modulus	Direct Tension Cyclic Fatigue	Indirect Tension Creep	Hamburg Wheel Tracking Device
Number of Replicates		3	5	4	4
Target air void (%)		7±0.5	7±0.5	7±0.5	7±1.0
Gyratory Compacted Specimen	**Diameter (mm)**	150	150	150	150
	Height (mm)	170	170	120	62
Test Specimen	**Diameter (mm)**	100	75	150	150
	Height (mm)	150	150	38	62

Using the optimal asphalt content and aggregate gradation presented in the JMF the cylindrical specimens were prepared and conditioned in accordance with AASHTO PP 60-13 (*18*) standard practice for the purpose of performance testing. Mixture bulk-specific gravity (G_{mb}) is measured before the material testing for all specimens in accordance with AASHTO T166-13 (*19*) to calculate the air void content and assure that air void content is within an acceptable range.

3. 2. MATERIAL CHARACTERIZATION TESTING

3.2.1. Dynamic Modulus (|*E**|) Testing

Dynamic modulus, |*E**|, is one of the key input data for the design of new pavements and rehabilitation practices in the Mechanistic-Empirical (M-E) Pavement design approach. The MEPDG (Mechanistic Empirical Pavement Design Guide) uses dynamic modulus as one of the primary material characterization parameters for pavement design. Also, it uses a hierarchical approach with three levels of materials characterization. The first level provides the highest design reliability and each succeeding level is a drop in the design reliability. The first or highest level entails the lab measured dynamic modulus of asphalt mixtures used in the pavement structure. The lab measured dynamic modulus is the absolute value of the complex modulus calculated by dividing the peak-to-peak stress by the peak-to-peak strain of a specimen subjected to a sinusoidal loading. The second and third levels of material characterization use predictive equations (*20*).

3.2.1.1. Preparation of Dynamic Modulus Test Specimen

Three replicates have been prepared in accordance with AASHTO PP 60-13 (*18*) using Superpave Gyratory compaction machine. The compacted specimens were prepared to a height of 170 mm and diameter of 150 mm. The mass required for each test specimens is calculated based on what was explained in the previous chapter. The SGC specimens were then cored and cut to diameter of 100 mm and height of 150 mm. Before testing, the G_{mb} values have been measured to determine the air void contents of specimens. Specimens with air void contents outside of the acceptable range of (AV%$\pm$0.5) have been discarded and replaced with new specimens having acceptable air void contents. Table 17 show the G_{mb} values and air void content of specimens tested for dynamic modulus.

Table 17 Bulk Specific Gravity, Air Void Content and Asphalt Binder Content of Specimens Used for Dynamic Modulus Test

Mixture Type	Replicate	G_{mb}	% Va	% AC
S3 64-22	1	2.287	7.4	4.4
	2	2.288	7.4	4.4
	3	2.308	6.6	4.4
S4 64-22	1	2.330	6.8	4.8
	2	2.338	6.5	4.8
	3	2.317	7.3	4.8
S4 70-28	1	2.294	6.8	5.5
	2	2.293	6.8	5.5
	3	2.279	7.4	5.5
S4 76-28	1	2.339	6.9	4.9
	2	2.332	7.2	4.9
	3	2.332	7.2	4.9
S5 76-28	1	2.334	6.6	5.3
	2	2.328	6.7	5.3
	3	2.330	6.6	5.3

3.2.1.2. Testing Procedure and Results

Brass buttons were attached to the specimens' surface 120 degree apart using a button gluing jig. Linear variable displacement transducers (LVDT) were instrumented on brackets attached to the brass buttons and the specimens are placed in the environmental chamber to reach to the testing temperature. The Asphalt Mixture Performance Tester (AMPT) was used for measuring the dynamic modulus of asphalt concrete samples. The compression dynamic modulus tests were performed at three different temperatures (4°, 20° and 40°C) and seven frequencies (25, 10, 5, 1, 0.5, 0.1 and 0.01 Hz). The testing started with the low to high temperatures and from high to low frequencies to minimize the amount of induced micro-damage to the specimens. The peak-to-peak strain level was within 75 to 125 micro-strains. All tests were performed in according to AASHTO TP79-13 (*21*). The calculation of dynamic modulus, phase angle, and the data quality indicator was performed automatically by the AMPT software. The testing measurements that met the criteria given in Table 18 were accepted; otherwise the dynamic modulus testing for each replicate was repeated to obtain the test data meeting the data quality statistic requirements.

Table 18 Data Quality Statistics Requirements

Data Quality Statistic	Limit
Load standard error	10%
Deformation standard error	10%
Deformation uniformity	30%
Phase uniformity	3 degree

The modulus of asphalt concrete is dependent on time, frequency of loading and temperature. Due to limitations of the machine capacity and testing time, dynamic modulus testing cannot be accomplished at full range of temperature and frequency. Therefore the use of time- temperature superposition concept reduces the required testing time. According to the time-temperature superposition principle, the same modulus value can be obtained either at low test temperature and long loading times or at high test temperature but short loading times. In fact, the time and temperature can be combined into a single parameter. This process can be performed by horizontally shifting the modulus values at different temperature to a certain reference temperature. The shifted frequency is called *reduced frequency*, f_R, which can be obtained by multiplying the original frequency by a shift factor as shown in Equation (5) and shift factors can be obtained by Equation (6). A single master-curve covering full range of temperature and frequency is developed and represented by a sigmoidal function as shown in Equation (7).

$$f_R = f \times a_T \tag{5}$$

where:

f = frequency in Hz; and
a_T = shift factor.

$$\log a_T = \alpha_1 T^2 + \alpha_2 T + \alpha_3 \tag{6}$$

where:
α_1, α_2, α_3 =fitting parameter; and
T = temperature.

$$\log\left|E^*\right| = a + \frac{b}{1+\frac{1}{e^{c+d\times \log f_R}}} \tag{7}$$

where:
a, b, c and d = fitting parameter; and
f_R = reduced frequency.

The modulus of HMA mixtures at all levels of temperature and frequency is determined from a master curve constructed at a reference temperature of 20°C. Using numerical optimization, the fitting parameters of Equations (5) and (6) were determined. The optimization was performed by using the Solver function in Microsoft Excel. This calculation is performed by a spreadsheet to compute the sum of the squared errors between the logarithm of the average measured dynamic modulus at each temperature/frequency combination and the values predicted by Equation (6). The solver function is used to minimize the sum of the squared errors by varying the fitting parameters in Equation (6).

Table 19 shows the final value of fitting parameters obtained by Solver for replicates of S3 PG 64-22, S4 PG 64-22, S4 PG 70-28, S4 PG 76-28, and S5 76-28. Dynamic modulus master-curves for all replicates of these mixtures are shown against the average result of them in Figure 22 through Figure 22 in logarithmic scale and Figure 23 through Figure 27 in logarithmic scale. Figure 28 and Figure 29 exhibit the average result of all replicates for different types of mixtures in one plot.

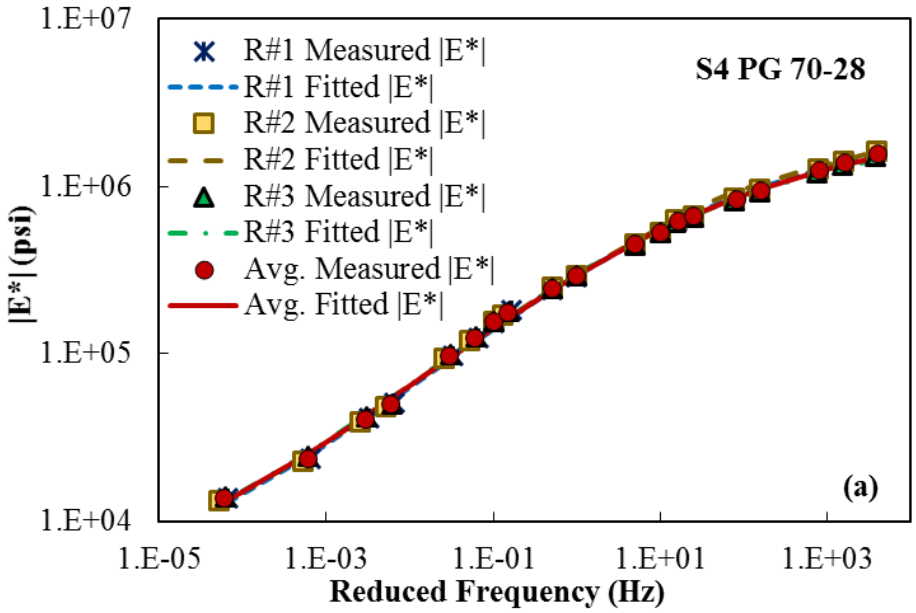

Figure 18 Dynamic Modulus Master-curve for S4 PG 70-28 Specimens in Logarithmic Scale

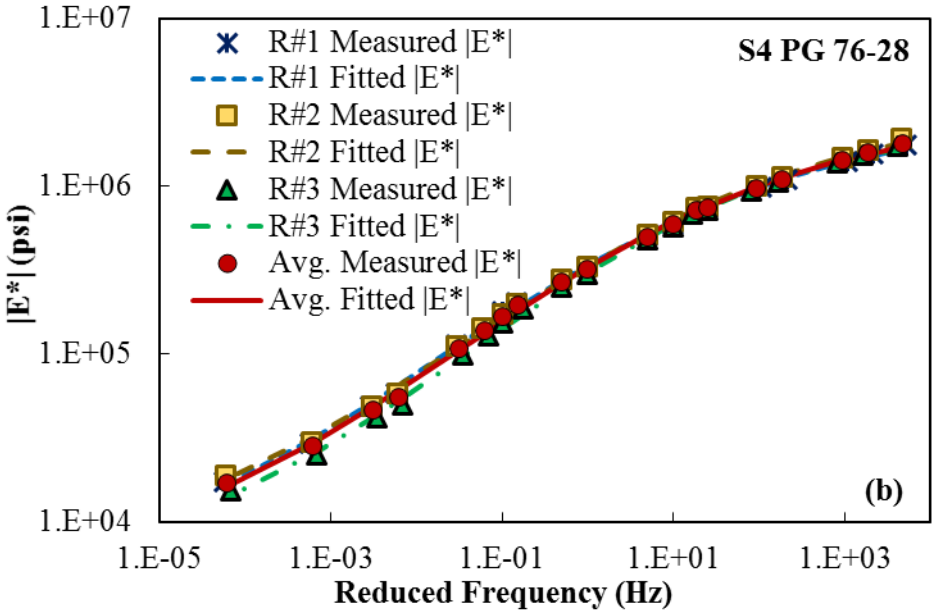

Figure 19 Dynamic Modulus Master-curve for S4 PG 76-28 Specimens in Logarithmic Scale

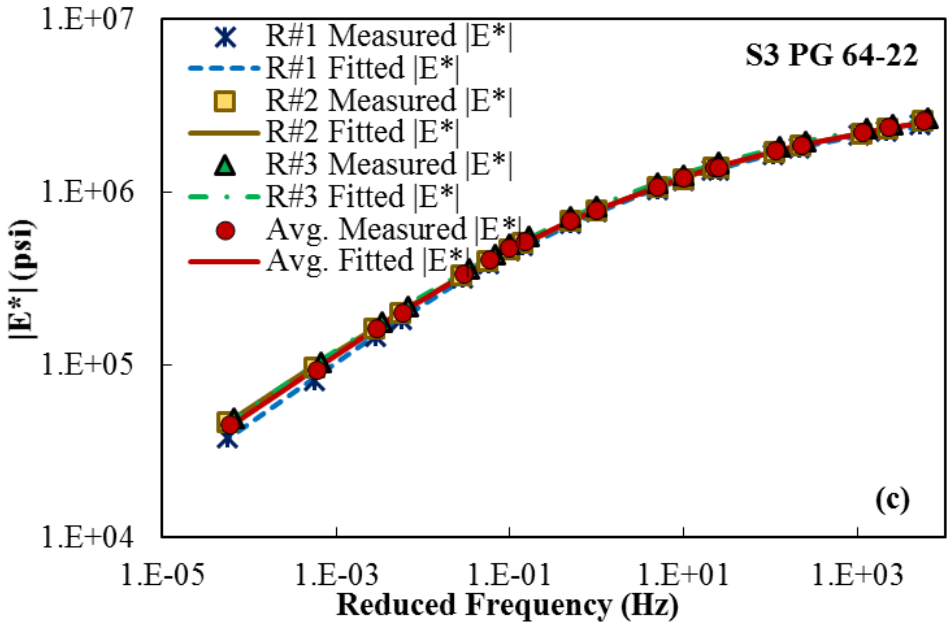

Figure 20 Dynamic Modulus Master-curve for S3 PG 64-22 Specimens in Logarithmic Scale

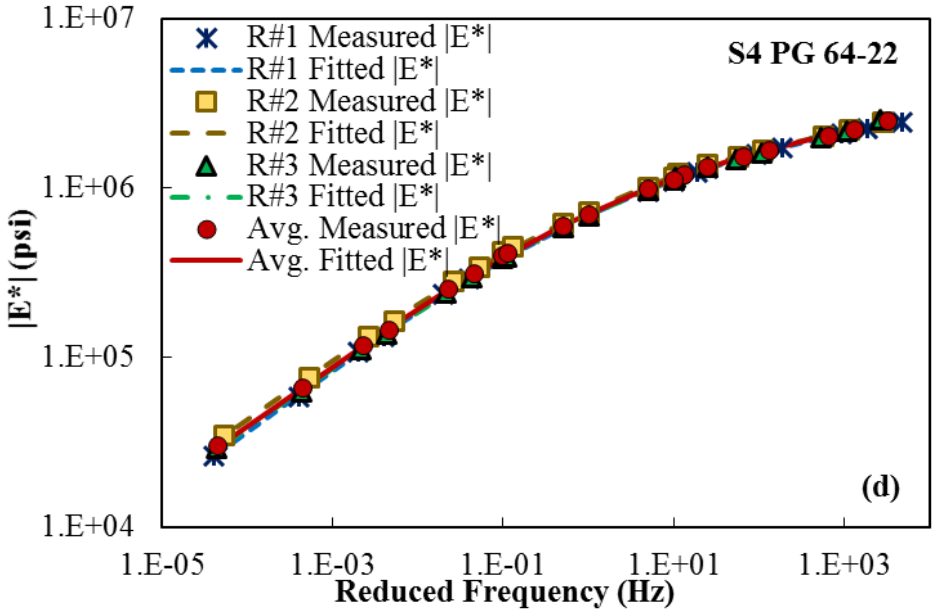

Figure 21 Dynamic Modulus Master-curve for S4 PG 64-22 Specimens in Logarithmic Scale

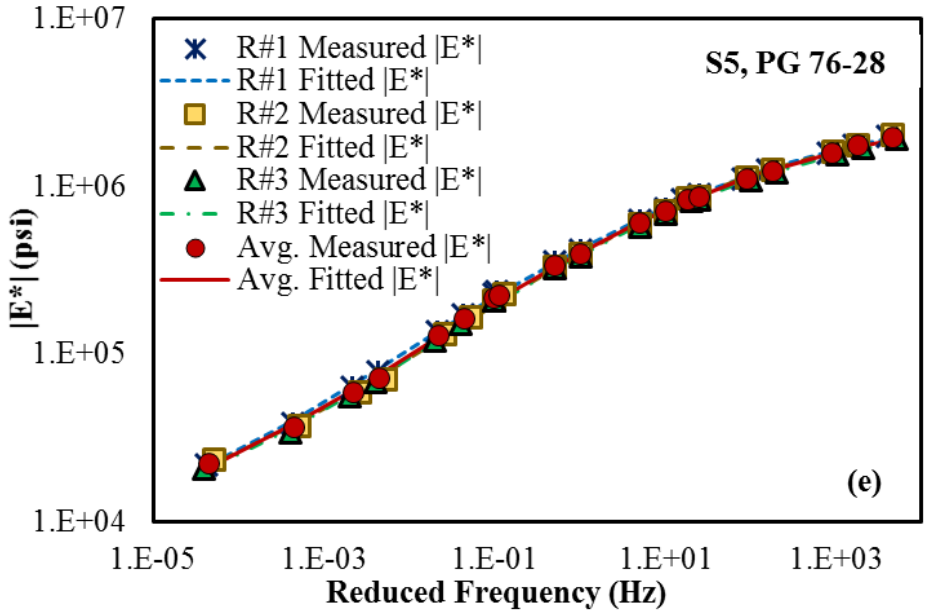

Figure 22 Dynamic Modulus Master-curve for S5 PG 76-28 Specimens in Logarithmic Scale

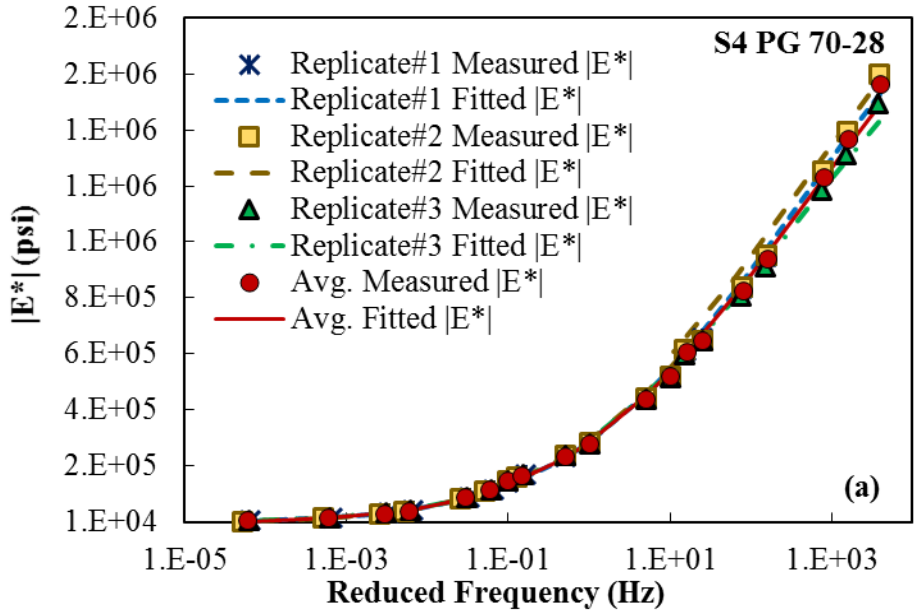

Figure 23 Dynamic Modulus Mastercurve for S4 PG 70-28 Specimens in Arithmetic Scale

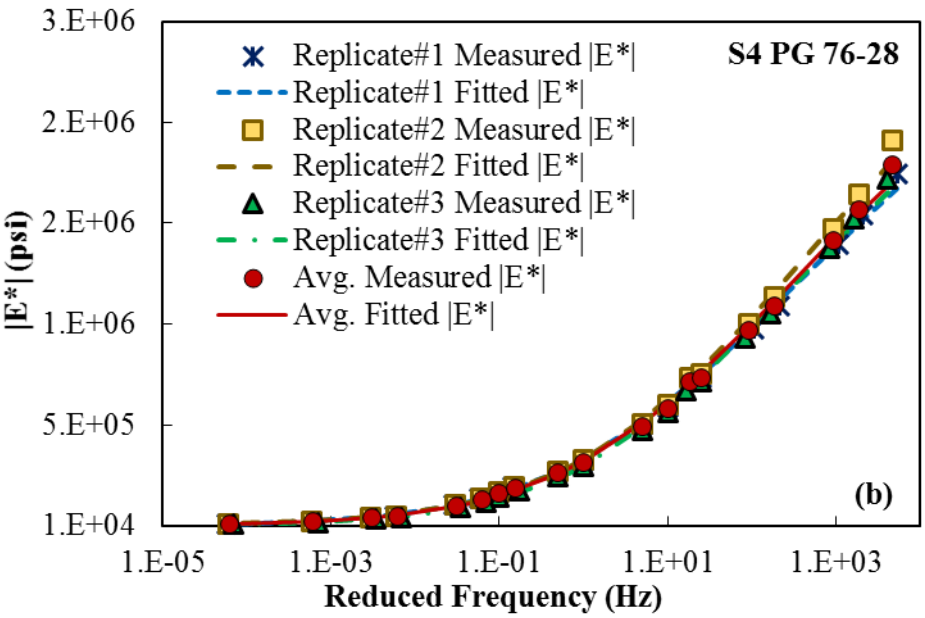

Figure 24 Dynamic Modulus Mastercurve for S4 PG 76-28 Specimens in Arithmetic Scale

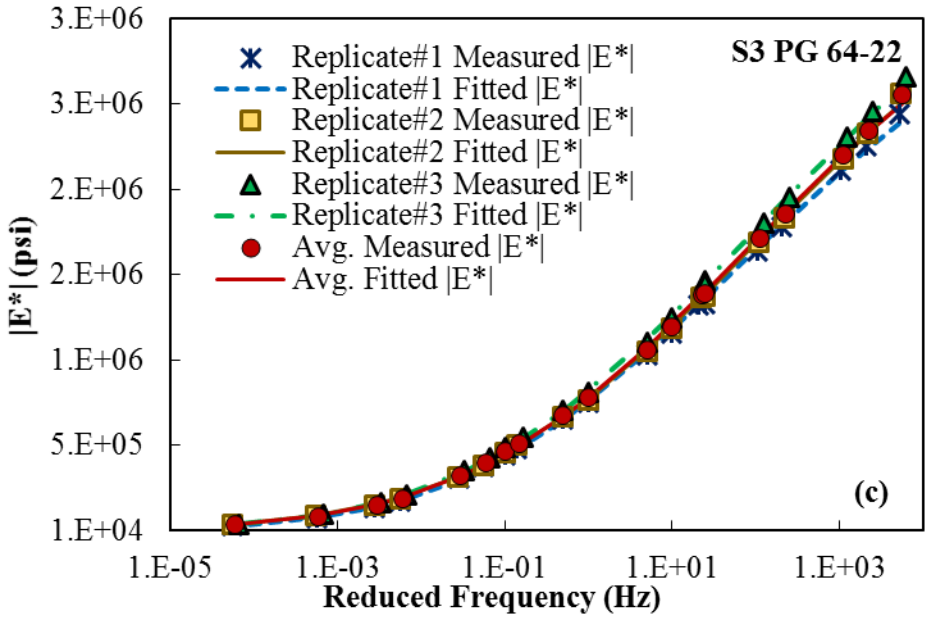

Figure 25 Dynamic Modulus Mastercurve for S3 PG 64-22 Specimens in Arithmetic Scale

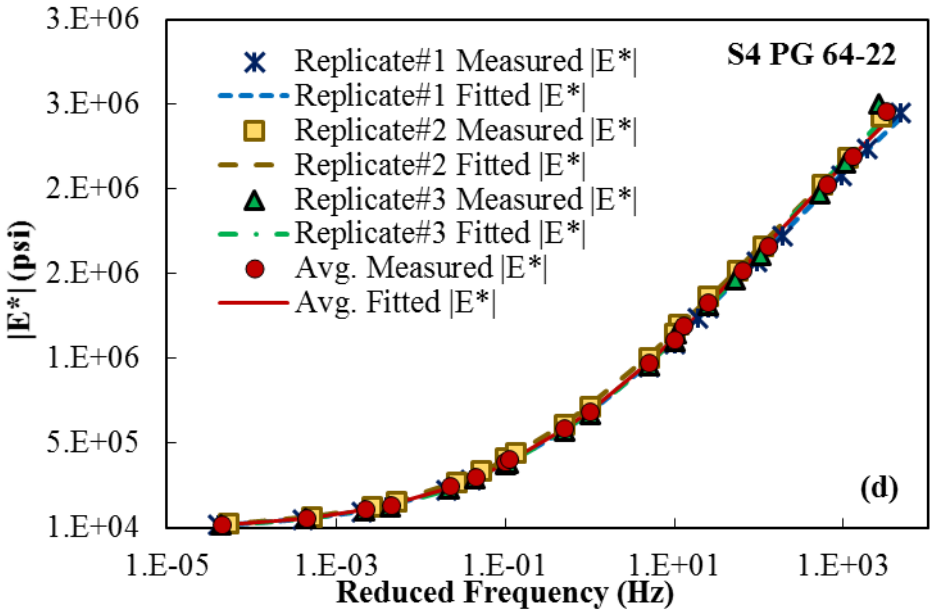

Figure 26 Dynamic Modulus Mastercurve for S4 PG 64-22 Specimens in Arithmetic Scale

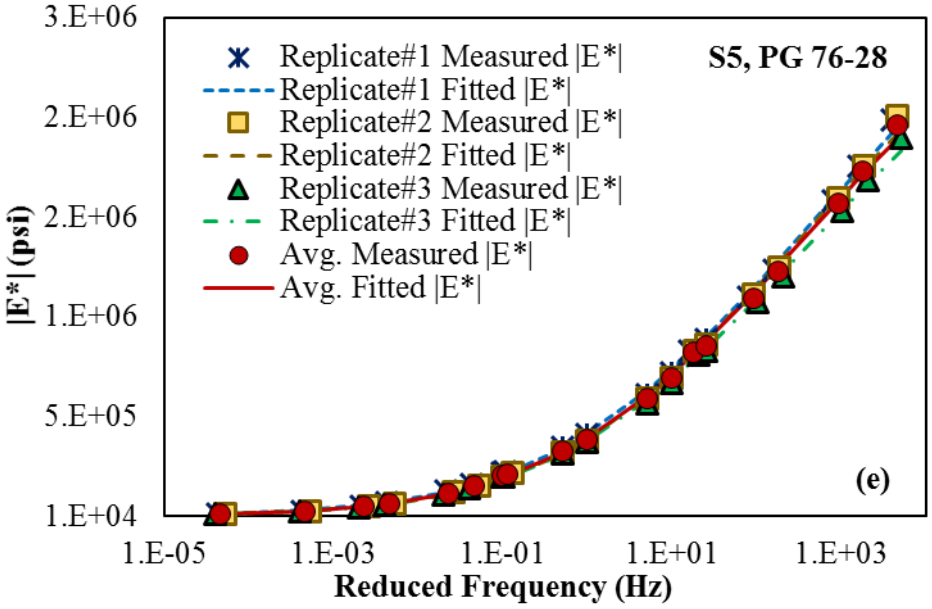

Figure 27 Dynamic Modulus Mastercurve for S5 PG 76-28 Specimens in Arithmetic Scale

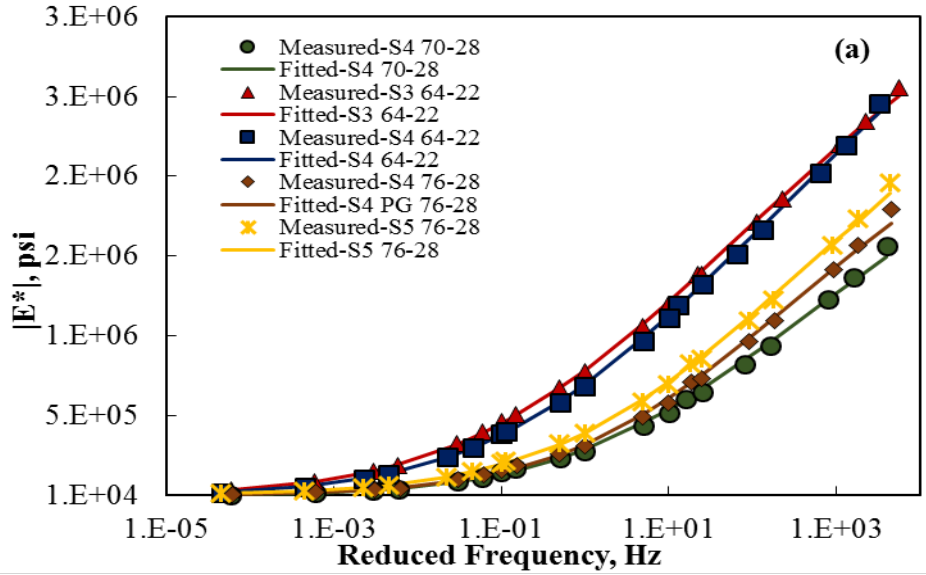

Figure 28 Average Dynamic Modulus Master-curves for Mixtures in Arithmetic Scale

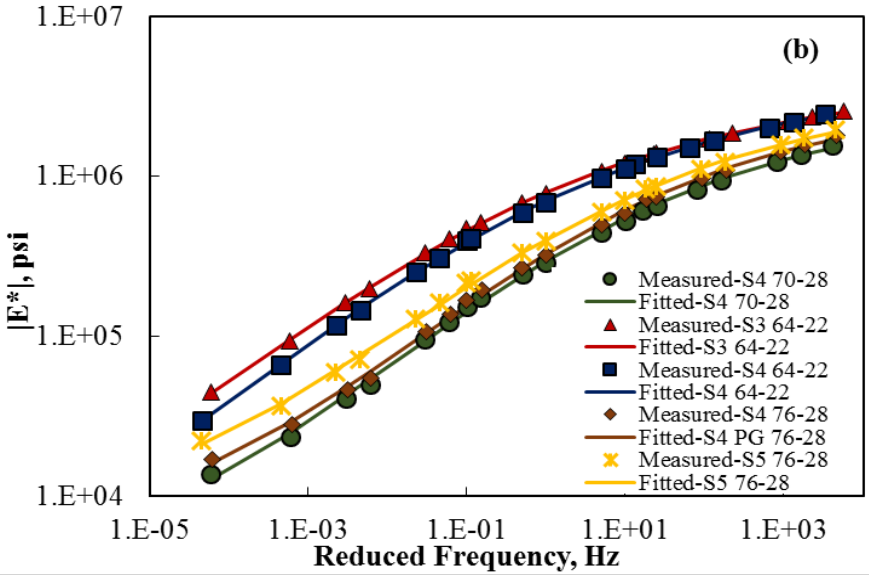

Figure 29 Average Dynamic Modulus Master-curves for Mixtures in Logarithmic Scale

Table 19 Optimized Value of Fitting Parameters

Mix. Type	Mix ID	Replicate	a	b	c	d	α_1	α_2	α_3
S3, PG 64-22	S3c00931100102	#1	0.72	3.69	1.48	0.39	9.09E-04	-0.17	2.97
		#2	0.85	3.60	1.38	0.36	9.41E-04	-0.17	3.01
		#3	0.88	3.58	1.42	0.38	1.15E-03	-0.18	3.09
		Avg.	0.82	3.62	1.43	0.38	1.00E-03	-0.71	3.03
S4, PG 64-22	S4pv0261201600	#1	0.56	3.89	1.39	0.38	6.18E-04	-0.16	2.89
		#2	0.78	3.67	1.36	0.37	4.01E-04	-1.38	2.6
		#3	0.66	3.83	1.31	0.37	2.30E-04	-0.13	2.55
		Avg.	0.69	3.78	1.35	0.38	4.20E-04	-0.14	2.68
S4, PG 70-28	S4qc0131304600	#1	1.17	3.12	0.78	0.45	7.70E-04	-0.16	2.80
		#2	1.16	3.13	0.79	0.44	6.23E-04	-0.15	2.78
		#3	1.20	3.04	0.83	0.46	7.15E-04	-0.15	2.78
		Avg.	1.15	3.12	0.81	0.44	7.44E-04	-0.16	2.82
S4, PG 76-28	S4qc0131304900	#1	1.36	2.93	0.78	0.46	9.36E-04	-0.17	2.98
		#2	1.47	2.88	0.66	0.46	8.47E-04	-0.16	2.90
		#3	1.44	2.83	0.69	0.51	8.51E-04	-0.16	2.84
		Avg.	1.43	2.87	0.71	0.48	8.76E-04	-0.16	2.91
S5, PG 76-28	S5qc0131402500	#1	1.33	3.06	0.83	0.42	5.37E-04	-0.15	2.8
		#2	1.62	2.72	0.70	0.47	7.60E-04	-0.16	2.9
		#3	1.48	2.85	0.76	0.45	6.76E-04	-0.16	2.9
		Avg.	1.49	2.87	0.76	0.45	6.59E-04	-0.16	2.9

A summary of specimens' dynamic modulus data is included in Appendix A.

3.2.1.3. Analysis of Dynamic Modulus Test Data

The result of dynamic modulus testing is used as level 1 input for MEPDG hierarchical approach for overlay design. As it can be seen in Figure 29, mixture S3 64-22 shows the highest dynamic modulus over the entire frequencies and the S4 PG 70-28 mixture shows the lowest value. Although no general trend is observed for ranking the mixtures in terms of the dynamic modulus value, it can be concluded that mixtures with larger NMAS containing high percentage of RAP and low binder content are in general stiffer than mixtures with smaller NMAS containing low RAP content and high binder content. Also, in case of having same NMAS and RAP percent, the mixture with stiffer binder and lower binder content has higher dynamic modulus value at some condition. The order of mixtures with decreasing dynamic modulus values are as follows: S3 PG 64-22, S4 PG 64-22, S5 PG 76-28, S4 PG 76-28 and S4 PG 70-28 respectively.

3.2.2. Hamburg Wheel-Track Testing

The Hamburg Wheel Tracking Test (HWTT) is a laboratory procedure that utilizes repetitive loading in the presence of water and measures the rut depth induced in an asphalt mixture with increasing load cycles. The test results are then processed to determine the asphalt mixture moisture susceptibility and rutting resistance.

3.2.2.1. Preparation of Hamburg Rut Test Specimen

Aggregate proportioning is done in accordance with the JMF. The aggregates and binder are conditioned at the mixing temperature provided in the mix design sheets of each mixture available through the ODOT database. Then mixtures are conditioned in accordance with short-term conditioning procedure in AASHTO R30 (*22*) and compacted by a Superpave Gyratory Compacter into 150-mm diameter and 62-mm height specimens. Four specimen replicates are fabricated for each mixture type. Mixture bulk-specific gravity (G_{mb}) is measured before material testing for all specimens in accordance with AASHTO T166-13 to calculate the air void content and assure that air void content is in an acceptable range. For laboratory-compacted specimens, the air void content should be 7.0 ± 1.0 percent. Bulk specific gravity, air void content and asphalt binder content specimens prepared for Hamburg test are summarized in Table 20.

Table 20 Bulk Specific Gravity, Air Void Content and Asphalt Binder Content of Specimens Used for Hamburg Tracking Test

Mixture Type	Replicate	G_{mb}	% Va	% AC
S3 64-22	1	2.263	8.3	4.4
	2	2.256	8.6	4.4
	3	2.252	8.6	4.4
	4	2.304	6.7	4.4
S4 64-22	1	2.316	7.3	4.8
	2	2.312	7.5	4.8
	3	2.315	7.3	4.8
	4	2.321	7.1	4.8
S4 70-28	1	2.262	8	5.5
	2	2.261	8	5.5
	3	2.262	8	5.5
	4	2.265	8	5.5
S4 76-28	1	2.341	6.8	4.9
	2	2.330	7.2	4.9
	3	2.310	8	4.9
	4	2.299	8	4.9
S5 76-28	1	2.308	7.5	5.3
	2	2.309	7.4	5.3
	3	2.307	7.5	5.3
	4	2.299	7.8	5.3

3.2.2.2. Testing Procedures and Results

Typically, two Superpave Gyratory Compacted cylindrical specimens with a diameter of 6.0 in (150 mm) and a thickness of 2.4 in (62 mm) are placed side-by-side, submerged in water at 122°F (50°C), and subjected to approximately 52 passes of a steel wheel per minute (AASHTO T324) (*23*). Each set of the specimens is loaded for a maximum of 20,000 load cycles or until the center of the specimen deforms 0.5 in (12.5 mm). For this project, four Superpave Gyratory compacted specimens have been prepared for each test.

During testing, rut depths at different positions along the specimens were recorded for each load cycle. The average rut depth of the 3 center measurements were then plotted and presented as the output of the test. Figure 30 through Figure 34 shows the result of Hamburg tests for all mixtures. In these figures, the results of all replicates are shown against the average curve. The Hamburg curves for the average of all replicates results are presented in Figure 35 in one plot. As shown in these figures, the resulting HWTT curves can be divided into the following three main phases: 1) post compaction phase, 2) creep phase, and 3) stripping phase. The post compaction phase is the deformation

measured at 1,000 passes, assuming that the wheel is densifying the mixture within the first 1,000 wheel passes. The creep slope is the number of repetitions or wheel passes to create a 1-mm rut depth due to viscous flow. The stripping phase starts once the bond between the asphalt binder and the aggregate starts degrading, causing visible damage such as stripping or raveling with additional load cycles. The stripping slope can be quantified as the number of passes required to create a 1-mm impression from stripping. The stripping inflection point is the number of passes at the intersection of the creep slope and the stripping slope. It represents the moisture damage resistance of the HMA and is assumed to be the initiation of stripping (*24*).

Table 21 shows the Hamburg rut test requirements adopted in Oklahoma Department of Transportation. The test results of the Hamburg Wheel Tracking test including the maximum impression at 20,000 cycles of loading, creep slope, strip slope and strip inflection point for all mixtures are summarized in Table 22. It can be seen that all mixtures meet the ODOT rut depth requirement.

Table 21 Oklahoma Hamburg Rut Test Requirements

Binder Grade	Minimum Number of Passes to 12.50 mm Rut Depth
PG 64	10,000
PG 70	15,000
PG 76	20,000

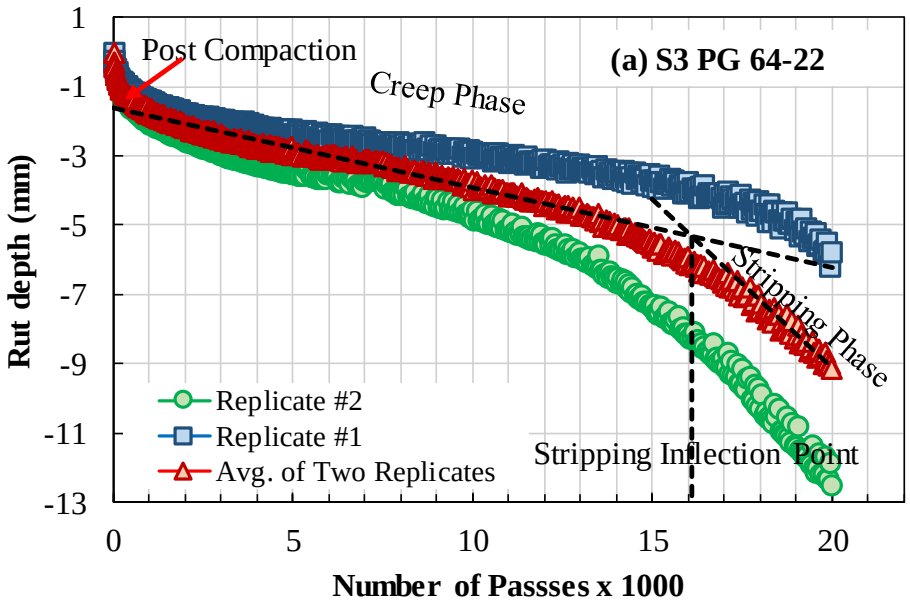

Figure 30 Hamburg Test Results for S3 PG 64-22 Mixture

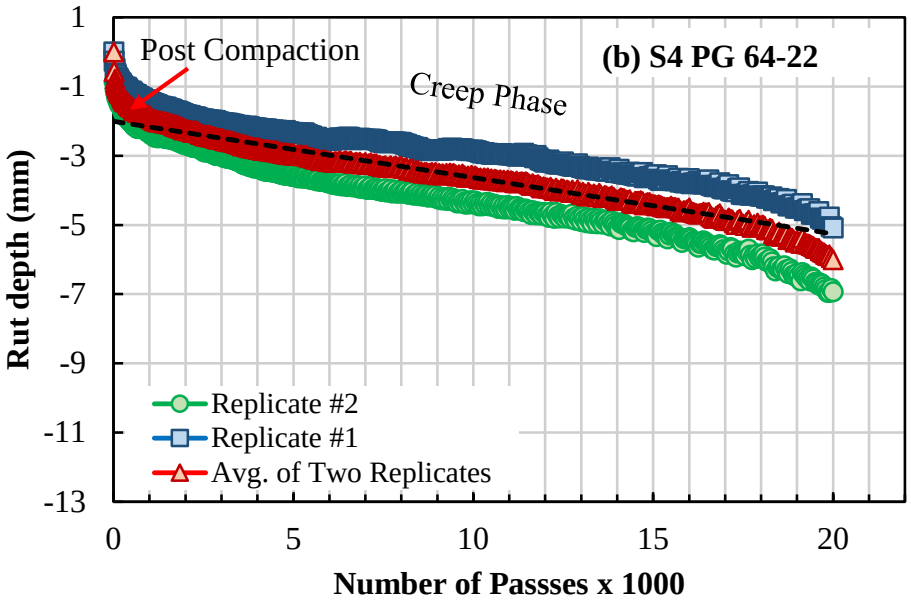

Figure 31 Hamburg Test Results for S4 PG 64-22 Mixture

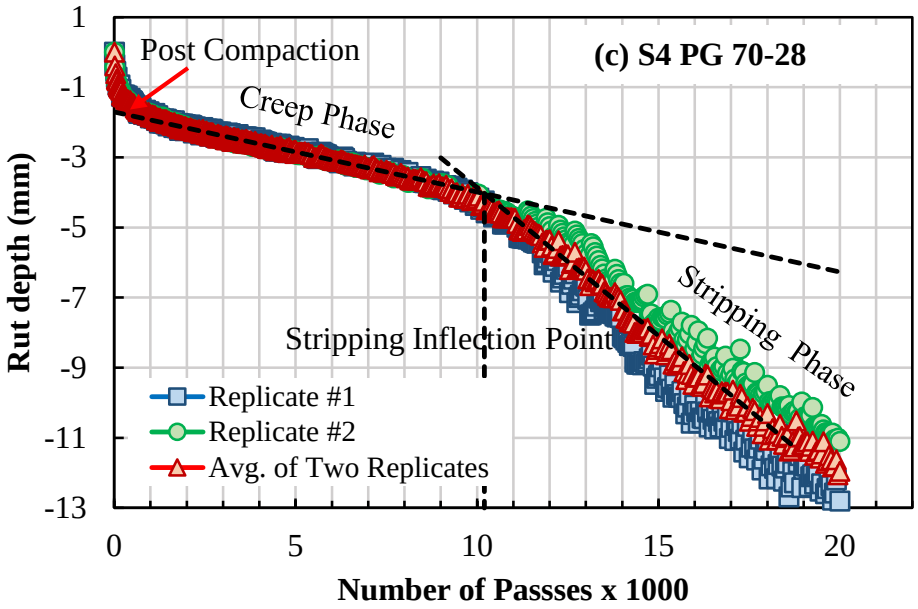

Figure 32 Hamburg Test Results for S4 PG 70-28 Mixture

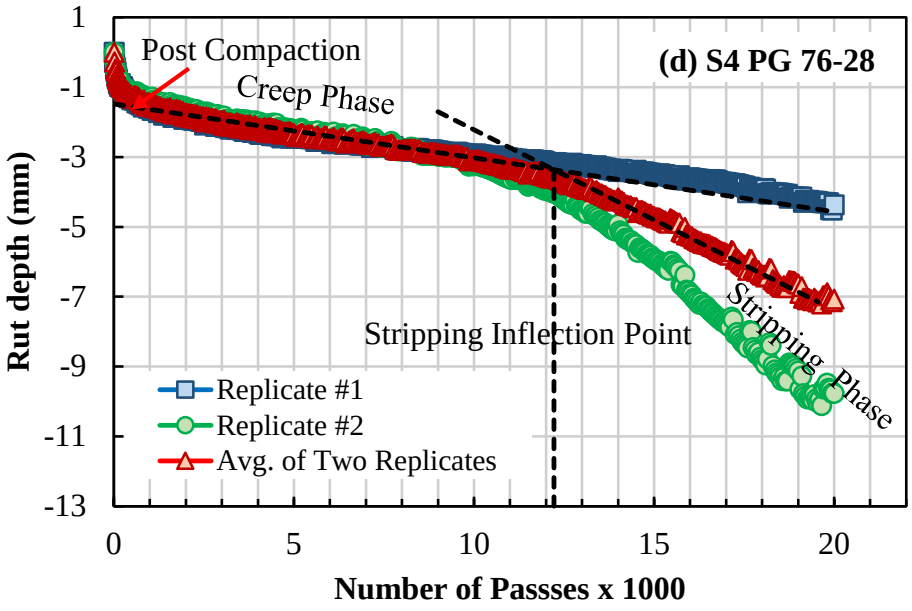

Figure 33 Hamburg Test Results for S4 PG 76-28 Mixtures

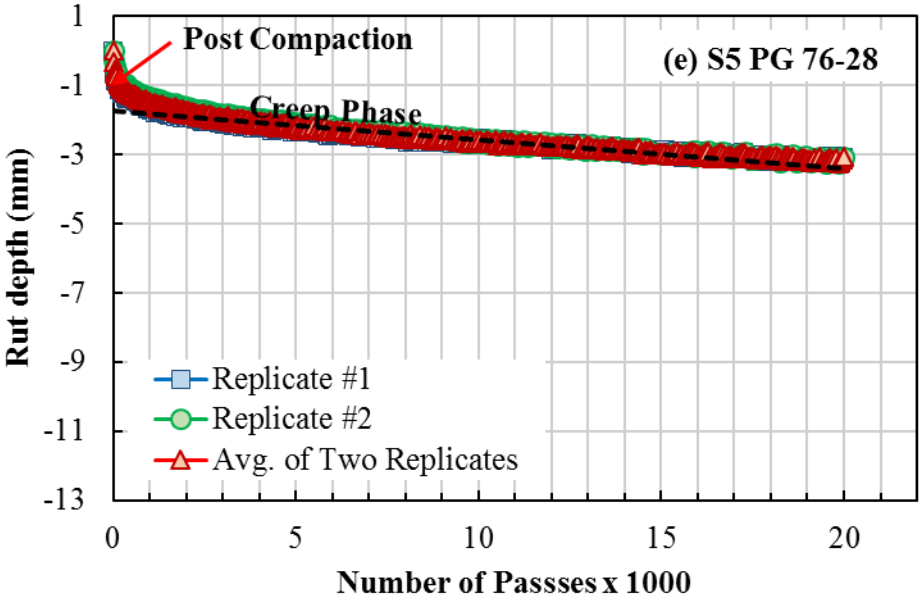

Figure 34 Hamburg Test Results for S5 PG 76-28 Mixtures

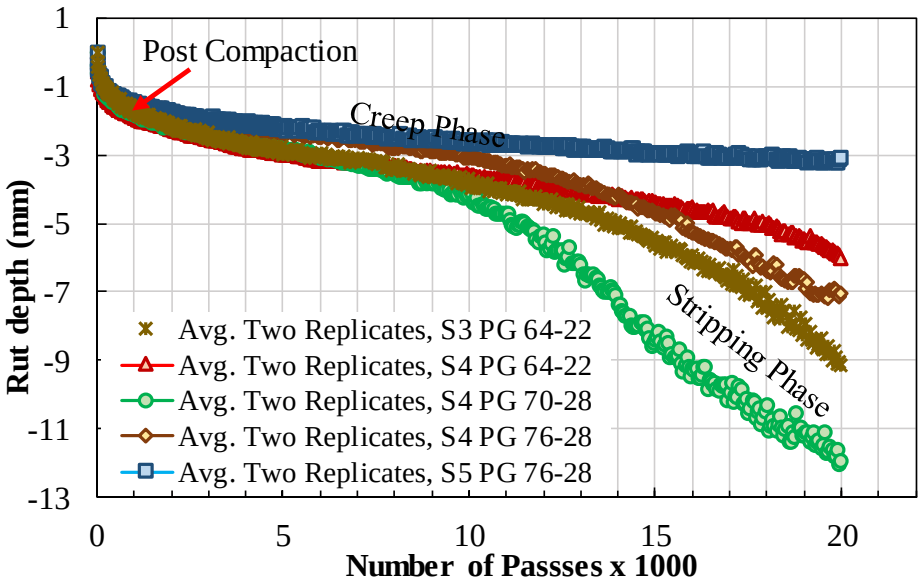

Figure 35 Hamburg Curve for the Average of Two Replicates for Tested Mixtures

Table 22 Summary of Hamburg Tracking Test

Mix ID	Binder Grade	Replicate	Maximum Impression @ 20,000 Cycles(mm)	Number of Passes to 12.5 mm Rut Depth	Creep Slope	Strip Slope	Strip. Inflection Point
S3c00931100102	PG 64	#1	6.2	> 20,000	7.69	1.38	17,460.00
		#2	12.52	20,000	3.70	0.90	13,950.00
		Average	9.15	> 20,000	4.35	1.02	16,120.00
S4pv0261201600	PG 64	#1	5.1	> 20,000	7.69	-	-
		#2	6.95	> 20,000	5.88	-	-
		Average	6	> 20,000	6.25	-	-
S4qc0131304600	PG 70	#1	13.08	18,600	4.75	1.01	9,950.00
		#2	11.1	> 20,000	4.92	1.26	11,170.00
		Average	12.05	> 20,000	4.39	1.18	10,200.00
S4qc0131304900	PG 76	#1	4.52	> 20,000	7.81	-	-
		#2	10.12	> 20,000	5.15	1.14	12,340.00
		Average	7.2	> 20,000	4.39	1.93	12,220.00
S5qc0131402500	PG 76	#1	3.24	> 20,000	12.76	-	-
		#2	3.24	> 20,000	9.95	-	-
		Average	3.24	> 20,000	12.18	-	-

3.2.2.3. Analysis of Hamburg Rut Test Data

Hamburg wheel Tracking Test results can be employed to rank mixtures used for rehabilitation projects with respect to their rutting and stripping resistance. Among five mixtures evaluated in this project, S5 PG 76-28 shows the highest rutting and stripping resistance and S4 PG 70-28 has the lowest resistance. The overall order of mixture performance in terms of decreasing rutting and stripping resistance is as follows: S5 PG 76-28, S4 PG 64-22, S4 PG 76-28, S3 64-22 and S4 PG 70-28. Therefore, S5 PG 76-28 shows the best rutting performance of those tested. According to obtained results in this study, fine dense graded aggregate mixed with high modified binder tend to have higher rutting resistance than coarse aggregate with unmodified binder. It should be noted that mineralogy and chemical composition of aggregates along with binder type, aggregate gradation, binder content, and RAP percentage are important contributing factors in characterizing stripping resistance of mixtures. However, this information is not available and thus a more complete discussion about the causes of rutting and stripping behavior of mixtures cannot be completed at this time.

3.2.3. Direct Tension Cyclic Fatigue Test

3.2.3.1. Preparation of Fatigue Test Specimens

Fatigue test specimens are first prepared by compacting asphalt concrete samples to a height of 180 mm and a diameter of 150 mm. Then, the specimens are cored and cut to a final testing geometry of 75 mm x 150 mm (d x h). After thoroughly drying, the specimens are measured for density using the AASHTO T 166 method. Afterwards, specimens are glued to steel end platens by using a gluing jig that ensured proper vertical alignment. Devcon 5 minute steel putty was used for the gluing. Once the end platen glue has cured, brass buttons are affixed to the specimen surface 90 degrees apart using another gluing jig. Brackets are attached to these buttons to instrument four sets of linear variable displacement transducers (LVDTs). MHR100 (± 0.1 in. or ±2.54 mm span) LVDTs are used for the testing with a gauge length of 100 mm. The fatigue sample gluing jig and sample set up inside the equipment are shown in Figure 36.

Figure 36 Uniaxial Fatigue Test Sample Gluing Process (left) and sample Setup inside Testing Chamber (right).

3.2.3.2. Testing Procedure and Results

After instrumentation, samples are placed into an IPC Global UTM 25 servo-hydraulic load frame temperature chamber and kept for conditioning inside at 18°C for approximately 6 hours. Once the sample reaches the proper test temperature the fatigue test is conducted by subjecting the specimens to a tension-compression mode of loading. Prior to the fatigue process a small magnitude (approximately 50 microstrain) sinusoidal load has been applied in order to measure the dynamic modulus of the specimen. This test is conducted at the same test temperature as the fatigue test and at a 10 Hz frequency and used to determine the |E*| of the test specimen in order to account for specimen to specimen variability. The fatigue tests are conducted using constant actuator controlled displacement at 18°C and a 10Hz frequency. During the testing, on specimen strain is measured using the four LVDTs. All five replicates from each mix are tested in the same procedure, but at different strain levels. The initial strain levels are selected to target fatigue lives of 10,000, 25,000, 50,000 and 100,000 cycles.

During the fatigue test the modulus and viscoelastic phase angle are tracked. Typical results from the axial fatigue test are shown in terms of apparent dynamic modulus and phase angle as a function of cycle number in Figure 37. The apparent dynamic modulus is calculated in the same way as the standard dynamic modulus, by taking the ratio of stress amplitude to strain amplitude, but is referred to as apparent to differentiate it from the non-damaged modulus. Following standard practice with the axial fatigue test, the failure cycle in these experiments is defined as the cycle when the viscoelastic phase angle shows a consistently decreasing trend (*25*, *26*).

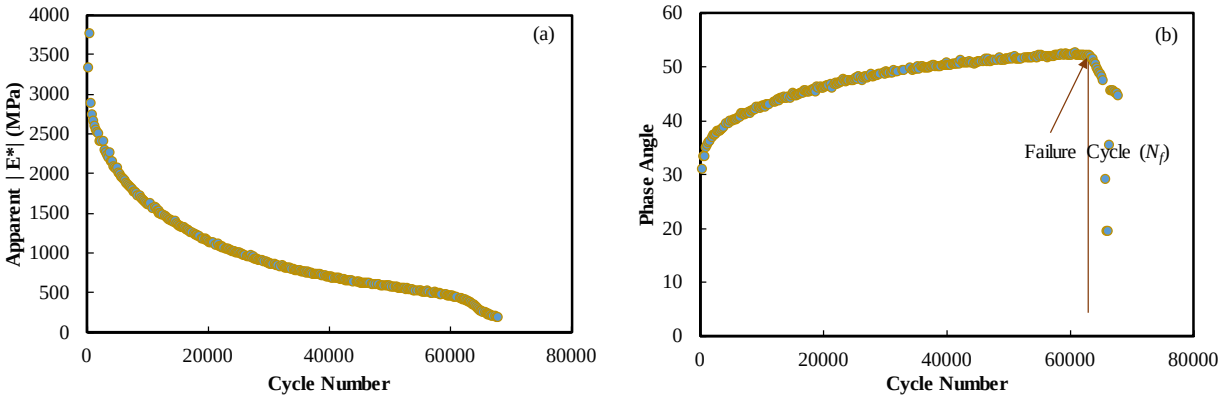

(a) **(b)**

Figure 37 Typical Cycle-Wise Test Results from The Axial Fatigue Test (a) Apparent Dynamic Modulus and (b) Phase Angle.

Fatigue test data results of each replicate at different strain levels from each asphalt concrete mixture were plotted together. Figure 38 shows the experimental fatigue life plots for all five asphalt concrete test samples at a test temperature of 18°C. Figure 67 in Appendix C presents the failure cycle and initial strain results from each experiment individually. Based on this data it appears that the S5 PG 76-28 mixture and S4 PG 76-28 show the best performance followed next by S4 PG 70-28, and finally by S4 PG 64-

22 and S3 PG 64-22. These results are somewhat expected given the stiffness of the different mixtures relative to one another, the RAP content, asphalt content, and presence of polymer modification.

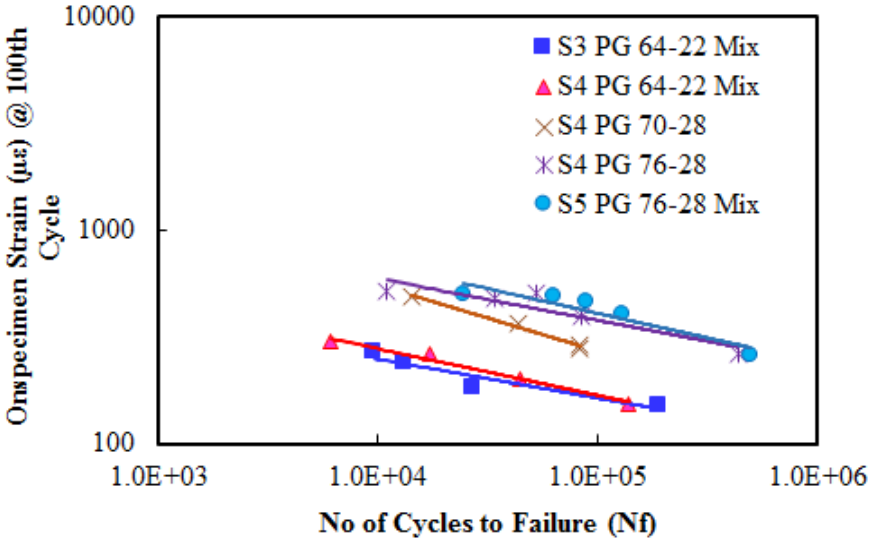

Figure 38 Experimental Fatigue Lives Plot for All Five Mixtures.

3.2.3.3. Analysis of Fatigue Test Data

The raw performance results from the fatigue test are only partly useful as the on-specimen strain amplitudes vary throughout the testing, which complicates interpretation. To overcome this limitation the fatigue test data was analyzed using simplified viscoelastic continuum damage theory (S-VECD). The S-VECD formulation and its functionality are explained in great detail in the literature (*26*, *27*, *28*, *29*, *30*, *31*) but in short some of model equations are described below.

1. the pseudo strain (ε^R) function in time and steady-state frequency domains;

$$\varepsilon^R = \frac{1}{E_R}\int_0^t E(t-\tau)\frac{d\varepsilon}{d\tau}d\tau$$
$$\varepsilon_0^R = \frac{1}{E_R}\left(|E^*| \times \varepsilon_0\right) \quad (8)$$

2. the pseudo strain energy density function, W^R,

$$W^R = \frac{1}{2}\left(\varepsilon^R\right)^2 C \quad (9)$$

3. the stress, σ, to ε^R relationship,

$$\sigma = \frac{dW^R}{d\varepsilon^R} = C \times \varepsilon^R \quad (10)$$

4. the damage evolution law with respect to time and cycles,

$$\left\{\begin{array}{l} \dfrac{dS}{dt} = \left(-\dfrac{\partial W^R}{\partial S}\right)^{\alpha} = \left(-\dfrac{1}{2}\left(\varepsilon^R\right)^2 \dfrac{dC}{dS}\right)^{\alpha} \\ \dfrac{dS}{dN} = \left(-\dfrac{\partial W^R}{\partial S}\right)^{\alpha} = \left(-\dfrac{1}{2}\left(\varepsilon_0^R\right)^2 \dfrac{dC}{dS}\right)^{\alpha} \dfrac{1}{f} K1 \end{array}\right\} \quad (11)$$

where;

$E(t)$ = LVE relaxation modulus,
τ = integration term,
t = time,
E_R = reference modulus (taken as 1),
α = damage evolution rate,
C = pseudo stiffness (material integrity),
S = damage, and
K_1 = loading shape factor.

As observed in the equations above, the primary functional relationship in the S-VECD model is the damage characteristic curve, or C-S curve. This function represents a fundamental relationship between the amount of damage in a material and its impact on the material integrity (S represents the damage and C represents the material integrity). From S-VECD analysis, damage characteristic curves (C-S) are developed for each replicate until failure at a test temperature of 18°C. Irrespective of strain levels these curves collapse together for all five replicates of each asphalt concrete mixes which is shown in Appendix C. One replicate from S3 PG 64-22 asphalt concrete mixture is discarded from the analysis due to measured high air void content. C-S replicate curves data from each mix is fitted to power function given in the Equation (12) below.

$$C = 1 - aS^b \quad (12)$$

The model fit parameters *a* and *b* for all five asphalt concrete mixes are given in the Table 23 below. Each mix replicates collapse and model fit graphs are shown in Appendix D**.** These curves are collapsing together from each mix and model fit is also corroborating with the C-S curves replicate data very well.

Table 23 C-S Curve Model Fit Parameters for Five Mixtures

Mixture Type	*a*	*b*
S3 PG 64-22	0.0006	0.5886
S4 PG 64-22	0.0016	0.5133
S4 PG 70-28	0.0121	0.3684
S4 PG 76-28	0.0233	0.2994
S5 PG 76-28	0.0167	0.3204

Figure 39 below shows the C-S curves model fit for all five asphalt concrete mixtures together. It was observed that the S3_64-22 and S4_64-22 mixture damage curves are positioned higher and fail much quicker than the other three mixtures. It is clearly seen that S5 and S4_76-28 mixtures sustain higher damage than the other three mixtures.

The average terminal C value for S3_64-22 mix is 0.553, S4_64-22 mix is 0.508, S4_70-28 mix is 0.253, S4_76-28 mix is 0.144 and S5 _76-28 mix is 0.161.

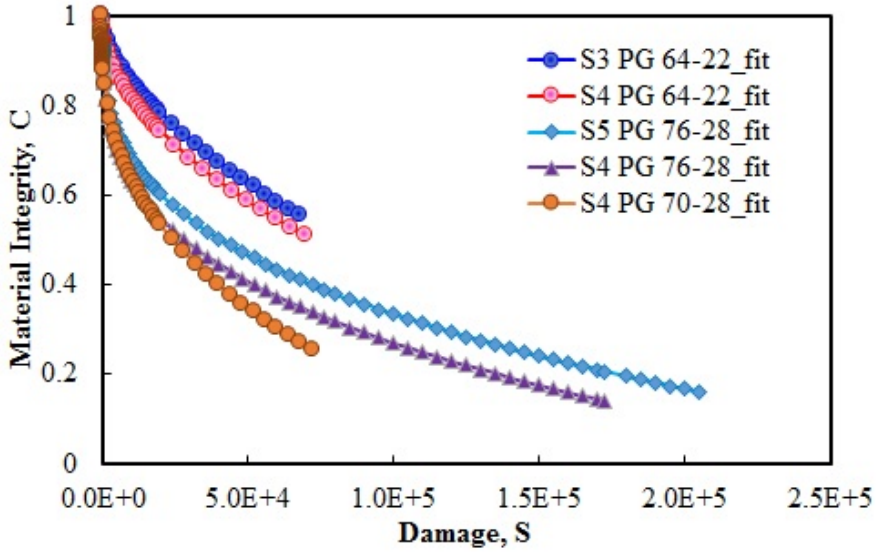

Figure 39 C-S Model Fit Curves for S3 and S4 Asphalt Concrete Mixtures

Damage curves alone are not sufficient to understand and predict the fatigue life of an asphalt concrete mixture. The damage curves and |*E**| of a mixture should be considered to evaluate the fatigue life of asphalt concrete mixtures. In order to gain additional information on fatigue performance, fatigue life of all mixtures is predicted using simulation predictive technique at test conditions. S-VECD theory is used to derive formulas for predicting the material response to fully reversed constant strain loadings. Figure 40 shows the simulated fatigue life of all asphalt concrete mixtures. The simulated fatigue life plot depicts that S4 PG 76-28 mixture have highest fatigue life and S3 PG 64-22 have least fatigue life of all tested mixtures in this study. Similar observations were also made from the experimental data; however, comparing Figure 38 to Figure 40 shows a better and more distinct separation of the material properties from the model predictions.

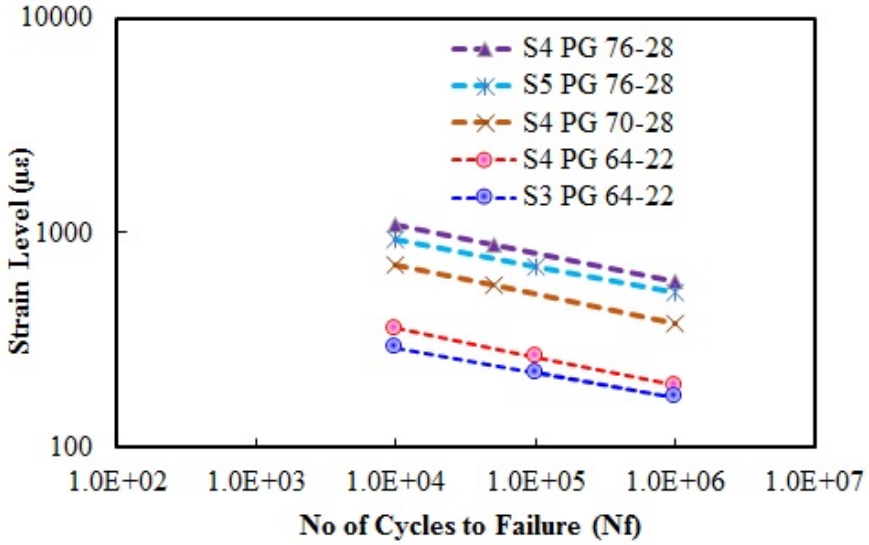

Figure 40 Fatigue Lives Plots for All Five Mixtures Using Simulated Data

3.2.4. Indirect Tension (IDT) Creep Compliance and Strength Test

Creep compliance, *D*(*t*), is a fundamental property of AC materials that explains the relationship between the time dependent strain and applied stress in viscoelastic materials. Determination of *D*(*t*) for AC materials is important as it is needed (in addition to the tensile strength) to evaluate the thermal and load induced cracking in AC pavements. Static creep test using the Superpave indirect tensile test is used to determine *D*(*t*) across multiple temperatures and times of loading, which is then used as input to the MEPDG to predict thermal cracking performance of AC pavements.

3.2.4.1. Preparation of IDT Test Specimens

To prepare IDT samples, two samples are compacted in the Superpave Gyratory compactor to a height of 120 mm and a diameter of 150 mm. Each of these samples is then cut into two IDT specimens with 38 mm thickness and 150 mm diameter. These specimens were cut from the center of the plug to achieve uniform air voids. After cutting, the specimens are dried in front of a fan for two days and the density is measured according to the AASHTO T166 procedure. Table 24 below contains the measured air voids of AC IDT samples, and shows that the samples are consistent with respect to air void content.

Table 24 Air Voids of IDT Test Specimens

Mix	Sample ID	Air Voids %	Mix	Sample ID	Air Voids %
S3 64-22	S3 64-22 1T	7.6	S4 76-28	S4 76-28 2T	7.3
	S3 64-22 1B	6.8		S4 76-28 2B	7.4
	S3 64-22 2T	7.3		S4 76-28 1T	7.6
	S3 64-22 2B	7.1		S4 76-28 1B	7
S4 64-22	S4 64-22 1T	7.6	S5 76-28	S5 76-28 1T	7.7
	S4 64-22 1B	7.1		S5 76-28 1B	7.8
	S4 64-22 2T	6.9		S5 76-28 2T	7.8
	S4 64-22 2B	6.3		S5 76-28 2B	7.6
S4 70-28	S4 70-28 1T	7.6			
	S4 70-28 1B	7.3			
	S4 70-28 2T	7.1			
	S4 70-28 2B	6.9			

Prior to testing, four brass buttons (2 in the horizontal direction and 2 in the vertical direction) are affixed on the front and back faces of each IDT specimen using Devcon 5 minute steel putty and a gluing plate that aligns the buttons properly. The buttons are set to a 50 mm gauge length. XS-B series LVDTs are then mounted in horizontal and vertical direction on both faces of the sample using brackets. These LVDTs are calibrated and connected to the external data acquisition system to record raw data of test. Once the sample is fully instrumented, it is installed in the creep compliance test fixture and kept inside the testing chamber for temperature conditioning. Thermocouples are installed on the surface and in the core of a separate dummy sample to monitor the temperature. Overall, six to eight hours of conditioning time is required to achieve temperature equilibrium. The test setup with fixture and magnified view of sample with LVDTs instrumentation is shown in Figure 41.

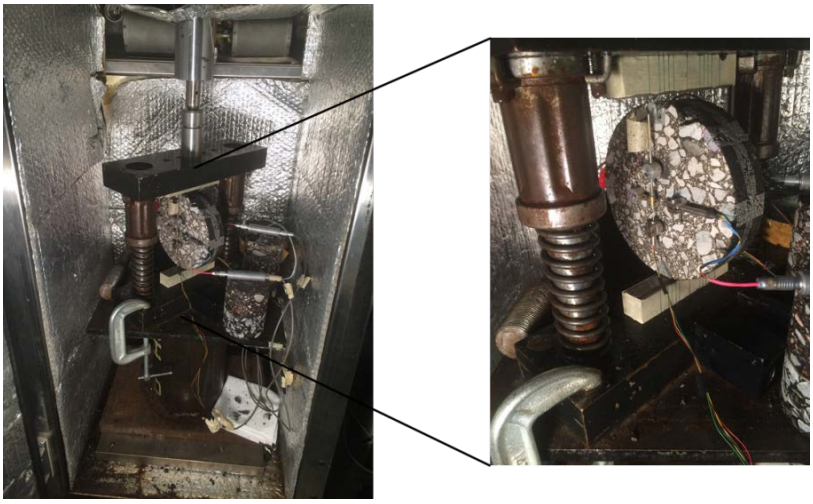

Figure 41 Creep Compliance Test Setup with Fixture inside the Testing Chamber (To right: Magnified View of Sample with LVDTS).

3.2.4.2. Testing Procedures and Results

After instrumentation, the sample is installed in the test fixture and kept inside the testing chamber for temperature conditioning to approximately -20°C. Once thermal equilibrium is reached, a creep load was applied for 100 seconds to produce a horizontal deformation of between 0.00125 to 0.0190 mm (25 to 380 με). At the completion of the creep loading at the -20°C, the temperature was adjusted and the process of thermal equilibrium and testing repeated at other two temperatures (-10 and 0°C). The same procedure was followed to test three replicates from all five asphalt concrete mixtures.

After the creep compliance test was completed at 0°C, the on-specimen LVDTs were removed and the samples were again conditioned to -10°C in order to determine the indirect tensile strength. The test was performed by applying a constant 12.5 mm/min vertical actuator displacement until the load began to decrease.

3.2.4.3. Analysis of IDT Test Data

IDT Creep Compliance

The test data at each temperature was analyzed to calculate the creep compliance using the calculation procedure described in AASHTO T-322 (*32*). The process described below and is based on experimental measurement of horizontal and vertical displacements ($\Delta X_{i,t}$ and $\Delta Y_{i,t}$) along with the applied load, P_n.

1. The average diameter (D_{Avg}), thickness (b_{Avg}) and creep load (P_{Avg}) for replicates are recorded.
2. The normalized horizontal and vertical deformations for each of the faces (two faces per replicate) are computed using Equation (13) and Equation (14).

$$\Delta X_{n,i,t} = \Delta X_{i,t} \times \frac{b_n}{b_{Avg}} \times \frac{D_n}{D_{Avg}} \times \frac{P_{Avg}}{P_n} \quad (13)$$

$$\Delta Y_{n,i,t} = \Delta Y_{i,t} \times \frac{b_n}{b_{Avg}} \times \frac{D_n}{D_{Avg}} \times \frac{P_{Avg}}{P_n} \quad (14)$$

where;

$\Delta X_{n,i,t}$ = normalized horizontal deformation for face *i* at time *t*,
$\Delta Y_{n,i,t}$ = normalized vertical deformation for face *i* at time *t*, and
b_n, D_n, P_n = thickness, diameter and creep load of replicate *n*.

3. The average normalized horizontal and vertical deformations at a time corresponding to half of the total creep time (*t*=50s) was extracted for all the replicate faces and ranked in ascending order.
4. The trimmed mean of horizontal (ΔX_t) and vertical (ΔY_t) deformations are calculated by eliminating lowest and highest measured horizontal and vertical deformations from all of the replicate faces using the Equation (15) and Equation (16).

$$\Delta X_t = \frac{\sum_{j=2}^{2n-1} \Delta X_{r,j}}{2n-2} \quad (15)$$

$$\Delta Y_t = \frac{\sum_{j=2}^{2n-1} \Delta Y_{r,j}}{2n-2} \quad (16)$$

where;
$\Delta X_{r,j}$ = $\Delta X_{n,i,t=50s}$ values sorted in ascending order and
$\Delta Y_{r,j}$ = $\Delta Y_{n,i,t=50s}$ values sorted in ascending order.

5. The ratio of horizontal and vertical deformation at *t*=50s is calculated using Equation (17).

$$\frac{X}{Y} = \frac{\Delta X_t}{\Delta Y_t} \quad (17)$$

6. The trimmed mean of horizontal deformation at time *t* is calculated using Equation (18).

$$\Delta X_{tm,t} = \frac{\sum_{j=2}^{2n-1} \Delta X_{r,j,t}}{2n-2} \quad (18)$$

where;
$\Delta X_{tm,t}$ = trimmed mean of horizontal deformation at time *t* and
$\Delta X_{r,j,t}$ = measured horizontal deformation at time *t*.

7. The creep compliance is calculated at time *t* using Equation (19) and Equation (20).

$$D(t) = \frac{\Delta X_{tm,t} \times D_{Avg} \times b_{Avg}}{P_{Avg} \times GL} \times C_{cmpl} \quad (19)$$

where;

D(t) = creep compliance at time *t* and
GL = gauge length in meters (50×10^{-3} m).

$$C_{cmpl} = 0.6354 \times \left(\frac{X}{Y}\right)^{-1} - 0.332 \quad (20)$$

Creep compliance test data at each temperature is then shifted to create a creep compliance mastercurve by using the shift factor function in Equation (21) along with the compliance function in Equation (22). D_0, D_1, E_a and n are determined via curve fitting the experimental data using the Excel solver optimization procedure. Figure 42 provides an example of shifted and unshifted data to demonstrate the outcomes. It should be noted that since the loading ramp occurs over a period of approximately 0.2 seconds,

the data for the first two seconds of the creep test are not included in the mastercurve analysis.

$$\log(a_T) = \frac{E_a}{2.303R}\left(\frac{1}{T} - \frac{1}{T_0}\right) \quad (21)$$

$$D(t) = D_0 + D_1 t_R^n \quad (22)$$

where;

E_a = activation energy (J/mol),
R = Universal gas constant (8.314 J/mol K),
T = temperature (Kelvin),
T_0 = reference temperature (Kelvin),
t_R = reduced time (s),
D_0 = elastic compliance (1/MPa),
D_1 = viscous compliance variable (1/MPa), and
n = log-log slope of the creep compliance curve.

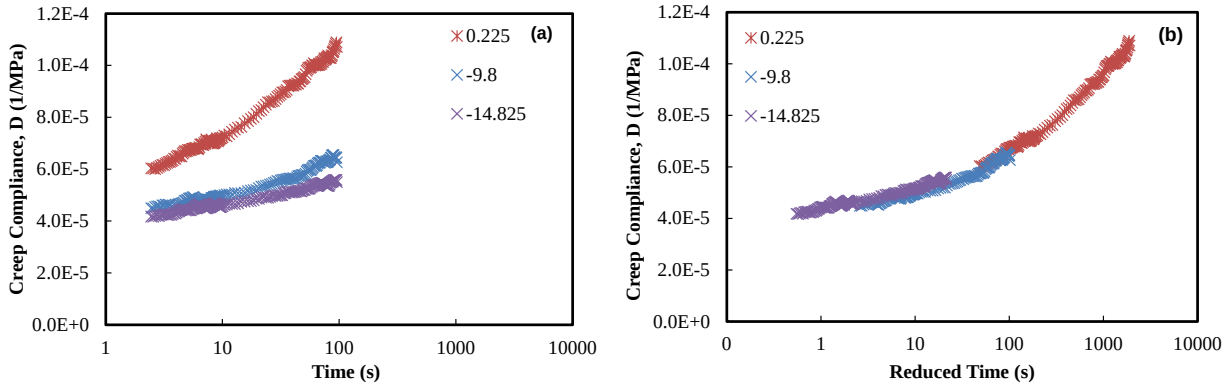

(a) **(b)**

Figure 42 Creep Compliance Test Data (a) before Shifting (b) after Shifting.

IDT Strength Test

The primary test parameter of interest in the IDT strength test is the tensile strength, which is calculated by using Equation (23).

$$S_t = \frac{2P_f}{\pi b D} \quad (23)$$

where;

S_t = tensile strength of AC sample (kPa),
P_f = peak load (kN),
b = thickness of sample (m), and
D = diameter of sample (m).

Figure 43 shows the average creep compliance master curves for all five asphalt concrete mixtures, while the replicate data and coefficient of variation for all five mixtures are shown in Appendix D. Average creep compliance master curves of all five

mixtures plotted together for possible comparisons. From the modulus test results it was observed that S3 64-22 mix (19 mm NMSA) is stiffest and S4 70-28 mix (12.5 mm NMSA) is softest among all five mixtures tested. The creep compliance mastercurves shown in Figure 43 indicates that the S4 70-28 mix have highest creep compliance and S3 64-22 mix have lowest creep compliance at all testing temperatures which is corroborating with the experimental findings from the dynamic modulus test results.

The predicted average creep compliance data for all five mixtures at precise temperatures and times are given in Table 25. The Mechanistic-Empirical thermal cracking model requires creep compliance data at precise temperatures and so once the average mastercurve was developed, creep compliance for all mixtures were predicted at the required times and temperatures using the average predicted shift factor and compliance equation coefficients. These predictions are shown in Table 26.

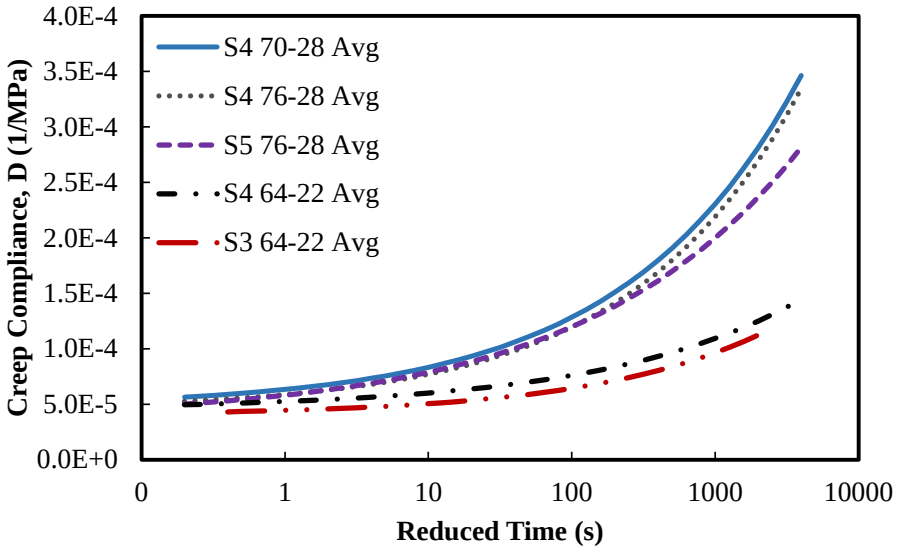

Figure 43 Creep Compliance Master Curves for S3 64-22 Mix (Average of 3 Replicates).

Table 25 Creep Compliance Coefficients for Mastercurves

Model Parameter	***Mix***				
	S3 64-22	***S4 70-28***	***S4 64-22***	***S4 76-28***	***S5 76-28***
***D_0* (1/MPa)**	4.00 x 10^{-5}	4.77 x 10^{-5}	4.5447E-05	4.528E-05	3.68E-05
***D_1* (1/MPa)**	4.61 x 10^{-6}	1.58 x 10^{-5}	7.1212E-06	1.36E-05	2.15E-05
N	0.363	0.355	0.318	0.369	0.293
E_a (J/mol)	1.76 x 10^5	1.93 x 10^5	1.58E+05	2.12E+05	2.20E+05

The average tensile strength of the different mixtures is shown below in Figure 44. These results show that the mix with a higher RAP content (S4 64-22 mix) has the highest strength and the mix with the highest asphalt content (S4 70-28 mix) shows the

lowest strength of all mixtures. The replicate data from each mix and test summary is given in Appendix D for each mixture type tested.

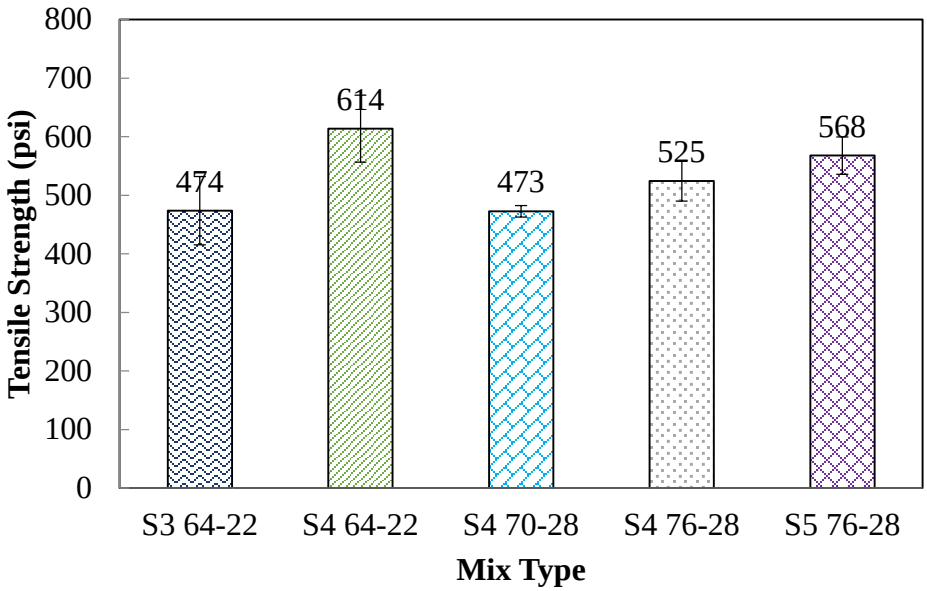

Figure 44 Average Tensile Strength of Study Mixtures (psi)

Table 26 Predicted Creep Compliance for Study Mixtures

Temp (°C)	Time (s)	S3 64-22 Avg		S4 70-28 Avg		S4 64-22 Avg		S4 76-28 Avg		S5 76-28 Avg	
		D(t) (1/MPa)	D(t) (1/psi)	D(t) (1/MPa)	D(t) (1/psi)	D(t) (1/MPa)	D(t) (1/psi)	D(t) (1/MPa)	D(t) (1/psi)	D(t) (1/MPa)	D(t) (1/psi)
-15	1	4.26E-05	2.94E-07	5.61E-05	3.87E-07	4.89E-05	3.37E-07	5.26E-05	3.62E-07	4.86E-05	3.35E-07
	2	4.34E-05	2.99E-07	5.85E-05	4.03E-07	4.99E-05	3.44E-07	5.47E-05	3.77E-07	5.13E-05	3.54E-07
	5	4.47E-05	3.08E-07	6.27E-05	4.32E-07	5.17E-05	3.56E-07	5.85E-05	4.03E-07	5.58E-05	3.85E-07
	10	4.61E-05	3.18E-07	6.68E-05	4.61E-07	5.34E-05	3.68E-07	6.23E-05	4.30E-07	6.01E-05	4.14E-07
	20	4.78E-05	3.30E-07	7.22E-05	4.97E-07	5.56E-05	3.83E-07	6.73E-05	4.64E-07	6.53E-05	4.50E-07
	50	5.09E-05	3.51E-07	8.15E-05	5.62E-07	5.93E-05	4.09E-07	7.61E-05	5.25E-07	7.41E-05	5.11E-07
	100	5.40E-05	3.72E-07	9.10E-05	6.27E-07	6.30E-05	4.34E-07	8.51E-05	5.87E-07	8.25E-05	5.69E-07
-10	1	4.26E-05	2.94E-07	6.35E-05	4.38E-07	5.13E-05	3.54E-07	5.89E-05	4.06E-07	5.83E-05	4.02E-07
	2	4.34E-05	2.99E-07	6.79E-05	4.68E-07	5.30E-05	3.65E-07	6.28E-05	4.33E-07	6.31E-05	4.35E-07
	5	4.47E-05	3.08E-07	7.56E-05	5.21E-07	5.58E-05	3.85E-07	6.99E-05	4.82E-07	7.13E-05	4.91E-07
	10	4.61E-05	3.18E-07	8.34E-05	5.75E-07	5.86E-05	4.04E-07	7.71E-05	5.31E-07	7.90E-05	5.45E-07
	20	4.78E-05	3.30E-07	9.34E-05	6.44E-07	6.20E-05	4.28E-07	8.63E-05	5.95E-07	8.86E-05	6.11E-07
	50	5.09E-05	3.51E-07	1.11E-04	7.65E-07	6.81E-05	4.69E-07	1.03E-04	7.09E-07	1.05E-04	7.21E-07
	100	5.40E-05	3.72E-07	1.29E-04	8.86E-07	7.40E-05	5.10E-07	1.20E-04	8.25E-07	1.20E-04	8.26E-07
0	1	4.26E-05	2.94E-07	9.91E-05	6.83E-07	6.07E-05	4.19E-07	8.96E-05	6.18E-07	1.03E-04	7.11E-07
	2	4.34E-05	2.99E-07	1.13E-04	7.82E-07	6.48E-05	4.47E-07	1.02E-04	7.07E-07	1.18E-04	8.14E-07
	5	4.47E-05	3.08E-07	1.39E-04	9.56E-07	7.18E-05	4.95E-07	1.25E-04	8.65E-07	1.43E-04	9.87E-07
	10	4.61E-05	3.18E-07	1.64E-04	1.13E-06	7.87E-05	5.43E-07	1.49E-04	1.03E-06	1.67E-04	1.15E-06
	20	4.78E-05	3.30E-07	1.96E-04	1.35E-06	8.74E-05	6.03E-07	1.79E-04	1.23E-06	1.97E-04	1.35E-06
	50	5.09E-05	3.51E-07	2.54E-04	1.75E-06	1.03E-04	7.07E-07	2.33E-04	1.60E-06	2.46E-04	1.69E-06
	100	5.40E-05	3.72E-07	3.11E-04	2.14E-06	1.17E-04	8.10E-07	2.87E-04	1.98E-06	2.93E-04	2.02E-06

CHAPTER 4. FALLING WEIGHT DEFLECTOMETER (FWD) DATA ANALYSIS

An important part of the pavement analysis performed to evaluate different rehabilitation scenarios was the determination of the existing pavement structural condition. This process was carried out with three major tasks. First, the ODOT FWD/GPR database was reviewed to better understand the available data for subsequent FWD analysis. Then, analysis was completed for both flexible and composite pavements using the AASHTO 1993 methodology in order to verify the design parameters in the database and verify the data quality. The properties calculated included the subgrade resilient modulus, M_r, the design subgrade modulus, M_{r_Design}, the design pavement modulus, E_{p_Design}, the modulus of subgrade reaction, k, and the effective static modulus of subgrade reaction, k_{eff_static}. The final step was backcalculation of the individual layer moduli and flexible layer damage ratios. The following sections detail these analyses.

4.1. FWD/GPR DATABASE REVIEW

Extensive work was conducted to extract data from the ODOT FWD/GPR database (2004_2011_data.mdb) and verify the calculated quantities presented along with data. This work was accomplished by first reviewing the database, verifying the data elements to the extent possible and performing initial calculations necessary to use data for later analyses. The data elements present in this database are summarized in Table 27.

As seen in Table 27, the current ODOT FWD database includes many columns with different calculated engineering parameters (E_p, M_r, E_{ac}, etc.). Considerable effort was spent to verify issues such as whether the drop data are corrected for temperature, what load level was used for calculation purposes, what thicknesses were used in calculations, etc. An example of the process followed is shown in Figure 45 and Figure 46, which presents analysis performed to decipher the meaning of the D_{i_9k} parameter. This parameter was found to yield the corrected deflections to a load level of exactly 9,000 pounds instead of the actual applied load, which varies slightly along the same section as showed in Figure 45. The conversion from D_i to D_{i_9k} was made assuming a linear relationship between the load and the measured deflections or by using Equation (24).

$$D_{i\_9k} = \frac{D_i \cdot 9000}{P} \tag{24}$$

where:

D_{i_9k} = corrected deflection for the i^{th} sensor (mils) to a 9,000 lb load,
D_i = measured deflection for the i^{th} sensor (mils), and
P = applied FWD drop load (lbs).

Table 27 A Summary of Data Elements in FWD/GPR Database

NLF_ID	10-digit unique ID for each control section. County (2), Control (2), Suffix (1), Lane ID (1), and begin mile of control section or 4-lane divided section (4).
IsInterstate	Checkbox indicating if the section belongs to the interstate system
IsNHS	Checkbox indicating if the section belongs to the NHS road system
FieldDiv	Field Divisions 1-8
Coll_Yr	Collection Year
ExpectedRecollectYr	Expected Recollection Year
CtlSect	Control Sections: 2-digit county, dash, 2-digit control section
Route	Route name
Direction	ODOT supplied value with 5=Primary and 6=Secondary
PaveType	Pavement type; AC, COMP, JPCP, DJMCP, DJCP, BRK, CRCP, GRV.
Chainage	Distance from beginning of control section, miles
SurfaceTemp	Surface temperature, °F
AirTemp	Air temperature, °F
Drop_Number	FWD drop number recorded in database
Stress	Stress generated from FWD drop, psi (11.8 in. diameter plate)
Force	Force applied in FWD drop, lb
Di	Measured deformations for sensors 1 to 7, mils (0, 203, 305, 457, 610, 914, and 1524 mm)
Di_Analysis	Analyzed deformations for sensors 1 to 7, mils
Di_9k	Calculated deformations for sensors 1 to 7 based on 9 kip load, mils
FWD[1]	Falling Weight Deflectometer
GPR[1]	Ground Penetrating Radar
Core[1]	Core taken from pavement
Design[1]	Values of parameters used in design
*_Latitude	Latitude where measurement was taken, degrees (WGS84 datum)
*_Longitude	Longitude where measurement was taken, degrees (WGS84 datum)
*_Comment	Field for comments
*_Test_Date	Test date in M/DD/YYYY format
*_Mr	Resilient modulus of subgrade layer, psi
*_Ep	Effective pavement modulus, psi
*_Ep_Mr	Ratio of effective pavement modulus to resilient modulus as per AASHTO
*_SN	Structural number
*_k	Coefficient of subgrade reaction, pcf
*_keff_static	Effective static coefficient of subgrade reaction, pcf
*_EAC_Corr	Corrected modulus of AC layer, psi
*_RMS_Error	Root mean square error
*_Li_Thick	Thickness of layer chosen layer i,in. (i goes up to 12 layers)
*_Li_Type	Type of chosen layer i (AC, PCC, Aggr Base, Subbase, Subgrade, bb, brick, cstb, ctb, fab, lime stb, sab, soil cement, stb base, stb soil)
*_Li_Modulus	Modulus of chosen layer i, psi

[1] prefix that accompanies headings indicated by "*_"

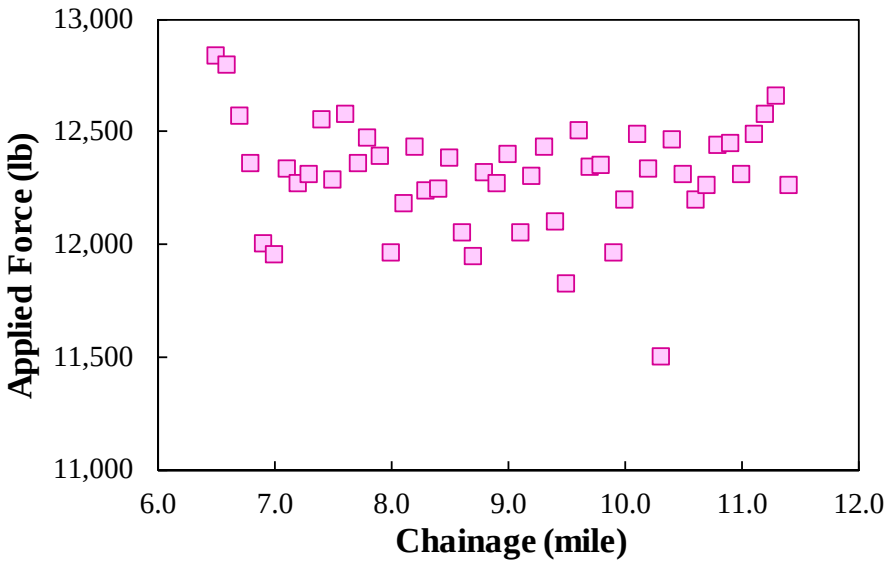

Figure 45 Applied Load over Versus Pavement Length, AC Control Section 66-18.

Similar to the analysis used to identify the meaning of D_{i_9k}, the interpretation of the $D_{i\_Analysis}$ was found to be the corrected deflections that are corresponding to a certain constant load. The applied constant load was found to vary from one section to another as shown in Figure 46. Three different reference loads (12,000, 15,000, 16,000 lb) were found to exist depending on whether the route was a U.S. highway or an interstate. The conversion from D_i to $D_{i\_Analysis}$ was made assuming a linear relationship between the load and the measured deflections or by using Equation (25).

$$D_{i\_Analysis} = \frac{D_i \cdot P_c}{P} \tag{25}$$

where:

$D_{i\_Analysis}$ = corrected deflection for the i^{th} sensor (mils) to a specific constant load,
D_i = measured deflection for the i^{th} sensor (mils),
P_c = normalized constant FWD drop load (lbs), and
P = applied FWD drop load (lbs).

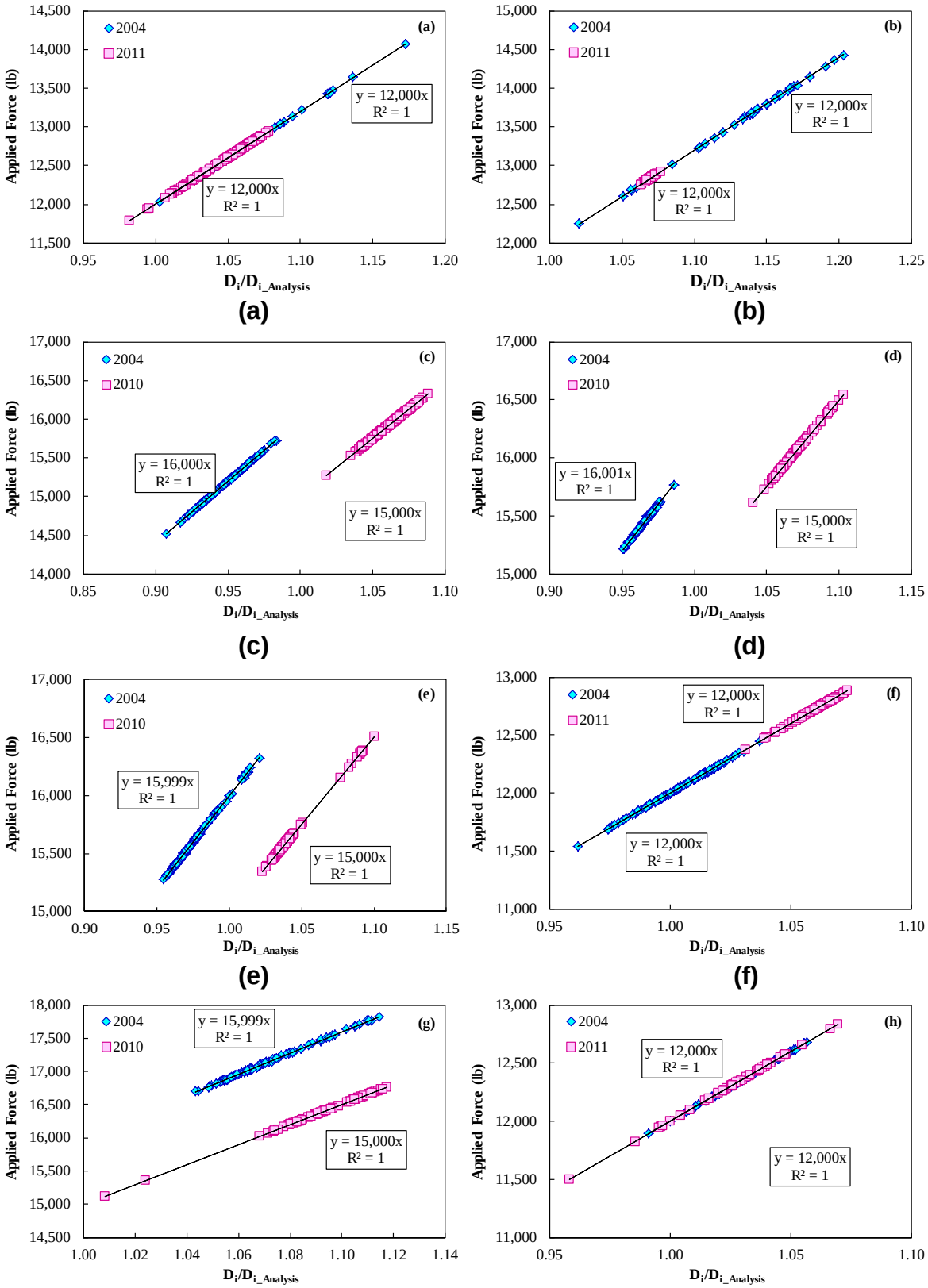
(a)
2004
2011
y = 12,000x
R² = 1
y = 12,000x
R² = 1
Applied Force (lb)
Di/Di_Analysis
(b)
2004
2011
y = 12,000x
R² = 1
y = 12,000x
R² = 1
Applied Force (lb)
Di/Di_Analysis
(c)
2004
2010
y = 16,000x
R² = 1
y = 15,000x
R² = 1
Applied Force (lb)
Di/Di_Analysis
(d)
2004
2010
y = 16,001x
R² = 1
y = 15,000x
R² = 1
Applied Force (lb)
Di/Di_Analysis
(e)
2004
2010
y = 15,999x
R² = 1
y = 15,000x
R² = 1
Applied Force (lb)
Di/Di_Analysis
(f)
2004
2011
y = 12,000x
R² = 1
y = 12,000x
R² = 1
Applied Force (lb)
Di/Di_Analysis
(g)
2004
2010
y = 15,999x
R² = 1
y = 15,000x
R² = 1
Applied Force (lb)
Di/Di_Analysis
(h)
2004
2011
y = 12,000x
R² = 1
y = 12,000x
R² = 1
Applied Force (lb)
Di/Di_Analysis

(g) (h)

Figure 46 Applied load versus Di/Di_Analysis Relationships: (a) Section 56-04; (b) Section 03-02; (c) Section 54-22; (d) Section 42-30; (e) Section 20-04; (f) Section 47-06; (g) Section 25-46; and (h) Section 66-18.

4.2. BACKCALCULATION USING AASHTO 1993 DESIGN GUIDANCE

After identifying the meaning of each variable in the database relevant control section data was extracted from the FWD/GPR database according to control section and data. This extraction was possible since the database was arranged in terms of control section, direction, and chainage (distance). The parameters of interest include:

- Subgrade resilient modulus, M_r, determined from the recorded deflections and known thickness values. Thickness can be obtained from either GPR (M_{r_GPR}) or from cores taken during FWD (M_{r_Core});
- Design subgrade modulus *Mr,* M_{r_Design}, calculated as the lower resilient modulus value from either the *GPR* or the core values then divided by a factor of three;

$$M_{r\_Design} = \frac{\min\left(M_{r\_GPR}, M_{r\_Core}\right)}{3} \quad (26)$$

- Design pavement modulus *Ep*, E_{p_Design}, calculated as the equivalent design modulus of pavement layers from the *GPR* calculations;
- Modulus of subgrade reaction, *k,* determined using the AASHTO 1993 procedure from M_{r_Design} values (for rigid pavements only); and
- Effective static modulus of subgrade reaction, k_{eff_static}: determined using AASHTO 1993 procedure (*33*) from recorded deflections via dividing the $k_{eff\_dynamic}$ by a factor of two using the pavement thickness from either *GPR* or core data.

4.2.1. Flexible Pavement Sections

4.2.1.1. Calculation Method

To determine the M_r of subgrade and the E_p for the database, the procedure outlined in the technical report prepared by Fugro Consultants (*34*, *35*) was followed. In this report, the M_r of subgrade and the E_p that are both computed from the deflection based on the 1993 AASHTO Design Guide. Equation (27) shows the function for calculating the resilient modulus.

$$M_r = \frac{0.24P}{d_r r} \quad (27)$$

where:
P = load (lb),
d_r = deflection at radius r (in.), and

r = radius (in.).

For the computation of E_p, the deflection at the plate (d_0) is used and requires a temperature correction to a standard temperature of 68°F. The value of E_p is found through iteration with Equation (28), which is used in the AASHTO Design Guide. This process can be done easily in Microsoft Excel using the Solver function. The field deflection at d=0 is corrected to 68°F using a relationship presented in the AASHTO Design Guide as shown in Figure 47. To ensure that temperature correction factors would be within a reasonable range, the 120°F factor was used with temperatures above 120°F, and the 12 in. AC thickness factor was used for AC thicknesses greater than 12 in. The verification process was carried out for the seven control sections. For each, M_r and E_p were calculated for both the 2004 and 2010 data based on the identified procedure and the calculated values were then to ones reported in the database.

$$d_0 = 1.5pa\left(\frac{1}{M_r\sqrt{1+\left(\frac{D}{a}\sqrt[3]{\frac{E_p}{M_r}}\right)^2}}+\frac{\left[1-\frac{1}{\sqrt{1+\left(\frac{D}{a}\right)^2}}\right]}{E_p}\right) \quad (28)$$

where:

d_0 = deflection at center of load at 68ºF (in.),
p = *FWD* plate pressure (psi),
a = *FWD* plate radius (5.91 in.),
D = total thickness of pavement layers above subgrade (in.),
M_r = subgrade resilient modulus (psi), and
E_p = effective pavement modulus of all layers above subgrade (psi).

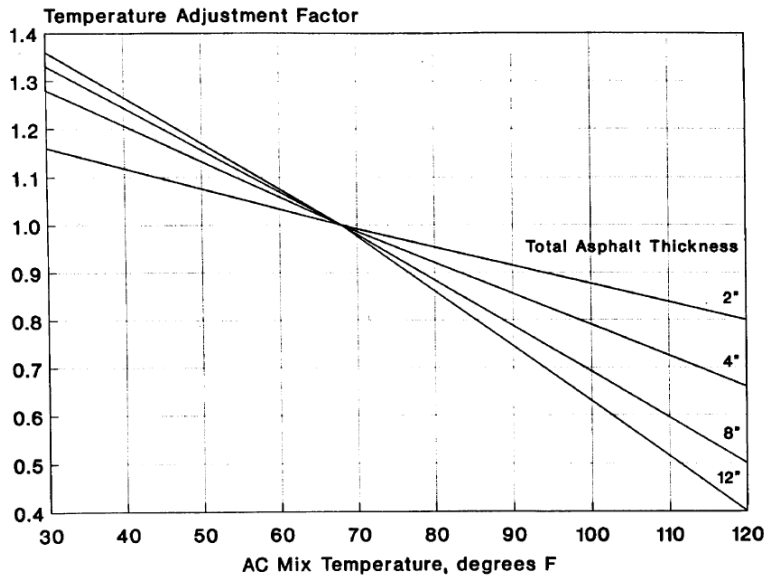

Figure 5.6. Adjustment to d_0 for AC Mix Temperature for Pavement with Granular or Asphalt-Treated Base

Figure 47 AASHTO 1993 Temperature Adjustment Factor for Pavement with Granular or Asphalt-Treated Base (3).

4.2.1.1. Verification and Results

For the verification of E_p, both GPR and core data were used separately as both provide different estimation of the pavement layer thickness, which is an input to calculate the E_p values, see Equation (28). Figure 78 to Figure 90 in Appendix E show comparisons of the reported and verified AASHTO 1993 M_r and E_p values for 2004 and 2010 using both GPR and core data. It can be observed from all figures that for the 2004 data, the E_p values match exactly with the reported E_p values. The only exception to this finding is the GPR values form control section 54-22, shown in Figure 79 For 2010 data, some control sections showed close agreement with the AASHTO 1993 E_p values; however, three control sections (54-22, 44-05, 09-05) showed that the AASHTO 1993 E_p values were extremely different than the reported values for both GPR and core cases. It was observed for these particular three control sections that the FWD data were measured at high pavement temperature (110 to 140°F) and that a low temperature correction factor was applied to the measured FWD d_0. This temperature correction resulted in a large increase to the AASHTO 1993 E_p values compared to the reported ones.

The LCCA (Life Cycle Cost Analysis) analysis of the preselected AC control section requires the identification of single M_r and E_p values that represent a specific homogeneous section or subsection. The identification of the sections or subsections with similar design parameters values which can be determined by looking into the change in the both M_r and E_p values along the length of the control sections. Appendix E (Figure 91 to Figure 97) shows the plotting of the M_r values versus chainage in miles for both 2004 and 2010 data and both 5 and 6 directions. In these figures the gross average including outliers is denoted and shown graphically as a bolded horizontal line. As described below these are not necessarily the final reported values for each section.

Similarly, Appendix E (Figure 98 to Figure 104) shows the variation of E_p values from both GPR and core data versus chainage in miles for 2004 and 2010 data and 5 and 6 directions. It can be observed for all the seven AC control sections that there is no sudden change or shift in both M_r and E_p values along specific distance of the section length except for some isolated individual spikes that are extremely higher or lower than the average trend. This finding means that the whole section can be considered as a uniform section without the need to subdivide the section into smaller subsections. In this case, each control section can be described by one representative M_r and E_p value which represents the average value of the design parameter after getting rid of any outliers. The excluded outliers were determined as the values outside data range calculated at 95% confidence level (values outside the mean ± 1.96 of standard deviation). The exclusion of the outliers is carried out through an iterative process wherein outliers are first identified and excluded, then the mean and standard deviation are recalculated and the process repeated until convergence. Figure 48 shows an example before and after the deletion of the outliers. After the completion of excluding the outliers, the average M_r, M_{r_Design}, E_{p_Design} were calculation for each section, each year, and each direction as summarized in Table 28.

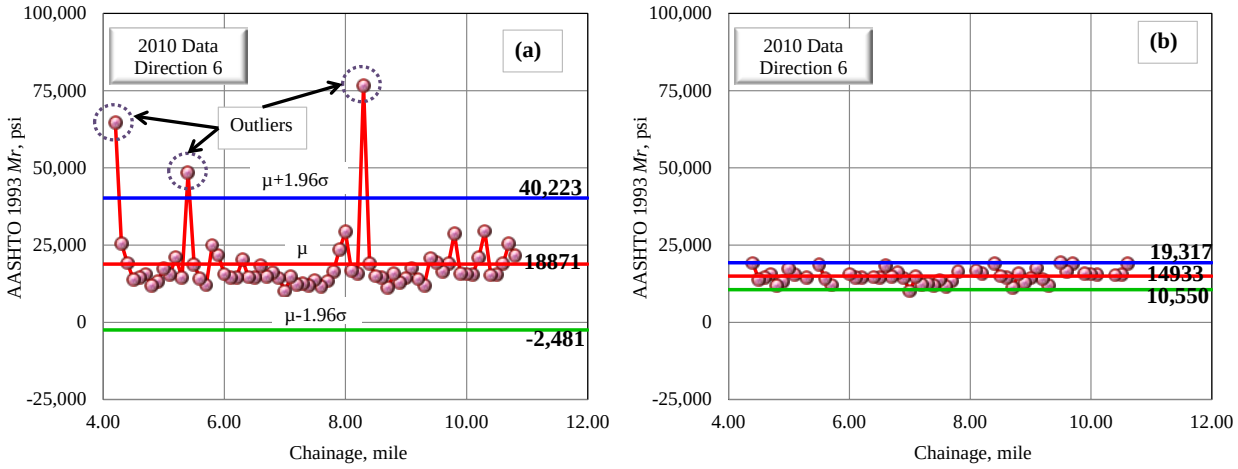

(a) **(b)**

Figure 48 AASHTO 1993 M_r versus Chainage of Control Section 09-05 (a) before Deletion of Outliers; and (b) after Deletion of Outliers.

Table 28 Summary of Representative Average Design Mr and Ep Values of Asphalt Pavement Control Sections

Control Section	Design Parameter	Year 2010		Year 2004	
		Direction 5	Direction 6	Direction 5	Direction 6
68-22	M_r	27,083	29,595	--	--
	M_{r_Design}	9,028	9,865	--	--
	E_{p_Design}	200,886	257,491	--	--
54-22	M_r	23,531	22,584	23,389	23,081
	M_{r_Design}	7,844	7,528	7,796	7,694
	E_{p_Design}	438,466	503,096	350,851	238,883

Control Section	Design Parameter	Year 2010		Year 2004	
		Direction 5	Direction 6	Direction 5	Direction 6
44-05	M_r	6,461	7,263	7,645	8,460
	M_{r_Design}	2,154	2,421	2,548	2,820
	E_{p_Design}	288,455	391,022	615,401	378,201
09-05	M_r	18,059	14,933	18,208	18,188
	M_{r_Design}	6,020	4,978	6,069	6,063
	E_{p_Design}	409,731	780,196	437,781	303,180
55-68	M_r	18,851	21,036	29,467	24,997
	M_{r_Design}	6,284	7,012	9,822	8,332
	E_{p_Design}	144,822	153,164	107,849	118,873
20-04	M_r	24,430	26,926	27,982	27,236
	M_{r_Design}	8,143	8,975	9,327	9,079
	E_{p_Design}	470,036	520,680	396,238	314,097
72-78	M_r	--	19,583	--	22,318
	M_{r_Design}	--	6,528	--	7,439
	E_{p_Design}	--	115,901	--	216,270

4.2.2. Composite Pavement Sections

4.2.2.1. Calculation Method

For composite pavement sections the modulus of subgrade reaction, *k*, and effective modulus of subgrade reaction were calculated in addition to M_r and E_p. For the calculation of subgrade reaction, k-value, there are four different methods identified by Fugro Consultants (*34*, *35*). Two of these methods that allow for an automated calculation algorithm were used for ODOT FWD/GPR database as detailed below:

Method 1:

Based on the AASHTO Design Guide Section 3.2.1, the composite k-value was determined using Equation (29), which is based on a single layered elastic simulation of the rigid plate loading test. This method leads to a composite k-value.

$$k = \frac{M_r}{19.4} \tag{29}$$

Method 2:

Method 2 is used for backcalculating a dynamic effective k-value from FWD testing. The dynamic value can be converted to a static effective k-value, $k_{eff\text{-}static}$, which is the value used for design purposes. The calculation and conversion method can be used for PCC and AC/PCC pavements. The first step of method 2 is to calculate the deflection bowl AREA from the drop data. This calculation is based on the deflections as shown in Equation (30) and the corrected deflection at zero distance (d_{0cor}).

$$AREA = 6\left[1 + 2\left(\frac{d_{12}}{d_{0cor}}\right) + \left(\frac{d_{24}}{d_{0cor}}\right) + \left(\frac{d_{36}}{d_{0cor}}\right)\right] \tag{30}$$

where:

d_i = deflection at 12, 24, and 36 in. from the plate center (in.) and

d_{0cor} = corrected deflection at 0 in sensor (in.).

The d_{0cor} value is obtained by subtracting the compression of the AC overlay ($d_{0compress}$) from the deflection at the plate (d_0). These correction equations are found in the AASHTO design guide as shown in Equation (31) and Equation (32), which are for bonded and unbounded AC and PCC interfaces respectively.

AC/PCC Bonded

$$d_{0compress} = -0.0000328 + 121.5006\left(\frac{D_{ac}}{E_{ac}}\right)^{1.0798} \quad (31)$$

AC/PCC Unbonded

$$d_{0compress} = -0.00002132 + 38.6872\left(\frac{D_{ac}}{E_{ac}}\right)^{0.94551} \quad (32)$$

where:
$d_{0compress}$ = AC compression at center of load (in.),
D_{ac} = AC thickness (in.), and
E_{ac} = AC elastic modulus (psi).

The dynamic effective modulus of subgrade reaction $k_{eff\_dynamic}$ is then calculated through Equation (33). To convert to a static effective modulus of subgrade reaction value k_{eff_static}, the $k_{eff\_dynamic}$ value is divided by 2.

$$k_{eff\_dynamic} = \left(\frac{P}{8d_{0cor}l_k^2}\right)\left\{1+\left(\frac{1}{2\pi}\right)\cdot\left[\ln\left(\frac{a}{2l_k}\right)+\gamma-1.25\right]\left(\frac{a}{l_k}\right)^2\right\} \quad (33)$$

where:
d_{0cor} = maximum corrected deflection (in.),
P = load, 9000 lb,
l_k = dense liquid radius of relative stiffness (in.),
γ = Euler's constant, 0.57721566490, and
a = radius of loading plate (5.9 in.).

$$l_k = \left[\frac{\ln\left(\frac{36-AREA}{1812.279133}\right)}{-2.559340}\right]^{4.387009} \quad (34)$$

To facilitate the calculation process, the following assumptions were made:

1. For method 1, the M_r used was multiplied by 0.25 to convert it to a theoretical lab value prior to performing the k-value computation. The factor of 0.25 is from the 1993 AASHTO Design Guide and is recommended for rigid pavements.

2. The simple equation in method 1 was used for rigid pavements despite the presence of any subgrade layers. Hence the k-value reported would be representative of a composite of all layers below the PCC.
3. To correct the deflection at d = 0 for method 2, an AC Elastic Modulus of 500,000 psi was assumed. This value is a typically used seed value for backcalculation, and was assumed in order to keep the computation as independent from the backcalculation as possible. The effect of changing this assumed AC modulus value on the correction to d_0 was minimal.
4. The interface between the AC and the PCC was bonded. The difference in the corrected deflection was minimal and information as to the bonding or lack thereof of the layers was not available.

For the composite sections, the verified subgrade M_r and the reported values matched completely for 2004 FWD data, while the 2010 data exhibited considerable scatter around the equality line. The verification process for the composite sections confirmed this observation as shown in Appendix E (Figure 105 to Figure 116), where both GPR and core M_r values were compared to the values computed by the 1993 AASHTO method. No clear explanation was found for this discrepancy. It was also found that the 2004 reported data used a threshold limit value of 50,000 psi for the reported GPR M_r values. This threshold was only applied to a single section (72-09), which leads to an unusual looking line of equality plot (see Figure 116). Such a threshold was not applied for the 2010 data (both GPR and core) and the 2010 core data.

4.2.2.2. Verification and Results

For the verification of E_p, both GPR and core data were used separately as both provide different estimation of the pavement layer thickness, which is an input to calculate the E_p values, see Equation (28). Figure 105 to Figure 116 in Appendix E show comparisons of the reported and verified AASHTO 1993 E_p values for 2004 and 2010 using both GPR and core data. It can be observed from all figures that for the 2004 data, the E_p values match exactly with the reported E_p values. For 2010 data, some control sections showed close agreement with the AASHTO 1993 E_p values; however, three control sections (42-30, 16-49, 72-09) showed that the AASHTO 1993 E_p values were extremely different than the reported values for both GPR and core cases. It was observed for control section 16-49 that the GPR data did not show any PCC layer and the calculation of the E_p value of this particular section was based on the core thickness data, which did show the presence of a PCC layer (Figure 110). For 42-30 and 72-09 sections, the AASHTO 1993 E_p values were lower compared to the reported values.

Appendix E also contains a comparison of the verified and the reported k, and k_{eff_static}. None of the seven composite control sections had either a k or k_{eff_static} values recorded for 2010. Therefore, the verification process included only the year 2004 data as shown in Figure 136 to Figure 159. Two control sections, 65-09 and 50-32, were not verified since neither of these sections were in the database for the year 2004. For the five verified composite control sections, it was observed that the AASHTO 1993 verified k

value match exactly the reported values, while the AASHTO 1993 verified k_{eff_static} values were higher than the reported values.

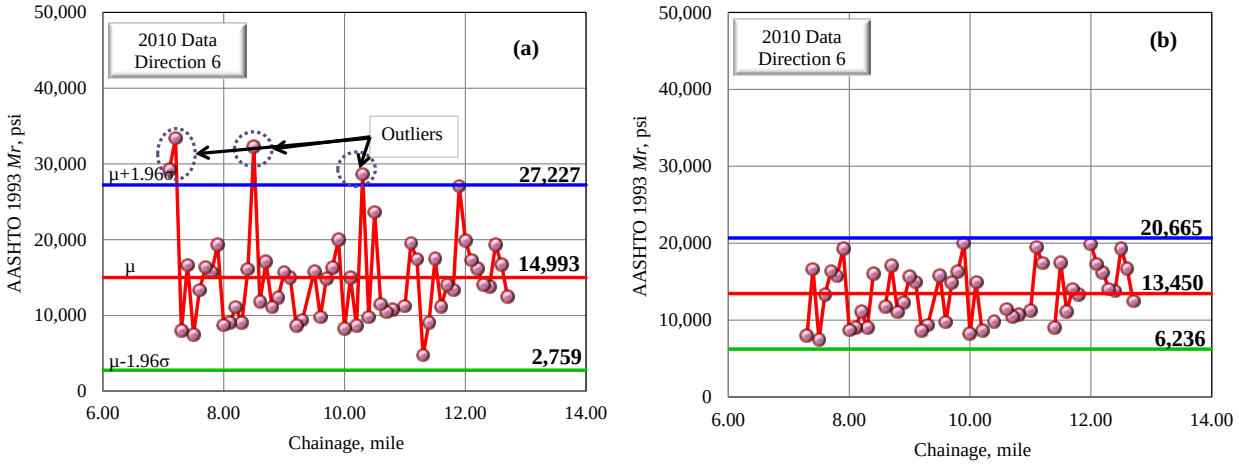

Figure 49 AASHTO 1993 M_r versus Chainage of Control Section 42-30 (a) before Deletion of Outliers; and (b) after Deletion of Outliers.

Table 29 Summary of Representative Average Design Mr and Ep, k and keff_stat Values of Composite Sections

Control Section	Design Parameter	Year 2010		Year 2004	
		Direction 5	Direction 6	Direction 5	Direction 6
25-46	M_r	23,800	22,878	23,931	25,959
	M_{r_Design}	7,933	7,626	7,977	8,653
	E_{p_Design}	872,909	1,074,843	608,515	613,701
	k	307	295	291	340
	$k_{eff\_static\_GPR}$	487	481	337	353
	$k_{eff\_static\_core}$	493	487	344	270
42-30	M_r	15,994	13,450	15,695	15,090
	M_{r_Design}	5,331	4,483	5,232	5,030
	E_{p_Design}	1,914,706	2,097,861	1,499,805	1,835,070
	k	206	173	204	194
	$k_{eff\_static\_GPR}$	242	205	172	170
	$k_{eff\_static\_core}$	241	204	175	176
55-09	M_r	14,591	12,079	--	--
	M_{r_Design}	4,864	4,026	--	--
	E_{p_Design}	300,489	400,327	--	--
	k	188	156	--	--
	$k_{eff\_static\_GPR}$	265	254	--	--
	$k_{eff\_static\_core}$	263	253	--	--
16-49	M_r	21,167	18,440	17,168	16,749
	M_{r_Design}	7,056	6,147	5,723	5,583
	E_{p_Design}	1,072,229	832,174	1,699,507	1,431,211
	k	273	238	221	216
	$k_{eff\_static\_GPR}$	--	--	228	193

Control Section	Design Parameter	Year 2010		Year 2004	
		Direction 5	Direction 6	Direction 5	Direction 6
	$k_{eff\_static\_core}$	--	--	239	201
50-32	M_r	50,264	50,791	--	--
	M_{r_Design}	16,755	16,930	--	--
	E_{p_Design}	1,345,680	1,204,797	--	--
	k	648	655	--	--
	$k_{eff\_static\_GPR}$	998	907	--	--
	$k_{eff\_static\_core}$	942	927	--	--
25-46	M_r	28,958	27,081	28,562	28,848
	M_{r_Design}	9,653	9,027	9,521	9,616
	E_{p_Design}	1,435,322	1,527,319	786,545	568,836
	k	373	349	368	364
	$k_{eff\_static\_GPR}$	451	556	290	306
	$k_{eff\_static\_core}$	429	563	289	296
72-09	M_r	37,184	41,972	53,174	73,148
	M_{r_Design}	12,395	13,991	17,725	24,383
	E_{p_Design}	1,216,856	1,168,473	1,156,380	977,498
	k	479	541	685	943
	$k_{eff\_static\_GPR}$	536	562	458	615
	$k_{eff\_static\_core}$	536	560	458	618

The LCCA of the preselected composite control sections requires the identification of single M_r E_p, k, and k_{eff_static} values that represent a specific homogeneous section or subsection. The identification of the sections or subsections with similar design parameters values which can be determined by looking into the change of any design parameter value along the length of the control sections. Appendix E (Figure 160 to Figure 176) shows the plotting of the M_r values versus chainage in miles for both 2004 and 2010 data and both 5 and 6 directions. In these figures the gross average including outliers is denoted and shown graphically as a bolded horizontal line. As described below these are not necessarily the final values reported for these sections. Similarly, Appendix E (Figure 129 to Figure 135) shows the variation of E_p values from both GPR and core data versus chainage in miles for 2004 and 2010 data and 5 and 6 directions as well as the variation in k and k_{eff_static} (Figure 136 to Figure 159). It can be observed for all the seven composite control sections that there is no sudden change or shift in in the design parameter values along the section length except for some isolated individual spikes that are much higher or lower than the average trend. This finding means that the whole section can be considered as a uniform section without the need to subdivide into smaller subsections.

In this case, each control section can be described by one representative *design* value which represents the average value of the design parameter after getting rid of any outliers. The excluded outliers were determined as the values outside data range calculated at 95% confidence level (values outside the mean ± 1.96 of standard deviation). The exclusion of the outliers is carried out through an iterative process wherein outliers are first identified and excluded, then the mean and standard deviation are recalculated and the process repeated until convergence. Figure 49 shows an

example before and after the deletion of the outliers. After the completion of excluding the outliers, the average M_r, M_{r_Design}, E_{p_Design}, k, and k_{eff_static} were calculation for each section, each year, and each direction as summarized in Table 29.

4.3. BACKCALCULATION FOR MEPDG ANALYSIS

While the AASHTO 1993 analysis provided very useful verification of the research team's understanding of the FWD/GPR data, its usefulness was limited to only the AASHTO 1993 design methodology. In this project, the Mechanistic-Empirical pavement analysis method was performed to ultimately consider rehabilitation strategy performance. This method requires individual layer moduli. As was the case for the 1993 AASHTO analysis, the data required to backcalculate the moduli values were available from 2004 and 2010. However, review of the records indicated that numerous control sections had received surface treatments or rehabilitation since 2004. Thus, analysis of 2004 data would not be representative of the pavement structure in place in 2010 and the research team decided to perform backcalculation using 2010 data only, with a few exceptions described in a following section.

For the purposes of this study, these individual layer values were backcalculated using Modulus 6.0. This decision was based on a small investigation comparing the usability and consistency of Evercalc, Elmod, and Modulus 6.0. In this process, the Modulus software was found to yield the most consistent and accurate prediction of deflection basins for the ODOT data. It was also the most usable for the massive number of backcalculations needed in this project (total of 1006). Modulus 6.0 was developed by the Texas Transportation Institute (TTI) for the Texas Department of Transportation deflection analysis. This program uses static, linear elastic analysis for the forward model and a system identification approach to interpret the deflection basins. The process begins by predicting surface deflections using layered elastic analysis with varying moduli ratios determined from the users input. Based upon the results of this analysis, a pattern search scheme is used to guide the optimization process. In practice this technique has shown to be more efficient than the standard iterative method. In this project deflection data was compiled from the ODOT database and entered into Modulus 6.0 for all stations along a given control section and direction. An example of the input data used is shown in Table 30 for the case of section 68-22 in the primary travel direction (D5).

Table 30 Example Backcalculation Input

Drop No.	Load (lb)	Measured Deflections (mils)						
		D1 (plate)	D2 (8 in.)	D3 (12 in.)	D4 (18.0 in.)	D5 (24.0 in.)	D6 (36 in.)	D7 (60 in.)
1	15042	23.74	18.49	15.49	12.00	8.87	5.72	2.46
2	15702	28.26	19.58	15.14	11.12	7.78	4.49	1.49
3	15681	24.94	16.64	12.51	9.12	6.07	3.06	0.81
•	•	•	•	•	•	•	•	•
•	•	•	•	•	•	•	•	•

Drop No.	Load (lb)	Measured Deflections (mils)						
		D1 (plate)	D2 (8 in.)	D3 (12 in.)	D4 (18.0 in.)	D5 (24.0 in.)	D6 (36 in.)	D7 (60 in.)
•	•	•	•	•	•	•	•	•
39	15368	32.19	23.87	18.75	14.99	11.20	7.12	3.24
40	15530	21.62	15.87	13.28	10.66	8.12	5.47	2.52

Once the data was input into the Modulus 6.0 software, the structural design and appropriate limits for the individual layer moduli were input. For analysis purposes, Poisson's ratios were assumed to be 0.38 for asphalt concrete, 0.20 for portland cement concrete and 0.35 for all other layers. Semi-infinite subgrade is a typical assumption for backcalculation analysis. However, in the case of the ODOT control sections, this assumption yielded high errors between measured and calculated sensor deflections. These values typically exceeded the commonly accepted average sensor error of 2.0% or less. The assumption of a rigid layer with the default ratio of bottom layer to stiff layer modulus of 100 was used in all backcalculation efforts (*36*). This assumption yielded more reasonable sensor errors for the majority of the sections analyzed.

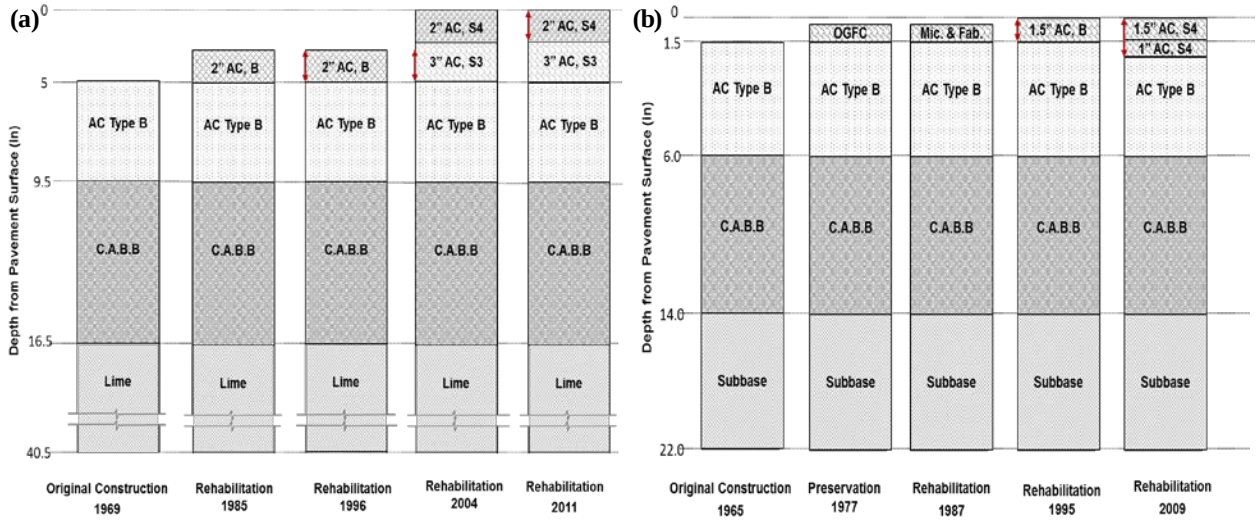

(a) **(b)**

Figure 50 Structural Configuration and Treatment History for; (a) Control Section 68-22 and (b) Control Section 54-22.

In the Modulus 6.0 software the user inputs a range for the moduli values of each layer. The backcalculation process was performed by varying these ranges until backcalculated moduli were within the defined ranges and the overall average sensor error for the group of sections was minimized. Once this process was completed, drop locations with individual average errors greater than 2% were removed from further analysis. Corrections were then applied to these raw backcalculated values in order to adjust the moduli for temperature and to identify and eliminate outliers. This process was slightly different for flexible and composite pavement sections and is described in more detail in each respective section. Finally, it should be mentioned that Modulus 6.0

is hardcoded to analyze pavement systems with a maximum of four layers. As described before, some sections contained more than four layers, and in these cases some pavements layers were combined based on engineering judgment. For example, in some cases adjacent granular layers were combined into a single layer and lime treated subbases/subgrade were combined.

4.3.1. Flexible Pavement Sections

4.3.1.1. Calculation Method

The layer moduli backcalculated from Modulus 6.0 are the values specific to the temperature when the FWD testing was performed. However, the method to use FWD data in MEPDG analysis requires the modulus at 68°F. So backcalculation in the flexible pavement sections involved first finding the uncorrected AC modulus and then applying a correction process to determine the modulus at 68°F and identify and eliminate outliers. Typical results from the uncorrected backcalculation are shown in Figure 51 where it is seen that the values can vary along the length of the section. Temperature correction of the moduli values was a two-step process; 1) first the asphalt layer temperatures were predicted and 2) the moduli are adjusted to a baseline temperature of 68°F based on the mid-layer temperature at the time of the FWD test.

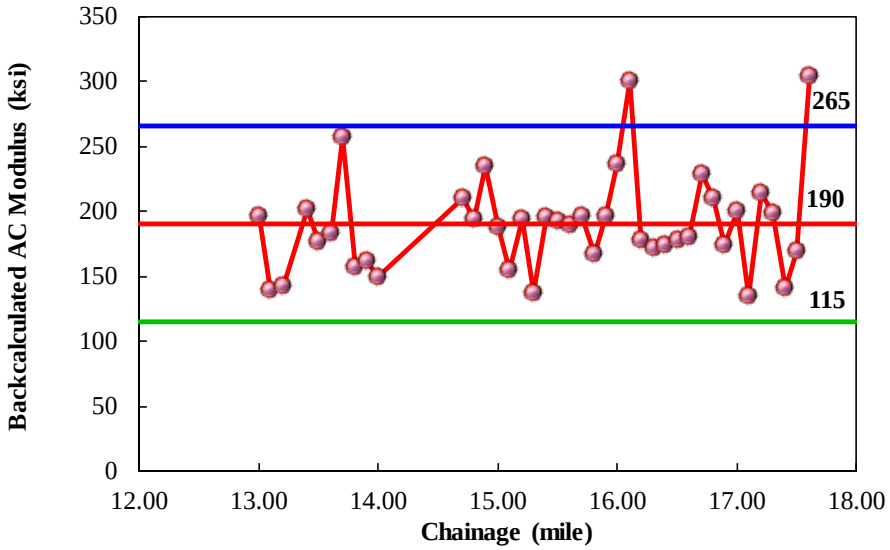

Figure 51 Raw Backcalculated AC Modulus for Primary Direction of Section 68-22 (Horizontal Lines Represent the Average and 95% Confidence Interval).

To predict the asphalt layer temperatures the research team investigated three different functions; Bells2, Bells3, and a procedure developed by the Texas Transportation Institute. The first two functions are shown in Equations (35) and (36) below and were developed to respectively predict pavement temperature during the LTPP protocol FWD testing and during routine FWD testing (*37*).

$$T_d = 2.78 + 0.912 \times IR + \left[\log(d) - 1.25\right] \times \left[-0.428 \times IR + 0.553\left(T_{(1-day)}\right) + 2.63 \times \sin\left(hr_{18} - 15.5\right)\right] + 0.027 \times IR \times \sin\left(hr_{18} - 13.5\right) \quad (35)$$

$$T_d = 0.95 + 0.892 \times IR + \left[\log(d) - 1.25\right] \times \left[-0.448 \times IR + 0.621\left(T_{(1-day)}\right) + 1.83 \times \sin\left(hr_{18} - 15.5\right)\right] + 0.042 \times IR \times \sin\left(hr_{18} - 13.5\right) \quad (36)$$

where:

T_d = pavement temperature at depth d (°C),
IR = pavement surface temperature (°C),
log = base 10 logarithm,
d = depth at which pavement temperature is to be predicted (mm),
$T_{(1\text{-}day)}$ = average air temperature the day before testing (°C),
sin = sine function on an 18-hr clock system, with 2π radians equal to one 18-hr cycle, and
hr_{18} = time of day, in a 24-hr clock system, but calculated using an 18-hr rise and fall time.

Fernando et al. (*38*) evaluated these two equations for pavements in Texas and Oklahoma and found that both exhibited notable bias with respect to the predicted pavement temperature. They subsequently developed an alternative temperature correction algorithm, referred to here as the TTI procedure and summarized in Equation (37). Since the TTI study included Oklahoma pavements and since the Bells3 equation was calibrated with relatively few sites (*39*), it was decided to follow the TTI procedure for this study. It should be noted that all three equations require the average daily air temperature on the day preceding the FWD test. Since this data was not recorded in the ODOT database the research team relied information published by the National Oceanic and Atmospheric Administration (*40*). Also note that the 2004 data did not include the time of day when FWD testing was performed. In these cases it was assumed that testing was conducted at 12:00 PM. Typical results of the temperature correction procedure are shown in terms of the air temperature, surface temperature (measured at the time of FWD testing), and mid-depth temperature from Equation (37) in Figure 52 for section 68-22.

$$T_d = 6.460 + 0.199\left(IR + 2\right)^{1.5} + \log(d)\left[-0.083\left(IR + 2\right)^{1.5} - 0.692 \times \sin^2\left(hr_{18} - 15.5\right) + 1.875 \times \sin^2\left(hr_{18} - 13.5\right) + 0.059\left(T_{(1-day)} + 6\right)^{1.5}\right] - 6.784 \times \sin^2\left(hr_{18} - 15.5\right)\sin^2\left(hr_{18} - 13.5\right) \quad (37)$$

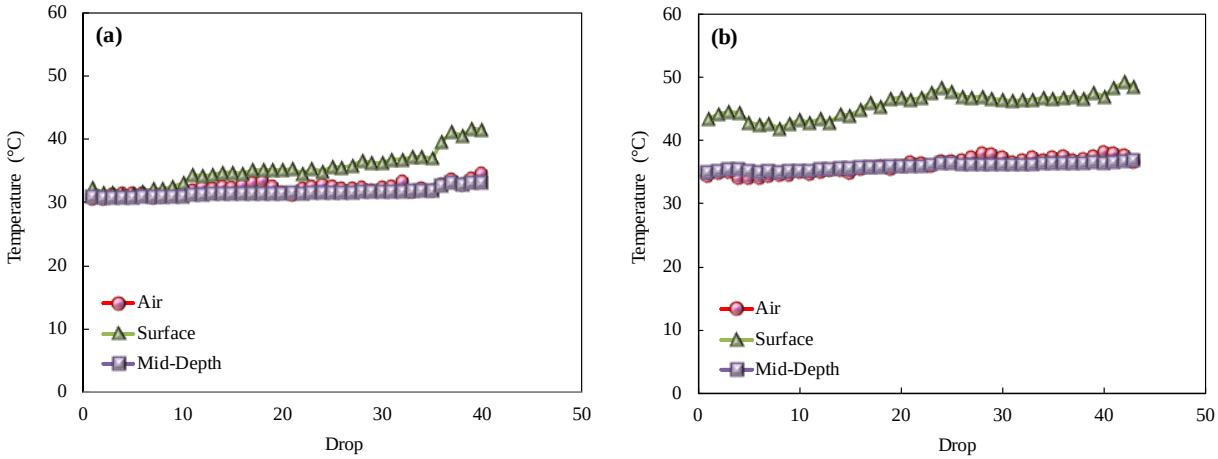

(a) **(b)**

Figure 52 Temperature Prediction for Section 68-22; (a) Primary Direction and (b) Secondary Direction.

Once mid-depth temperatures were established the moduli were corrected to a temperature of 68°F and a frequency of 14 Hz (the approximate loading frequency imparted by a moving truck at normal highway speed). Fernando et al. (*38*) evaluated Chen's model, Equation (38), and the Witczak-Fonesca model, Equation (39).

Their conclusion was that the Witczak-Fonesca model was most appropriate and thus it was chosen for the purposes of this study. The research team did investigate this issue and found that the differences between the Witczak-Fonesca function and the Chen function were small. Based on analysis conducted during the NCHRP 1-37A project and the suggestions of Fernando et al. (*38*) the reference loading frequency (f_R) was chosen as 14 Hz and the FWD frequency (f_T) was set at 16.7 Hz (*41*). The viscosity-temperature relationship used in Equation (40) was also chosen based on the representative PG grade of the section along with the correlations currently used in the mechanistic-empirical analysis process (*42*). Figure 53 shows a comparison of the uncorrected backcalculated asphalt concrete moduli for section 68-22 along with the temperature corrected values.

$$E_{68} = E_T \left(\frac{T}{68} \right)^{2.4462} \tag{38}$$

where:
E_{68} = corrected modulus (to 68°F),
E_T = backcalculated modulus of AC layer, and
T = mid-depth layer temperature at the time of the FWD test (°F).

$$\log\left(E_{68}\right) = \log\left(E_T\right) + \alpha \left[\frac{1}{1+e^{-\left(B_R + 0.7425\log\left(\eta_{68}\right)\right)}} - \frac{1}{1+e^{-\left(B_T + 0.7425\log\left(\eta_T\right)\right)}} \right] \tag{39}$$

where:
E_{68} = corrected modulus (to 68°F),
E_T = backcalculated modulus of AC layer,

α = $1.87+0.003p_4+0.00004p_{3/8}-0.00018(p_{3/8})^2+0.164p_{3/4}$,
B_R = $0.716 \times \log(f_R)$,
B_T = $0.716 \times \log(f_T)$, Corrected modulus (to 68°F),
p_4 = cumulative percent retained on No. 4 sieve by total aggregate weight,
$p_{3/8}$ = cumulative percent retained on 3/8-inch sieve by total aggregate weight,
$p_{3/4}$ = cumulative percent retained on 3/4-inch sieve by total aggregate weight,
f_R = reference loading frequency (Hz),
f_T = test frequency (Hz),
η_{68} = viscosity of asphalt cement at 68°F (10^6 Poises) calculated from Equation (40), and
η_T = viscosity of asphalt cement at mid-depth layer temperature at the time of the FWD test (10^6 Poises) calculated from Equation (40).

$$\log\log(\eta) = A + VTS\log(T_{rankine}) \quad (40)$$

where:

η = viscosity (cP),
A, VTS = model coefficients for given binder, and
$T_{rankine}$ = temperature (Rankine).

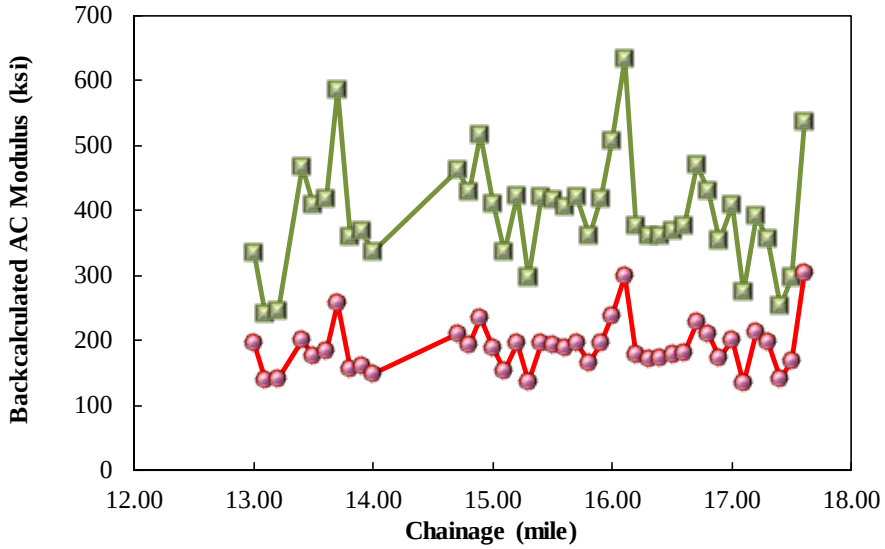

Figure 53 Comparison of Raw Backcalculated AC Modulus and Temperature Corrected AC Modulus (68°F).

The data shown in Figure 53 demonstrates that the overall variation in moduli along the control section does not show sudden changes or shifts in the moduli values. This finding mirrors the observations in the AASHTO 1993 based analysis and means that the whole section can be considered as uniform and thus further sectional subdivision is not needed. As was done previously, outliers are determined as the values outside the data range calculated at 95% confidence level (values outside the mean ± 1.96 of standard deviation). The exclusion of the outliers is carried out through an iterative process wherein outliers are first identified and then excluded. Next, the mean and standard deviation are recalculated and the process repeated until convergence (or until

5 iterations have been carried out). Figure 54 shows an example before and after the deletion of the outliers. The same correction procedure was applied separately for any individually analyzed asphalt layers, but always using the mid-depth temperature of the respective layer.

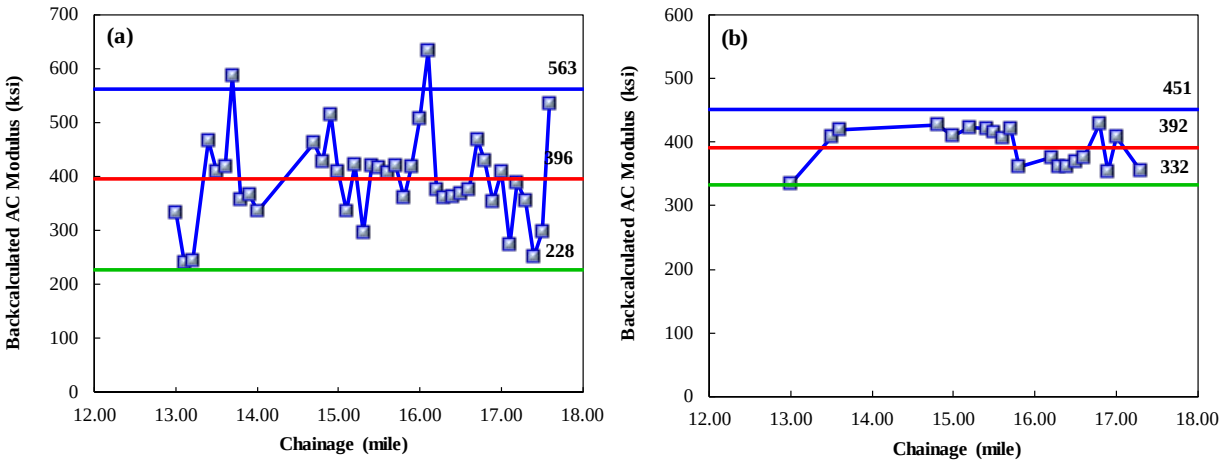

(a) **(b)**

Figure 54 Temperature Corrected Modulus (a) before Deletion of Outliers and (b) after Deletion of Outliers.

Once the layer moduli were determined for each direction in a control section, the asphalt concrete layer damage ratio was determined according to Equation (41). This value can be defined as the ratio of the backcalculated AC layer modulus at 68°F to the undamaged modulus of a representative mixture subjected to dynamic modulus testing.

$$Damage\ Ratio = DR = 1 - \frac{E_{68}}{|E^*|_{68,14\,Hz}} \quad (41)$$

where:

DR = damage ratio,
E_{68} = backcalculated AC layer modulus at 68°F, and
$|E^*|_{68,14\ Hz}$ = dynamic modulus of representative mixture at 68°F, 14 Hz.

Dynamic modulus test results of representative asphalt concrete mixtures were used to represent the stiffness behavior of undamaged asphalt concrete. The dynamic modulus master curve sigmoidal coefficients and shifting parameters were used to calculate the dynamic modulus values of a representative asphalt concrete mixture at 68°F and 14 Hz which represented the frequency of the corrected modulus.

Once the damage ratio was known it was used to estimate the damaged layer mastercurve. The process followed in this study is the same as that suggested by the MEPDG. First, the undamaged mastercurve is estimated according to the form shown in Equation (42). Note in the MEPDG literature that the mastercurve equation is shown in a slightly different but equivalent form using reduced time instead of reduced frequency.

$$\log\left|E^*\right| = a + \frac{b}{1 + \frac{1}{e^{c+d\times log f_R}}} \quad (42)$$

where:
l*E**l = dynamic modulus,
a,b,c,d = fitting coefficients, and
f_r = reduced frequency.

The damaged material mastercurve is estimated by adjusting the *b* parameter based on the damage ratio according to Equation (43).

$$b' = b \times (1 - DR) \quad (43)$$

where:
b' = adjusted mastercurve fitting coefficient,
b = mastercurve fitting coefficient, and
DR = damage ratio.

One challenge in estimating the undamaged modulus of an AC pavement layer is that there are typically multiple mixtures that comprise the AC layer. See for example Figure 50, which shows that after the 2009 rehabilitation that the AC layer was in control section 54-22 was actually comprised of three different dense graded asphalt layers. This section is also interesting because in addition to the dense graded mixes it also contained a coarse aggregate bituminous base (CABB) layer. For such pavements the dense graded asphalt concrete layers were combined into a single layer for analysis purposes. The undamaged properties of this layer were taken as the average of each material type weighted according to the proportion of that material in the total AC layer. In the case of control section 54-22, the 1.5 inches of surface mixture (S4 PG 76-28), 1 inch of leveling course (S4 PG 64-22), and 3.5 inches of “AC Type B” (S4 PG 64-22) accounted for 25%, 16.7%, and 58.3% of the AC layer, respectively. The CABB layer was considered an independent AC layer for FWD backcalculation purposes.

4.3.1.2. Results

Table 31and Table 32 present the backcalculated moduli values for all layers in the pavement structure. Note that the backcalculated values of the subgrade in these tables have not been corrected to laboratory values. This correction is necessary because it has been recognized that FWD backcalculated values of subgrade moduli are generally higher than those from laboratory testing. Since design procedures are based on laboratory derived moduli the backcalculated values must be corrected.
During the backcalculation process discrepancies in the AC (surface and base) layer thicknesses between the record drawing and pavement core information in the PMS database were identified. Three scenarios were evaluated to overcome this issue and produce the most accurate backcalculation possible:

1. Surface and base AC layer thicknesses were used as shown on the record drawings,

2. Surface and base AC layer thicknesses determined from ODOT PMS database pavement core thicknesses and averaged over the entire section, and
3. Base AC layer thickness determined from record drawings and surface AC layer thickness determined by subtracting the base AC layer thickness given in the record drawings from total pavement core thickness from ODOT PMS database cores (averaged over the entire section).

Option 3 was considered because the research team's experience suggested that the discrepancy between the core and record drawing was more likely to occur because of a failure to document some maintenance or overlay rehabilitation activity rather than the initial base construction. To decide between these scenarios a sub-group of direction 5 data from sections 68-22, 54-22, and 44-05 was evaluated with each. It was found that Option 1 yielded the greatest error between backcalculated and measured deflections, and was thus eliminated. Option 2 tended to yield the least error in prediction, but the ODOT PMS database did not always record separate thicknesses for the surface and base (CABB, FABB, and OGBB) layers. Thus, Option 3 was chosen in order to balance accuracy and data availability.

The research team decided to exclude 2004 FWD data from backcalculation because several sections received rehabilitation since 2004. Thus, analysis based on 2004 data will not accurately reflect the structural capacity of the pavement. Control section 20-04 was an exception to this rule. For this section backcalculation using 2010 data yielded questionable results and average errors between predicted and measured sensor deflections greater than the acceptable maximum value of two percent. These high errors occurred because FWD testing was conducted at very high pavement surface temperatures (134°F) and there existed a UTBWC (known as Novachip in other parts of country) that complicated the analysis. Since this section received the UTBWC surface treatment after 2004, backcalculation was performed using 2004 data which yielded average errors less than two percent. Using 2004 data eliminated both of these factors because the surface temperature was around 80°F in the 2004 testing and the UTBWC was applied after 2004. The research team believes that backcalculation based on 2004 data better represents pavement structural capacity for control section 20-04 in light of the fact that the UTBWC is generally considered to yield no structural capacity. Finally, 2010 FWD data were not available for section 66-36 and record drawings show a rehabilitation treatment after the 2004 FWD data were obtained. Since 2004 data would not accurately represent the section, it was eliminated from further analysis.

During analysis of FWD data, several challenges with the 2010 PMS database that need to be considered when interpreting the backcalculation results given in Table 31 and Table 32 are two issues that need to be kept in mind. First, the FWD testing on numerous sections was performed with pavement surface temperatures greater than 90°F. The viscous behavior of asphalt becomes predominant at higher temperatures which introduces inaccuracies into the FWD analysis that assumes elastic behavior (*42*). Second, testing of sections were completed during the summer months but are not consistent. Therefore, unbound layer moduli should be adjusted to account for seasonal variation in moduli.

4.3.2. Composite Pavement Sections

4.3.2.1. Calculation Method

Backcalculation analysis was carried out for seven composite (AC-PCC) sections. As described in a preceding chapter, four basic types of composite sections exist, each of which require slightly different analysis approaches for backcalculation:

- Type 1 – Very thin AC surface layer (< 3.0”) over a thick PCC layer (Section 42-30);
- Type 2 – Thick AC surface layer (> 3.0”) over a thick PCC layer (Section 55-09);
- Type 3 – Thin bituminous stabilized layer under thick PCC layer (Sections 25-46 MP 0, 25-46 MP 17, 16-49, and 50-32); and
- Type 4 – Thin AC surface layer, thick PCC layer, and thin bituminous stabilized layer (Section 72-09).

One limitation of the backcalculation process that is particularly relevant to the composite sections is that reliable moduli values cannot be determined for thin surface layers less than three inches (*43*). In this case, the user must either pre-assign a fixed modulus value to the thin layer or combine the first and second layers into a single analysis unit and smear the individual layer properties into the backcalculated value. This latter approach typically underestimates PCC layer moduli values so the research team chose to follow the first method and assigned a pre-defined value to the thin AC layers for backcalculation purposes.

Table 31 Backcalculated Layer Moduli Values for Flexible Pavement Sections (Direction 5)

Section	Year	Layer	Thickness (in.)	Backcalculated Modulus @ 68°F (ksi)[1]	Damage Ratio
68-22	2010	AC	5.7	419.7	0.67
		CABB	7	105.5	0.92
		Lime Base	24	36.3	-
		Subgrade	-	12.2	-
54-22	2010	AC	8.7	374.0	0.69
		CABB	8	221.0	0.83
		Subbase	8	77.6	-
		Subgrade	-	17.6	-
44-05 MP 10.8	2010	AC	7.5	758.7	0.22
		FABB	12	239.1	0.81
		Subgrade	-	15.9	-
09-05	2010	AC	12.8	985.9	0.21
		OGBB/FABB	6	15.8	0.99
		Subbase	6	8.5	-
		Subgrade	-	14.3	-
55-68	2010	AC	11.8	341.6	0.70
		Sand Asphalt	8	173.7	0.87
		Subgrade	-	13.7	-
20-04	2004	AC	11.1	787.1	0.22
		FABB	8	144.3	0.88
		Select	6	58.1	-
		Subgrade	-	21.3	-
44-05 MP 13.85	2010	AC	14	539.4	0.55
		Soil Cement	10	436.2	-
		Subgrade	-	22.0	-
14-06[2]	2010	AC	14.1	544.4	0.54
		Agg. Base	8	30.8	-
		Stab. Sub	8	158.3	-
		Subgrade	-	14.9	-

1. Sensors with error 2.0 and greater were removed from analysis.

2. Record drawings indicate reconstruction in 2010. FWD data may have been collected on the old pavement section but actual dates of reconstruction are not clear in the records. Assume as undamaged pavement section.

Table 32 Backcalculated Layer Moduli Values for Flexible Pavement Sections (Direction 6)

Section	Year	Layer	Thickness (in.)	Backcalculated Modulus @ 68°F (ksi)[1]	Damage Ratio
68-22	2010	AC	11.3	277.1	0.78
		CABB	7	24.2	0.98
		Lime Base	24	89.6	-
		Subgrade	-	9.3	-
54-22	2010	AC	10.4	608.6	0.49
		CABB	8	119.6	0.91
		Subbase	8	76.3	-
		Subgrade	-	17.7	-
44-05[2] MP 10.8	2010	AC	5	1060.3	0
		FABB	12	422.9	0.66
		Subgrade	-	19.5	-
09-05	2010	AC	12	1023.5	0.18
		OGBB/FABB	6	10.2	0.99
		Subbase	6	8.6	-
		Subgrade	-	13.0	-
55-68	2010	AC	10.5	295.0	0.75
		Sand Asphalt	8	184.9	0.86
		Subgrade	-	15.7	-
20-04	2004	AC	11	524.1	0.48
		FABB	8	123.7	0.9
		Select	6	92.7	-
		Subgrade	-	19.9	-
44-05 MP 13.85	2010	AC	13.5	510.1	0.57
		Soil Cement	10	679.2	-
		Subgrade	-	23.7	-
14-06[3]	2010	AC	13.3	643.0	0.46
		Agg. Base	8	28.4	-
		Stab. Sub	8	27.4	-
		Subgrade	-	16.4	-

1. Sensors with error 2.0 and greater were removed from analysis.

2. Sensors with error 3.0 and greater were removed for Direction 6, no further improvement possible with available pavement structure information.

3. Record drawings indicate reconstruction in 2010. FWD data may have been collected on the old pavement section but actual dates of reconstruction are not clear in the records. Assume as undamaged pavement section.

For the thin dense graded AC layers, a value of 1,000 ksi for the modulus at 68°F was selected by evaluating several backcalculation scenarios and finding that increasing the AC layer modulus yielded overall lower errors in predicting the surface deflections. An upper bound limit of 1,000 ksi for the modulus was established because this value represented a damage ratio approaching one and thus backcalculated moduli that were similar to the laboratory measured dynamic moduli. For bituminous stabilized base/subbase layers a layer modulus value of 175 ksi at 68°F (14 Hz) was selected based on review of backcalculated moduli values of similar layers in flexible pavement

control sections. It is important to note that assumed layer moduli values for the thin AC surface layers and bituminous treated subbase layers were based on the conditions of 68°F and 14 Hz loading frequency. Since the FWD testing was not performed at this temperature or frequency, the modulus value entered into the Modulus 6.0 software was adjusted. The adjustment procedure was essentially the mathematical inverse of the process used to correct the flexible pavement sections backcalculated moduli to 68°F and 14 Hz.

The first step in the adjustment process was to determine the mid-depth temperature of the AC and/or bituminous treated base layers by using to the TTI algorithm shown in Equation (37). The second step was to apply the Witczak-Fonesca function, Equation (39), to solve for the modulus at the mid-depth temperature, Equation (44) (the variables in this function were defined previously with respect to Equation (39)). As with the backcalculation correction in the flexile sections, FWD loading frequency was assumed to be 16.7Hz. Examples of the moduli resulting from this process are shown in Table 33.

$$\log\left(E_T\right) = \log\left(E_{68}\right) - \alpha\left[\frac{1}{1+e^{-\left(B_R+0.7425\log\left(\eta_{68}\right)\right)}} - \frac{1}{1+e^{-\left(B_T+0.7425\log\left(\eta_T\right)\right)}}\right] \quad (44)$$

Table 33 Example of Assumed AC Layer Moduli Used for Composite Sections

Control Section	Layer Type	Assumed Modulus, 68°F, 14 Hz (ksi)	Assumed Layer Modulus Input for Modulus 6 (ksi)
25-46 MP 17	Hot Sand	175	136
72-09	Asphalt Sand	175	44
42-30	AC	1000	641
72-09	AC	1000	265

4.3.2.2. Results

Table 34 shows the backcalculated layer moduli for all composite control sections included in this study. It is important to note the following when reviewing these data:

1. The unbound layer moduli have not been corrected to laboratory values.
2. Unbound layers were combined into a single layer and lime stabilized layers were combined with subgrade layers because Modulus 6 can analyze a maximum of four layers.
3. Section 16-49 shows an AC treatment in 2011 which was not reflected in the 2010 FWD core data so an undamaged (D=1.0) AC layer assumption may apply to this scenario.
4. The backcalculated PCC modulus for Section 72-09 Direction 5 appears high compared to the rest of the control sections so Direction 6 was evaluated which yielded similar results.
5. FWD data from 2004 were used for Section 42-30 since the drop temperature in 2010 was around 137°F and 2010 backcalculation results did not appear reasonable.

6. For section 55-09, both directions were analyzed because average PCC moduli values were very low. Analysis of Direction 6 data yielded similar results. Records show this plain PCC was constructed in 1959.

Table 34 Backcalculated Layer Moduli Values for Composite Pavement Sections

Section	Year	Layer	Thickness (in.)	Direction	Backcalculated Modulus @ 68°F (ksi)	Damage Ratio
25-46 MP 17	2010	AC	5.4	5	361.6	0.68
		Plain PCC	9.3		4638.3	-
		Hot Sand[1]	4.0		175.0	N/A
		Lime / Subgrade	-		19.9	-
42-30[3]	2004	AC	2.4	6	1019.3	0.01
		Doweled / MPCC[5]	9.1		4415.9	-
		SC / Select	12.0		69.4	-
		Subgrade	-		11.1	-
55-09	2010	AC	8.0	5	428.8	0.58
		Plain PCC	7.8		611.8	-
		SC[5] / Select	12.0		65.0	-
		Subgrade	-		10.4	-
		AC	7.6	6	496.6	0.52
		Plain PCC	8.8		1319.0	-
		SC[5] / Select	12.0		58.1	-
		Subgrade	-		12.8	-
16-49[2]	2010	AC	3.8	6	803.6	0.35
		Plain PCC	10.5		4107.5	-
		Soil Asphalt[1]	6.0		175.0	N/A
		Lime / Subgrade	-		15.6	-
50-32	2010	AC	7.4	6	921.3	0.23
		CRCP	8.2		4384.0	-
		FABB[1]	4.0		175.0	N/A
		Subgrade	-		39.0	-
25-46 MP 0	2010	AC	7.0	5	654.2	0.43
		Plain PCC	9.3		4039.6	-
		Hot Sand[1]	4.0		175.0	N/A
		Lime / Subgrade	-		22.9	-
72-09	2010	AC	1.9	5	1076.0	0.15
		Plain PCC	8.7		6219.0	-
		Asphalt Sand[1]	4.0		175.0	-
		Subgrade	-		34.6	-
		AC[4]	2.0	6[6]	1054.9	N/A
		Plain PCC	9.4		5791.3	-
		Asphalt Sand[1]	4.0		175.0	-
		Subgrade	-		28.0	-

1. FABB and Hot Sand modulus fixed at 175 ksi due to thin section under PCC. This value is an engineering estimate based on the FABB layer moduli from AC-AC control sections.
2. Backcalculation was performed using 2010 core data which did not reflect the 2011 AC treatment.

3. 2004 data was used in this case. 2010 FWD testing was conducted at 137° F and the backcalculated values for PCC were low, most likely due to high d_o deflections.
4. AC modulus fixed at approximately 1,000 ksi due to thin AC section over PCC.
5. MPCC = Meshed PCC, SC = Sand Cushion
6. Drops with error greater than 2.5% were eliminated.

4.4. FWD DATA ANALYSIS SUMMARY

A total of 1,006 individual FWD drops on 15 different control sections have been analyzed according to both the 1993 AASHTO design guide and MEPDG input requirements. There were several issues that had to be solved in performing this analysis, notably temperature corrections and reconciliation of pavement plans and pavement cores taken during the testing. For the 1993 AASHTO design guide based analysis temperature corrections were applied to the drop plate deflections using an iterative method described in the design guide. The moduli backcalculated for the individual layers were corrected according to a two-step process using a TTI model to predict the mid-depth temperature and the Witczak-Fonesca model to correct for temperature and frequency of loading. Since both analyses were performed using the same basic deflection data they provide very similar conclusions regarding which control sections are more structurally compromised. Specifically they show that overall the flexible sections are less structurally sound than the composite sections. The application of the resultant backcalculated moduli values is described in detail in the following chapter as is the implications on rehabilitation performance.

CHAPTER 5. MECHANISTIC-EMPIRICAL PAVEMENT ANALYSIS

5.1. MEPDG OVERVIEW

Structural design and performance prediction of rehabilitated pavements are conducted in this study by using the MEPDG analysis tool. This tool uses a mechanistic approach to predict the responses of pavements to the traffic loads and then pavement performance is estimated based on the empirical relationship developed from field data. The accuracy of analysis results highly depends on using detailed design inputs. A comprehensive set of data is measured in the laboratory or collected from different sources for this study to conduct the design analysis. The MEPDG provides three hierarchical levels of design reliability for inputs. The required inputs for level 1 are determined through comprehensive laboratory test measurements and field measurements. The needed inputs for levels 2 and 3 are estimated based on experience, predictive models or correlation with other material properties. A summary of collected database catalog for MEPDG analysis are illustrated in Table 35 and described below:

Table 35 Database Catalog Collection for Rehabilitation Selection

Type of Data	Description
Pavement Structure	Pavement Profile: Layer Types, Thickness and Design
Traffic	Average Annual Daily Truck Traffic (AADTT), Percent Truck, Traffic Volume Adjustment Factors
Climate	Seasonal Depth of Water Table, Geographic Coordinates
Historical Pavement Performance (PMS Database)	Structural Integrity (Nondestructive Testing)
	Surface Distress: Type, Severity and Extent
Material Characterization & Performance Testing	Binder Properties: Frequency Sweep, Multiple Stress Creep Recovery
	Mixture Properties: Dynamic Modulus, Cyclic Tension Fatigue, Hamburg, Indirect Tension Creep

5.1.1.Traffic

Traffic information including two-way AADTT, percent of single and combination truck, traffic growth factor, vehicle class distribution, and hourly truck distribution are provided by ODOT for representative pavement sections. However, level 3 is employed for axle load distribution input.

5.1.2. Climate Data

The MEPDG climate data covers 15 different weather stations from the national Climatic Data Center (NCDC) database for Oklahoma. The software will display six closest weather stations to each site specified by geographical coordination and the annual

average of water table depth. The virtual weather station is generated by selecting the three closest available stations to the site. The average groundwater tables for representative pavement sections investigated in this study are obtained from USGS groundwater Watch website and the geographical coordination information are extracted from ODOT PMS database.

5.1.3. Pavement Structure and Material Data

Type of mixtures and binder grade used in original construction and rehabilitation projects of representative pavement sections are extracted from the design plan provided by ODOT. A project number is assigned to each construction and rehabilitation project applied on existing pavements. Mix design sheet of mixtures used in projects are categorized based on project numbers found through ODOT website. These data are gathered and used as level 2 inputs in MEPDG. However, there is no mixture information including job mix formula and binder content recorded for original construction of old sections. Level 3 inputs are used for this sections based on default value obtained from ODOT Standard Specification Book (*44*).

Also, the detailed information about base and subbase are not available. Typical values are assumed according to the base and subbase requirement defined in the ODOT Standard Specification Books. Also, Course Aggregate Bituminous Base (CABB) and Fine Aggregate Bituminous Base (FABB) are used largely on original construction of old pavements. These are old techniques which are quite different than Superpave mixtures. Based on the recommendations one inch of asphaltic concrete can be substituted for one and a half inches (1 1/2") of fine aggregate bituminous base or one and a quarter inch (1 1/4") of coarse aggregate bituminous base (*45*). Also, subgrade soil data is not available for any of the representative sections. Subgrade data including soil AASHTO classification, sieve analysis, soil constant and typical resilient modulus are obtained from ODOT's Geologic Materials (Red Books) (*46*) and a technical report (*47*) conducted for developing database catalog for calibration of MEPDG for Oklahoma. The backcalculated resilient modulus of unbound materials used for base, subbase and subgrade are employed as level 1 inputs in MEPDG.

The dynamic modulus and indirect tension creep compliance test results of five commonly used mixtures in Oklahoma rehabilitation projects, which were discussed in previous chapters, are used as level 1 inputs in MEPDG analysis. In addition to the material properties of overlay mixtures, the condition of existing pavement has a significant effect on the selection of appropriate design and its performance. Backcalculation of FWD field testing provides a viable resource to evaluate this condition. The ODOT PMS database includes deflection, temperature, load, and location data for FWD tests conducted in 2010/2011 and 2004.
The damaged dynamic mastercurve along with the rutting depth acquired from PMS database are employed as level 1 inputs in MEPDG overlay design. Initial IRI which is a required input for overlay design analysis is also extracted from ODOT PMS database for representative pavement sections.

5.2. MEPDG ANALYSIS

The representative pavement sections are modeled in MEPDG version 1.1 using detailed data described in previous sections. It should be noted that calibration of MEPDG is beyond the scope of this research study. However, using national calibration coefficient introduces large amount of error in the results. Therefore, research team has decided to apply calibration factors conducted by Arkansas State for analysis of flexible pavement sections. The decision was made after discussion with ODOT's engineers due to similar conditions covered in the study. However, national calibration coefficients are employed for analysis of composite pavement since no calibration effort was found for composite pavement on literature. Table 36 shows the Arkansas calibration factors applied in this study.

Table 36 Calibration Coefficient Applied for MEPDG Analysis

Distress Type	Calibration Factor	Default	Calibrated Coefficient
Alligator Cracking	C_1	1.0	0.654
	C_2	1.0	0.263
	C_3	6000	6000
AC Rutting	βr_1	1.0	0.68
	βr_2	1.0	1.0
	βr_3	1.0	1.0
Base Rutting	βs_1	1.0	1.0
Subgrade Rutting	βs_2	1.0	0.85

Three rehabilitation categories including light rehabilitation (2" milling with overlay thickness of 2" or less), medium rehabilitation (2" milling with overlay thickness between 2" and 4") and heavy rehabilitation (2" milling with overlay thickness more than 4") are considered as feasible alternatives for each representative sections. The objective of such analysis is to find the extension in service life of existing pavements with different damage condition resulted from placing these three rehabilitation categories. The alternative scenarios are selected based on the commonly used rehabilitation designs on the state's highways. The extension is determined by changing the analysis period ranging from 1 to 30 years. The number of years after which design criteria and threshold recommended by AASHTO 2008 (*48*) at 95% reliability is met, has been considered as the extended service life. Table 37 shows the design criteria recommended by AASHTO 2008 (*48*) for use in evaluating the acceptability of a trial design for interstate highways.

Table 37 Threshold Values Used in This Study for Interstate Highways

Pavement Type	Performance Criteria	Maximum Value at End of Design Life
Asphalt Concrete Overlay on Asphalt Concrete Pavement	Alligator Cracking	10% Lane Area
	Rut Depth	0.4 in
	Thermal Cracks Length	500 ft./mi
	IRI	160 in/mi
Asphalt Concrete Overlay on JPCP, CRCP	Alligator Cracking	10% Lane Area
	Rut Depth	0.4 in
	Thermal Cracks Length	500 ft./mi
	IRI	160 in./mi
	Mean joint Faulting	0.15 in
	Reflection Cracks	10%

Once the analysis is accomplished for all identified scenarios, the evaluation matrix is developed to consolidate the analysis results and collected database into a decision support tool. This matrix presented in Table 38 and

Table 39 can serve as a guideline for identification of rehabilitation treatments which satisfy the pavement needs to a great extent. The computed structural numbers and damage factors in output matrix account for structural integrity of investigated pavements. The structural number, *SN*, is computed from Equation (45) which is suggested in AASHTO 1993 Design Guide:

$$SN = \sum a_i D_i \tag{45}$$

where D_i and a_i are layer thickness and layer coefficients respectively. a_i is function of backcalculated modulus and calculated from different equations in AASHTO Guide for asphalt concrete layer, granular base, cement treated base, bituminous treated base and granular subbase. Project information of representative sections including division, county, route, pavement type and etc. are presented in Appendix G.

Table 38 Evaluation Matrix for Identification of Rehabilitation Treatments for Composite Pavement Sections

Control Section	Family Group	Pavement Profile	Thickness (in.)	2010 AADT	Existing Pavement Condition							Rehabilitation Alternatives		Structural Life
					Pavement Performance Indexes						Damage (d_j)			
					Ride Index	Rut Index	Functional Index	Structural Index	PQI	SN				
												Light Rehab.	2" S5 76-28 (2" milling)	3
		Plain PCC	9.3		57	26	56	66	53	6.24	0.68	Medium Rehab.	3" S4 76-28 (2" milling)	6
		Hot Sand	4									Heavy Rehab.	2" S4 76-28, 3" S3 64-22 (2" milling)	15
		Lime/Subgrdae	-											
16-49	2	AC	3.8	6800	82	89	39	89	71	10.3	0.35	Light Rehab.	2" S5 76-28 (2" milling)	5
		Plain PCC	10.5									Medium Rehab.	4" S4 76-28, 2" milling	7
		Soil Asphalt	6											
		Subbase/Subgrade	-									Heavy Rehab.	2" S4 76-28, 3" S3 64-22, 2" milling	15
42-30	3	AC	2.4	23627	84	91	72	98	83	8.56	0.01	Light Rehab.	2" S5 76-28 (2" milling)	6
		PCC	9.1									Medium Rehab.	4" S4 76-28 (2" milling)	9
		Sand Cushion/Select	12									Heavy Rehab.	2" S4 76-28, 3" S3 64-22 (2" milling)	18
		Subgrade	-											
55-09	4	AC	7.6	48100	100	99	100	100	100	5.17	0.52	Light Rehab.	2" S5 76-28 (2" milling)	4
		Plain PCC	8.8									Medium Rehab.	4" S4 76-28 (2" milling)	9
		Sand Cushion/Select	12									Heavy Rehab.	2" S4 76-28, 3" S3 64-22 (2" milling)	12
		Subgrade	-											
50-32	5	AC	7.4	29631	100	97	99	100	99	7.05	0.23	Light Rehab.	2 S5 76-28, 2" milling	5
		CRCP	8.2									Medium Rehab.	3" S4 76-28, 2" milling	8
		FABB	4											
		Subgrade	-									Heavy Rehab.	2" S4 76-28, 3" S3 64-22, 2" milling	18
25-46 MP. 0	6	AC	7	29631	100	100	98	100	99	8.03	0.43	Light Rehab.	2" S5 76-28 (2" milling)	5
		Plain PCC	9.3									Medium Rehab.	4" S4 76-28 (2" milling)	8
		Hot Sand	4											
		Lime/Subgrade	-									Heavy Rehab.	2" S4 76-28, 3" S3 64-22 (2" milling)	17
72-09	7	AC	2	62600	91	96	99	100	95	8.13	0.15	Light Rehab.	2" S5 76-28,2" milling	4
		Plain PCC	9.4									Medium Rehab.	4" S4 76-28,2" milling	7
		Asphalt Sand	4									Heavy Rehab.	2" S4 76-28, 3" S4 64-22, 2" milling	16
		Subgrade	-											

Table 39 Evaluation Matrix for Identification of Rehabilitation Treatments for Flexible Pavement Sections

Control Section	Family Group	Pavement Profile	Thickness (in.)	2010 AADT	Existing Pavement Condition							Rehabilitation Alternatives		Structural Life
					Pavement Performance Indexes						Damage (d_i)			
					Ride Index	Rut Index	Functional Index	Structural Index	PQI	SN				
68-22	1	A.C.	5.7	17502	92	91	51	47	79	3.21	0.67	Light Rehab.	2" S5 76-28, 2" milling	7
		C.A.B.B.	7									Medium Rehab.	4" S4 76-28, 2" milling	8
		Lime	24									Heavy Rehab.	2" S4 76-28, 3" S3 64-22, 2" milling	20
		Subgrade	-											
44-05 MP.10.8	2	A.C.	7.5	30984	99	94	100	100	97	5.75	0.22	Light Rehab.	2" S5 76-28 , 2" milling	7
		F.A.B.B.	12									Medium Rehab.	1.5" S5 76-28, 2" S4 76-28, 2" milling	9
		Subgrade	-									Heavy Rehab.	2" S4 76-28, 3" S3 64-22, 2" milling	18
09-05	3	A.C.	12.8	25728	100	98	100	100	100	5.98	0.21	Light Rehab.	2" S5 76-28, 2" milling	6
		O.G.B.B.	3									Medium Rehab.	4" S4 76-28, 2" milling	9
		F.A.B.B.	3									Heavy Rehab.	2" S4 76-28, 3" S3 64-22, 2" milling	21
		Select borrow	6											
20-04	4	A.C.	11.1	22500	100	100	51	99	93	6.31	0.22	Light Rehab.	2" S5 76-28, 2" milling	7
		F.A.B.B.	8									Medium Rehab.	4" S4 76-28, 2" milling	9
		Select borrow	6									Heavy Rehab.	2" S4 76-28, 3" S3 64-22, 2" milling	20
		Subgrade	-											
44-05 MP.13.8	5	A.C.	14	35900	100	95	98	99	98	7.83	0.55	Light Rehab.	2.5" S4 76-28, 2" milling	9
		Soil Cement	10									Medium Rehab.	4" S4 76-28, 2" milling	15
		Subgrade	-									Heavy Rehab.	2" S4 76-28, 3" S3 64-22, 2" milling	20
55-68	6	A.C.	11.8	39309	88	85	89	100	89	4.74	0.7	Light Rehab.	2" S5 76-28, 2" milling	6
		Sand Asphalt	8									Medium Rehab.	4" S4 76-28, 2" milling	9
		Subgrade	-									Heavy Rehab.	2" S4 76-28, 3" S3 64-22, 2" milling	17
14-06	7	A.C.	14.25	81464	100	92	100	100	98	5.58	0	Light Rehab.	2" S5 76-28, 2" milling	7
		Agg. Base	8									Medium Rehab.	4" S4 76-28, 2" milling	11
		Stabilized Subgrade	8									Heavy Rehab.	2" S4 76-28, 3" S4 64-22, 2" milling	22
		Natural Subgrade	-											

CHAPTER 6. DEVELOPMENT OF TIME-BASED REHABILITATION STRETEGIES

The service life of rehabilitation obtained from MEPDG analysis served as an important guide in development of time-based rehabilitation strategies. The slight modification is applied on extended lives based on expert's opinion to account for field consideration and inaccuracy of some of performance prediction equations in MEPDG. Oklahoma Pavement Preservation Program (PPP) is studied to consider the commonly used maintenance activities and trigger value in the development of rehabilitation strategies for pavement family groups.

6.1. DEFINITION OF TYPICAL FLEXIBLE AND COMPOSITE PAVEMENT SECTIONS

Although different pavement groups investigated in this study have different structures, performance measures, and damage factors, the extension in service life obtained by applying overlays are almost similar for each rehabilitation category. The similarities for the effect of each rehabilitation category on different pavements can be explained to some extent by the thickness of pavements. Representative sections identified in this study are adequately thick such that almost none of the distresses initiated in these thick pavements are propagated more than 2-3 inches into the depth of the asphalt surface layer according to the recorded observations. Furthermore, regular milling off of the top 2 inches provides almost similar appropriate existing pavement condition for the entire pavement family groups. Due to the same structural integrity, flexible and composite pavement groups are shrunk to three typical flexible and two typical composite pavement sections which are illustrated in Figure 55 and Figure 56respectively. The range of typical thickness of each layer is also shown in these figures.

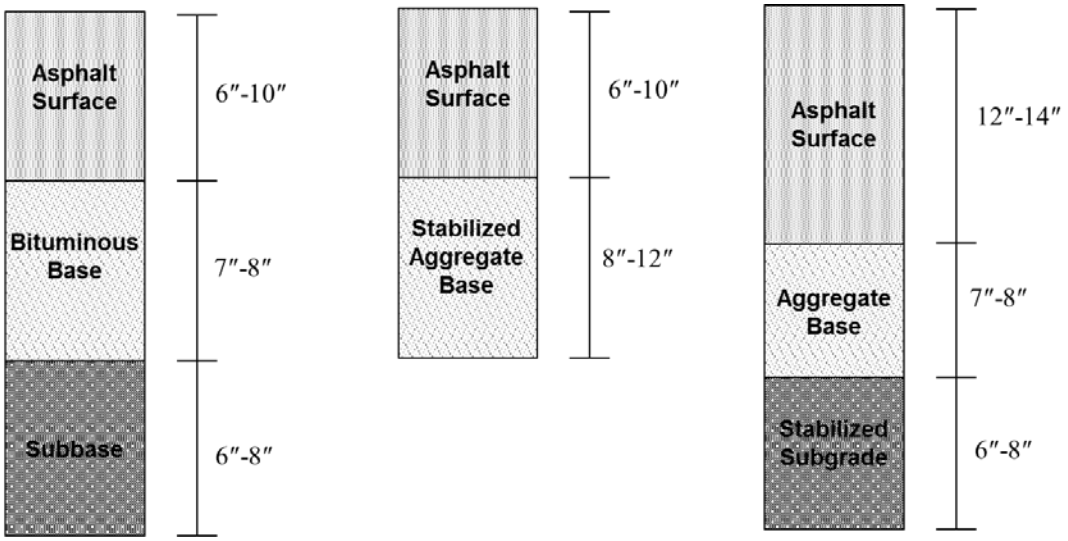

Figure 55 Three Typical Flexible Pavement Sections

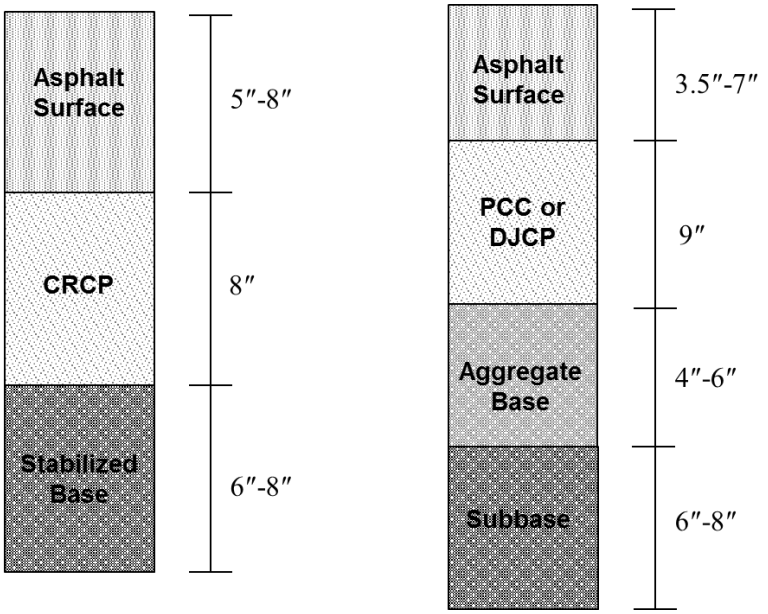

Figure 56 Two Typical Composite Pavement Sections

6.2. TIME-BASED REHABILITATION STRATEGIES

A series of time-based rehabilitation strategies are suggested for the aforementioned typical sections for high-volume traffic roads. The structural index is used as trigger value for categorizing rehabilitation strategies. Structural index of asphalt concrete and composite pavement is a load-related distresses measure defined in ODOT PMS database, which accounts for structural pavement rating as a result of propagating fatigue cracking, patches and pothole distresses built in pavements. Two trigger values of 80 and 60 are chosen for categorizing rehabilitation strategies. Two alternatives are suggested for each category and 2016 is assumed as the starting year of analysis period for all strategies. These strategies are illustrated in Figure 57 to Figure 62. Short and tall arrows in figures represent maintenance and rehabilitation activities respectively.

Time intervals are obtained based on service lives obtained from Mechanistic-Empirical analysis with MEPDG and modified properly to be in line with Oklahoma common rehabilitation practices. It must be noted that these strategies are developed based on the overlay design analysis of typical pavements mentioned in the previous section. Therefore, they can be applied merely for aforementioned sections. These simplified solutions are believed to provide a viable decision making tool for the agency's decision makers for the purpose of cost-effectiveness analysis of investigated renewal solutions in this study.

When the structural index is higher than 80, adequate structural integrity exists and no rehabilitation is required in 2016. When pavements reach to the threshold, which is assumed 60 in this study, medium or heavy rehabilitation are required to restore the pavement condition. Applying routine maintenance in a proper interval can extend the

service life of pavements. Routine maintenance in this study refers to maintenance activities which are common in Oklahoma such as Ultra-Thin Bonded Wearing Course, Microsurface and crack sealing, etc. Two solutions suggested for each level of structural category differ in the type and time of applying maintenance and/or the suggested rehabilitation activities. Among different combinations of mixtures and thickness that can be considered for light, medium and heavy rehabilitation (some of them are presented in Table 38 and
Table 39) four rehabilitation including 2" of mixture S5 PG 76-28 with 2" milling, 3" of mixture S4 PG 76-28 with 2" milling, 4" of mixture S4 PG 76-28 with 3" milling, 2" of mixture S4 PG 76-28 and 3" mixture of S3 64-22 with 3" milling are used in the development of rehabilitation solutions.

When the structural index is between 60 and 80, applying light rehabilitation in 2016 decreases the deterioration rate and delays the need for major rehabilitation. However, when the structural index is less than 60, pavements are in need of major rehabilitations in 2016. In general, placing overlay and milling on flexile pavements result in 5 more years of extended service life than that of the composite pavements. Including the aforementioned major considerations, time-based rehabilitation solutions are developed for Oklahoma interstate highways.

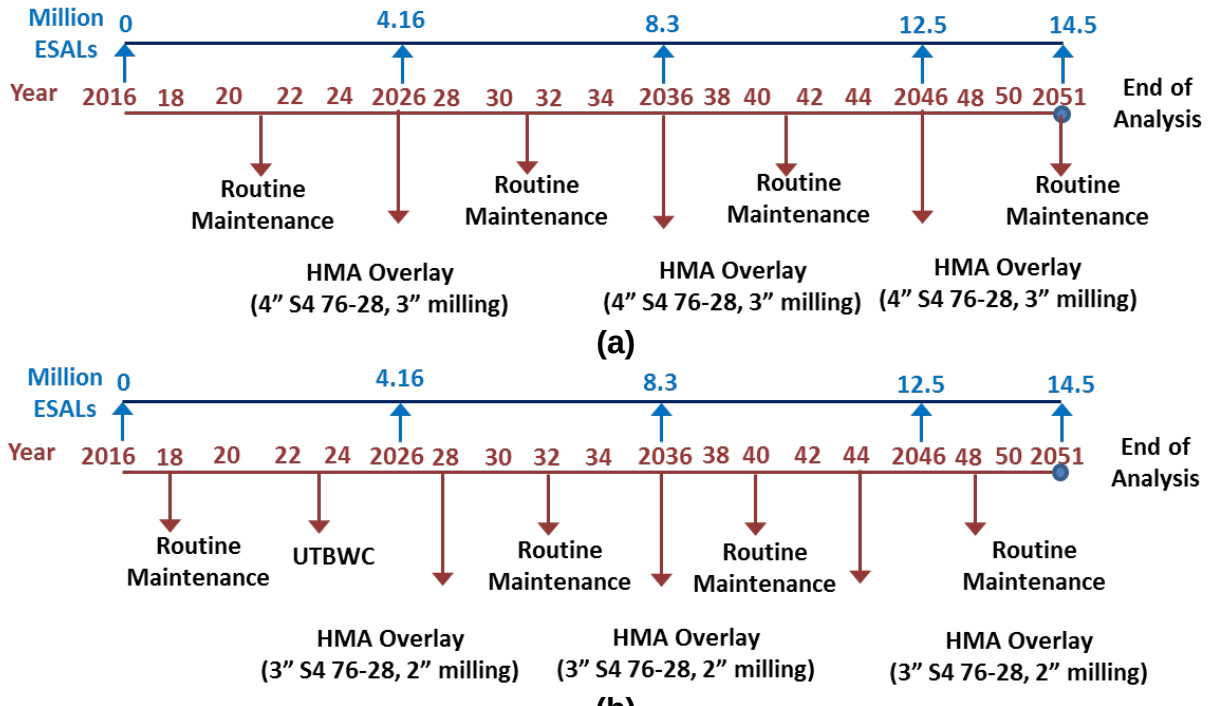

Figure 57 Two Suggested Rehabilitation Strategies, Alternatives (a) and (b), for Flexible Pavements with Structural Index>80

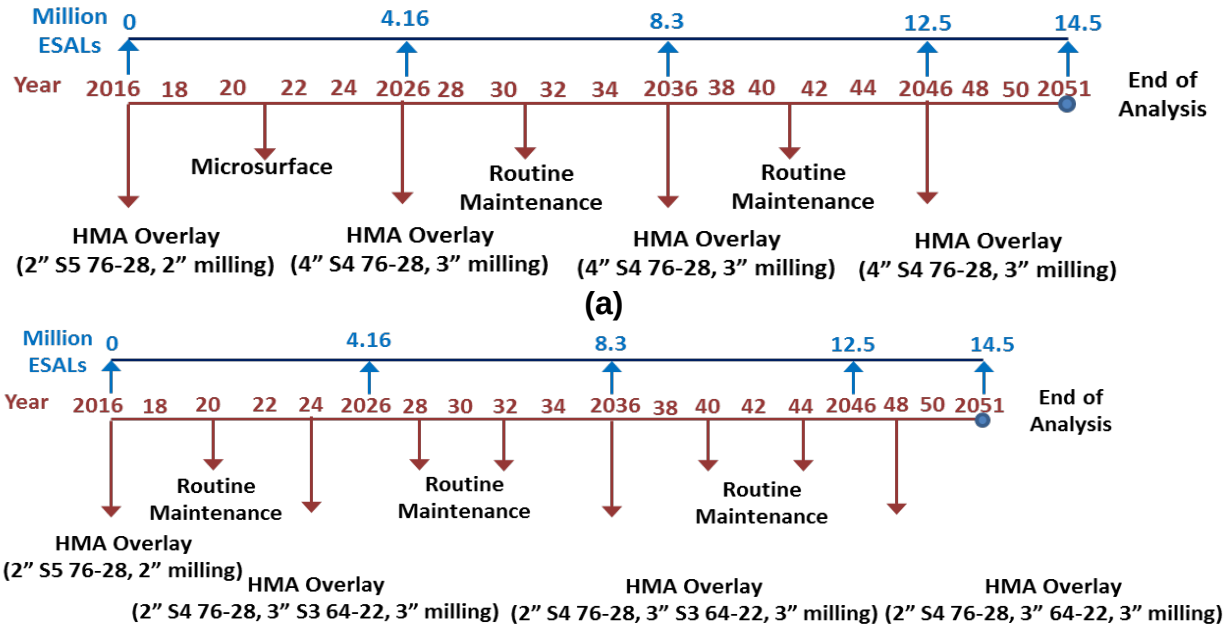

(a)

(b)

Figure 58 Two Suggested Rehabilitation Strategies, Alternatives a and b, for Flexible Pavements with 60≤ Structural Index ≤80

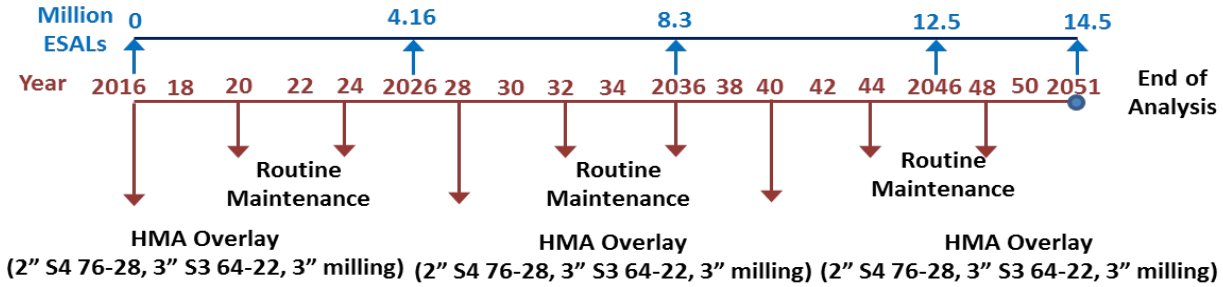

(a)

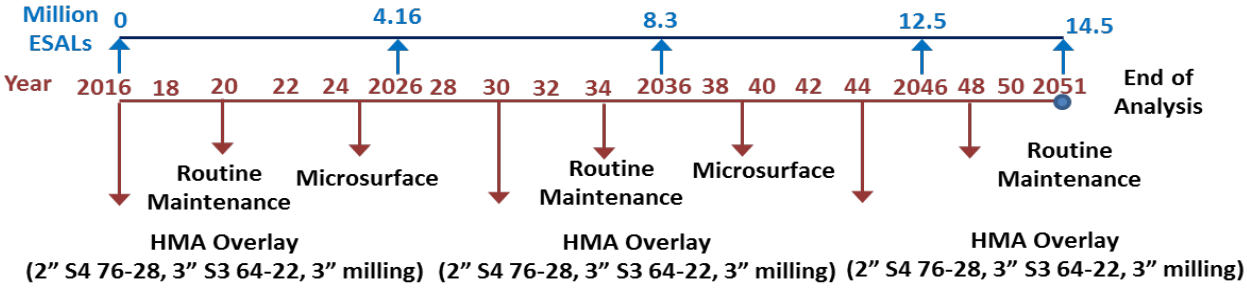

(b)

Figure 59 Two Suggested Rehabilitation Strategies, Alternatives a and b, for Flexible Pavements with Structural Index <60

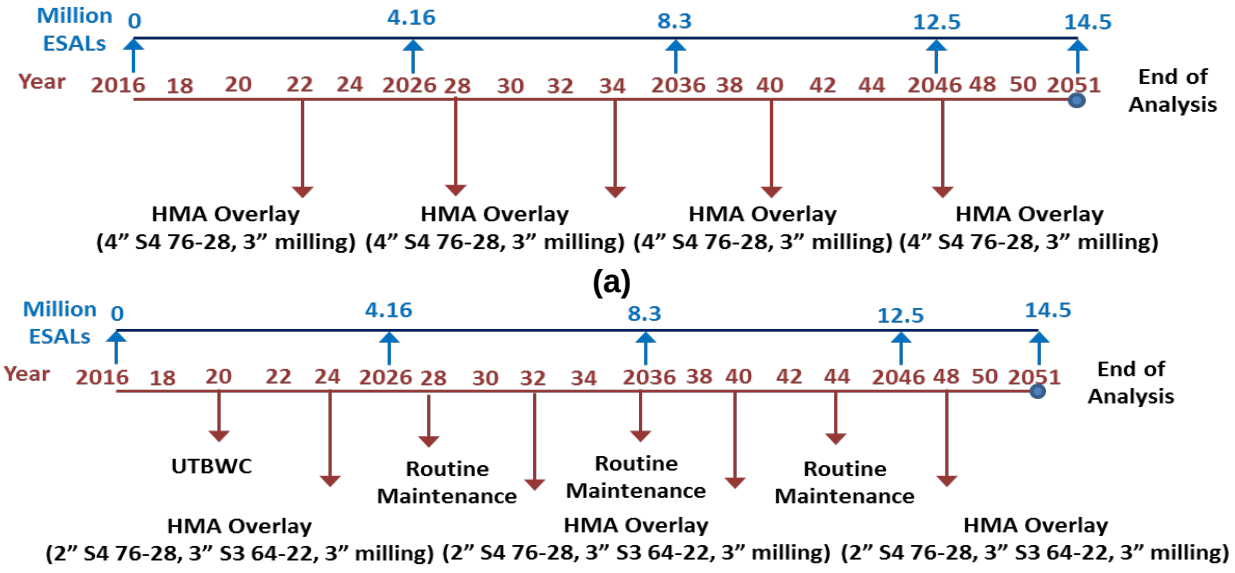

(a)

(b)

Figure 60 Two Suggested Rehabilitation Strategies for Composite Pavements with Structural index>80

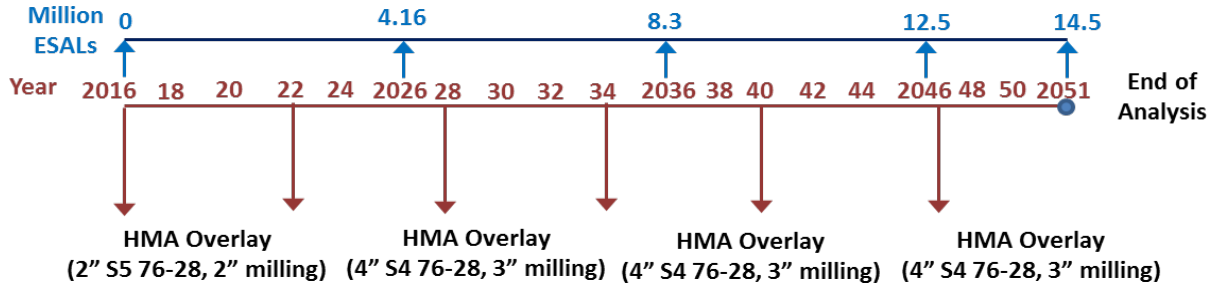

(a)

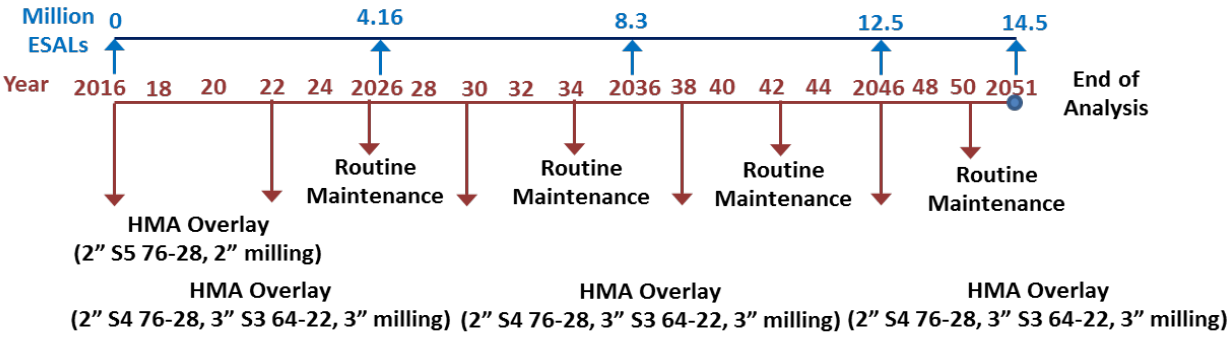

(b)

Figure 61 Two Suggested Rehabilitation Strategies for Composite Pavements with 60≤ Structural Index ≤80

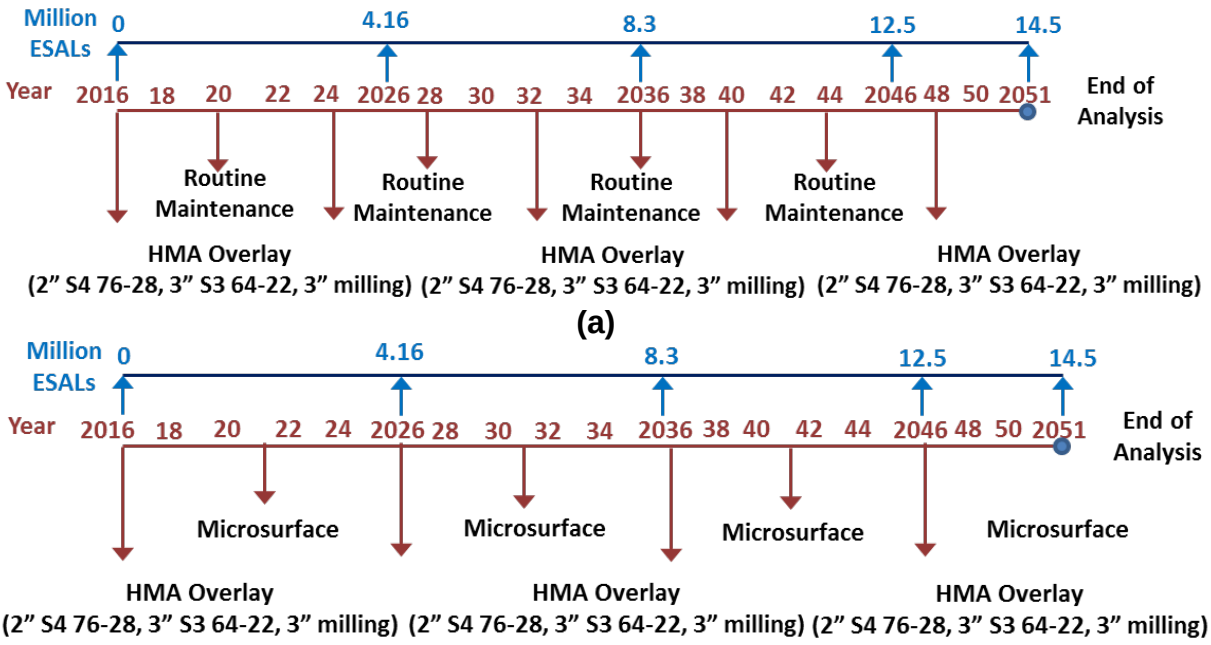

Figure 62 Two Suggested Rehabilitation Strategies, Alternatives a and b, for Composite Pavements with Structural index <60

CHAPTER 7. LIFE CYCLE COST ANALYSIS

The long-term economic efficiency of rehabilitation strategies is evaluated by performing life cycle cost analysis (LCCA). LCCA is an engineering economic analysis tool for comparing the competing design alternatives for transportation projects. For the purpose of this study, LCCA was conducted using Real-Cost 2.5 software, which is available through FHWA to calculate the agency and user costs for construction and rehabilitation solutions of highways (49, 50).

7.1. LCCA INPUTS AND ASSUMPTIONS

To make a reasonable life cycle cost comparison of alternatives, rehabilitation strategies are considered for sections with one mile length and total of four lanes in both directions (2 lanes each direction). Also, the AADT of 30,000 is assumed for all sections, and 2016 is adopted as the starting year for 35 years of analysis period. According to the ODOT PMS database, the cost of routine maintenance is assumed $60,000 per lane and mile.

The work zone time-delay and vehicle operation cost arising from the restriction of normal flow of the roadways as well as the increasing users' travel time due to creating queues or speed change through the work zone are calculated in the RealCost software based on FHWA's method as user costs. The appropriate estimate of activity work zone inputs such as work zone length, duration, hours and the number of lanes open in each direction during work zone are influential in calculating the value of user cost. In this study, work zone duration is calculated from Equation (46) (51):

$$WZD = \frac{Lane - miles}{PR} \quad (46)$$

where,

WZD = work zone duration

Lane-miles = the multiplication of the total length of pavement section and total number of lanes in both directions

PR = Productivity rate in lane-miles per day

Productivity rates of typical rehabilitation strategies are functions of lane closure strategies, and rehabilitation types. The work zone hours are assumed to be from 10 p.m. to 5 a.m. for rehabilitation activities and the total number of lanes in both directions (inbound and outbound) which is open under normal condition is four for all representative sections. It is assumed that one lane in each direction remains open during work zone. The extended pavement service lives of rehabilitation categories are considered as the structural lives of rehabilitation activities in RealCost software.

The historical bid price data of 2015 is extracted from the provided ODOT sources to compute the rehabilitation cost estimates (agency construction costs). The agency construction cost of existing pavements, user-delay cost associated with the routine maintenance and the cost associated with traffic control, preparation of pavements for placing overlays such as laying tack coat are excluded in this analysis. This decision

was made based on the assumption that these costs are almost the same for all investigated alternatives. Therefore, the agency cost includes only the cost of overlays and millings. The value of alternative at the end of the analysis period, called salvage value, is included in agency cost. Real-Cost estimates remaining service life value based on the project cost and the percentage of design life remaining at the end of analysis period. The major components, inputs and assumptions made for LCCA in this study are summarized in Table 40.

Table 40 Major LCCA Components Used in This Study

LCCA Component		Assumption
Analysis Period (Years)		35
Discount Rate (%)		4
Beginning of Analysis Period		2016
AADT Construction Year (total for both directions)		30,000
Single Unit Trucks as Percentage of AADT (%)		8
Combination Trucks as Percentage of AADT (%)		21
Annual Growth Rate of Traffic (%)		2.7
Speed Limit Under Normal Operating Conditions (mph)		65
Work Zone Speed Limit (mph)		40
Lanes Open in Each Direction Under Normal Condition		2
Free Flow Capacity (vphpl)		2127
Queue Dissipation Capacity (vphpl)		1700
Maximum Queue Length (miles)		5
Lane Width (ft)		12
Proportion of Trucks and Buses (%)		29
Lane Open in Each direction during work zone		1
Work Zone Capacity(vphpl)		1510
FHWA's Recommended User Delay Cost		
Vehicle Class	$ Value Per Vehicle Hour	
	Value of Time for Passenger Cars	12.8
	Value of Time for Single Unit Trucks	31.7
	Value of Time for Combination Trucks	31.7

7.2. LIFE CYCLE COST RESULTS AND DISCUSSION

The agency and user costs of suggested rehabilitation strategies for typical flexible and composite pavement sections are presented in Figure 64. Table 41 summarizes the user and agency cost of different alternatives. The alternatives which are shown as “alternative a” and alternative “b” in following figures, do not refer to the same

strategies. In fact, alternatives “a” in rehabilitation strategy which is assigned to pavements with structural index higher than 80, is different from the one that is assigned to pavement with structural index less than 60.

As it can be seen from figures, when structural index is higher than 80 for flexible pavements, alternative “b” yields lowest user cost and alternative “a” results in lower agency cost. In general, alternative “a” is more cost-effective than alternative “b” in the long term. For flexible pavements with structural index between 60 and 80, alternative “a” has the lower total cost while for pavements with structural index less than 60 alternative “b” shows the lower total cost. A review of composite pavements reveals that alternative “a” leads to lower total cost for pavements with a structural index higher than 80 and between 60 and 80 while alternative “b” yields lower total cost for pavements with a structural index less than 60. The more cost-effective alternatives for flexible and composite pavements are presented in Figure 65 and Figure 66 respectively. Although the rehabilitation strategies with lower total cost are selected as the preferred solutions, it should be noted that both alternatives for flexible and composite pavements provide feasible and effective solutions.

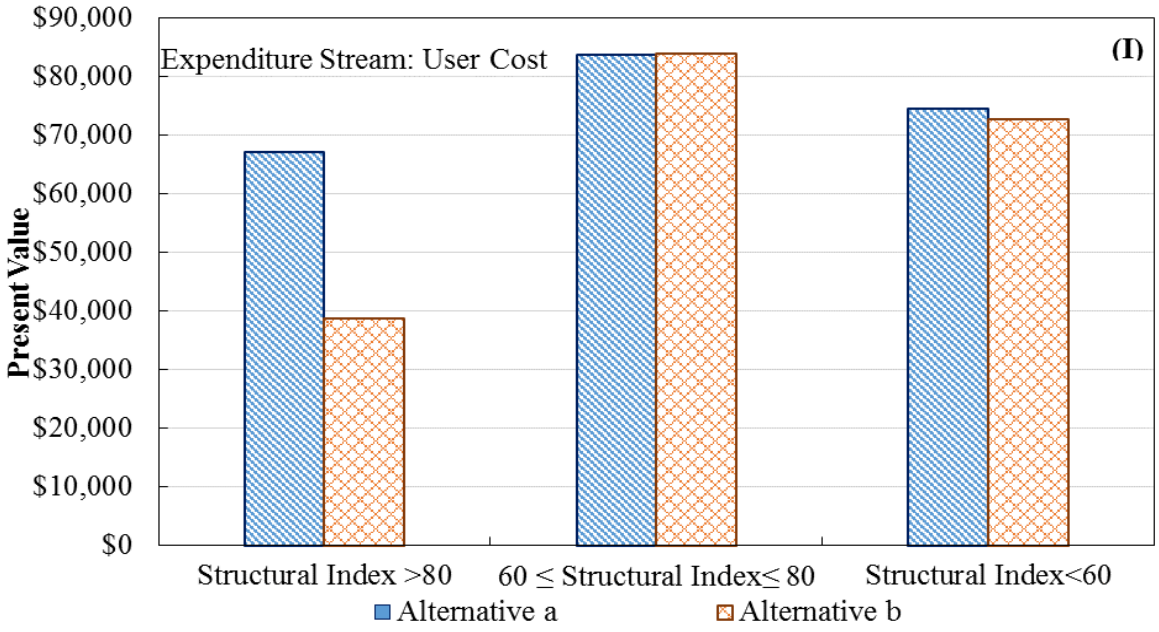

(I)

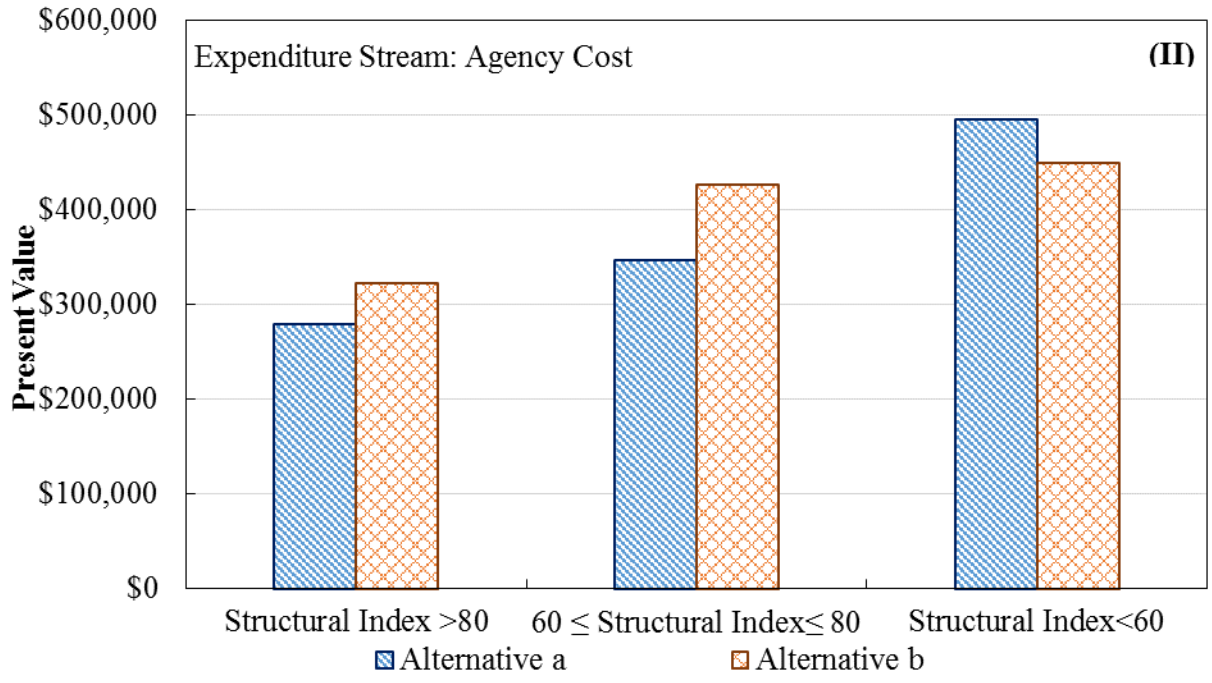

(II)

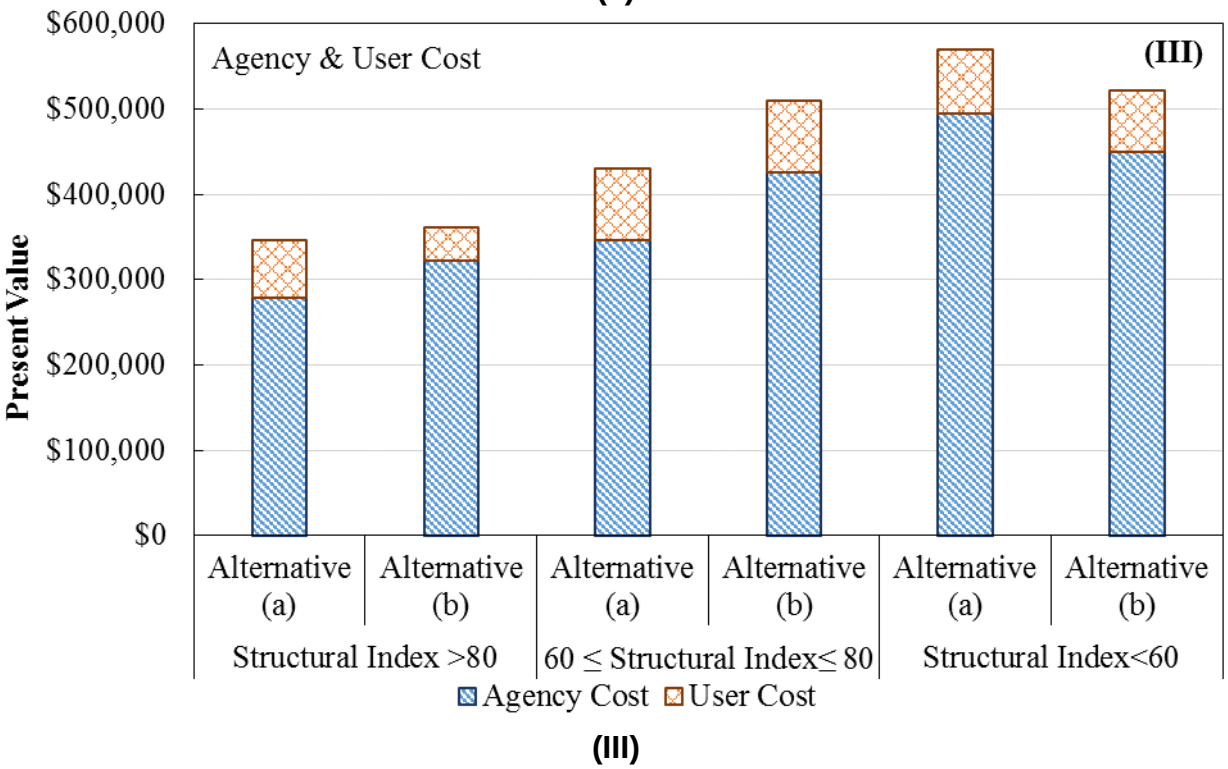

(III)

Figure 63 Comparison of Net Present Value (NPV) in Terms of (I) User, (II) Agency and (III) Total (Agency and User) Life-Cycle Cost for Rehabilitation Alternatives of Typical Flexible Pavement Sections.

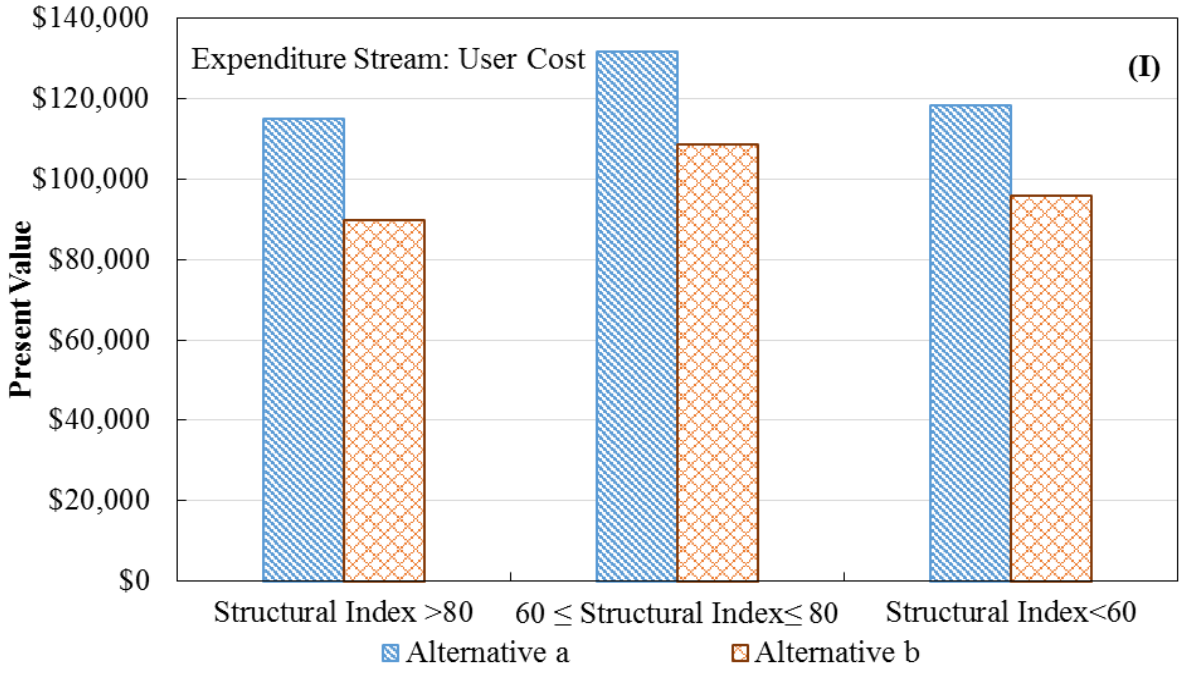
Expenditure Stream: User Cost
(I)
$140,000
$120,000
$100,000
$80,000
$60,000
$40,000
$20,000
$0
Present Value
Structural Index >80
60 ≤ Structural Index≤ 80
Structural Index<60
Alternative a
Alternative b

(I)

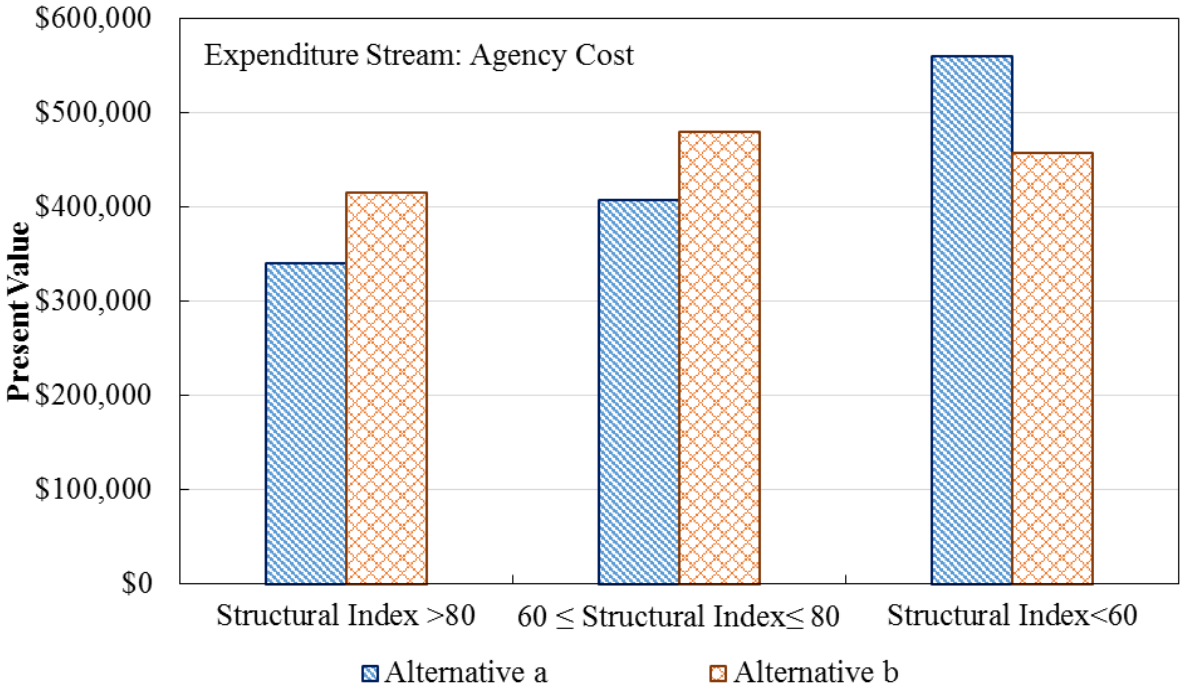
Expenditure Stream: Agency Cost
$600,000
$500,000
$400,000
$300,000
$200,000
$100,000
$0
Present Value
Structural Index >80
60 ≤ Structural Index≤ 80
Structural Index<60
Alternative a
Alternative b

(II)

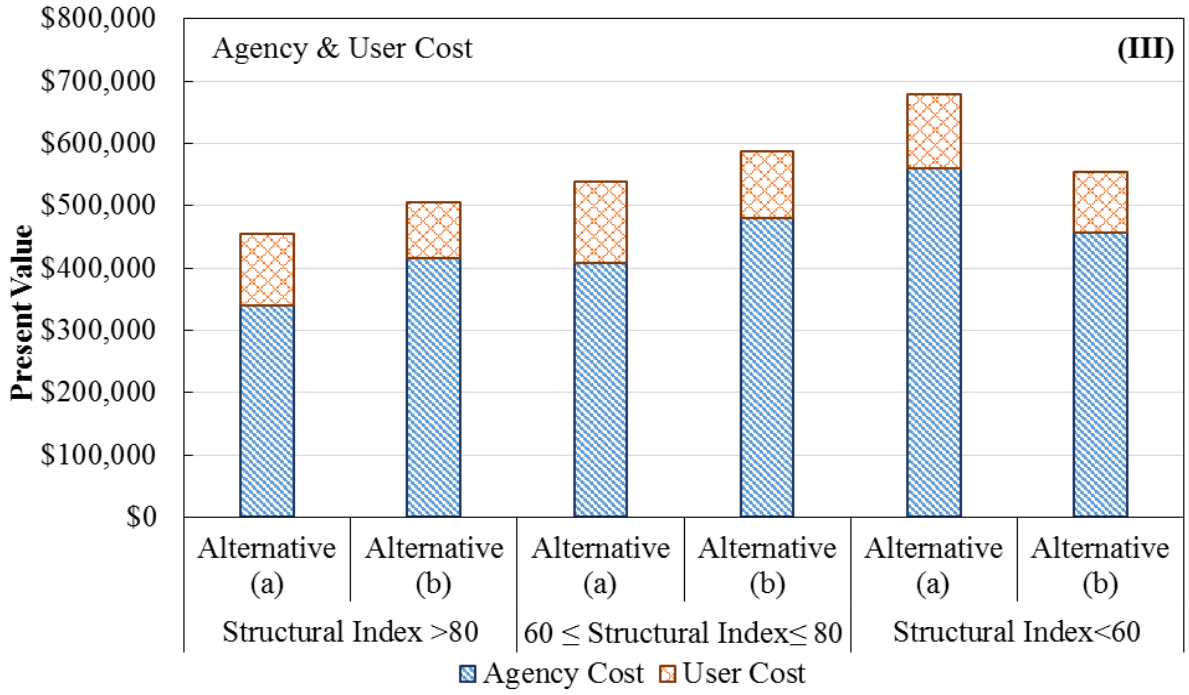

(III)

Figure 64 Comparison of Net Present Value (NPV) in Terms of (I) User, (II) Agency and (III) Total (Agency and User) Life Cycle Cost for Rehabilitation Alternatives of Typical Composite Pavement Sections.

Table 41 Life Cycle Cost Associated with Alternatives

Cost $	Pavement Type	Structural Index >80		60 ≤ Structural Index≤ 80		Structural Index<60	
		Alternative (a)	Alternative (b)	Alternative (a)	Alternative (b)	Alternative (a)	Alternative (b)
User Cost	Composite	114,903	89,695	131,494	108,571	118,352	95,857
	Flexible	67,201	38,832	83,791	83,947	74,487	72,835
Agency Cost	Composite	340,444	415,029	407,141	479,367	559,765	457,496
	Flexible	279,501	322,799	346,198	426,173	495,287	449,466
Total Cost	Composite	455,347	504,724	538,635	587,938	678,117	553,353
	Flexible	346,701	361,631	429,989	510,119	569,774	522,301

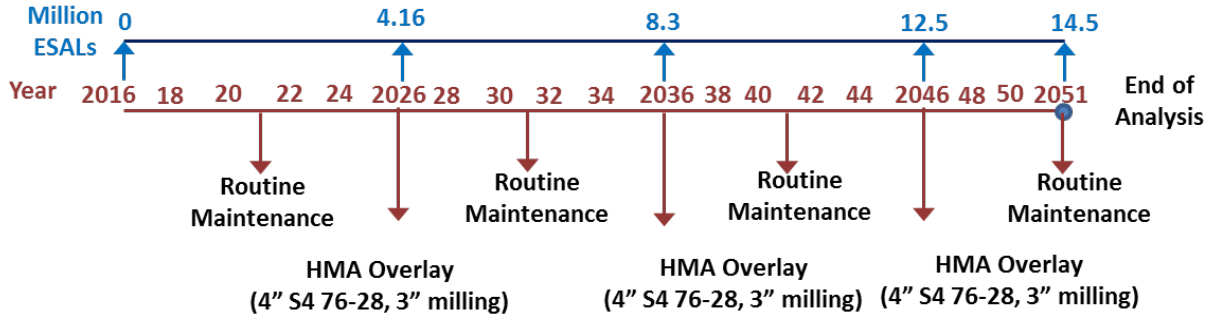

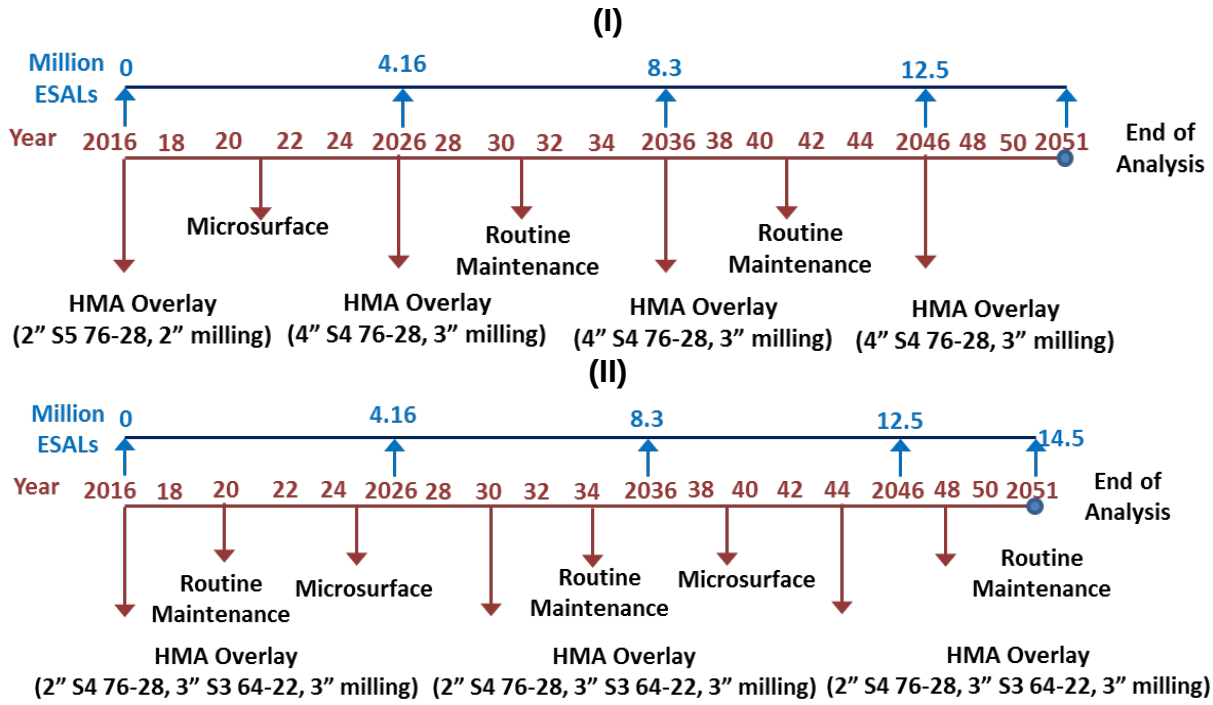

Figure 65 Cost-effective Time-based Rehabilitation Strategies for Flexible Pavements Sections with (I) Structural Index>80, (II) 60≤ Structural Index ≤80, (III) Structural Index<60

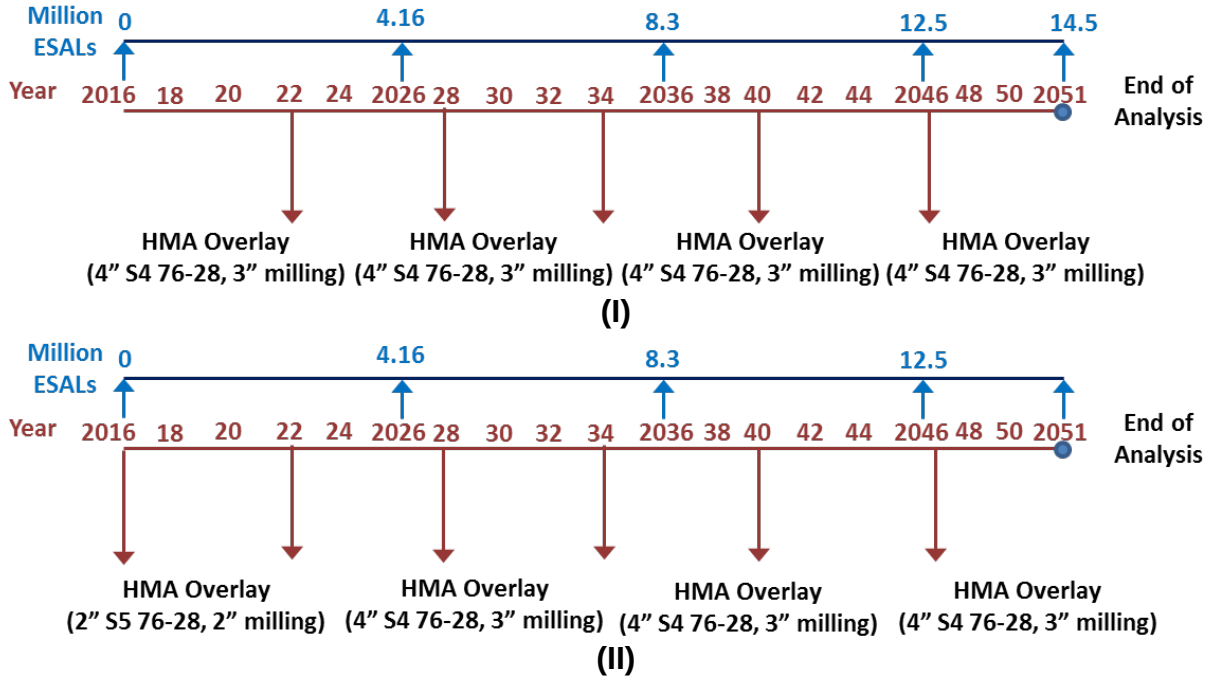

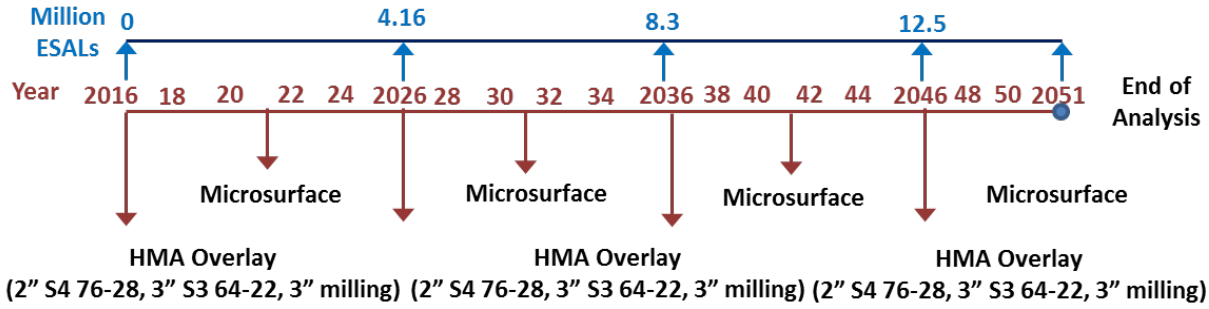

(III)

Figure 66 Cost-effective Time-based Rehabilitation Strategies for Composite Pavements Sections with (I) Structural Index>80, (II) 60≤ Structural Index ≤80, (III) Structural Index<60

CHAPTER 8. SUMMARY AND RECOMMENDATION

The findings presented in this section are based on the analysis of national highways located in the State of Oklahoma. National highways are divided into seven flexible and composite pavement family groups. The representative pavement sections for family groups are identified and required database including laboratory and field data are either extracted from existing data or measured to evaluate the condition of existing pavements and material characteristic of overlay mixtures. The summary of findings from performed tasks is presented in the following sections.

8.1. DYNAMIC MODULUS TEST

The dynamic modulus values of five representative mixtures commonly used in overlay projects in Oklahoma including S3 PG 64-22, S4 PG 64-22, S4 PG 70-28, S4 PG 76-28 and S5 PG 76-28 mixture types are tested in the laboratory to provide the level 1 hierarchical inputs for overlay design using MEPDG. The test results show that the mixture S3 64-22 have the highest dynamic modulus and S4 PG 70-28 mixture have the lowest values over the entire ranges of testing conditions. According to the observed results, it can be concluded that course mixtures containing high percentage of RAP and low binder content show higher dynamic modulus than fine mixtures with low RAP content and high binder content. Also, in case of having same nominal maximum aggregate size and RAP percent, mixtures containing binder with a higher high-temperature grade and lower binder content have higher dynamic modulus values. So, the order of mixtures with decreasing dynamic modulus values is S3 PG 64-22, S4 PG 64-22, S5 PG 76-28, S4 PG 76-28, S4 PG 70-28.

8.2. HAMBURG WHEEL TRACKING TEST

The rutting and stripping resistance of listed mixtures in previous section is evaluated using Hamburg wheel Tracking test device. Of five mixtures evaluated in this study, mixture S5 PG 76-28 shows the highest rutting and stripping resistance and S4 PG 70-28 mixture shows the lowest resistance. Therefore, S5 PG 76-28 mixture can be considered as one of the most balanced design mixtures for rehabilitation when surface rutting is a major problem. According to obtained results in this study, fine dense graded aggregate mixed with high modified binder tend to have higher rutting resistance than coarse aggregate with unmodified binder. To properly study the effect of all contributing factors on rutting and stripping resistance of mixtures, mineralogy and chemical composition of aggregates along with binder type, aggregate gradation, binder content, and RAP percentage were needed however they were not available during this research study. The order of mixtures with decreasing rutting and stripping resistance is S5 PG 76-28, S4 PG 64-22, S4 PG 76-28, S3 64-22, S4 PG 70-28.

8.3. DIRECT TENSION CYCLIC FATIGUE TEST

The fatigue resistant of mixtures are evaluated by using uniaxial fatigue test. It was observed that the S3 64-22 and S4 64-22 mixture damage curves are positioned higher and fail much quicker than the other three mixtures. It's clearly seen that S5 and S4 76-28 mixtures sustain higher damage than the other three mixtures. The simulated fatigue life plot depicts that S4 76-28 mixture have highest fatigue life and S3 64-22 have least fatigue life of all tested mixtures in this study.

8.4. INDIRECT TENSION (IDT) CREEP COMPLIANCE AND STRENGTH TEST

The tensile strength and creep compliance property of mixtures are evaluated through IDT test. From the modulus test results it was observed that S3 64-22 mix is stiffest and S4 70-28 mix is softest among all five mixtures tested. The creep compliance mastercurves indicates that the S4 70-28 mix have highest creep compliance and S3 64-22 mix have lowest creep compliance at all testing temperatures which is corroborating with the experimental findings from the dynamic modulus test results. Also, the results of tensile strength test of the different mixtures show that the mix with a higher RAP content (S4 64-22 mix) has the highest strength and the mix with the highest asphalt content (S4 70-28 mix) shows the lowest strength of all mixtures.

8.5. FALLING WEIGHT DEFLECTOMETER (FWD) DATA ANALYSIS

A total of 1006 individual FWD drops on 15 different control sections have been analyzed according to both the 1993 AASHTO design guide and MEPDG input requirements. For the 1993 AASHTO design guide based analysis temperature corrections were applied to the drop plate deflections using an iterative method described in the design guide. The moduli backcalculated for the individual layers were corrected according to a two-step process using a TTI model to predict the mid-depth temperature and the Witczak-Fonesca model to correct for temperature and frequency of loading. Both analyses provide similar conclusions regarding which control sections are more structurally compromised. They show that overall the flexible sections are less structurally sound than the composite sections.

8.6. MECHANISTIC-EMPIRICAL PAVEMENT ANALYSIS

The representative pavement sections are modeled in MEPDG version 1.1 using gathered and measured data. Three rehabilitation categories, which are in line with commonly used rehabilitation on Oklahoma highways, including light rehabilitation (2" milling with overlay thickness of 2" or less), medium rehabilitation (2" milling with overlay thickness between 2" and 4") and heavy rehabilitation (2" milling with overlay thickness more than 4") are considered as feasible alternatives for each representative sections. The extension in life resulting from different overlay alternatives is then determined by changing the analysis period ranging from 1 to 30 years. The number of years after which design criteria and threshold recommended by AASHTO 2008 at 95% reliability is met, has been considered as the extended service life. The results of design analysis

show that the light, medium and heavy rehabilitation treatments extend the life of existing flexible pavement by 5-7, 8-11 and 17-22 years respectively. Also, placing light, medium and heavy rehabilitation on composite pavements extend the life of existing pavements by 3-5, 6-9 and 15-18 years respectively.

The evaluation matrix is developed in this study to consolidate the analysis results and collected database into a decision support tool. This matrix can be served as a guideline for identification of rehabilitation treatments which satisfy the pavement needs to a great extent.

8.7. DEVELOPMENT OF TIME-BASED REHABILITATION STRATEGIES AND LIFE CYCLE COST

The service life of rehabilitation obtained from MEPDG analysis served as a guide in the development of time-based rehabilitation strategies. The slight modification is applied on extended service lives based on expert opinions to account for field consideration and inaccuracy of some of performance prediction equations in MEPDG. Three typical flexible and two typical composite pavement groups with specified thickness of layers are defined to cover major Oklahoma interstate highways. A series of time-based rehabilitation solutions are suggested for these typical sections and structural index is used as trigger value for categorizing rehabilitation strategies. Two alternatives are considered for pavements with different levels of structural index. These simplified solutions are believed to provide a viable decision making tool for the agency's decision makers for the purpose of cost-effectiveness analysis of investigated renewal solutions in this study.

The results of life cycle cost analysis on suggested alternatives reveal the more cost-effective rehabilitation solution compared to other alternative candidates for typical pavements.

8.8. RECOMMENDATION FOR FUTURE RESEARCH

- The selected pavement family groups are good representatives of different high-volume traffic pavements and cover a variety of pavement conditions. Therefore, it is recommended that the identified pavement sections be monitored over time to collect the additional field observations that can be used for local calibration of MEPDG for the state and enhance the results of this study.

- A deterministic life cycle cost analysis is conducted in this study. However, in order to incorporate the various probabilistic parameters into the analysis, the probabilistic life cycle cost analysis is recommended to be conducted for future research.

- Five mixtures are studied in the current study as common rehabilitation mixtures. However, it is recommended to assess more mixture types and develop a database catalog of all mixtures used in different Oklahoma field divisions for rehabilitation projects in future.

REFERENCES

1. American Association of State Highway and Transportation Officials (AASHTO), (1993). *Guide for Design of Pavement Structures*, AASHTO, Washington, DC.
2. National Cooperative Highway Research Program, (2004). *Mechanistic-Empirical Pavement Design Guide*, Transportation Research Board, Washington, DC.
3. Rauhut, J.B, Von Quintus, H.L., and Eltahan, A.A., (2000). *Performance of Rehabilitated Asphalt Concrete Pavements in the LTPP Experiments—Data Collected Through February 1997*, Report No. FHWA-RD-00-029, Federal Highway Administration, Washington, DC.
4. Von Quintus, H.L., Simpson, A.L., and Eltahan, A.A., (2001). *Rehabilitation of Asphalt Concrete Pavements—Initial Evaluation of the SPS-5 Experiment*, Report No. FHWA-RD-01-168, Federal Highway Administration, Washington, DC.
5. Hall, K.T., Correa C.E., and Simpson, A.L., (2002). *LTPP Data Analysis: Effectiveness of Maintenance and Rehabilitation Options*, NCHRP Web Document 47 (Project 20-50(3/4)), National Cooperative Highway Research Program, Washington, DC.
6. Von Quintus, H.L. and Mallela, J., (2005). *Reducing Flexible Pavement Distress in Colorado Through the Use of PMA Mixtures*, Final Report Number 16729.1/1, Colorado Asphalt Pavement Association, Denver, CO.
7. Carvalho, R., Ayres, M., Shirazi, H., Selezneva, O., Darter, M., (2011). *Impact of Design Features on Pavement Response and Performance in Rehabilitated Flexible and Rigid pavements,* Final Report No. FHWA-HRT-10-066, Federal Highway Administration, Washington, DC.
8. Peshkin, D., Smith, K. L., Wolters, A., Krstulovich, J., Moulthrop, J., Alvarado, C., (2011). *Preservation Approaches for High-Traffic-Volume Roadways,* Transportation Research Board, Washington, D.C., Obtained from: http://www.trb.org/Main/Blurbs/165280.aspx
9. Wu, Zh., Groeger, J. L., Simpson, Amy L., Hicks, R.G., (2010). *Performance Evaluation of various Rehabilitation and Preservation Treatments,* Final Report No. FHWA-HIF-10-020, Federal Highway Administration, Washington, DC.
10. Oklahoma department of Transportation (ODOT), (2011). *2011 Conditions and Performance of Pavements on the National Highway System in Oklahoma*, Oklahoma Department of Transportation, Pavement Management Branch..
11. AASHTO T 308, “Determining the Asphalt Binder Content of Hot Mix Asphalt (HMA) by the Ignition Method”, AASHTO, Washington, D.C.
12. McDaniel, R., Anderson, R., (2001). *Recommended Use of Reclaimed Asphalt Pavement in the Superpave Mix Design Method*, NCHRP Report No. 452, Transportation Research Board, Washington, D.C.

13. Kvasnak, A., (2010). *What to Consider When Designing a High RAP Content Mix*, Hot Mix Asphalt Technology, National Asphalt Pavement Association, Vol. 18, pp. 18-19.

14. Zhou, Fujie, Hu, Sheng, Das, G., Scullion, Tom, (2011). *High RAP Mixes Design Methodology with Balanced Performance*, FHWA/TX-11/0-6092-2.

15. AASHTO T 27-14, "Standard Method of Test for Sieve Analysis of Fine and Coarse Aggregates", AASHTO, Washington, D.C.

16. AASHTO T 209, "Theoretical Maximum Specific Gravity and Density of Hot Mix Asphalt Paving Mixtures", AASHTO, Washington, D.C.

17. Prowell, B. D., Brown, E. R., (2007). *Superpave Mix Design: Verifying Gyration Levels in the Ndesign Table,* Transportation Research Board, Washington, D.C., http://onlinepubs.trb.org/onlinepubs/nchrp/nchrp_rpt_573.pdf. Last accessed October 2015.

18. AASHTO PP 60-13, "Standard Practice for Preparation of Cylindrical Performance Test Specimens Using the Superpave Gyratory Compactor (SGC)", AASHTO, Washington, D.C.

19. AASHTO T166-13, "Bulk Specific Gravity of Compacted Hot Mix Asphalt Using Saturated Surface- Dry Specimens", AASHTO, Washington, D.C.

20. Cross, Stephen A., Jakatimath, Y., KC, S., (2007). *Determination of Dynamic Modulus Master Curves for Oklahoma HMA Mixtures*, Final report sponsored by Oklahoma Department of Transportation.

21. AASHTO TP79-13, "Determining the Dynamic Modulus and Flow Number for Asphalt Mixtures Using the Asphalt Mixture Performance Tester (AMPT)", AASHTO, Washington, D.C.

22. AASHTO R 30-02, "Standard Practice for Mixtures Conditioning of HOT-Mix Asphalt", AASHTO, Washington, D.C.

23. AASHTO T 324-11, "Hamburg Wheel-Track Testing of Compacted Hot Mix Asphalt", AASHTO, Washington, D.C.

24. Aschenbrener, T., and G. Currier, (1993). *Influence of Testing Variables on the Results from the Hamburg Wheel-Tracking Device*, CDOT-DTD-R-93-22. Colorado Department of Transportation.

25. Reese, R. (1997). *Properties of Aged Asphalt Binder Related to Asphalt Concrete Fatigue Life*, Journal of the Association of Asphalt Paving Technologists, Vol. 66, pp. 604-632.

26. Kim, Y. R., D. N. Little., and R. L. Lytton. (2003). *Fatigue and Healing Characterization of Asphalt 27 Mixtures.* Journal of Materials in Civil Engineering, Vol. 15(1), pp. 75-83.

27. Daniel, J.S., and Y. R. Kim. (2002). *Development of a Simplified Fatigue Test and Analysis 20 Procedure Using a Viscoelastic Continuum Damage Model*, Journal of the Association of Asphalt Paving Technologists. Vol. 71, pp. 619-650.

28. Chehab, G. R., Kim, Y. R., Schapery, R. A., Witczack, M.W., Bonaquist, R., (2003). *Characterization of Asphalt Concrete in Uniaxial Tension Using a Viscoelastoplastic Model,* Journal of the Association of Asphalt Paving Technology, Vol. 72, pp. 315-355.

29. Underwood, B. S., Kim, Y. R., Guddati, M. N., (2010). *Improved Calculation Method of Damage Parameter in Viscoelastic Continuum Damage Model*, International Journal of Pavement Engineering, Vol. 11, No. 6, pp. 459-476.

30. Hou, T., Underwood, B. S., Kim, Y. R., (2010). *Fatigue Performance Prediction of North Carolina Mixtures Using the Simplified Viscoelastic Continuum Damage Model*, Journal of the Association of Asphalt Paving Technologists, Vol. 79, pp. 35-80.

31. Sabouri, M., Kim, Y. R., (2014). *Development of a Failure Criterion for Asphalt Mixtures Under Different Modes of Fatigue Loading*, Transportation Research Record: Journal of the Transportation Research Board, No. 2447, Transportation Research Board of the National Academies, Washington, D.C., pp. 117-125.

32. AASHTO T 322-07, *Determining the Creep Compliance and Strength of Hot Mix Asphalt Using the Indirect Tensile Test Device*, AASHTO, Washington, D.C.

33. AASHTO (1993), "AASHTO Guide for Design of Pavement Structures," AASHTO, Washington, D.C.

34. Fugro Consultants LP. (2006), *Description of Variables for Analyzing Results of FWD, GPR, and Coring Information*, Project 1409, Final Report Submitted to Oklahoma Department of Transportation, Transportation Planning and Research Division, Engineering Services Branch.

35. Fugro Consultants LP. (2006), *Summary Report for Falling Weight Deflectometer (FWD) and Ground Penetrating Radar (GPR) Pavement Evaluation*, Project 3201-14091409, Report Submitted to Oklahoma Department of Transportation, Transportation Planning and Research Division, Engineering Services Branch.

36. Liu, W., Scullion, T., (2001), *Modulus 6.0 for Windows: User's Manual*, Report No. FHWA/TX-05/0-1869-2, Federal Highway administration.

37. Lukanen, E.O., Stubstad, R.N., Briggs, R., (1998). *Temperature Predictions and Adjustment Factors for Asphalt Pavements*, Report No. FHWA-RD-98-085. Federal Highway Administration.

38. Fernando, E.G., Liu, W., Ryu D., (2001). *Development of a Procedure for Temperature Correction of Backcalculated AC Modulus*, Report No. FHWA/TX-02/1863-1, Texas Department of Transportation, Austin TX.

39. Stubstad, R.N., Lukanen, E.O, Richter, C.A., Baltzer, S., (1998). *Calculation of AC Layer Temperatures from FWD Field Data*, Proceedings of the 5th International Conference on the Bearing Capacity of Roads and Airfields, Trondheim, Norway.

40. National Oceanic and Atmospheric Administration, *Daily Summary Observations*, Online: https://gis.ncdc.noaa.gov/map/viewer/#app=clim&cfg=obs&theme=ghcn, Accessed May 2015.

41. Lytton, R. L., Germann, F.P., Chou, Y.J., Stoffels, S.M., (1990). *Determining Asphaltic Concrete Pavement Structural Properties by Nondestructive Testing*, National Cooperative Highway Research Program (NCHRP) Report 327, Transportation Research Board, Washington D.C.

42. ARA, Inc., (2004). *Guide for Mechanistic-Empirical Design of New and Rehabilitated Pavement Structures*, National Cooperative Highway Research Program (NCHRP) 1-37A. Transportation Research Board, Washington D.C.

43. Texas Department of Transportation (TXDOT), (2011). *Pavement Design Guide*, Texas Department of Transportation, Revised 2011.

44. Oklahoma Department of Transportation, *2009 Standard Specification Book*, http://www.odot.org/c_manuals/specbook/oe_ss_2009.pdf, Last accessed October, 2015.

45. Hartronft, B.C., (1976). *Performance of Coarse Aggregate, Hot Sand and Asphaltic Concrete Bases in Oklahoma*, Transportation Research Circular Journal, Vol. 177, pp. 20-eoa.

46. Oklahoma Highway Department (OHD), (1965). *Engineering Classification of Geologic Materials (Red Books)*, Oklahoma Research Project 61-01-1, Research and Development Division. Oklahoma City, Oklahoma.

47. Hossein, Z., Zaman, M., Doiron, C., Cross, S., (2011). *Development of Flexible Pavement Database for Local Calibration of MEPDG*, Report NO. FHWA-OK-11-06(1), Washington, DC.

48. American Association of State Highway and Transportation Officials (AASHTO). (2008). *Mechanistic-Empirical Pavement Design Guide: A Manual of Practice*. AASHTO Designation: MEPDG-1. Washington, DC.

49. FHWA. U.S. Department of Transportation, (2004). *Life-Cycle Cost Analysis RealCost User Manual*, www.fhwa.dot.gov/infrastructure/asstmgmt/rc210704.pdf, Accessed June 1, 2015.

50. FHWA, U.S. Department of Transportation, (2002). *Life-Cycle Cost Analysis Primer*, isddc.dot.gov/OLPFiles/FHWA/010621.pdf, Accessed June 1, 2015.

51. State of California, Department of Transportation (Caltrans), *Life-Cycle Cost Analysis Procedures Manual*, State of California, Department of Transportation, Pavement Standards Team & Division of Design. 2010.

APPENDIX A. AGGREGATE PROPORTION AND JMF OF TESTED MIXTURES

Table 42 Aggregate Proportion and JMF of Tested Mixture: S3 PG 64-22

S3 PG 64-22, Mix ID: S3c00931100102	
Aggregate	**%Used**
#67 Rock	30
1/2" Chips	10
Man. Sand	35
Sand	10
Fine Rap	15
Combined Gradation	
Sieve Size	**JMF**
3/4"	100
1/2"	90
3/8"	79
#4	57
#8	41
#16	28
#30	19
#50	12
#100	7
#200	5.1
Asphalt Binder Content	
% Asphalt Cement	**% New asphalt cement**
4.4	3.6
Specific Gravity	
Gmm	2.47
Gse	2.644
Gsb	2.61

Table 43 Aggregate Proportion and JMF of Tested Mixture: S4 PG 64-22

S4 PG 64-22, Mix ID: S4pv0261201600	
Aggregate	**%Used**
5/8" Chips	25
Stone Sand	20
3/16" Scrns	20
Sand	10
Fine Rap	25
Combined Gradation	
Sieve Size	**JMF**
3/4"	100
1/2"	98
3/8"	89
#4	67
#8	50
#16	36
#30	28
#50	20
#100	10
#200	5.6
Asphalt Binder Content	
% Asphalt Cement	**% New asphalt cement**
4.8	3.7
Specific Gravity	
Gmm	2.499
Gse	2.707
Gsb	2.662

Table 44 Aggregate Proportion and JMF of Tested Mixture: S4 PG 70-28

S4 PG 70-28, Mix ID: S4qc0131304600	
Aggregate	**%Used**
5/8" Chips	35
Man. Sand	20
Stone Sand	18
Sand	12
Fine Rap	15
Combined Gradation	
Sieve Size	**JMF**
3/4"	100
1/2"	94
3/8"	85
#4	65
#8	48
#16	35
#30	27
#50	18
#100	7
#200	3
Asphalt Binder Content	
% Asphalt Cement	**% New asphalt cement**
5.0	4.2
Specific Gravity	
Gmm	2.463
Gse	2.655
Gsb	2.625

Table 45 Aggregate Proportion and JMF of Tested Mixture: S4 PG 76-28

S4 PG 76-28, Mix ID: S4qc0131304900	
Aggregate	**%Used**
5/8" Chips	37
Man. Sand	22
Stone Sand	14
Sand	12
Fine Rap	15
Combined Gradation	
Sieve Size	**JMF**
3/4"	100
1/2"	93
3/8"	83
#4	64
#8	44
#16	31
#30	24
#50	16
#100	7
#200	3.7
Asphalt Binder Content	
% Asphalt Cement	**% New asphalt cement**
4.9	4.1
Specific Gravity	
Gmm	2.513
Gse	2.697
Gsb	2.66

Table 46 Aggregate Proportion and JMF of Tested Mixture: S5 PG 76-28

S5 PG 76-28, Mix ID: S5qc0131402500	
Aggregate	**%Used**
3/8" Chips	30
Man. Sand	30
Stone Sand	15
Sand	10
Fine Rap	15
Combined Gradation	
Sieve Size	**JMF**
3/4"	100
1/2"	100
3/8"	98
#4	71
#8	50
#16	34
#30	25
#50	14
#100	6.0
#200	3.5
Asphalt Binder Content	
% Asphalt Cement	**% New asphalt cement**
5.1	4.5
Specific Gravity	
Gmm	2.496
Gse	2.687
Gsb	2.655

APPENDIX B. DYNAMIC MODULUS DATA

Table 47 Summary of Dynamic Modulus Data for Mixtures Tested by October 2014

Mixture ID	Replicate	Temp.(°C)	|E*| (psi)						
			0.01 Hz	0.1 Hz	0.5 Hz	1 Hz	5 Hz	10 Hz	25 Hz
S3c00931100102	1	4	-	1,331,011	1,649,079	1,790,781	2,124,078	2,265,780	2,450,413
		20	-	455,854	662,822	763,624	1,039,050	1,164,653	1,340,004
		40	38,058	81,468	145,183	181,877	315,747	384,350	488,922
	2	4	-	1,379,019	1,701,293	1,845,170	2,186,589	2,338,298	2,569,344
		20	-	469,052	676,456	778,708	1,060,371	1,193,371	1,386,851
		40	46,717	96,320	163,022	198,992	327,350	395,228	509,227
	3	4	-	1,473,148	1,816,888	1,966,132	2,316,253	2,464,336	2,667,679
		20	-	494,869	714,746	820,914	1,117,371	1,256,027	1,462,416
		40	49,385	103,165	176,511	219,007	362,014	437,579	558,250
S4pv0261201600	1	4	-	1,250,805	1,578,591	1,729,285	2,085,498	2,246,054	2,460,420
		20	-	389,426	583,052	681,387	962,035	1,100,111	1,307,950
		40	26,237	59,175	107,357	133,681	235,396	291,091	386,671
	2	4	-	1,209,180	1,525,797	1,671,705	2,031,834	2,197,177	2,436,634
		20	-	421,190	622,357	722,723	1,012,653	1,155,371	1,379,454
		40	34,998	76,435	134,044	164,908	281,663	344,175	451,793
	3	4	-	1,156,241	1,473,438	1,621,957	1,978,895	2,166,284	2,514,809
		20	-	387,396	583,342	682,403	967,112	1,108,088	1,321,729
		40	28,979	62,961	111,897	138,351	241,778	297,908	395,083
S4qc0131304600	1	4	-	620,326	843,249	956,524	1,260,233	1,405,561	1,606,728
		20	-	152,435	242,648	286,740	447,296	529,823	664,708
		40	13,793	23,685	41,118	50,778	97,175	124,486	181,152
	2	4	-	625,838	849,486	962,470	1,260,813	1,402,660	1,608,614
		20	-	155,045	247,434	293,701	450,922	530,548	658,471
		40	13,343	22,843	39,117	48,269	93,332	119,540	169,549

Mixture ID	Replicate	Temp.(°C)	|E*| (psi)						
			0.01 Hz	0.1 Hz	0.5 Hz	1 Hz	5 Hz	10 Hz	25 Hz
	3	4	-	608,433	817,288	920,119	1,192,935	1,322,454	1,502,881
		20	-	156,351	246,129	289,785	445,991	525,762	655,135
		40	13,996	24,410	41,800	50,473	99,075	126,894	178,832
S4qc0131304900	1	4	-	739,257	983,211	1,102,142	1,406,721	1,548,858	1,753,796
		20	-	178,541	280,648	330,686	506,182	595,960	740,418
		40	17,376	29,182	48,950	58,175	112,883	143,573	201,312
	2	4	-	744,914	1,009,753	1,142,752	1,481,851	1,651,835	1,918,994
		20	-	145	279,343	332,426	514,739	609,449	762,028
		40	18,797	29,994	48,820	58,131	110,809	141,803	200,587
	3	4	-	679,502	936,944	1,061,821	1,383,080	1,529,858	1,730,880
		20	-	152,000	250,915	300,953	480,800	573,624	721,998
		40	15,214	25,063	41,379	49,733	98,916	128,402	184,778
S5qc0131402500	1	4	-	827,576	1,128,883	1,268,528	1,602,620	1,746,396	1,932,432
		20	-	218,589	350,914	424,763	638,194	747,733	907,067
		40	21,275	39,985	65,200	81,074	135,168	168,144	223,130
	2	4	-	832,807	1,143,774	1,285,395	1,615,402	1,752,987	1,926,573
		20	-	197,039	325,130	398,543	614,963	727,261	890,853
		40	22,281	38,954	61,864	76,563	128,020	160,229	214,997
	3	4	-	812,624	1,103,776	1,236,448	1,547,282	1,677,996	1,844,229
		20	-	196,518	319,617	389,168	591,903	696,372	848,271
		40	19,980	35,755	57,183	70,809	117,973	147,195	196,549

APPENDIX C. UNIAXIAL FATIGUE TEST RESULTS

Table 48 Summary of Fatigue Test Results

Mix	Sample No.	Initial strain level (με)	N_f (Experimental)
S4 64-22	S4_64_1	299	6130
	S4_64_2	217	16000
	S4_64_3	262	17229
	S4_64_4	154	139213
	S4_64_5	201	44580
S3 64-22	S3_64_1	184	26975
	S3_64_2	270	9611
	S3_64_3	175	49253
	S3_64_4	152	189326
	S3_64_5	237	13323
S4 70-28	S4_70_1	490	14123
	S4_70_2	279	83290
	S4_70_3	273	46003
	S4_70_4	367	43572
	S4_70_5	288	83400
S4 76-28	S4_76_1	261	435889
	S4_76_2	395	84349
	S4_76_3	476	33926
	S4_76_4	509	52607
	S4_76_5	520	11036
S5 76-28	S576_5	497	24620
	S5_76_3	458	90115
	S5_76_2	493	63037
	S5_76_1	403	129961
	S5_76_4	258	499805

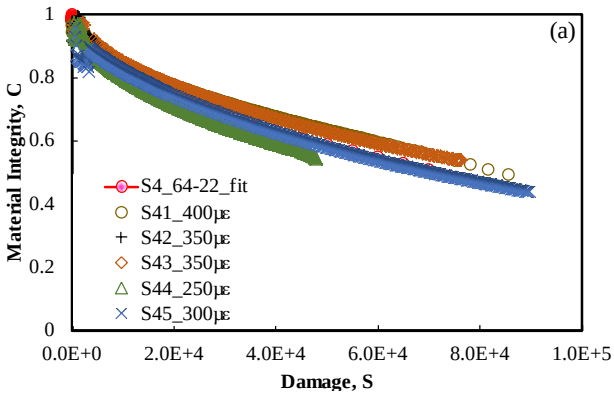
(a)
Material Integrity, C
Damage, S
S4_64-22_fit
S41_400με
S42_350με
S43_350με
S44_250με
S45_300με
0
0.2
0.4
0.6
0.8
1
0.0E+0
2.0E+4
4.0E+4
6.0E+4
8.0E+4
1.0E+5

(a)

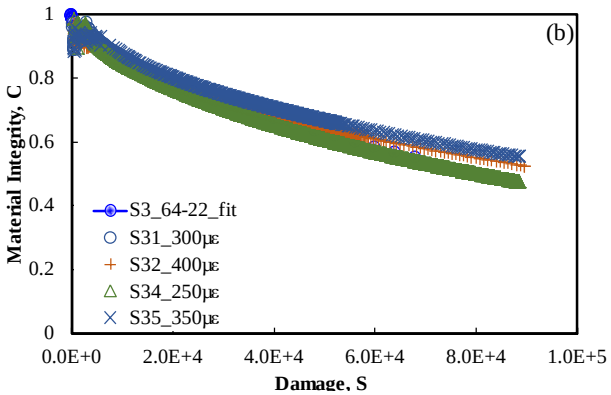
(b)
Material Integrity, C
Damage, S
S3_64-22_fit
S31_300με
S32_400με
S34_250με
S35_350με
0
0.2
0.4
0.6
0.8
1
0.0E+0
2.0E+4
4.0E+4
6.0E+4
8.0E+4
1.0E+5

(b)

(c)

(d)

APPENDIX D. INDIRECT TENSION (IDT) CREEP COMPLIANCE AND STRENGTH TEST

S3 64-22 Mix

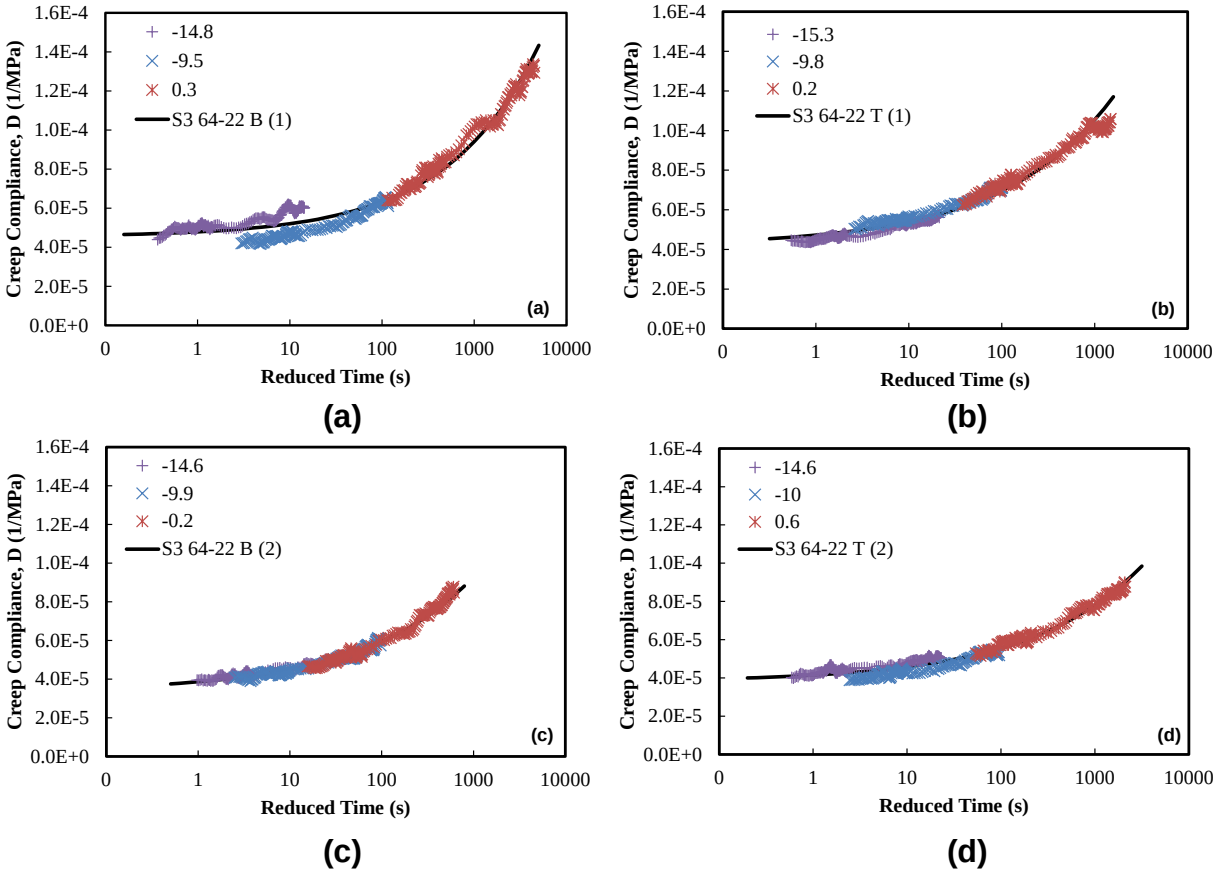

Figure 68 Creep Compliance Master Curves for S3 64-22 Mix Replicates; (a) Compacted Sample 1 Bottom Slice, (b) Compacted Sample 1 Top Slice, (c) Compacted Sample 2 Bottom Slice, and (d) Compacted Sample 2 Top Slice.

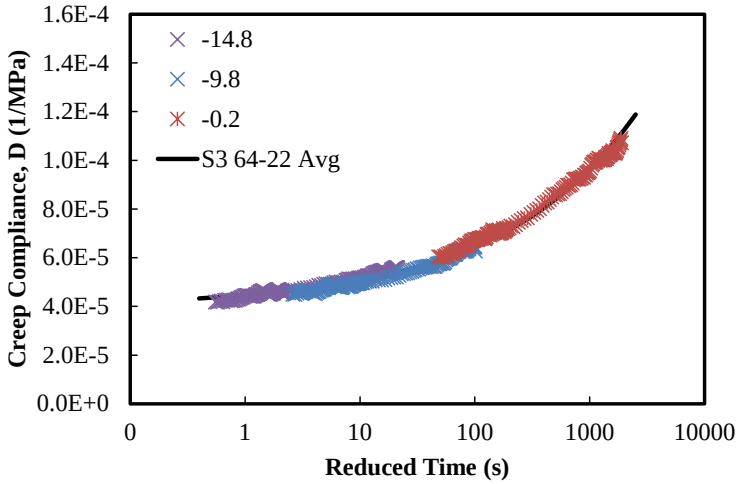

Figure 69 Creep Compliance Master Curves Fit for S3 64-22 Mix (Average of 3 Replicates)

Table 49 Creep Compliance of S3 64-22 Mix Replicates

Temp (°C)	Time (s)	D(t) (1/MPa) (Experimental)			Average D(t) (1/MPa)	Standard Deviation	CV
		S3 64-22 B (1)	S3 64-22 T (1)	S3 64-22 T (2)			
-15	2.45	4.39E-05	4.47E-05	4.02E-05	4.29E-05	2.4E-06	5.6%
	5.05	4.95E-05	4.56E-05	4.32E-05	4.61E-05	3.2E-06	6.9%
	10.02	5.10E-05	4.68E-05	4.43E-05	4.74E-05	3.4E-06	7.2%
	20.5	5.09E-05	4.86E-05	4.61E-05	4.85E-05	2.4E-06	5.0%
	50.5	5.51E-05	5.29E-05	4.92E-05	5.24E-05	3.0E-06	5.7%
	95.5	6.02E-05	5.62E-05	5.05E-05	5.56E-05	4.9E-06	8.7%
-10	2.45	4.20E-05	5.04E-05	4.74E-05	4.66E-05	4.3E-06	9.2%
	5.05	4.42E-05	5.30E-05	4.20E-05	4.64E-05	5.8E-06	12.6%
	10.02	4.56E-05	5.61E-05	4.24E-05	4.80E-05	7.2E-06	14.9%
	20.5	4.98E-05	5.97E-05	4.52E-05	5.16E-05	7.4E-06	14.4%
	50.5	5.62E-05	6.47E-05	5.02E-05	5.70E-05	7.3E-06	12.8%
	95.5	6.10E-05	7.12E-05	5.18E-05	6.14E-05	9.7E-06	15.8%
0	2.45	6.40E-05	6.24E-05	5.29E-05	5.98E-05	6.0E-06	10.0%
	5.05	7.31E-05	7.10E-05	5.95E-05	6.78E-05	7.3E-06	10.8%
	10.02	8.32E-05	7.47E-05	6.26E-05	7.35E-05	1.0E-05	14.1%
	20.5	1.01E-04	8.62E-05	6.84E-05	8.50E-05	1.6E-05	18.9%
	50.5	1.17E-04	9.86E-05	7.84E-05	9.80E-05	1.9E-05	19.6%
	95.5	1.29E-04	1.06E-04	8.77E-05	1.08E-04	2.1E-05	19.4%

Table 50 Tensile Strength Test Summary of S3 64-22 Mix Replicates

Parameter	S3 64 22 1B	S3 64 22 2T	S3 64 22 1T	Average
Average temperature (°C)	-10.7	-9.5	-10.4	-10.2
Peak load (kN)	26.6	35.3	31.3	31.1
Tensile strength (psi)	414	530	476	473
Tensile strength (kPa)	2855	3659	3284	3266
Time at failure (s)	4.8	5.3	7.1	5.7

S4 64-22 Mix

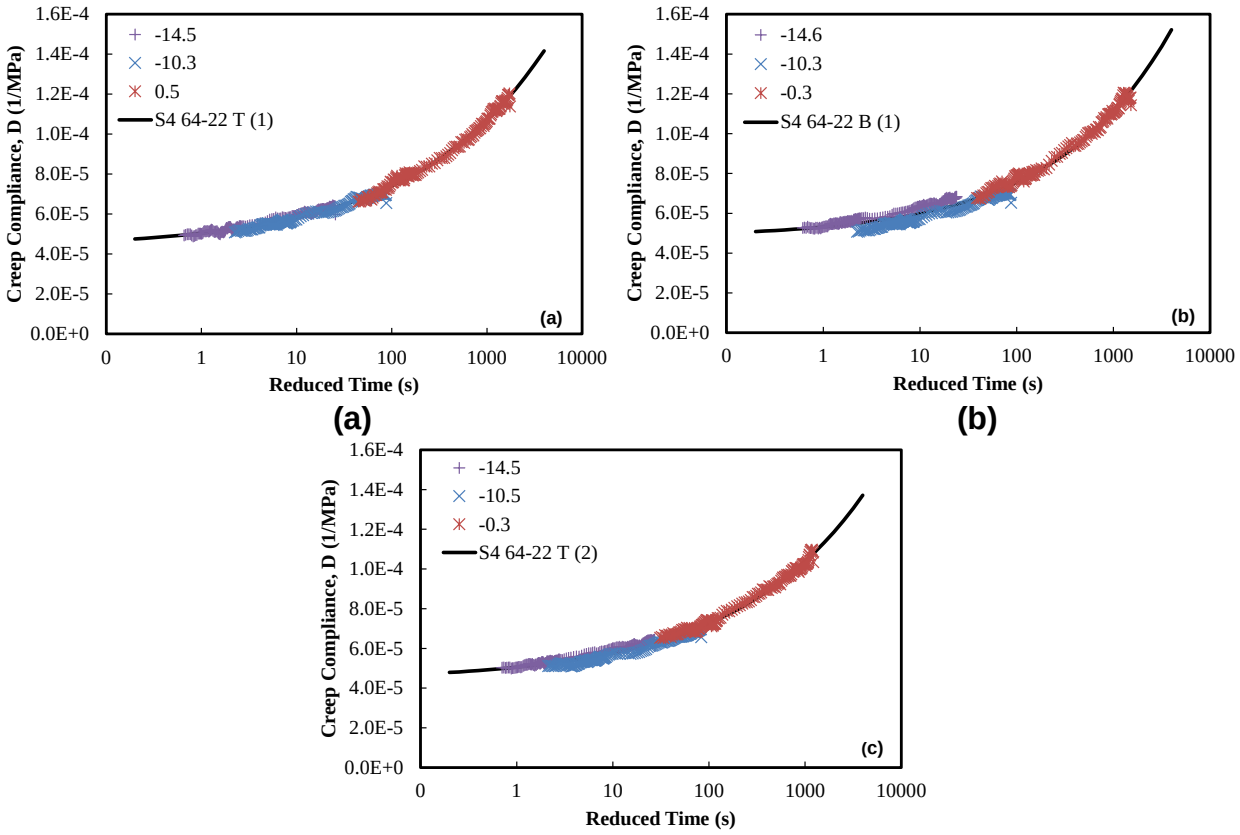

Figure 70 Creep Compliance Master Curves for S4 64-22 Mix Replicates; (a) Compacted Sample 1 Top Slice, (b) Compacted Sample 1 Bottom Slice, and (c) Compacted Sample 2 Top Slice.

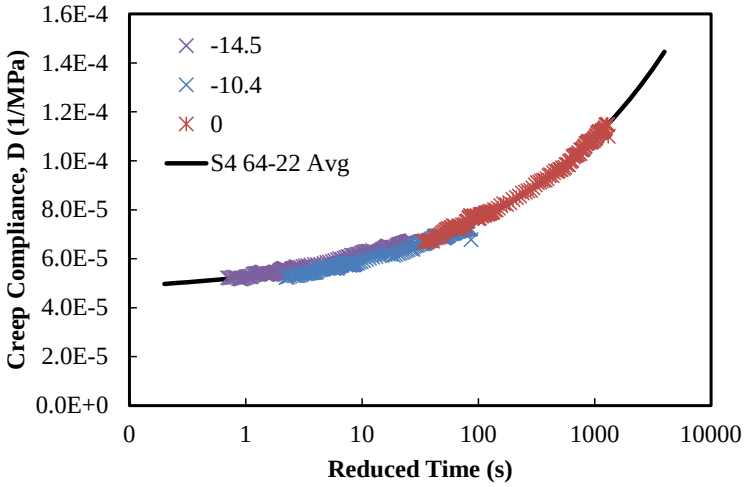

Figure 71 Creep Compliance Master Curve Fit for S4 64-22 Mix (Average of 3 Replicates).

Table 51 Creep Compliance of S4 64-22 Mix Replicates

Temp (°C)	Time (s)	D(t) (1/MPa) (Experimental)			Average D(t) (1/MPa)	Standard Deviation	CV
		S4 64-22 T (1)	S4 64-22 B (1)	S4 64-22 T (2)			
-15	2.45	4.93E-05	5.26E-05	5.02E-05	5.07E-05	1.7E-06	3.4%
	5.05	5.12E-05	5.46E-05	5.21E-05	5.26E-05	1.8E-06	3.4%
	10.02	5.39E-05	5.77E-05	5.42E-05	5.53E-05	2.1E-06	3.8%
	20.5	5.75E-05	5.93E-05	5.75E-05	5.81E-05	1.0E-06	1.8%
	50.5	6.07E-05	6.48E-05	6.06E-05	6.20E-05	2.4E-06	3.8%
	95.5	5.97E-05	6.83E-05	6.12E-05	6.31E-05	4.6E-06	7.2%
-10	2.45	5.08E-05	5.07E-05	5.10E-05	5.08E-05	1.8E-07	0.4%
	5.05	5.48E-05	5.47E-05	5.22E-05	5.39E-05	1.5E-06	2.8%
	10.02	5.67E-05	5.65E-05	5.64E-05	5.65E-05	1.6E-07	0.3%
	20.5	6.05E-05	6.04E-05	5.79E-05	5.96E-05	1.5E-06	2.5%
	50.5	6.82E-05	6.81E-05	6.53E-05	6.72E-05	1.6E-06	2.4%
	95.5	6.55E-05	6.53E-05	6.56E-05	6.55E-05	1.6E-07	0.2%
0	2.45	6.62E-05	6.77E-05	6.53E-05	6.64E-05	1.2E-06	1.8%
	5.05	7.29E-05	7.32E-05	6.96E-05	7.19E-05	2.0E-06	2.8%
	10.02	8.03E-05	8.18E-05	7.51E-05	7.91E-05	3.5E-06	4.4%
	20.5	8.88E-05	9.27E-05	8.36E-05	8.84E-05	4.6E-06	5.2%
	50.5	1.04E-04	1.08E-04	9.63E-05	1.03E-04	5.9E-06	5.7%
	95.5	1.14E-04	1.14E-04	1.03E-04	1.10E-04	6.1E-06	5.5%

Table 52 Tensile Strength Test Summary of S4 64-22 Mix Replicates

Parameter	S4 64 22 1B	S4 64 22 1T	S4 64 22 2T	Average
Average temperature (°C)	-10.7	-11.0	-11.0	-10.9
Peak load (kN)	36.97	40.27	43.21	40.1
Tensile strength (psi)	564.69	600.19	676.76	613.88
Tensile strength (kPa)	3893	4138	4666	4233
Time at failure (s)	5.3	5.5	6.2	5.7

S4 70-28 Mix

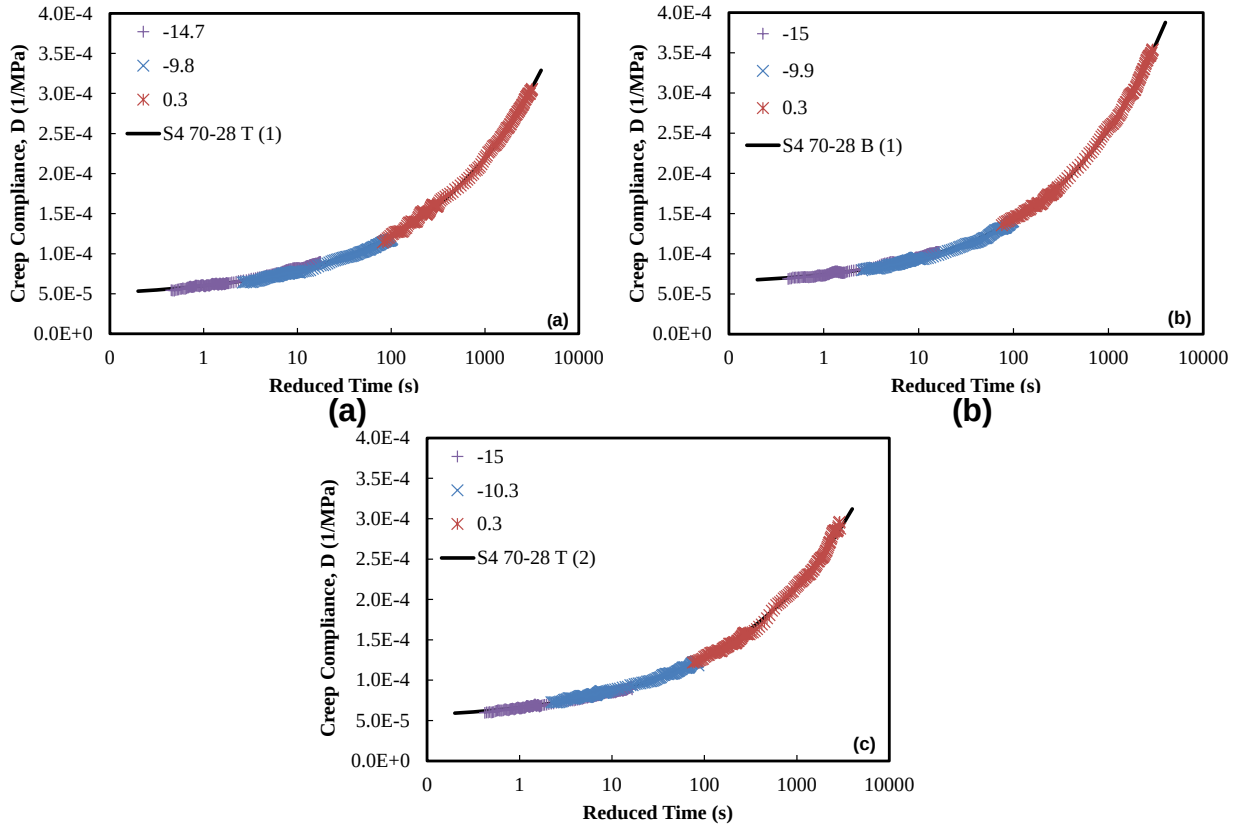

Figure 72 Creep Compliance Master Curves for S4 70-28 Mix Replicates; (a) Compacted Sample 1 Top Slice, (b) Compacted Sample 1 Bottom Slice, and (c) Compacted Sample 2 Top Slice.

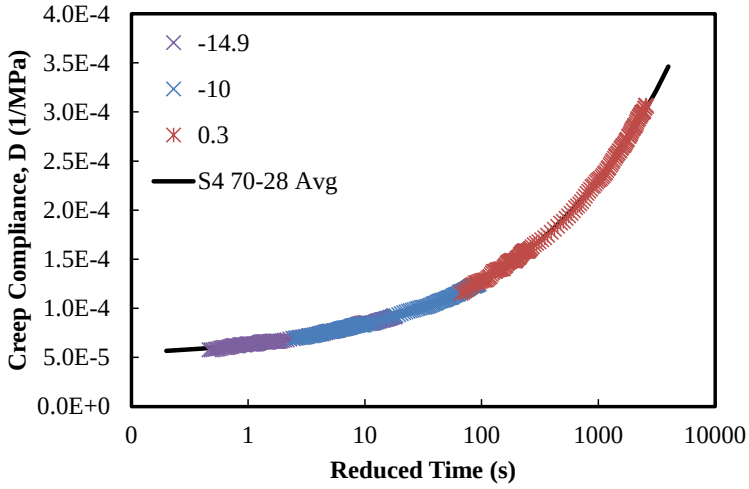

Figure 73 Creep Compliance Master Curves Fit for S4 70-28 Mix (Average of 3 Replicates)

Table 53 Creep Compliance of S4 70-28 Mix Replicates

Temp (°C)	Time (s)	D(t) (1/MPa)			Average D(t) (1/MPa)	Standard Deviation	CV
		S4 70-28 T (1)	S4 70-28 T (2)	S4 70-28 B (1)			
-15	2.45	5.46E-05	5.97E-05	6.88E-05	6.1E-05	7.2E-06	11.8%
	5.05	6.02E-05	6.39E-05	7.32E-05	6.6E-05	6.7E-06	10.2%
	10.02	6.33E-05	6.87E-05	7.75E-05	7.0E-05	7.2E-06	10.3%
	20.5	7.03E-05	7.48E-05	8.37E-05	7.6E-05	6.8E-06	9.0%
	50.5	8.21E-05	8.46E-05	9.33E-05	8.7E-05	5.9E-06	6.8%
	95.5	8.99E-05	8.90E-05	1.02E-04	9.4E-05	7.4E-06	7.9%
-10	2.45	6.41E-05	7.27E-05	7.96E-05	7.2E-05	7.8E-06	10.8%
	5.05	7.19E-05	8.04E-05	8.67E-05	8.0E-05	7.4E-06	9.3%
	10.02	7.71E-05	8.66E-05	9.34E-05	8.6E-05	8.2E-06	9.6%
	20.5	8.90E-05	9.57E-05	1.04E-04	9.6E-05	7.6E-06	7.9%
	50.5	1.04E-04	1.09E-04	1.20E-04	1.1E-04	8.2E-06	7.4%
	95.5	1.19E-04	1.19E-04	1.40E-04	1.3E-04	1.3E-05	10.0%
0	2.45	1.14E-04	1.22E-04	1.35E-04	1.2E-04	1.1E-05	8.7%
	5.05	1.40E-04	1.37E-04	1.59E-04	1.5E-04	1.2E-05	8.4%
	10.02	1.66E-04	1.57E-04	1.84E-04	1.7E-04	1.4E-05	8.1%
	20.5	1.95E-04	1.95E-04	2.25E-04	2.0E-04	1.7E-05	8.5%
	50.5	2.55E-04	2.40E-04	2.89E-04	2.6E-04	2.5E-05	9.6%
	95.5	3.06E-04	2.88E-04	3.54E-04	3.2E-04	3.4E-05	10.9%

Table 54 Tensile Strength Test Summary of S4 70-28 Mix Replicates

Parameter	S4 70-28 1T	S4 70-28 2T	S4 70-28 1B	Average
Average temperature (°C)	-10.2	-10.6	-10.3	-10.4
Peak load (kN)	30.7	30.3	31.2	30.7
Tensile strength (psi)	476	461	479	472
Tensile strength (kPa)	3285	3182	3308	3258
Time at failure (s)	6.8	6.3	7.4	6.8

S4 76-28 Mix

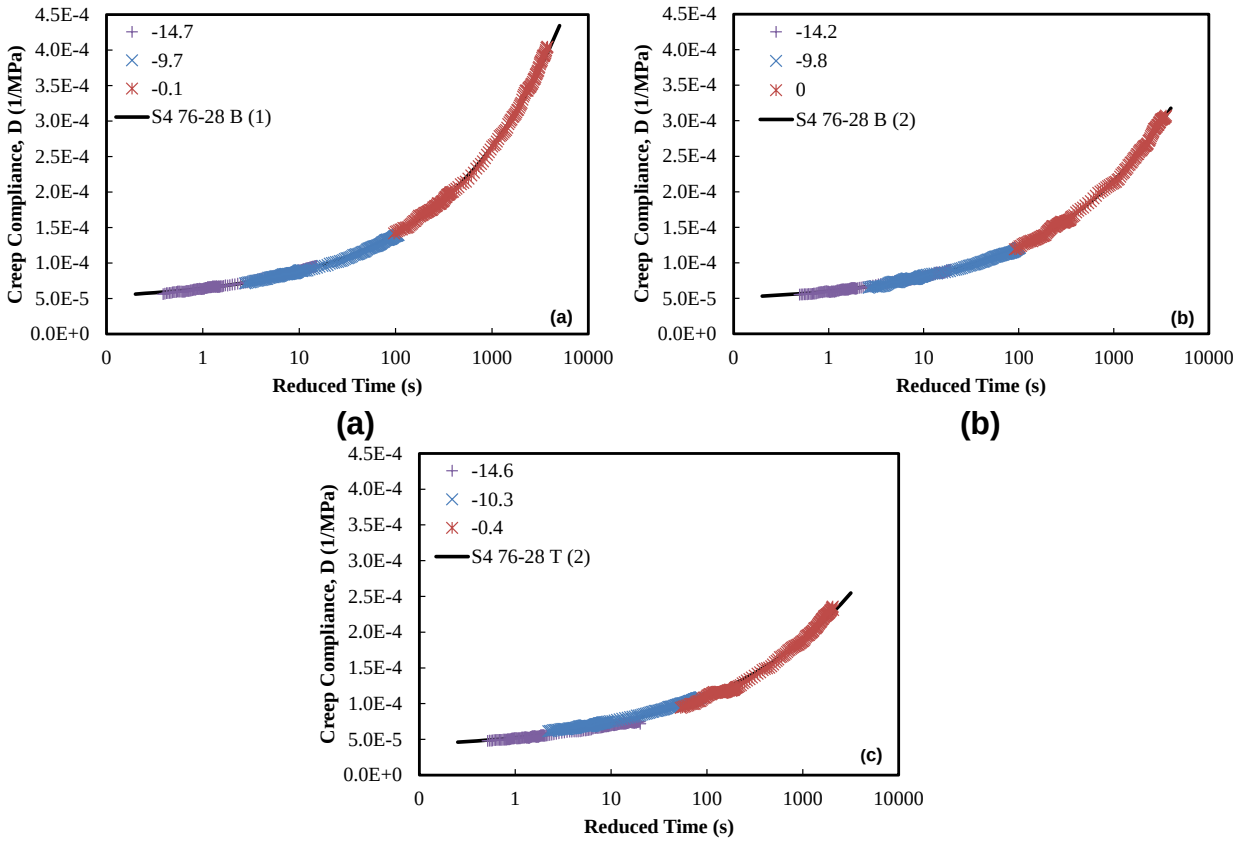

Figure 74 Creep Compliance Master Curves for S4 76-28 Mix Replicates; (a) Compacted Sample 1 Bottom Slice, (b) Compacted Sample 2 Bottom Slice, and (c) Compacted Sample 2 Top Slice.

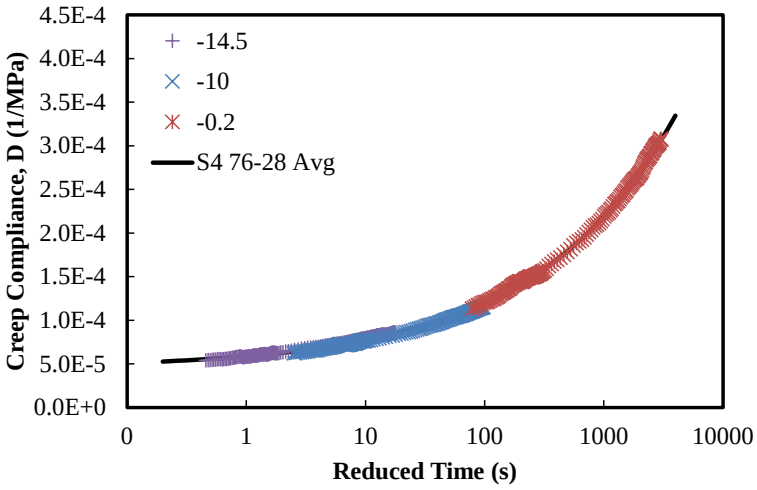

Figure 75 Creep Compliance Master Curve Fit for S4 76-28 Mix (Average of 3 Replicates)

Table 55 Creep Compliance of S4 76-28 Mix Replicates

Temp (°C)	Time (s)	D(t) (1/MPa) (Experimental)			Average D(t) (1/MPa)	Standard Deviation	CV
		S4 76-28 B (1)	S4 76-28 B (2)	S4 76-28 T (2)			
-15	2.45	5.63E-05	5.55E-05	4.81E-05	5.33E-05	4.50E-06	8.50%
	5.05	6.26E-05	5.91E-05	5.14E-05	5.77E-05	5.70E-06	9.90%
	10.02	6.72E-05	6.44E-05	5.56E-05	6.24E-05	6.10E-06	9.70%
	20.5	7.50E-05	7.15E-05	6.12E-05	6.92E-05	7.20E-06	10.40%
	50.5	8.58E-05	8.10E-05	7.01E-05	7.89E-05	8.00E-06	10.20%
	95.5	9.58E-05	8.97E-05	7.20E-05	8.59E-05	1.20E-05	14.40%
-10	2.45	7.16E-05	6.52E-05	6.17E-05	6.62E-05	5.00E-06	7.60%
	5.05	8.08E-05	7.30E-05	6.77E-05	7.38E-05	6.60E-06	8.90%
	10.02	8.96E-05	8.34E-05	7.48E-05	8.26E-05	7.40E-06	9.00%
	20.5	1.01E-04	9.07E-05	8.36E-05	9.16E-05	8.60E-06	9.40%
	50.5	1.22E-04	1.08E-04	9.72E-05	1.09E-04	1.20E-05	11.40%
	95.5	1.40E-04	1.21E-04	1.09E-04	1.23E-04	1.60E-05	12.60%
0	2.45	1.42E-04	1.19E-04	9.43E-05	1.18E-04	2.40E-05	20.10%
	5.05	1.71E-04	1.39E-04	1.13E-04	1.41E-04	2.90E-05	20.40%
	10.02	2.01E-04	1.66E-04	1.25E-04	1.64E-04	3.80E-05	23.20%
	20.5	2.43E-04	2.02E-04	1.51E-04	1.99E-04	4.60E-05	23.40%
	50.5	3.24E-04	2.58E-04	1.95E-04	2.59E-04	6.50E-05	24.90%
	95.5	4.05E-04	3.07E-04	2.31E-04	3.14E-04	8.70E-05	27.70%

Table 56 Tensile Strength Test Summary of S4 76-28 Mix Replicates

Parameter	S4 76-28 B (1)	S4 76-28 B (2)	S4 76-28 T (2)	Average
Average temperature (°C)	-11.5	-10.0	-11.2	-10.9
Peak load (kN)	37.16	33.84	32.40	34.5
Tensile strength (psi)	563.34	514.31	496.09	524.58
Tensile strength (kPa)	3884	3546	3420	3617
Time at failure (s)	7.5	8.7	8.7	8.3

S5 76-28 mix

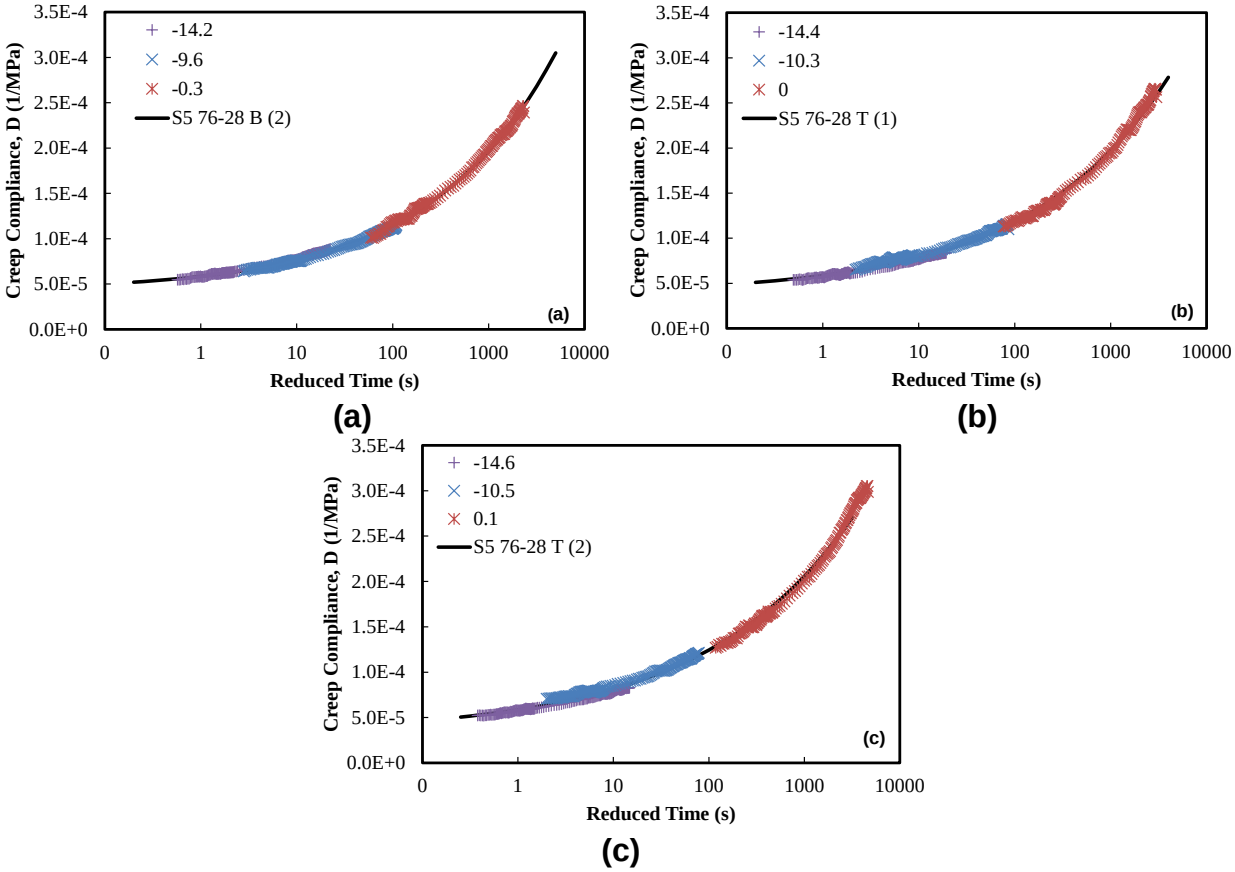

Figure 76 Creep Compliance Master Curves for S5 76-28 Mix Replicates; (a) Compacted Sample 2 Bottom Slice, (b) Compacted Sample 1 Top Slice, and (c) Compacted sample 2 Top Slice.

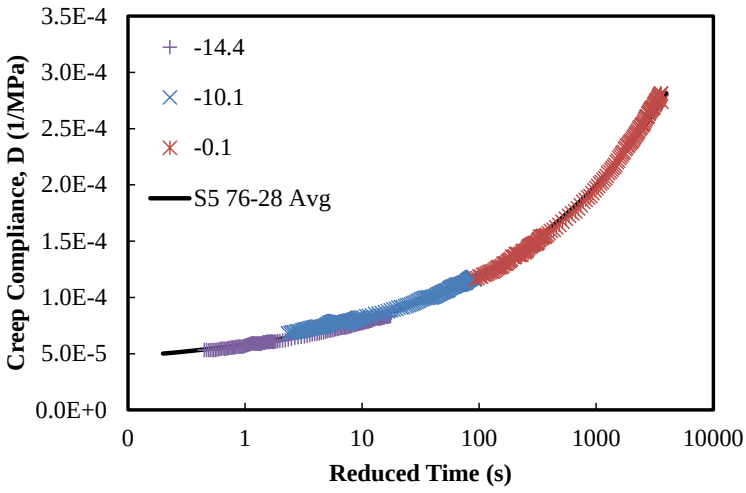

Figure 77 Creep Compliance Master Curve Fit for S5 76-28 Mix (Average of 3 Replicates).

Table 57 Creep Compliance of S5 76-28 Mix Replicates

Temp (°C)	Time (s)	D(t) (1/MPa) (Experimental)			Average D(t) (1/MPa)	Standard Deviation	CV
		S5 76-28 B (2)	S5 76-28 T (1)	S5 76-28 T (2)			
-15	2.45	5.48E-05	5.40E-05	5.23E-05	5.37E-05	1.30E-06	2.40%
	5.05	5.89E-05	5.67E-05	5.54E-05	5.70E-05	1.80E-06	3.10%
	10.02	6.39E-05	6.14E-05	6.03E-05	6.19E-05	1.80E-06	3.00%
	20.5	6.96E-05	6.79E-05	6.63E-05	6.79E-05	1.70E-06	2.50%
	50.5	7.99E-05	7.70E-05	7.60E-05	7.76E-05	2.00E-06	2.60%
	95.5	8.85E-05	8.41E-05	8.31E-05	8.52E-05	2.90E-06	3.40%
-10	2.45	6.40E-05	6.51E-05	7.06E-05	6.66E-05	3.60E-06	5.40%
	5.05	6.95E-05	7.31E-05	7.64E-05	7.30E-05	3.40E-06	4.70%
	10.02	7.66E-05	8.02E-05	8.35E-05	8.01E-05	3.50E-06	4.30%
	20.5	8.71E-05	8.86E-05	9.08E-05	8.88E-05	1.80E-06	2.10%
	50.5	1.02E-04	1.02E-04	1.06E-04	1.04E-04	2.30E-06	2.20%
	95.5	1.15E-04	1.10E-04	1.21E-04	1.16E-04	5.60E-06	4.90%
0	2.45	1.01E-04	1.13E-04	1.27E-04	1.14E-04	1.30E-05	11.40%
	5.05	1.22E-04	1.27E-04	1.50E-04	1.33E-04	1.50E-05	11.40%
	10.02	1.40E-04	1.49E-04	1.67E-04	1.52E-04	1.40E-05	9.40%
	20.5	1.65E-04	1.74E-04	2.01E-04	1.80E-04	1.90E-05	10.30%
	50.5	2.09E-04	2.20E-04	2.57E-04	2.29E-04	2.50E-05	10.90%
	95.5	2.39E-04	2.57E-04	2.99E-04	2.65E-04	3.10E-05	11.60%

Table 58 Tensile Strength Test Summary of S5 76-28 Mix Replicates

Parameter	S5 76-28 B (2)	S5 76-28 T (1)	S5 76-28 T (2)	Average
Average temperature (°C)	-10.4	-10.8	-10.9	-10.7
Peak load (kN)	36.09	39.24	34.47	36.6
Tensile strength (psi)	555.4	603.9	544.0	567.8
Tensile strength (kPa)	3830	4164	3751	3915
Time at failure (s)	8.1	7.8	7.7	7.9

APPENDIX E. VERIFICATION DATA FOR FWD ANALYSIS

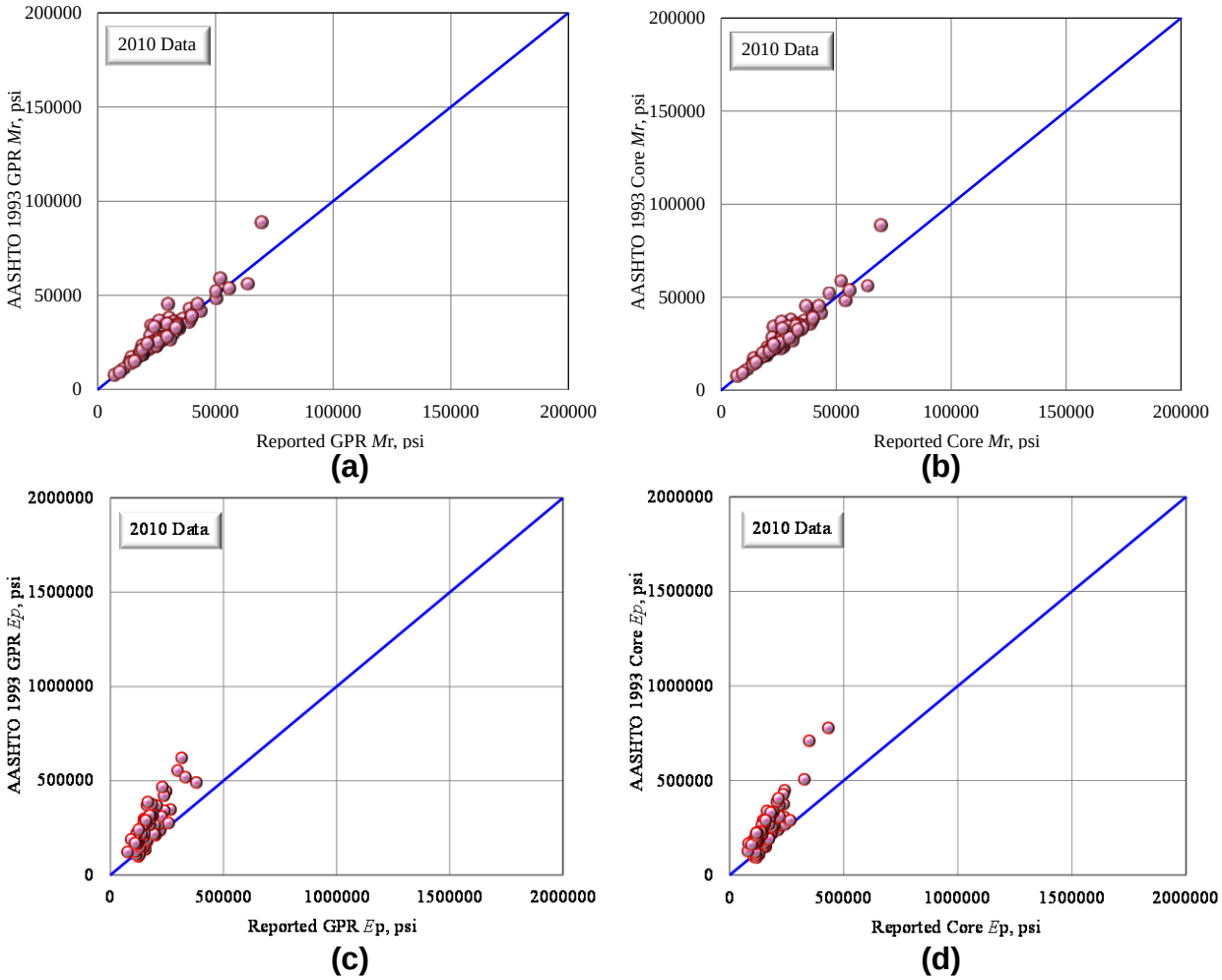

Figure 78 Comparison of 2010 Reported and AASHTO 1993 Verified values of (a) Mr Based on GPR and (b) Mr Based on Core, (c) Ep Based on GPR and (d) Ep based on Core for Control Section 68-22

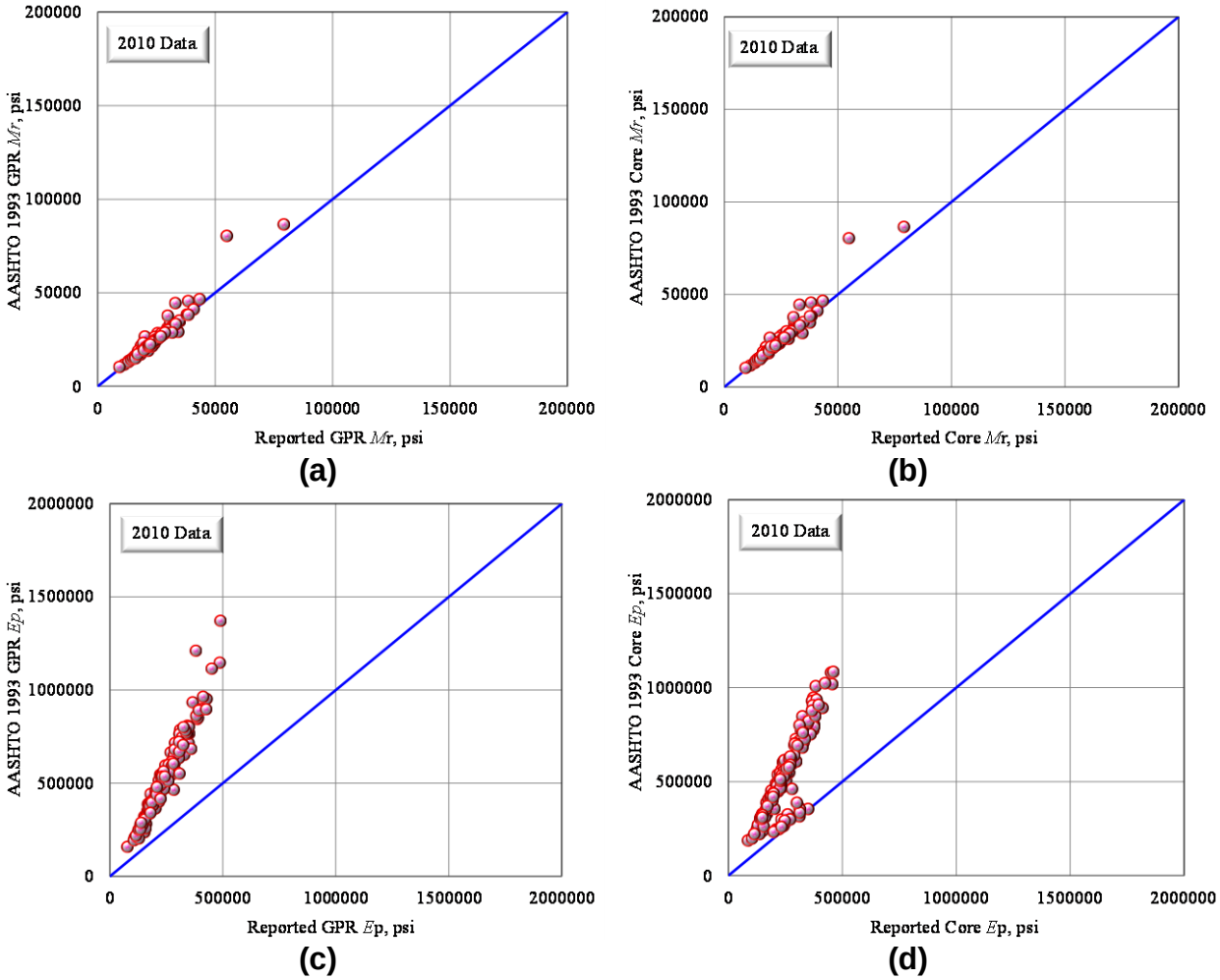

Figure 79 Comparison of 2010 Reported and AASHTO 1993 Verified Values of (a) Mr Based on GPR and (b) Mr Based on Core, (c) Ep Based on GPR and (d) Ep based on Core for Control Section 54-22.

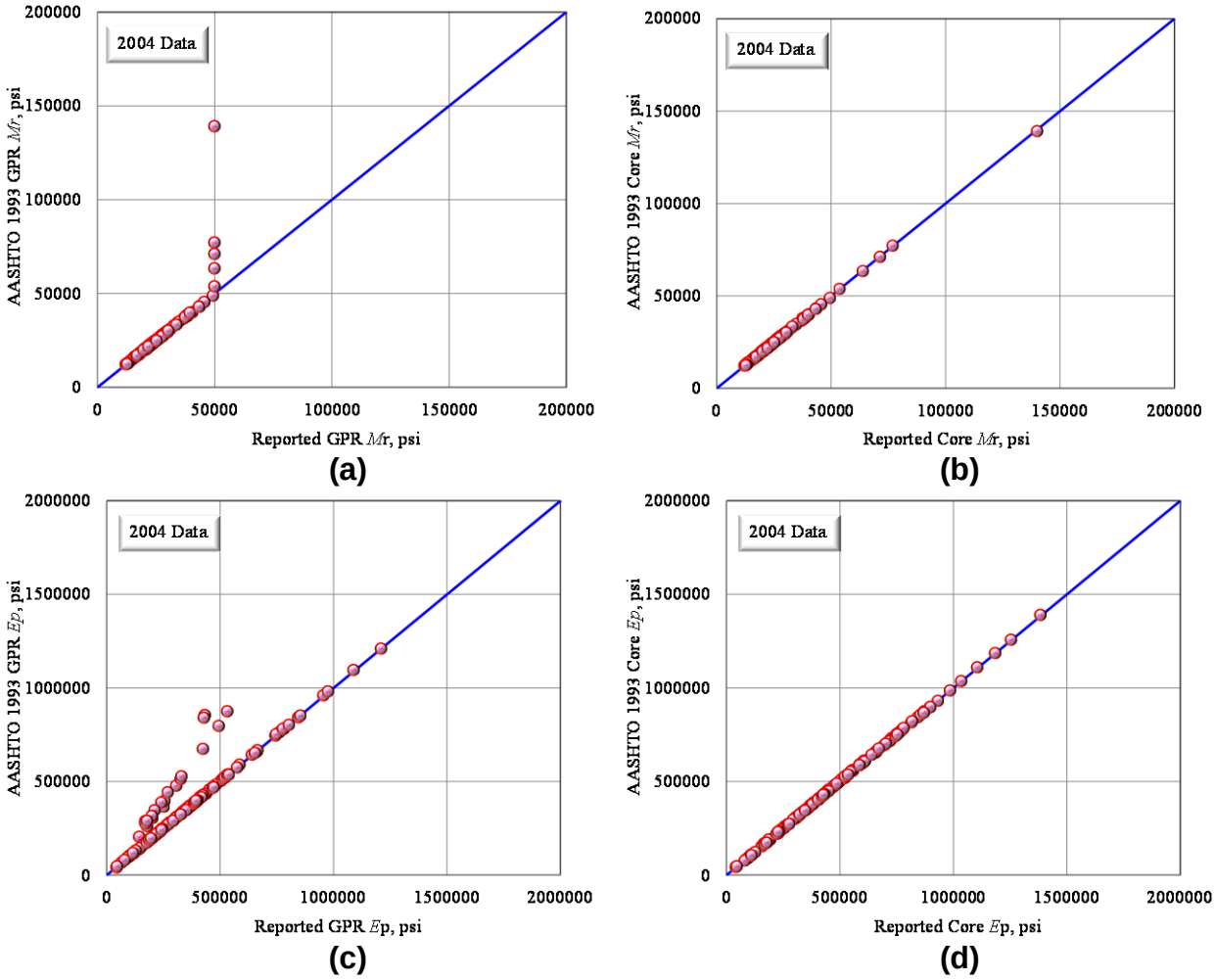

Figure 80 Comparison of 2004 Reported and AASHTO 1993 Verified Values of (a) Mr Based on GPR and (b) Mr Based on Core, (c) Ep Based on GPR and (d) Ep based on Core for Control Section 54-22.

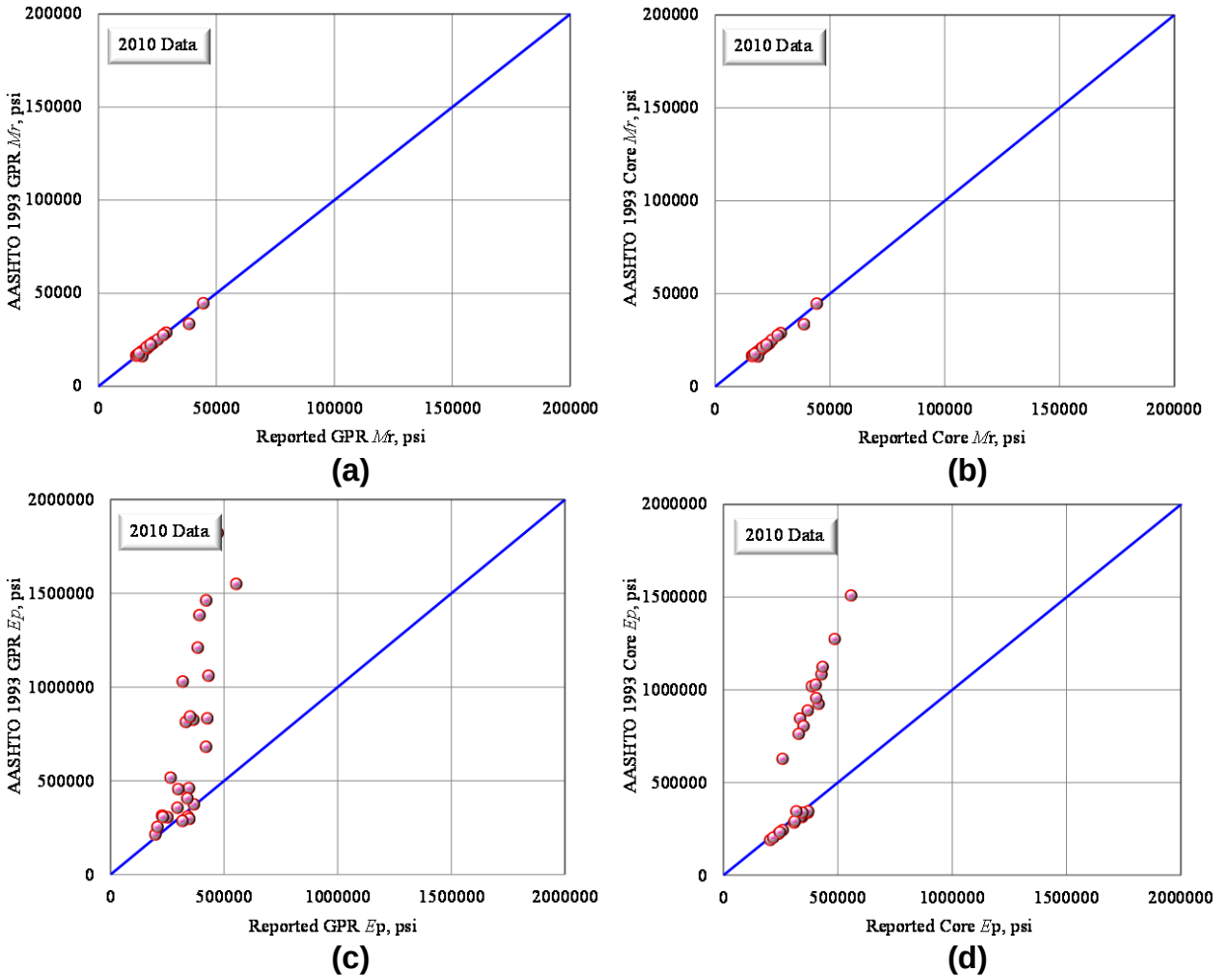

Figure 81 Comparison of 2010 Reported and AASHTO 1993 Verified Values of (a) Mr Based on GPR and (b) Mr Based on Core, (c) Ep Based on GPR and (d) Ep based on Core for Control Section 44-05.

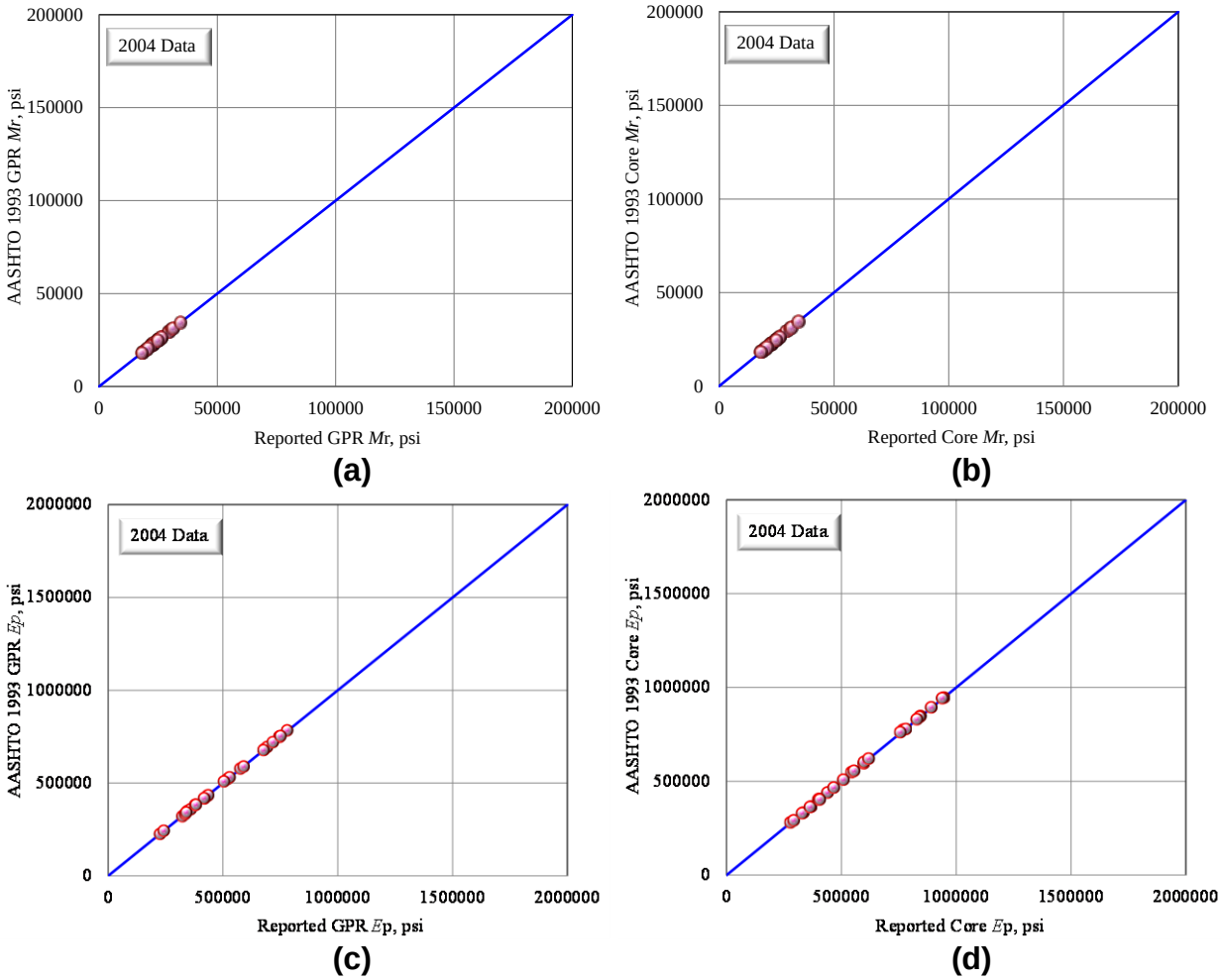

Figure 82 Comparison of 2004 Reported and AASHTO 1993 Verified Values of (a) Mr Based on GPR and (b) Mr Based on Core, (c) Ep Based on GPR and (d) Ep Based on Core for Control Section 44-05.

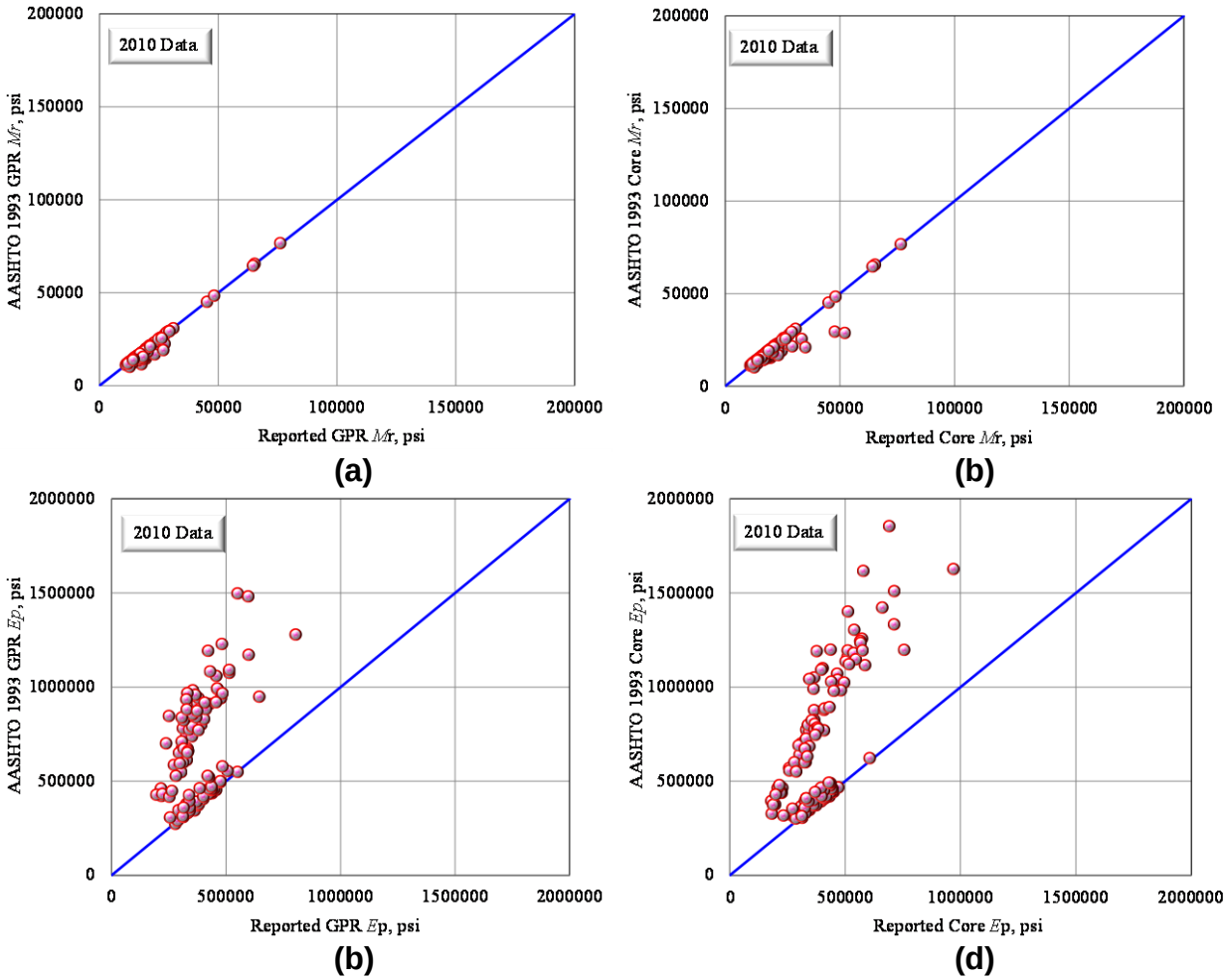

Figure 83 Comparison of 2010 Reported and AASHTO 1993 Verified Values of (a) Mr Based on GPR and (b) Mr Based on Core, (c) Ep Based on GPR and (d) Ep Based on Core for Control Section 09-05.

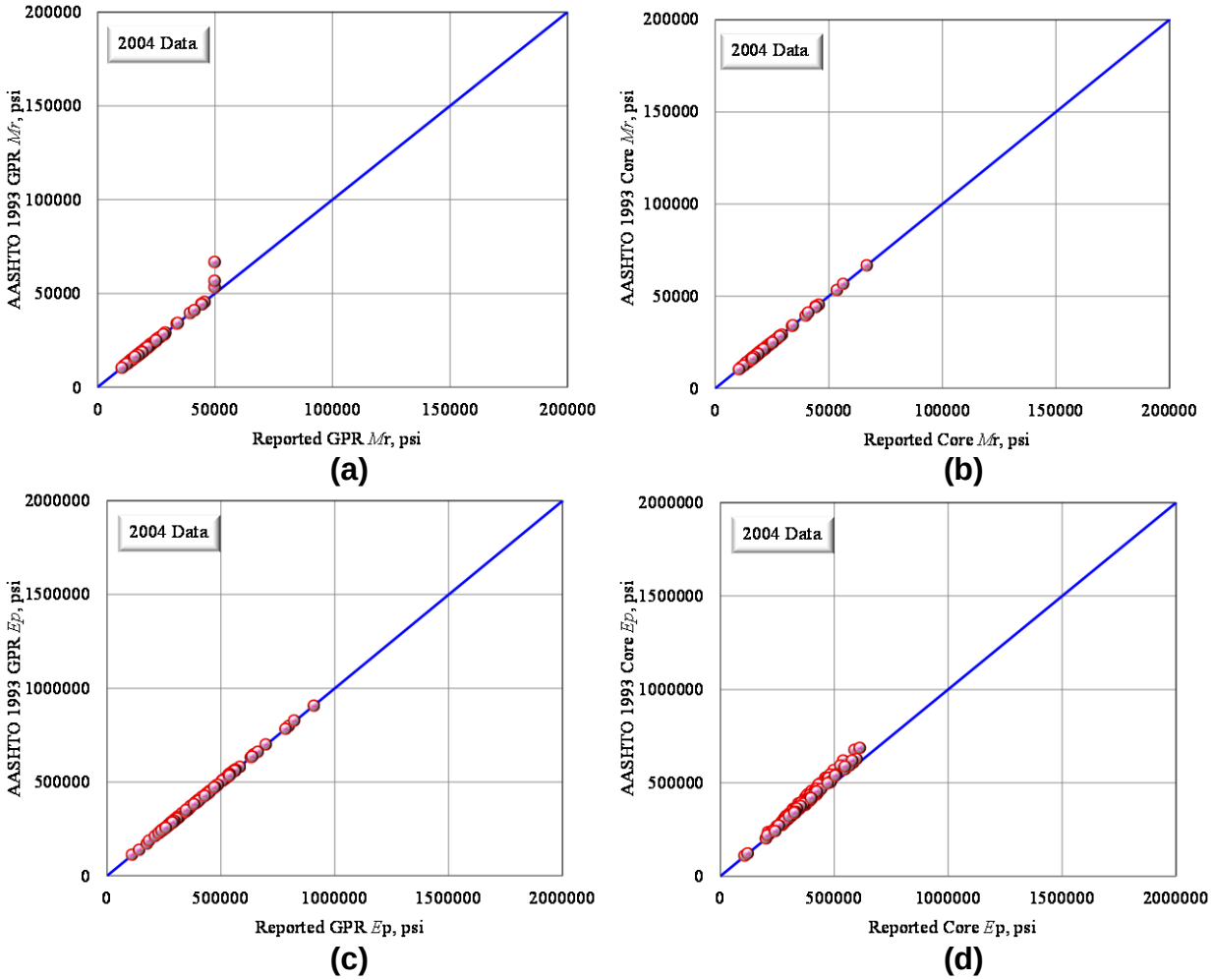

Figure 84 Comparison of 2004 Reported and AASHTO 1993 Verified Values of (a) Mr Based on GPR and (b) Mr Based on Core, (c) Ep Based on GPR and (d) Ep Based on Core for Control Section 09-05.

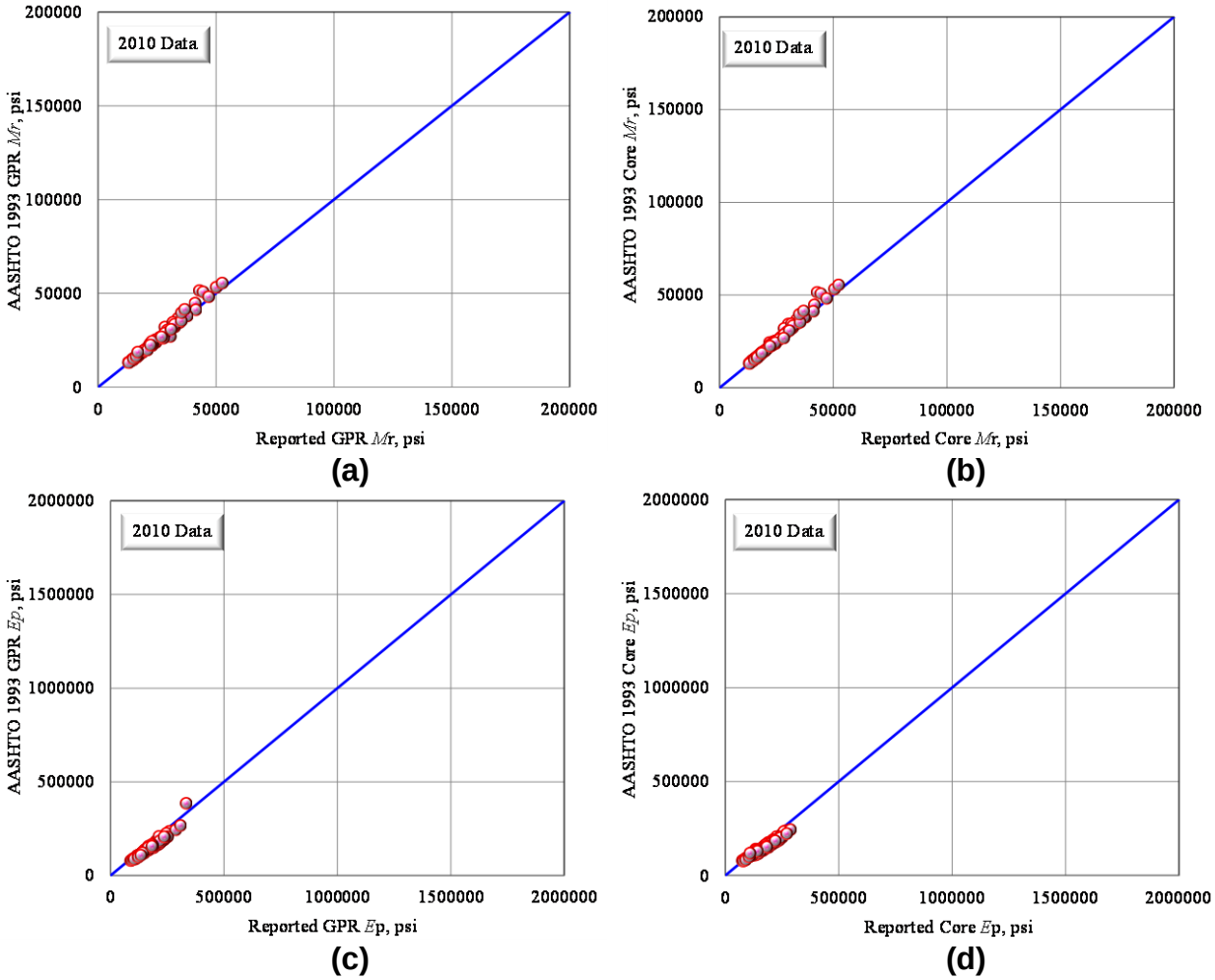

Figure 85 Comparison of 2010 Reported and AASHTO 1993 Verified Values of (a) Mr Based on GPR and (b) Mr Based on Core, (c) Ep Based on GPR and (d) Ep Based on Core for Control Section 55-68.

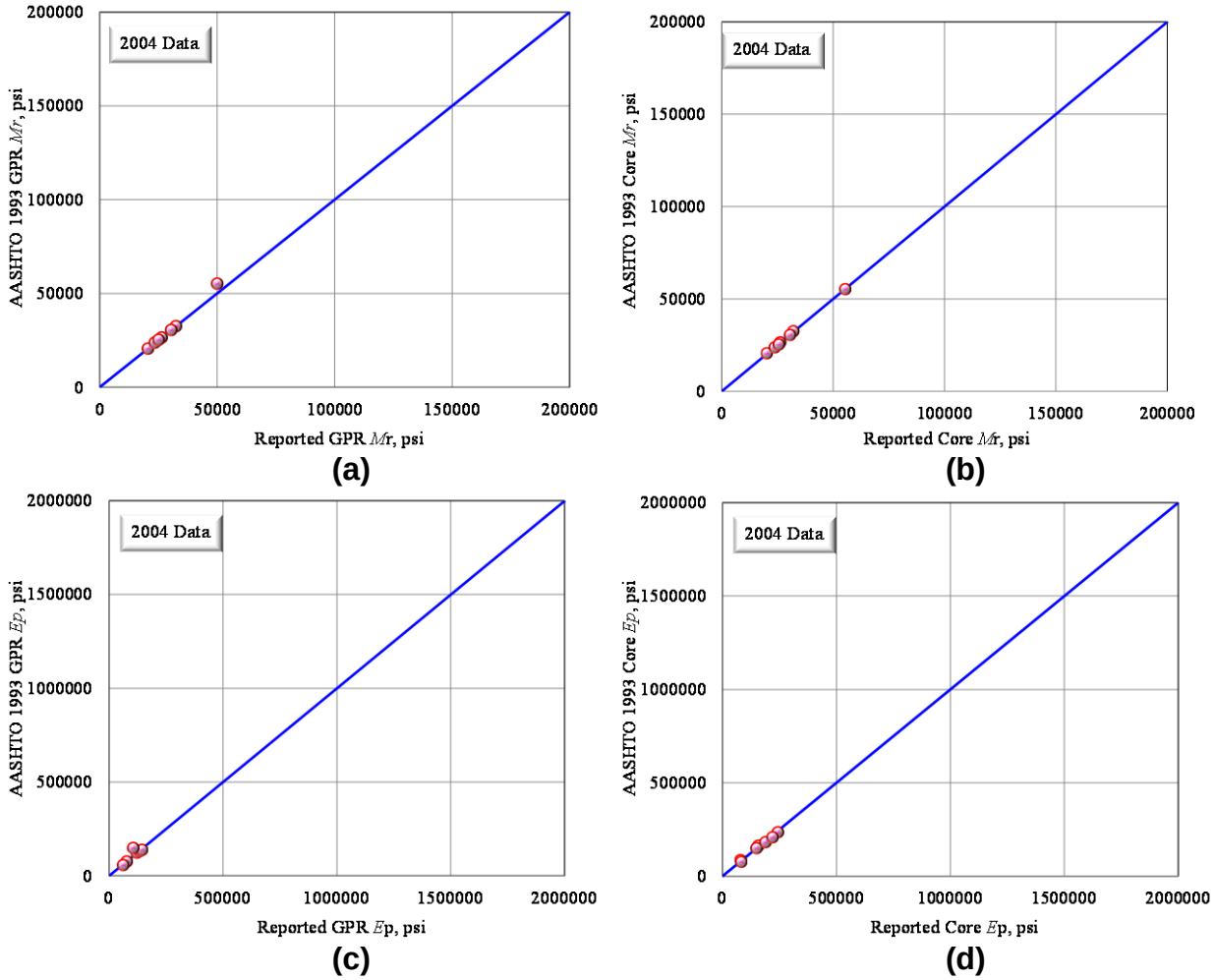

Figure 86 Comparison of 2004 Reported and AASHTO 1993 Verified Values of (a) Mr Based on GPR and (b) Mr Based on Core, (c) Ep Based on GPR and (d) Ep Based on Core for Control Section 55-68.

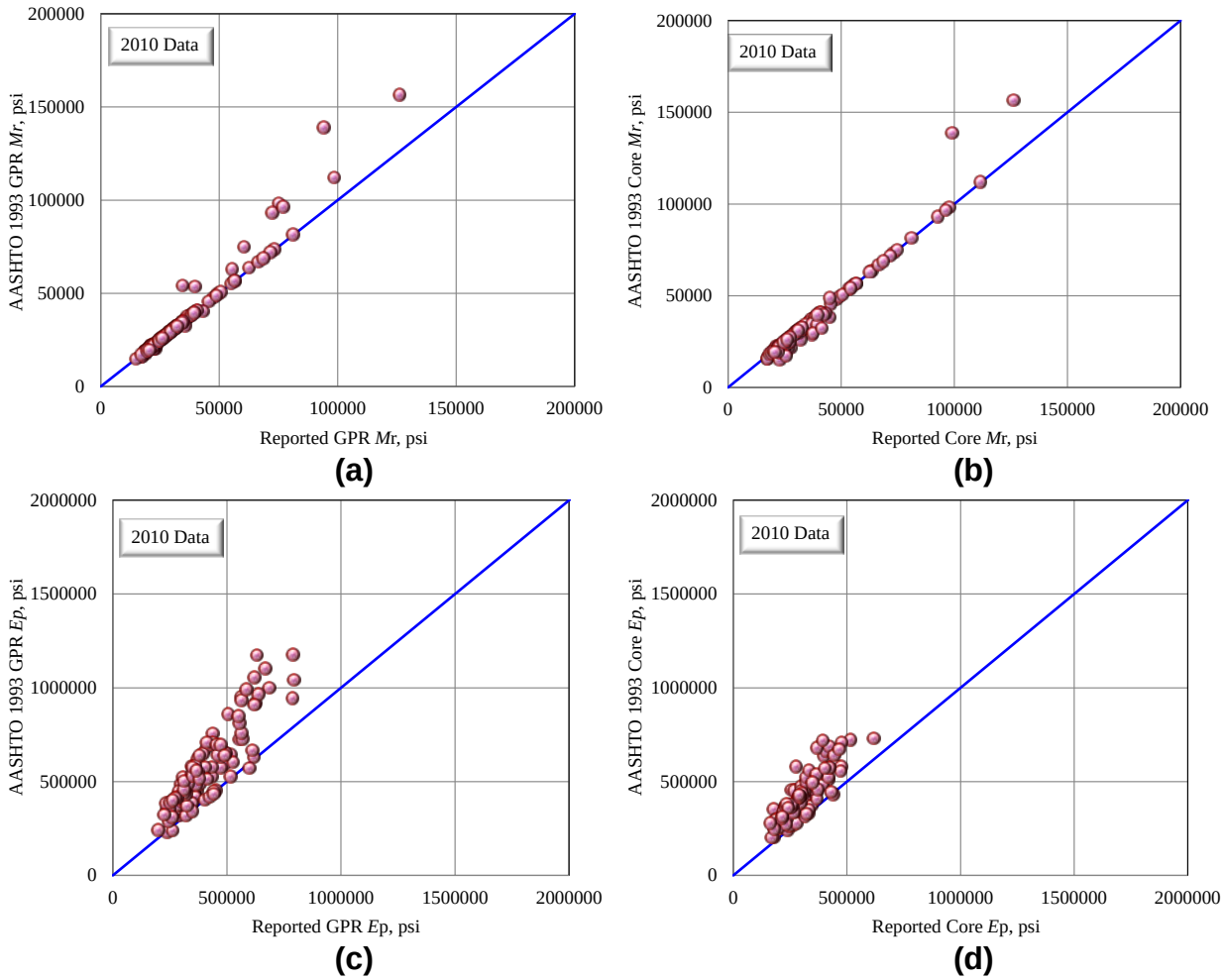

Figure 87 Comparison of 2010 Reported and AASHTO 1993 Verified Values of (a) Mr Based on GPR and (b) Mr Based on Core, (c) Ep Based on GPR and (d) Ep Based on Core for Control Section 20-04.

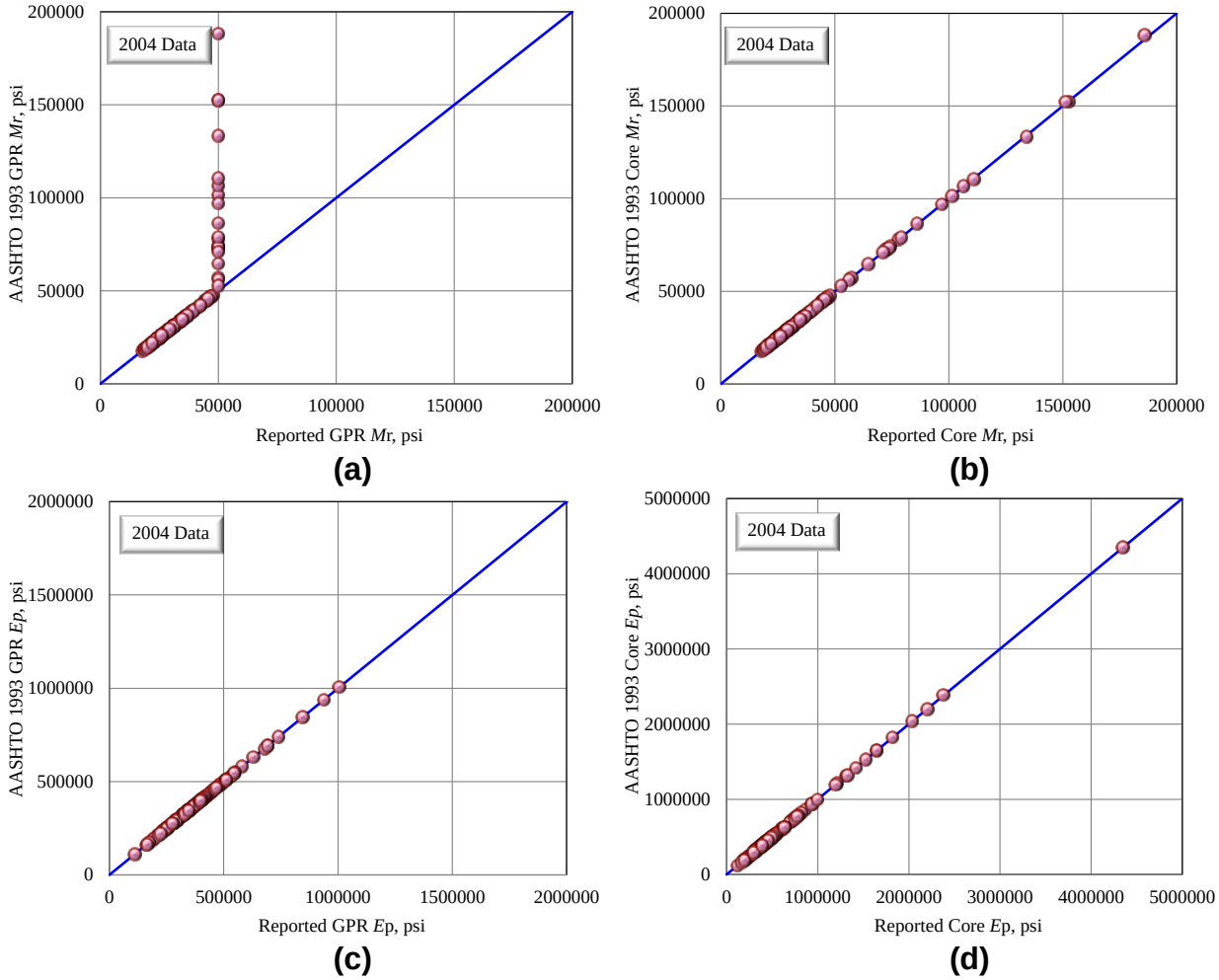

Figure 88 Comparison of 2004 Reported and AASHTO 1993 Verified Values of (a) Mr Based on GPR and (b) Mr Based on Core, (c) Ep Based on GPR and (d) Ep Based on Core for Control Section 20-04.

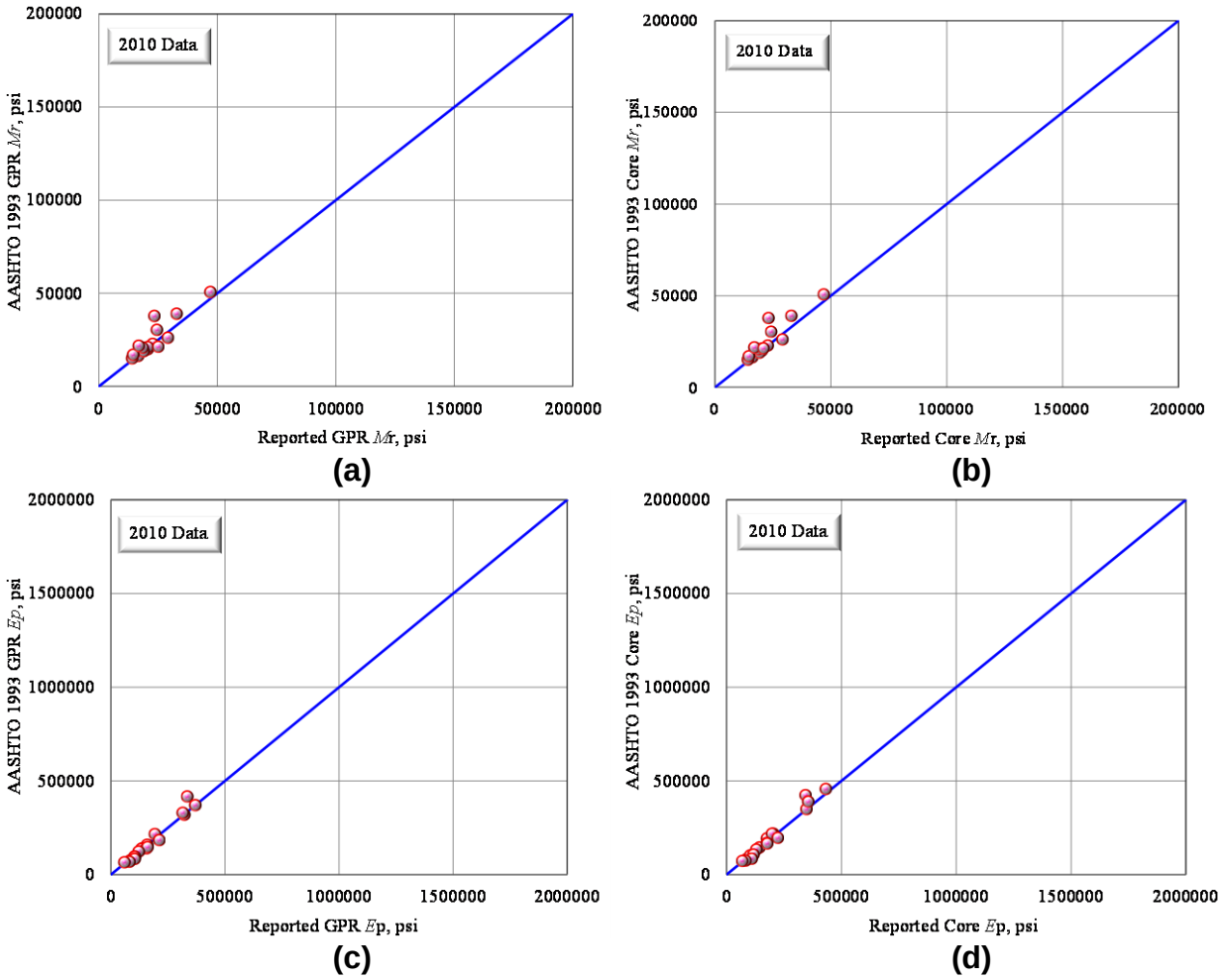

Figure 89 Comparison of 2010 Reported and AASHTO 1993 Verified Values of (a) Mr Based on GPR and (b) Mr Based on Core, (c) Ep Based on GPR and (d) Ep Based on Core for Control Section 72-78.

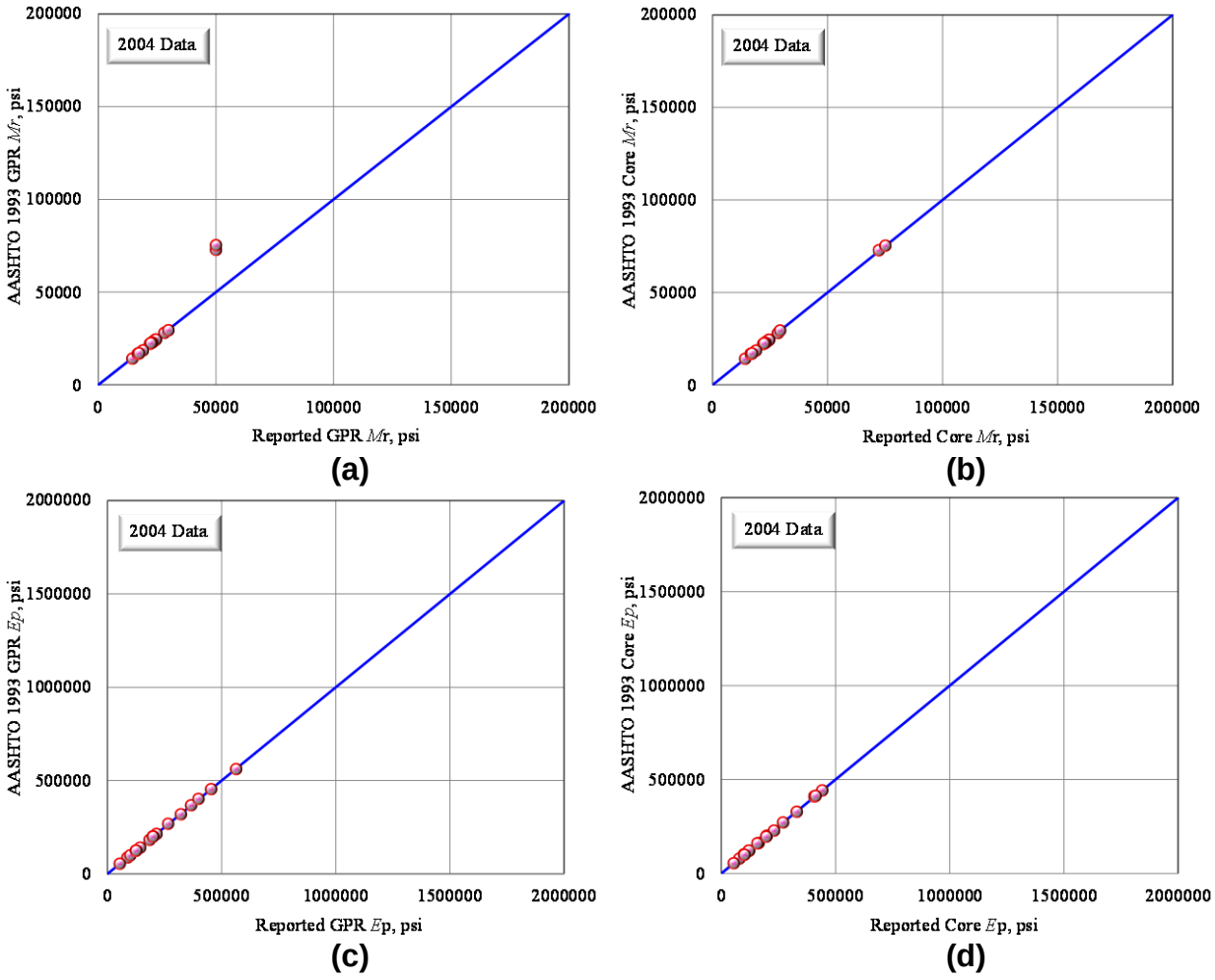

Figure 90 Comparison of 2004 Reported and AASHTO 1993 Verified Values of (a) Mr Based on GPR and (b) Mr Based on Core, (c) Ep Based on GPR and (d) Ep Based on Core for Control Section 72-78.

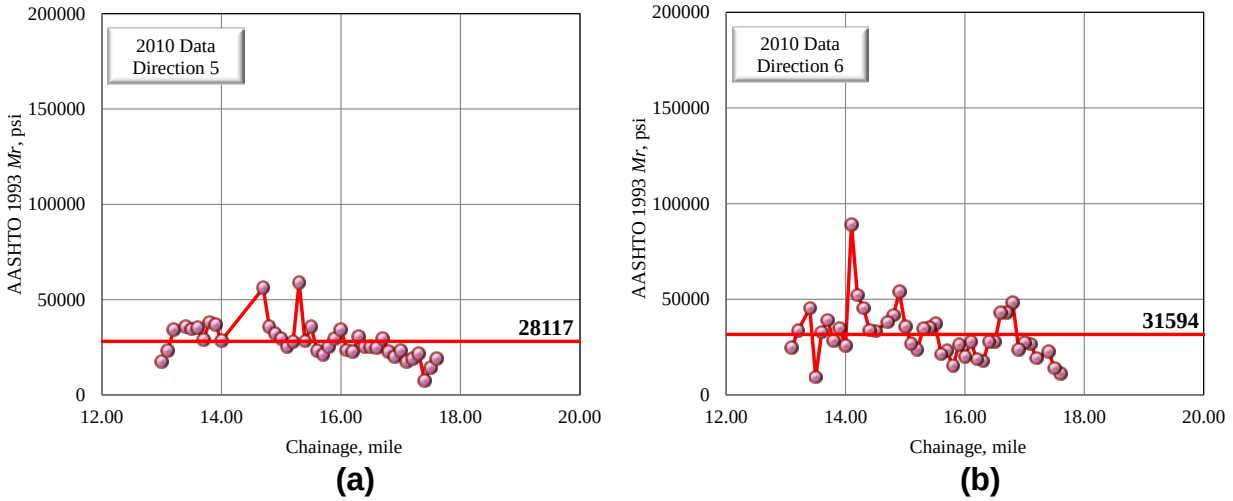

Figure 91 AASHTO 1993 Verified Mr Values Versus Distance in (a) Direction 5 and (b) Direction 6 for Control Section 68-22.

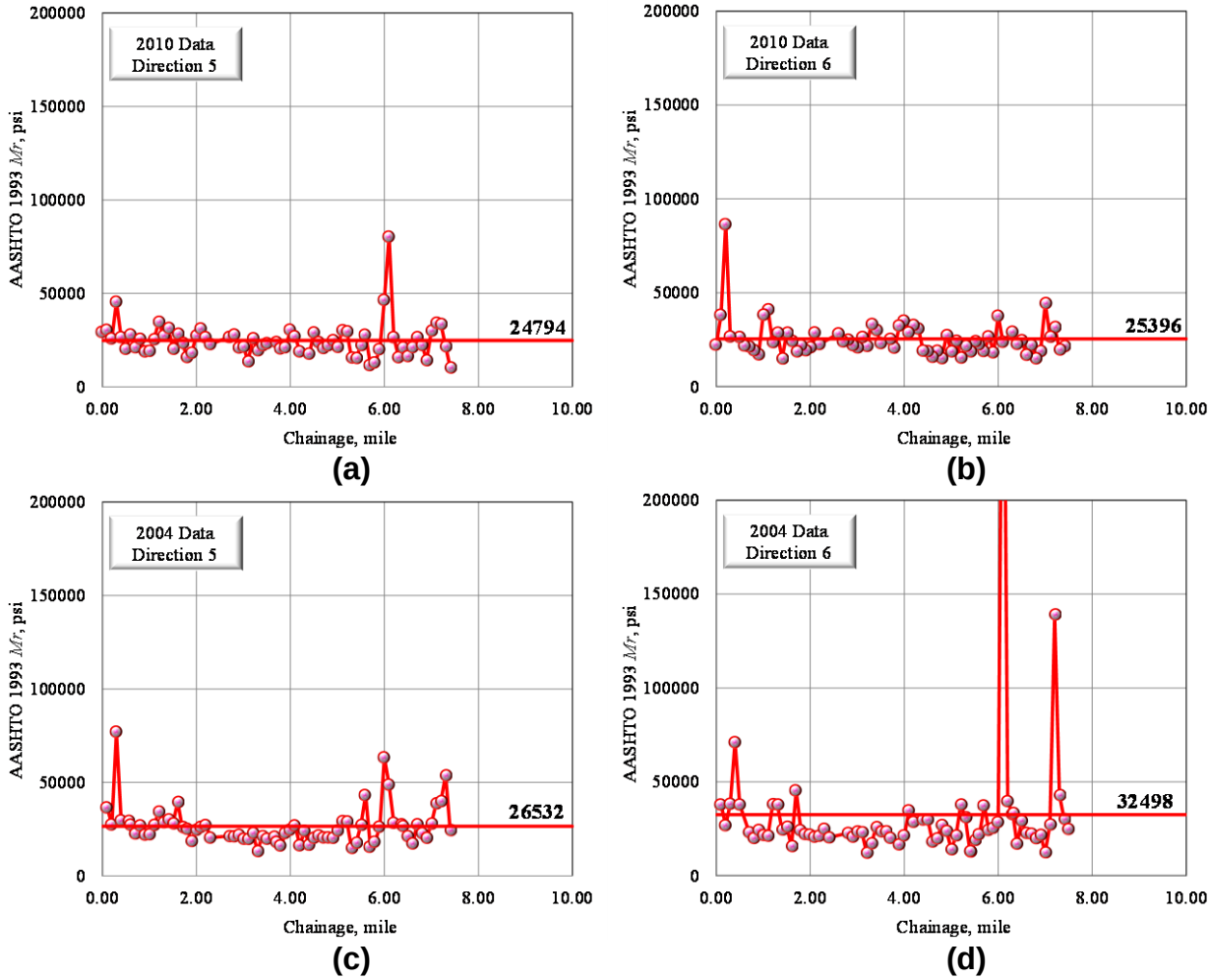

Figure 92 AASHTO 1993 Verified M_r Values Versus Distance for (a) 2010 data in Direction 5, (b) 2010 Data in Direction 6, (c) 2004 Data in Direction 5, and (d) 2004 Data in Direction 6 for Control Section 54-22.

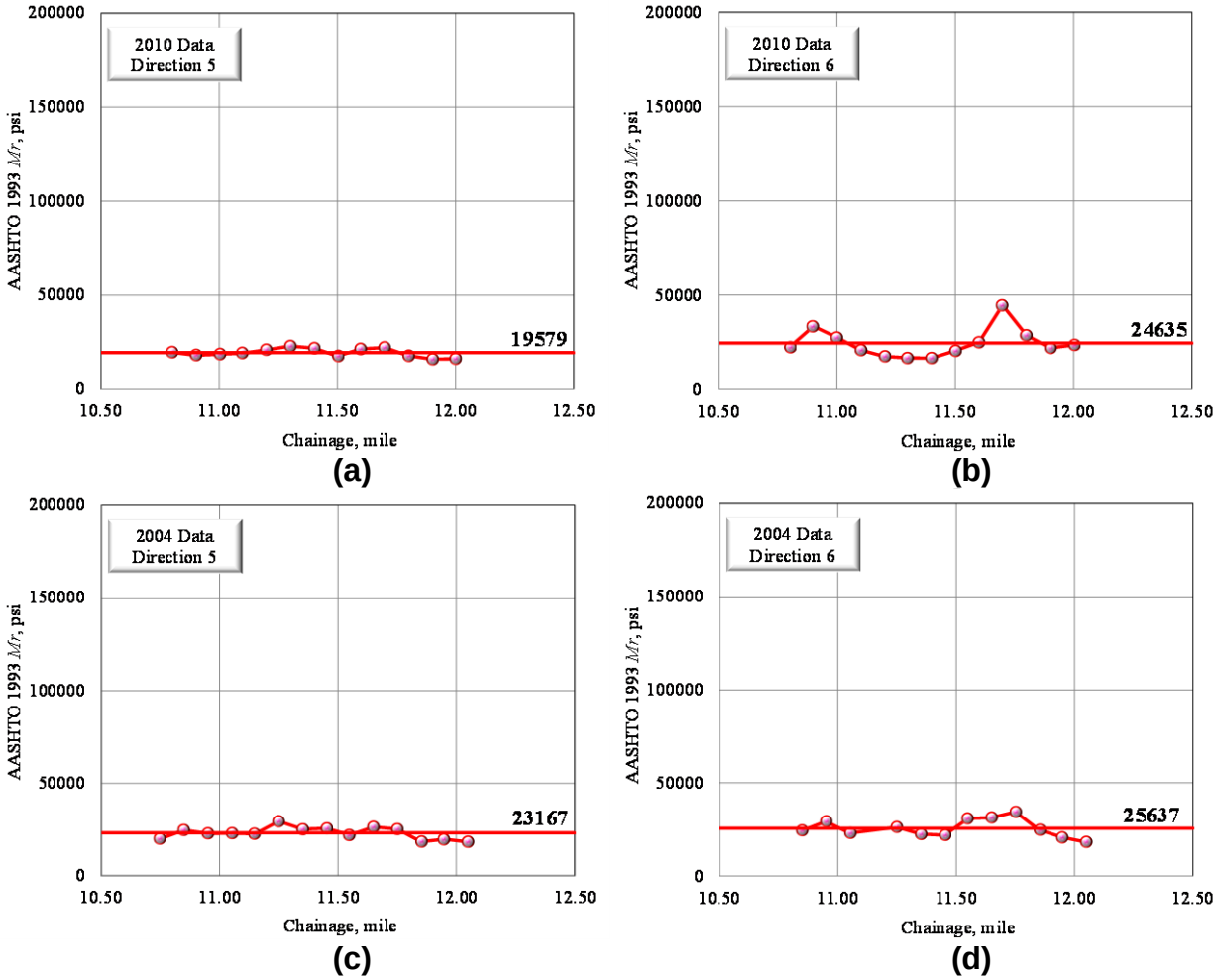

Figure 93 AASHTO 1993 Verified M_r Values Versus Distance for (a) 2010 data in Direction 5, (b) 2010 Data in Direction 6, (c) 2004 Data in Direction 5, and (d) 2004 Data in Direction 6 for Control Section 44-05.

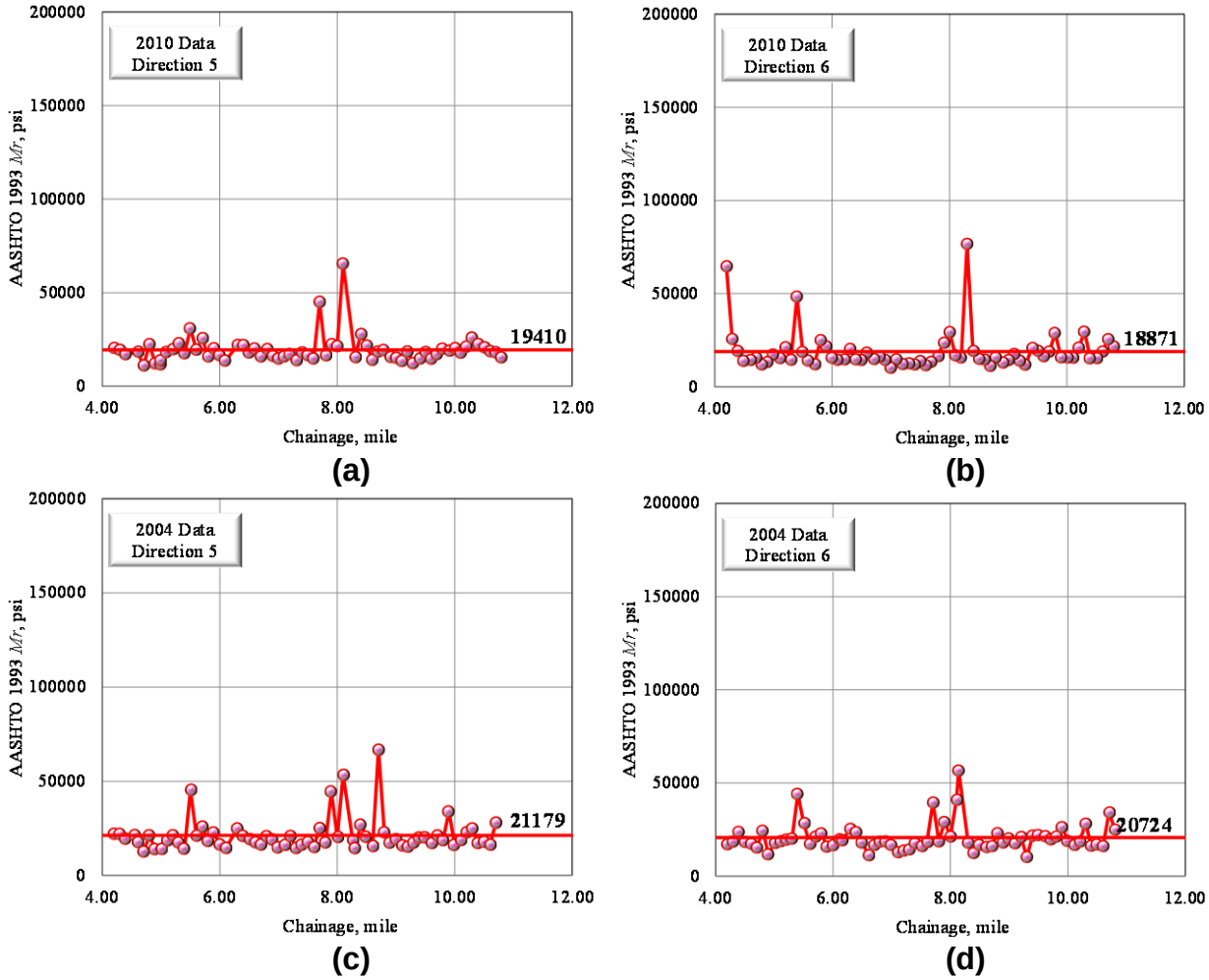

Figure 94 AASHTO 1993 Verified *Mr* Values Versus Distance for (a) 2010 data in Direction 5, (b) 2010 Data in Direction 6, (c) 2004 Data in Direction 5, and (d) 2004 Data in Direction 6 for Control Section 09-05.

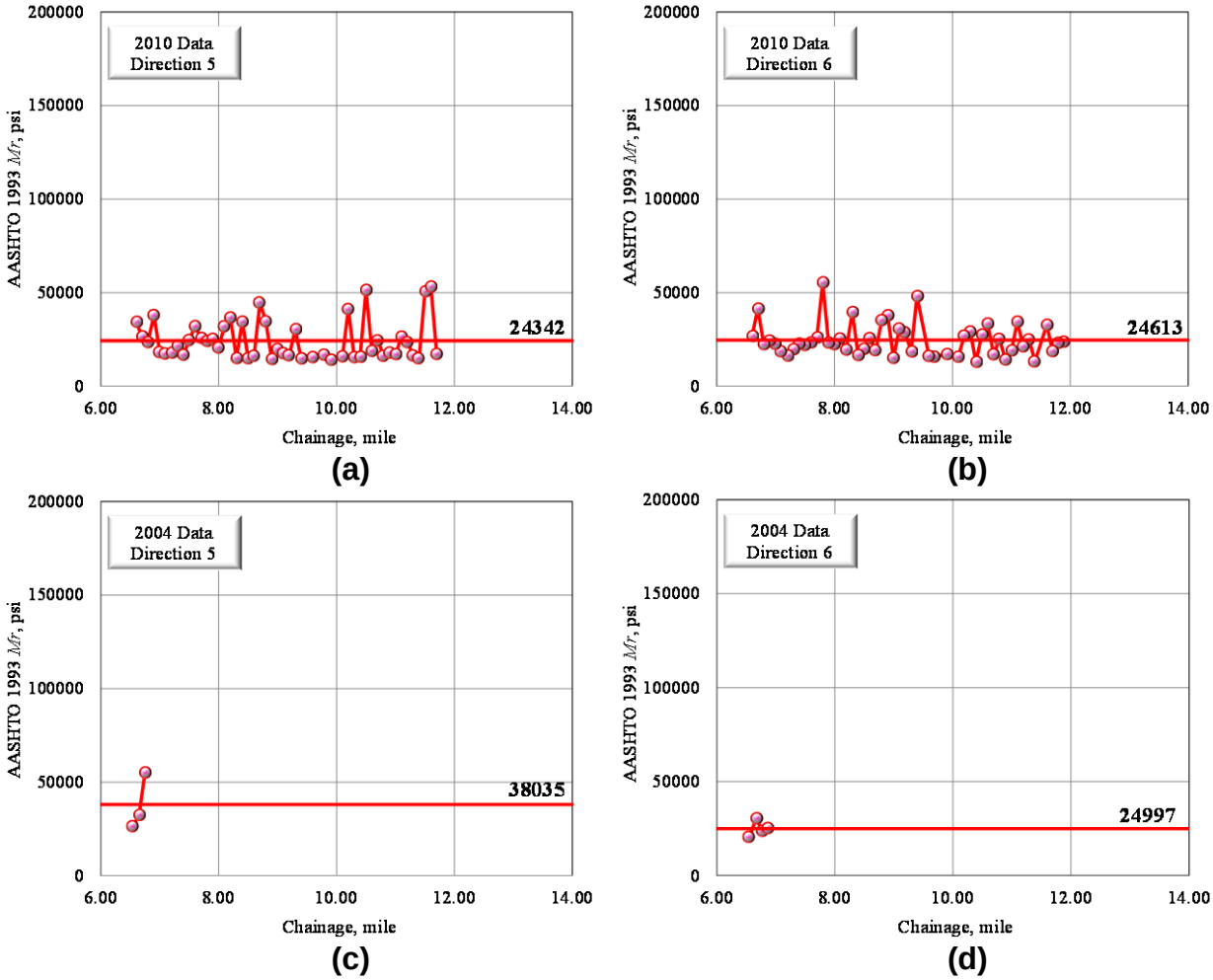

Figure 95 AASHTO 1993 Verified M_r Values Versus Distance for (a) 2010 Data in Direction 5, (b) 2010 Data in Direction 6, (c) 2004 Data in Direction 5, and (d) 2004 Data in Direction 6 for Control Section 55-68.

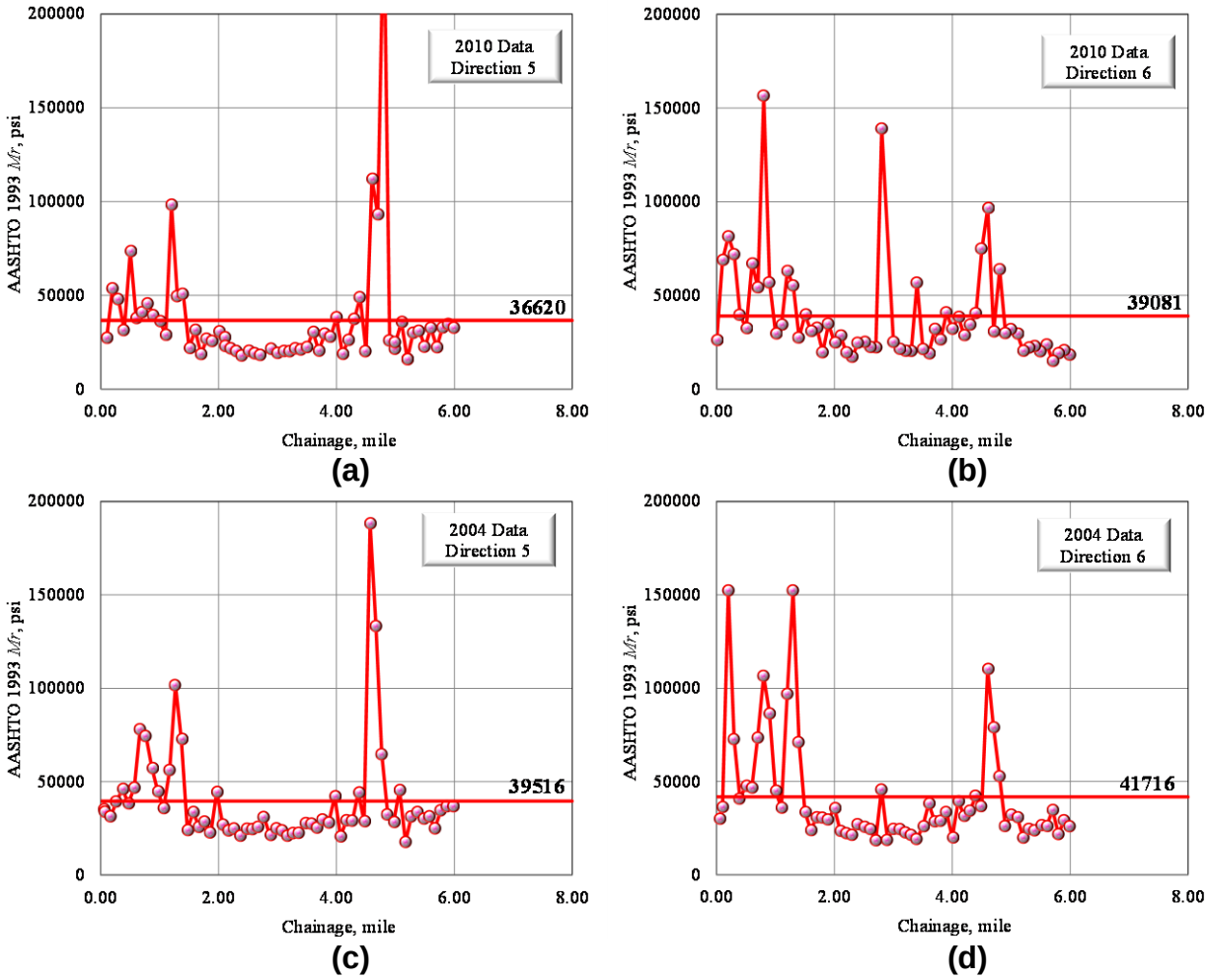

Figure 96 AASHTO 1993 Verified M_r Values Versus Distance for (a) 2010 Data in Direction 5, (b) 2010 Data in Direction 6, (c) 2004 Data in Direction 5, and (d) 2004 Data in Direction 6 for Control Section 20-04.

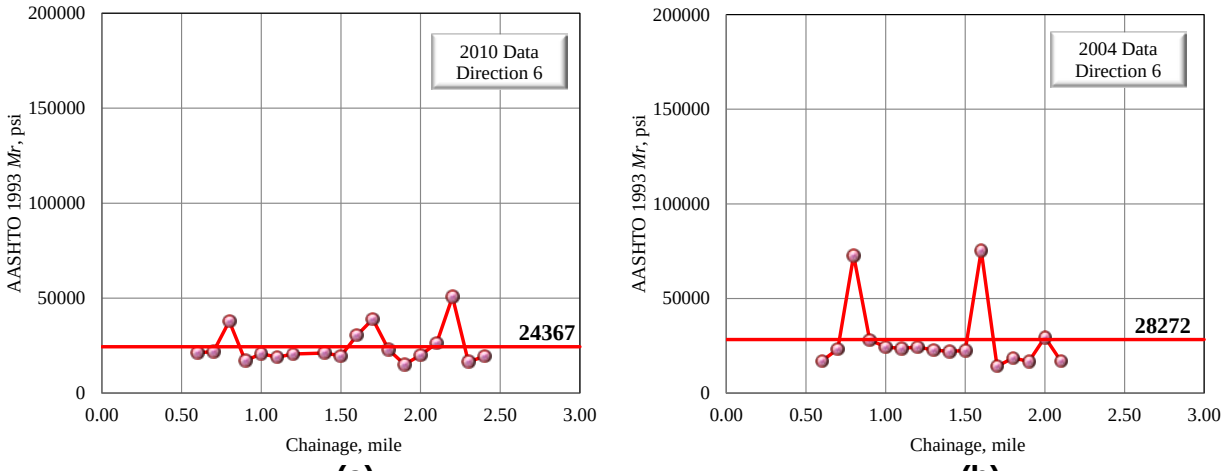

Figure 97 AASHTO 1993 Verified M_r Values Versus Distance for (a) 2010 Data in Direction 5, (b) 2004 Data in Direction 6 for Control Section 72-78.

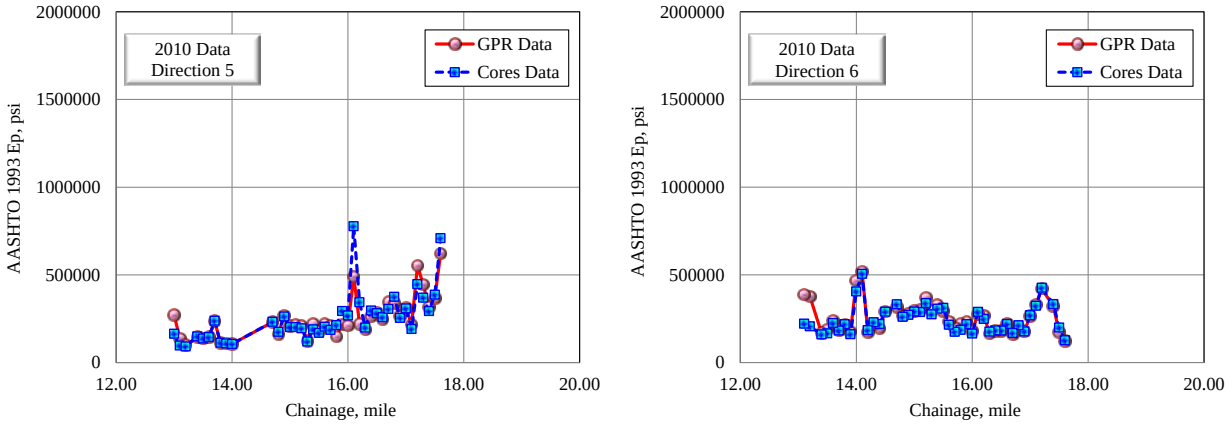

Figure 98 GPR and Core AASHTO 1993 Verified E_p Values Versus Distance for (a) 2010 Data in Direction 5, (b) 2010 Data in Direction 6 for Control Section 68-22.

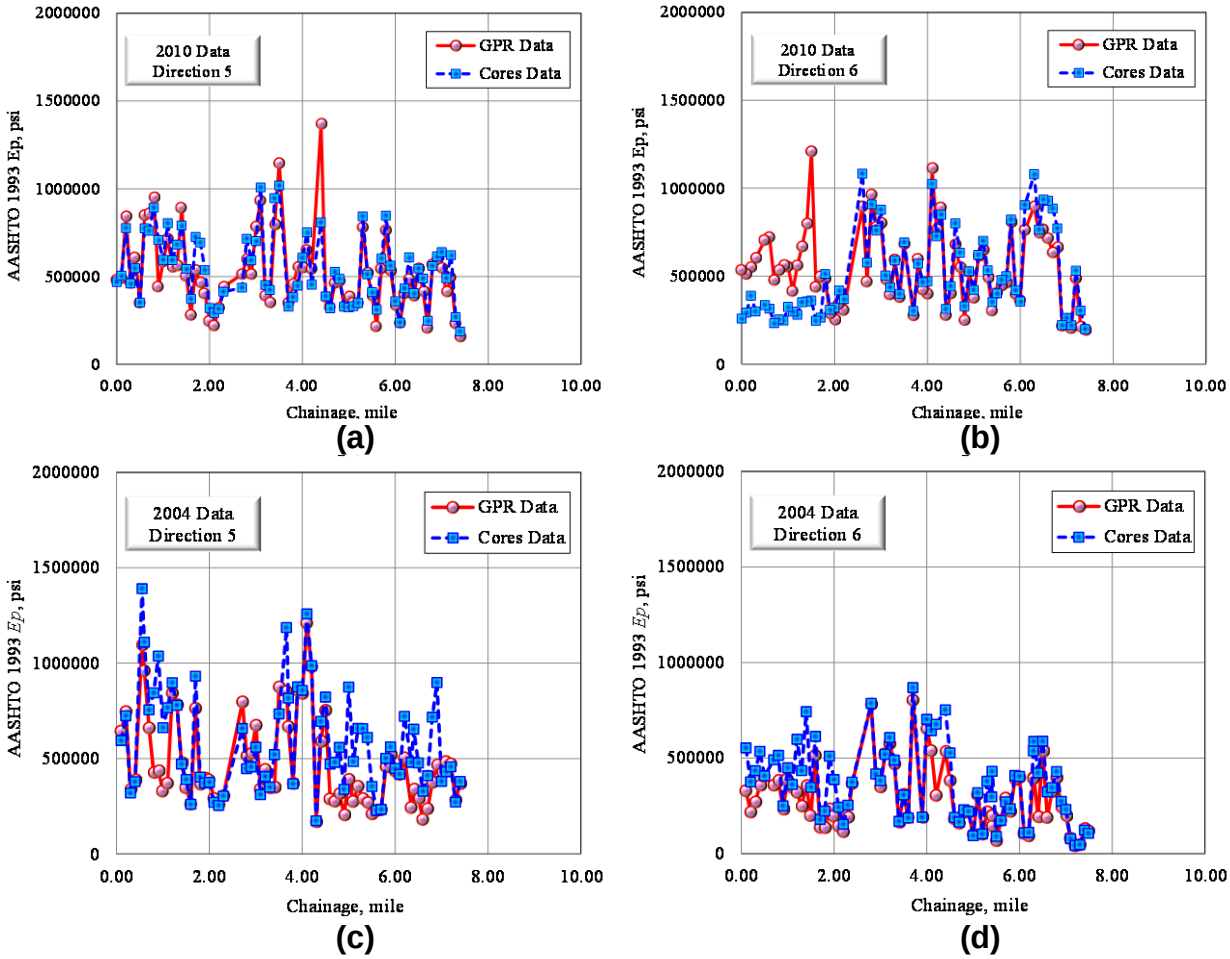

Figure 99 GPR and Core AASHTO 1993 Verified E_p Values Versus Distance for (a) 2010 Data in Direction 5, (b) 2010 Data in Direction 6, (c) 2004 Data in Direction 5, and (d) 2004 Data in Direction 6 for Control Section 54-22.

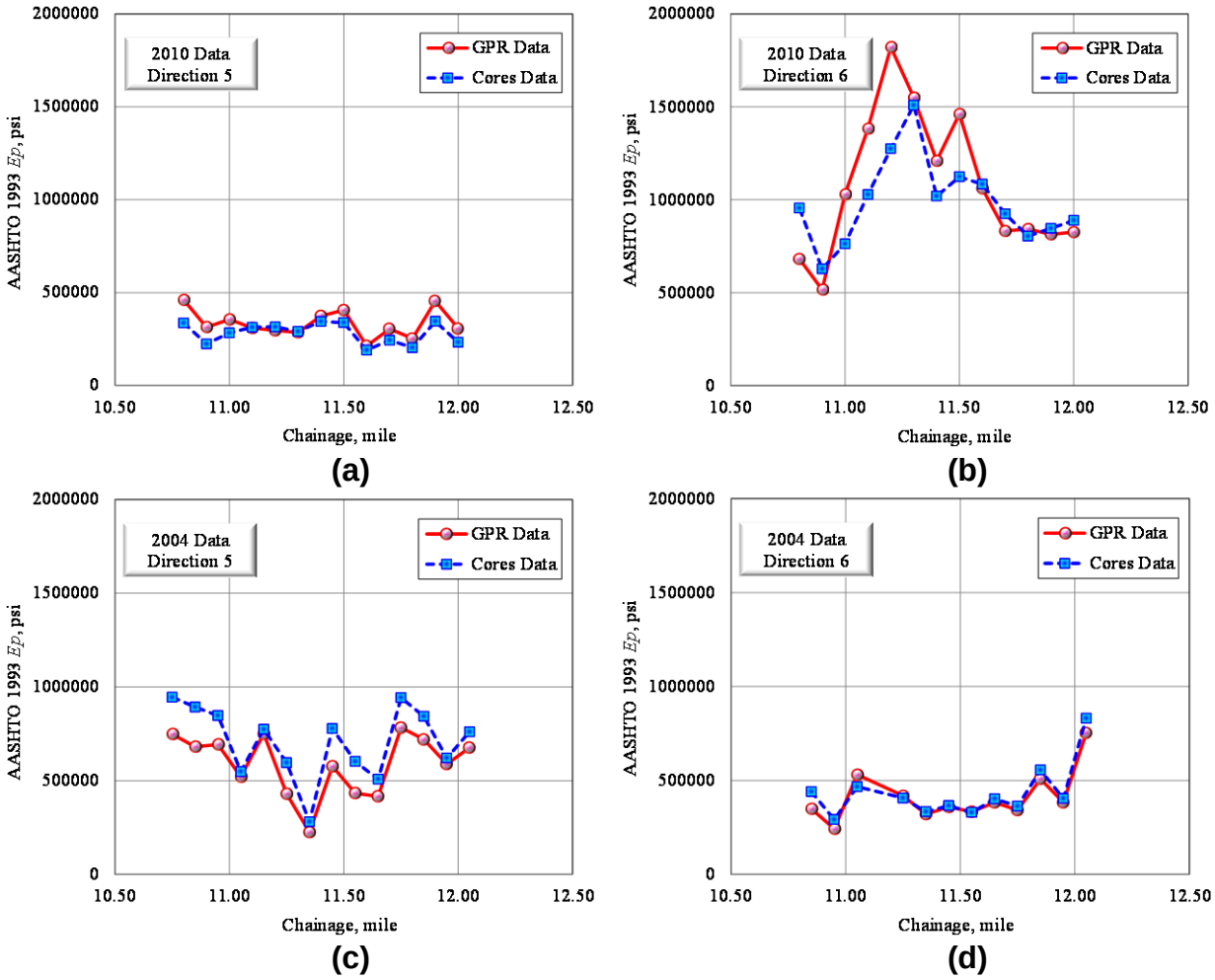

Figure 100 GPR and Core AASHTO 1993 Verified E_p Values Versus Distance for (a) 2010 Data in Direction 5, (b) 2010 Data in Direction 6, (c) 2004 Data in Direction 5, and (d) 2004 Data in Direction 6 for Control Section 44-05.

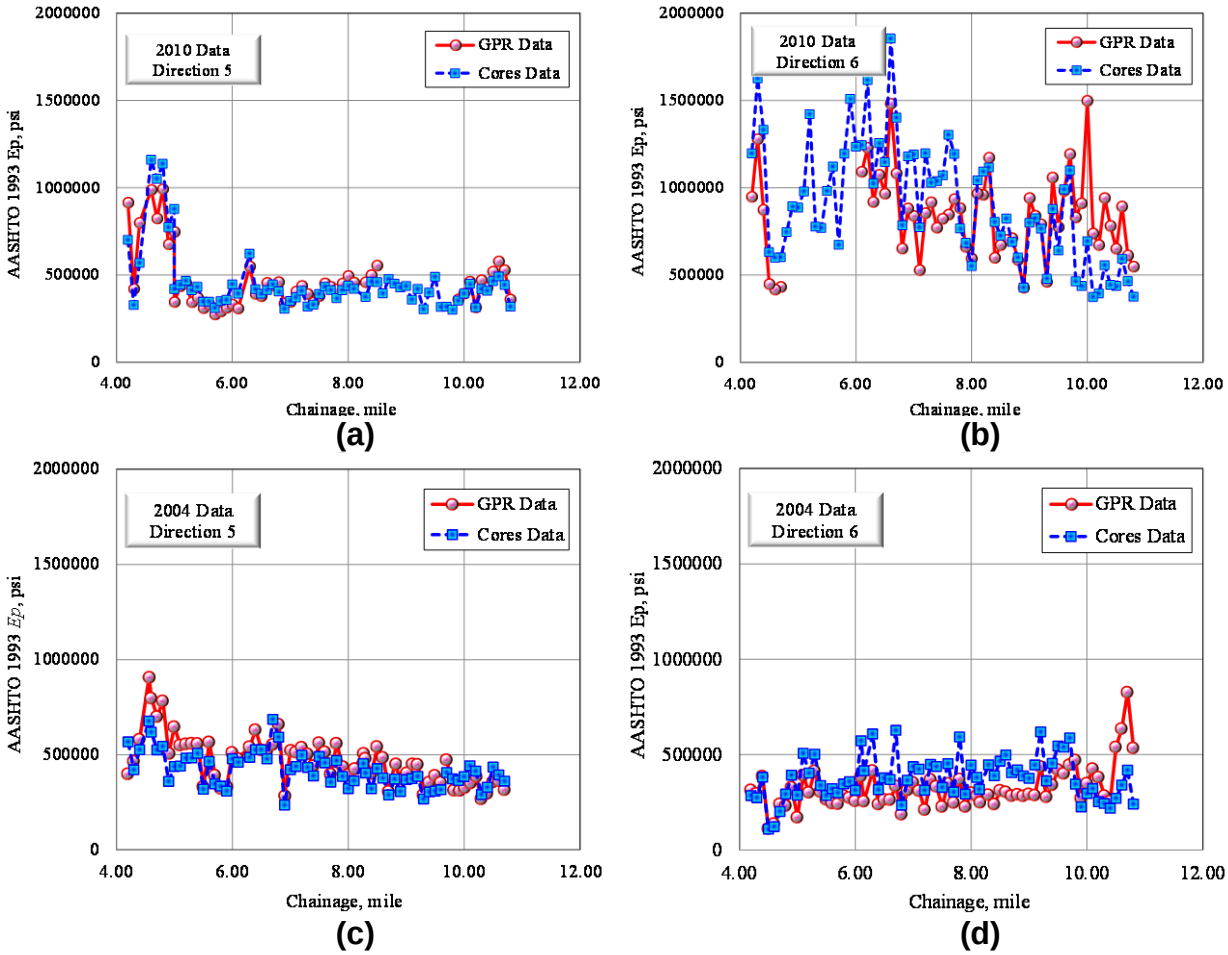

Figure 101 GPR and Core AASHTO 1993 Verified E_p Values Versus Distance for (a) 2010 Data in Direction 5, (b) 2010 Data in Direction 6, (c) 2004 Data in Direction 5, and (d) 2004 Data in Direction 6 for Control Section 09-05.

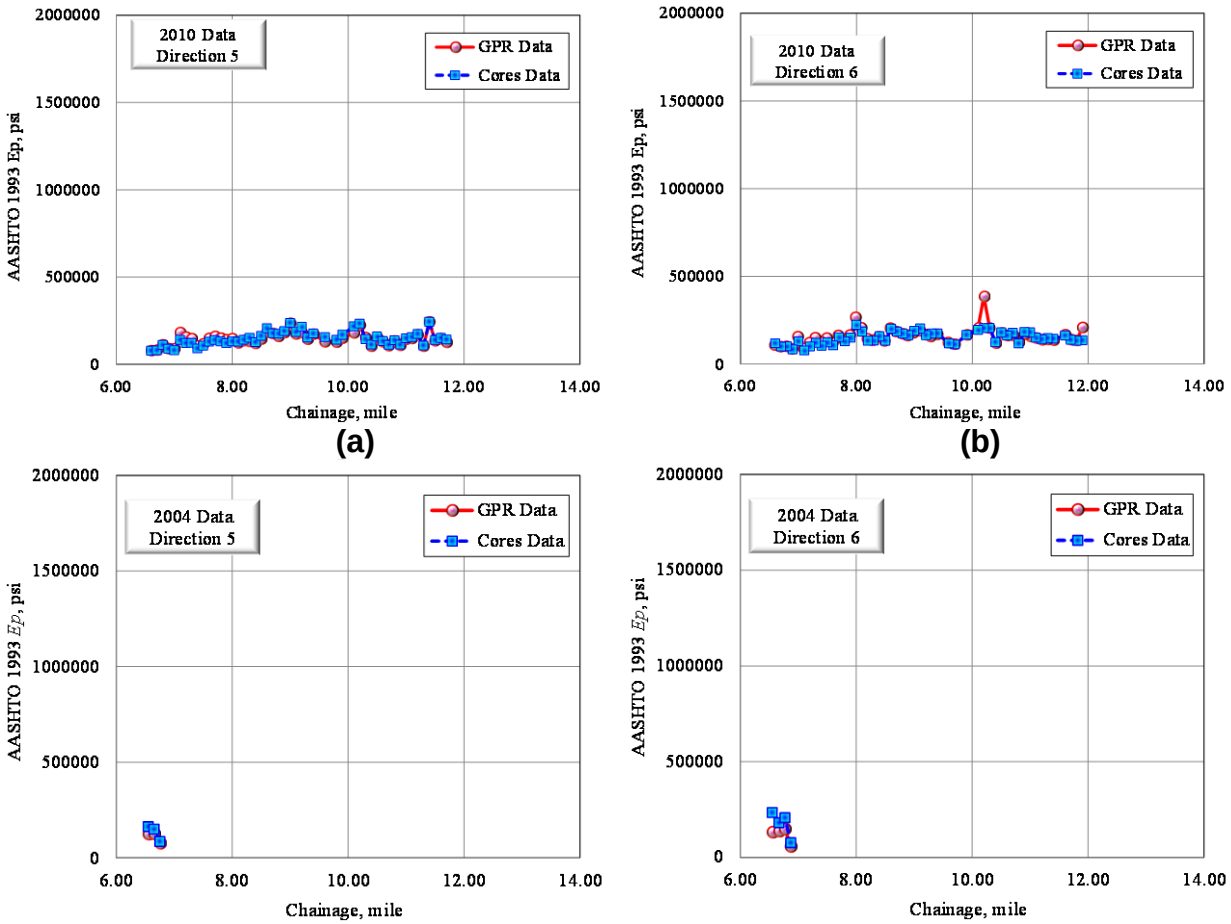

Figure 102 GPR and Core AASHTO 1993 Verified E_p Values Versus Distance for (a) 2010 Data in Direction 5, (b) 2010 Data in Direction 6, (c) 2004 Data in Direction 5, and (d) 2004 Data in Direction 6 for Control Section 55-68.

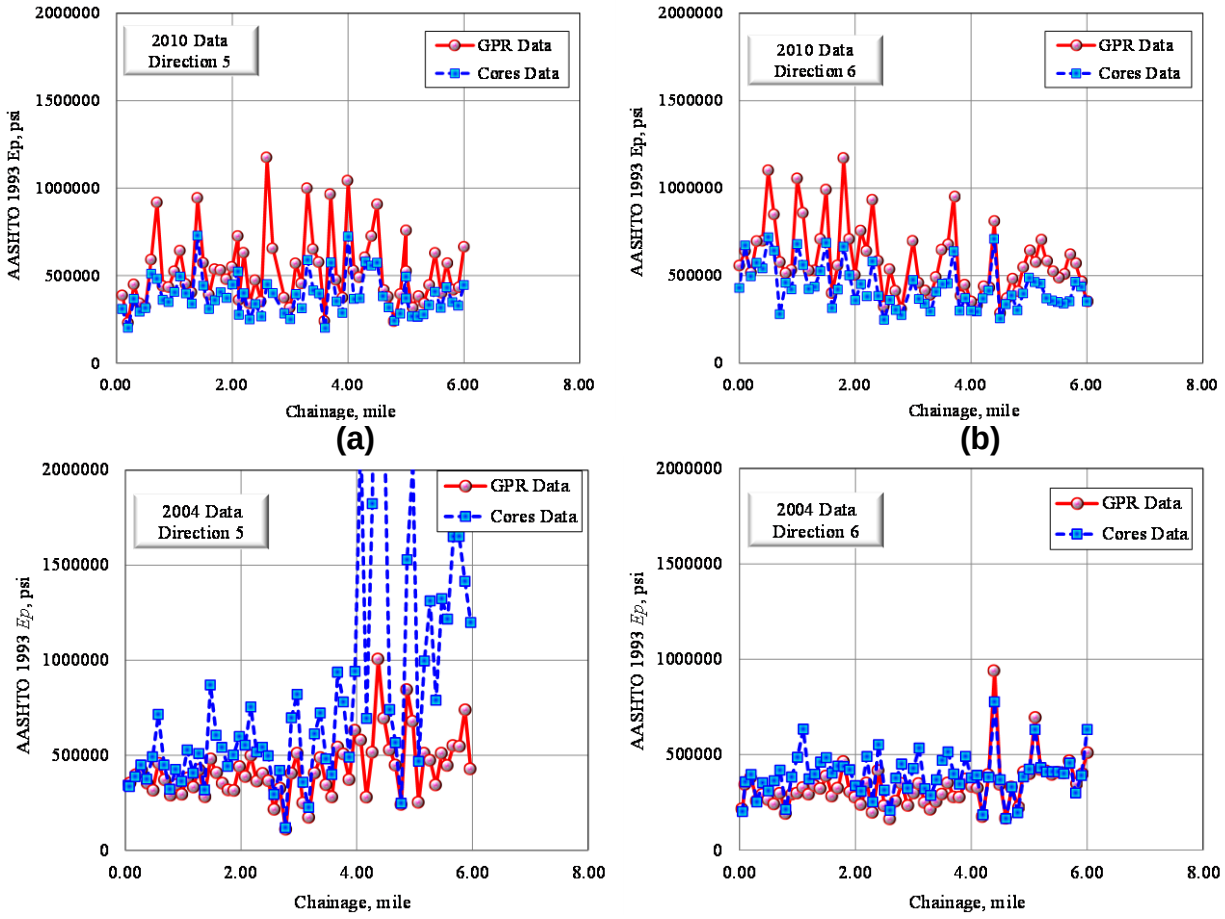

Figure 103 GPR and Core AASHTO 1993 Verified E_p Values Versus Distance for (a) 2010 Data in Direction 5, (b) 2010 Data in Direction 6, (c) 2004 Data in Direction 5, and (d) 2004 Data in Direction 6 for Control Section 20-04.

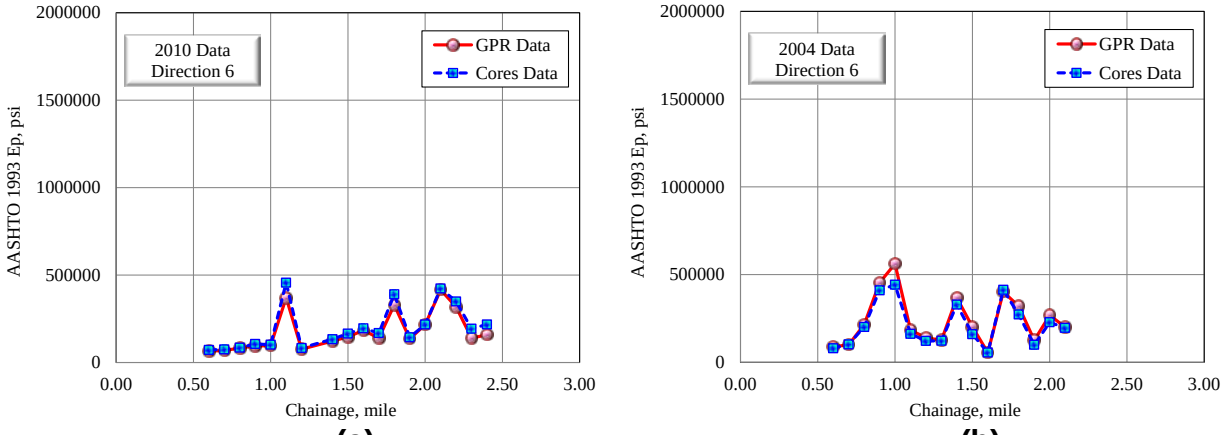

Figure 104 GPR and Core AASHTO 1993 Verified E_p Values Versus Distance for (a) 2010 Data in Direction 6, and (b) 2004 Data in Direction 6 for Control Section 72-78.

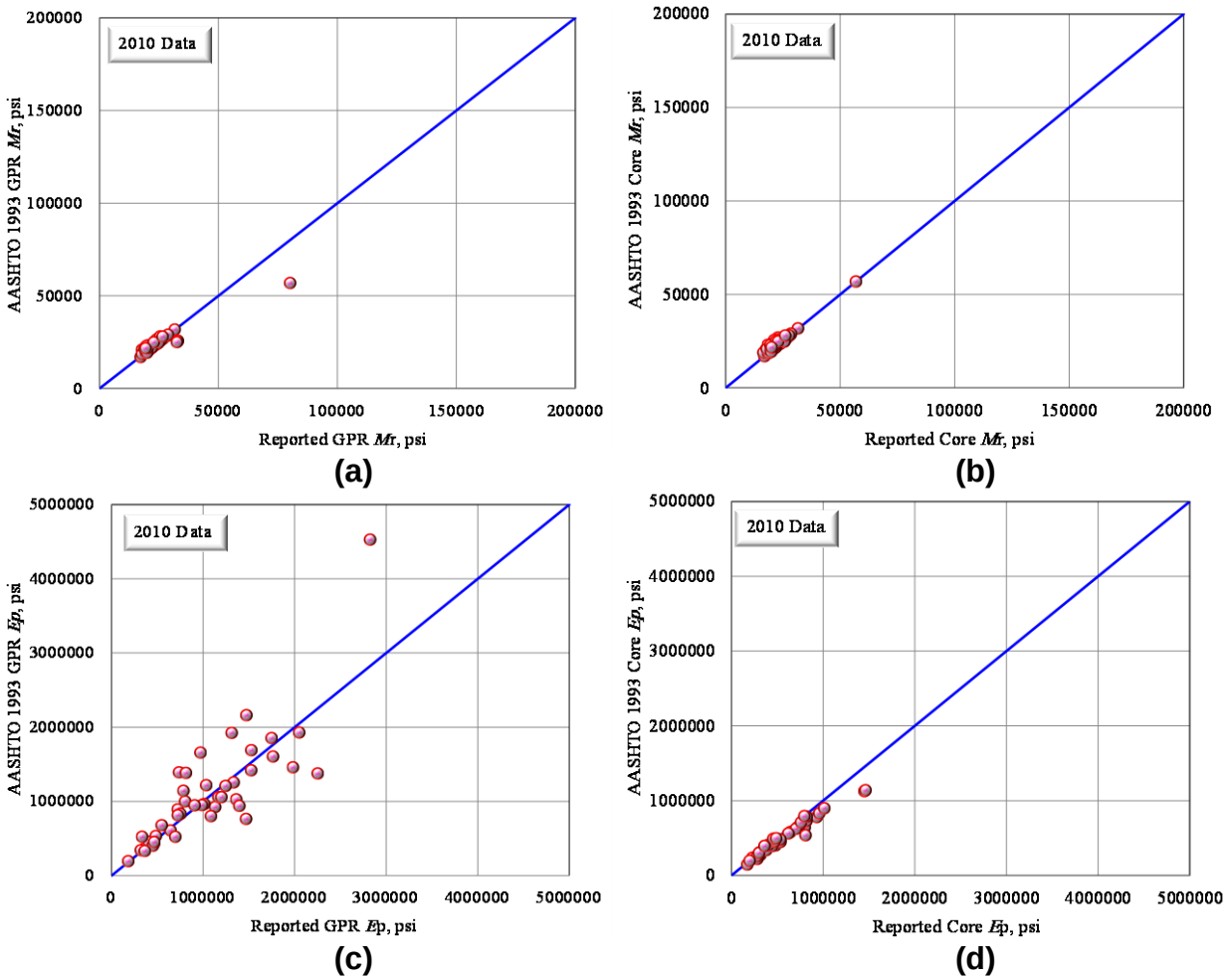

Figure 105 Comparison of 2010 Reported and AASHTO 1993 Verified Values of (a) Mr Based on GPR and (b) Mr Based on Core, (c) Ep Based on GPR and (d) Ep Based on Core for Control Section 25-46.

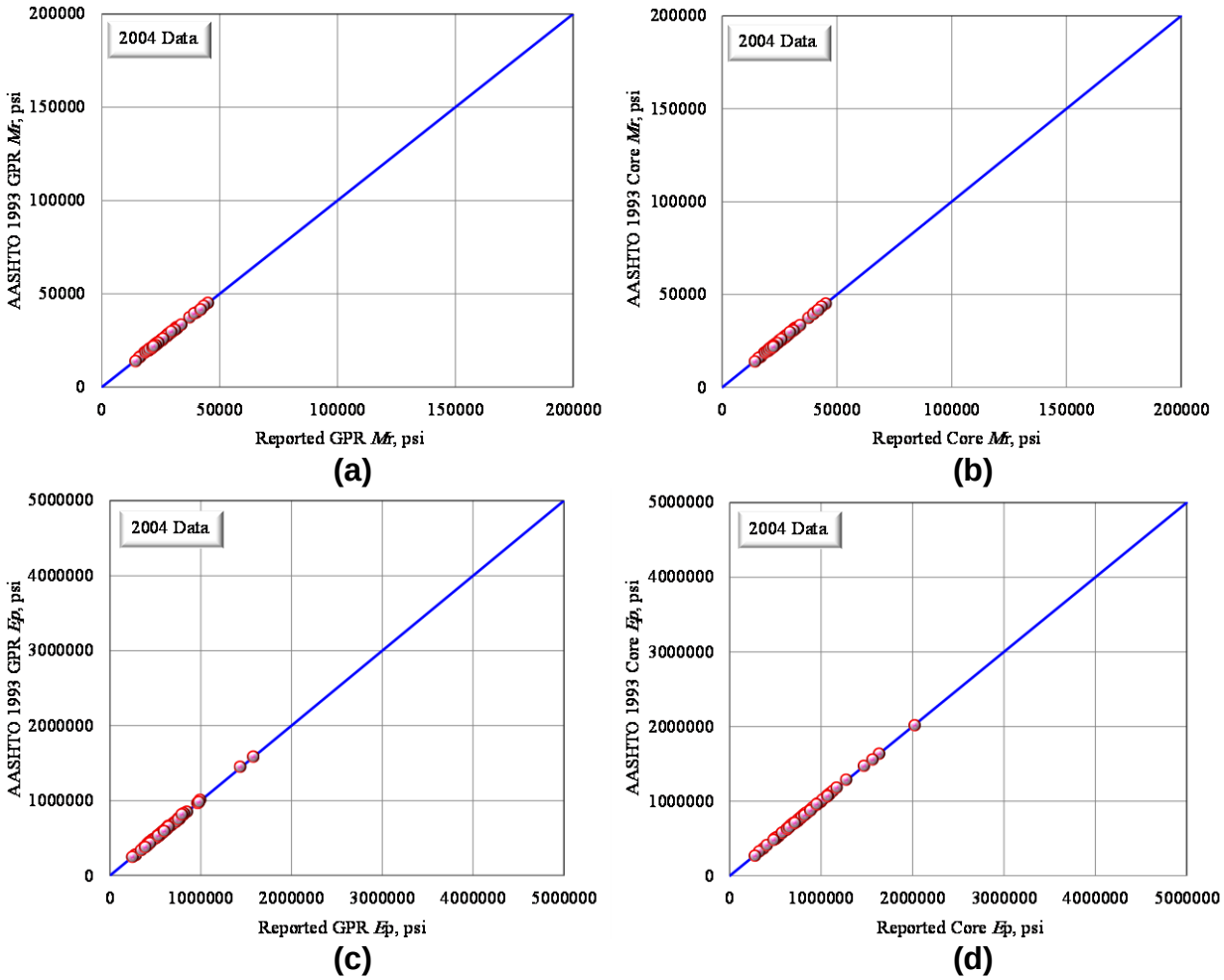

Figure 106 Comparison of 2004 Reported and AASHTO 1993 Verified Values of (a) Mr Based on GPR and (b) Mr Based on Core, (c) Ep Based on GPR and (d) Ep Based on Core for Control Section 25-46.

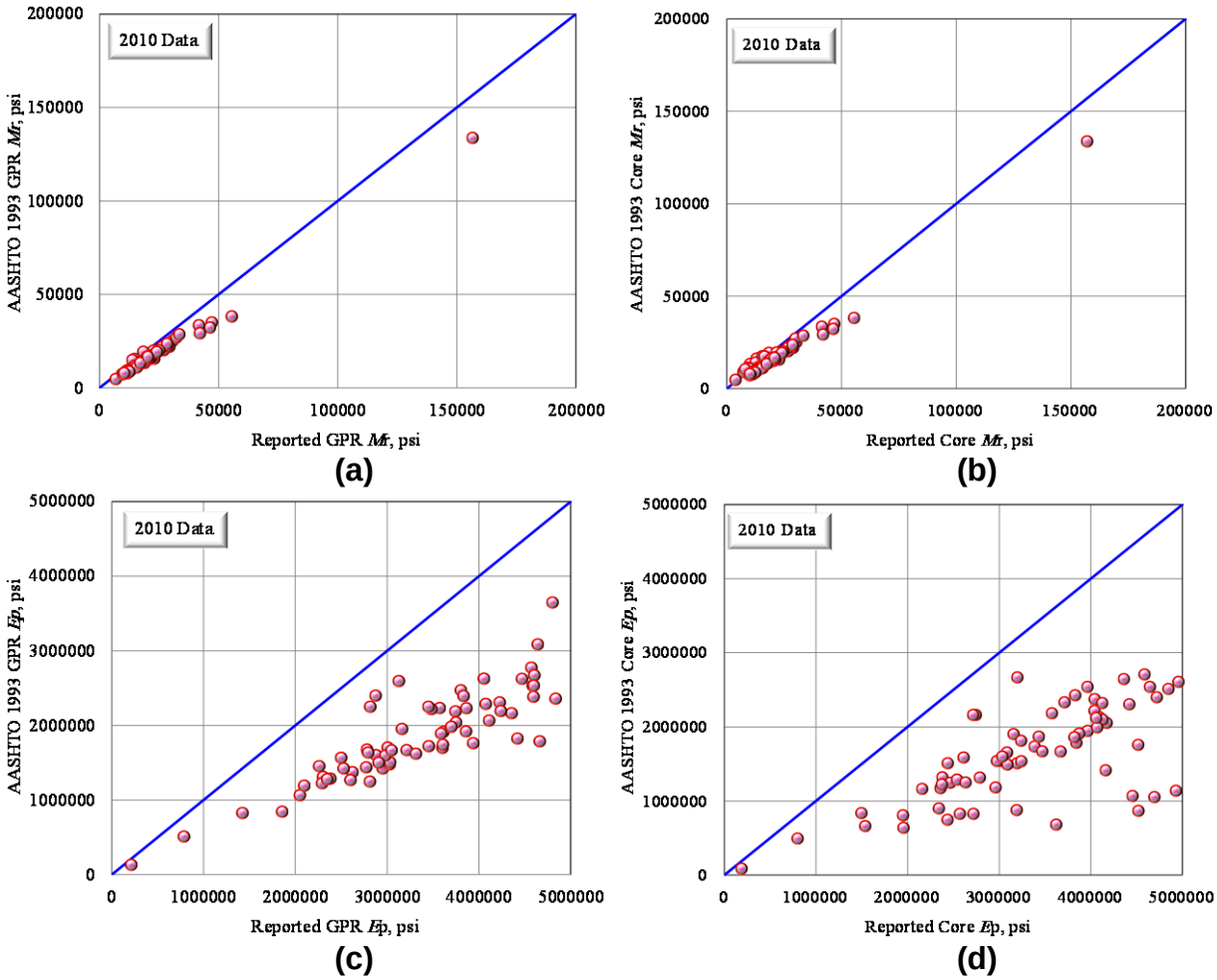

Figure 107 Comparison of 2010 Reported and AASHTO 1993 Verified Values of (a) Mr Based on GPR and (b) Mr Based on Core, (c) Ep Based on GPR and (d) Ep Based on Core for Control Section 42-30.

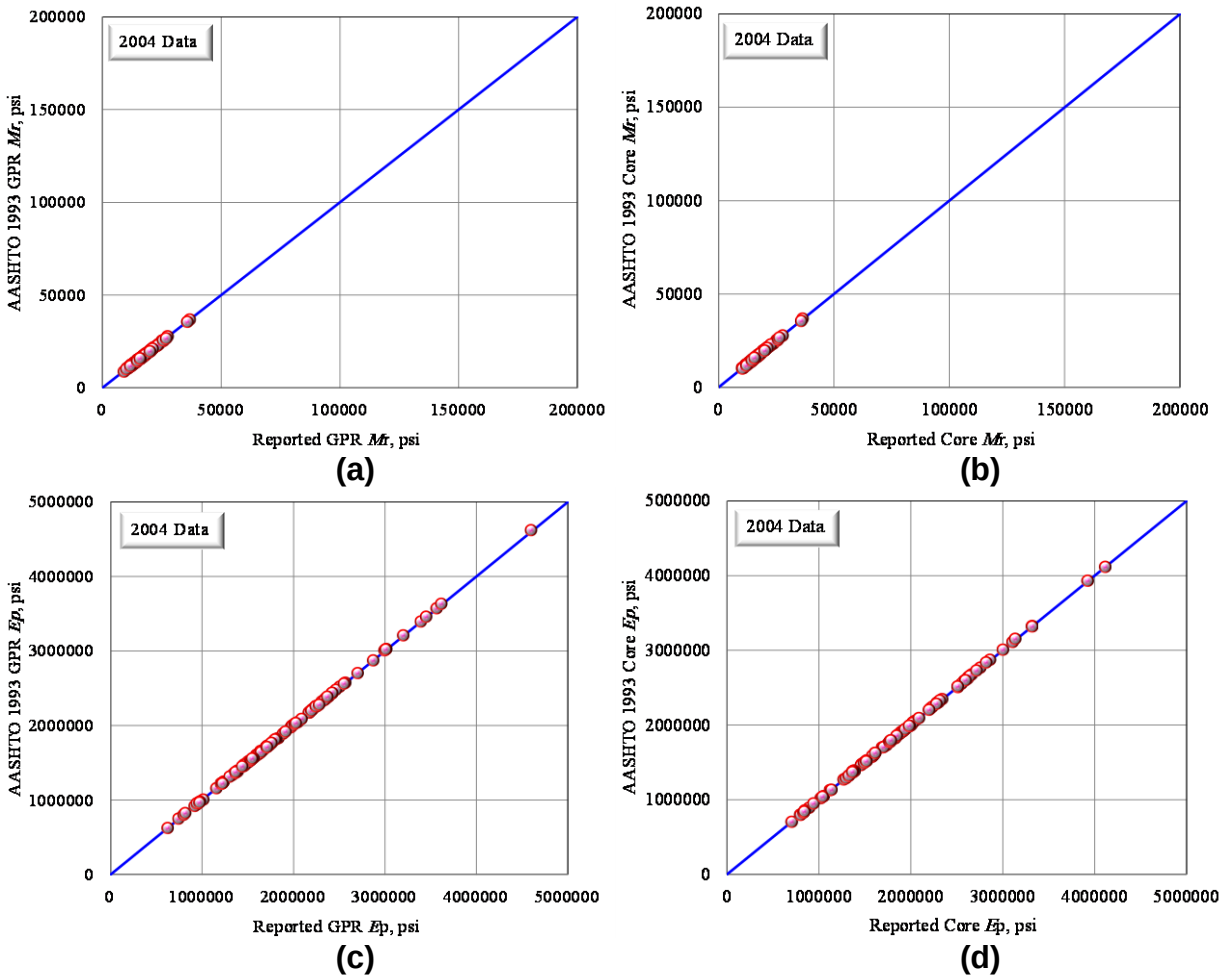

Figure 108 Comparison of 2004 Reported and AASHTO 1993 Verified Values of (a) Mr Based on GPR and (b) Mr Based on Core, (c) Ep Based on GPR and (d) Ep Based on Core for Control Section 42-30.

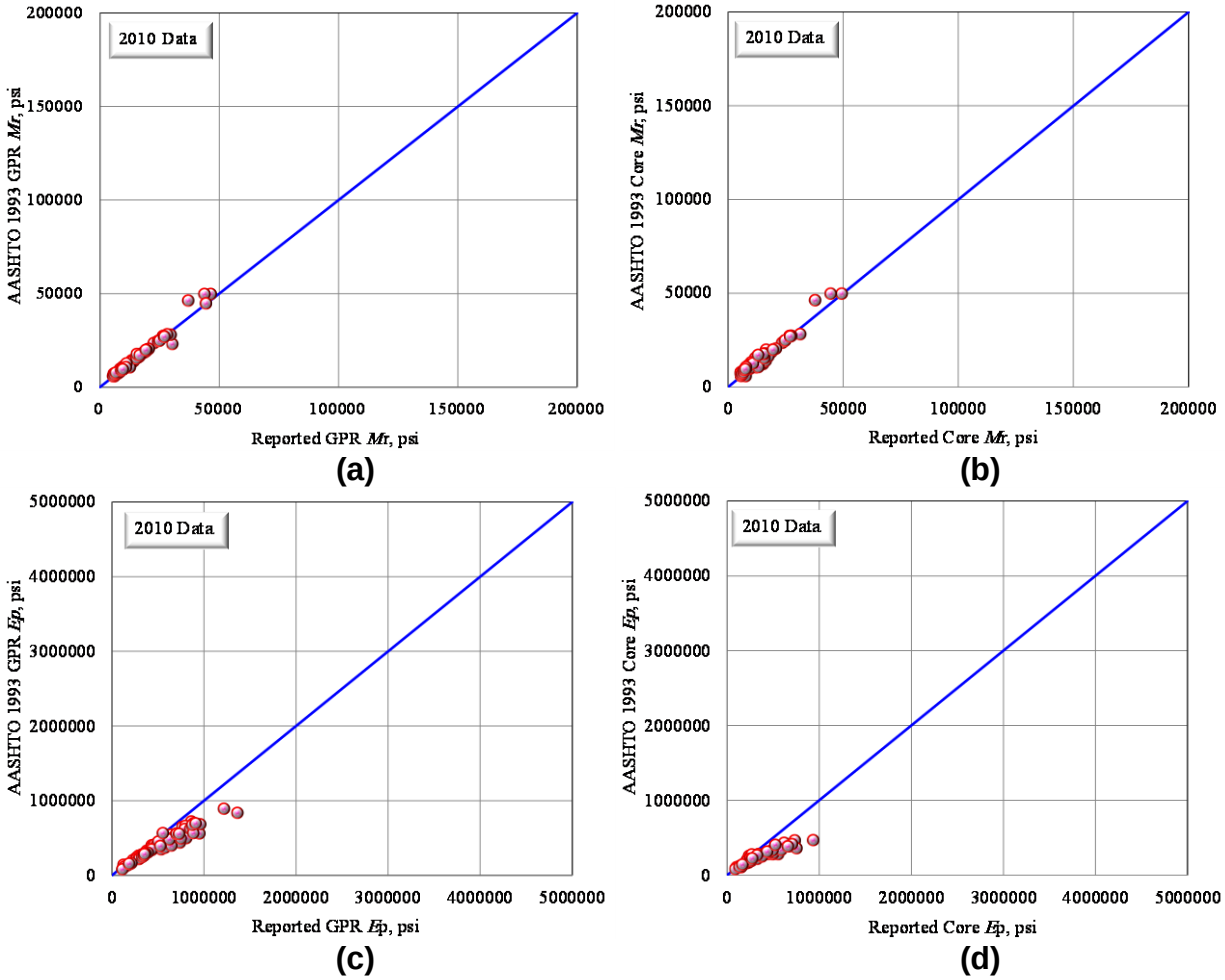

Figure 109 Comparison of 2010 Reported and AASHTO 1993 Verified Values of (a) Mr Based on GPR and (b) Mr Based on Core, (c) Ep Based on GPR and (d) Ep Based on Core for Control Section 65-09.

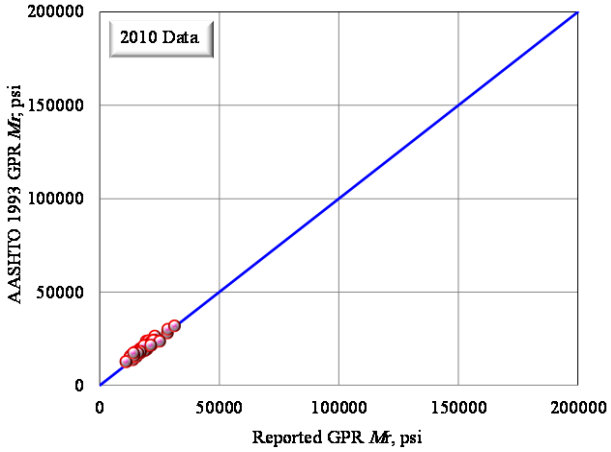

(a)

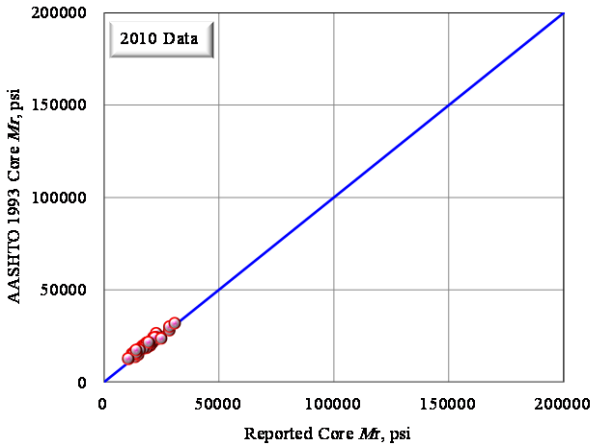

(b)

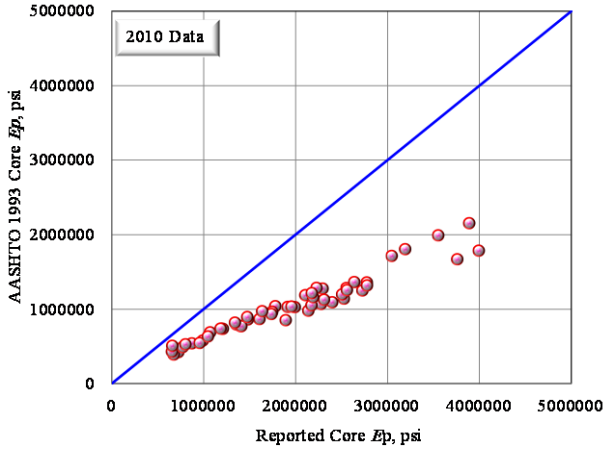

(c)

Figure 110 Comparison of 2010 Reported and AASHTO 1993 Verified Values of (a) Mr Based on GPR and (b) Mr Based on Core, (c) Ep Based on GPR for Control Section 16-49 (Note: the GPR data for this section did not include thickness of PCC layer so E_p could not be calculated from the GPR values).

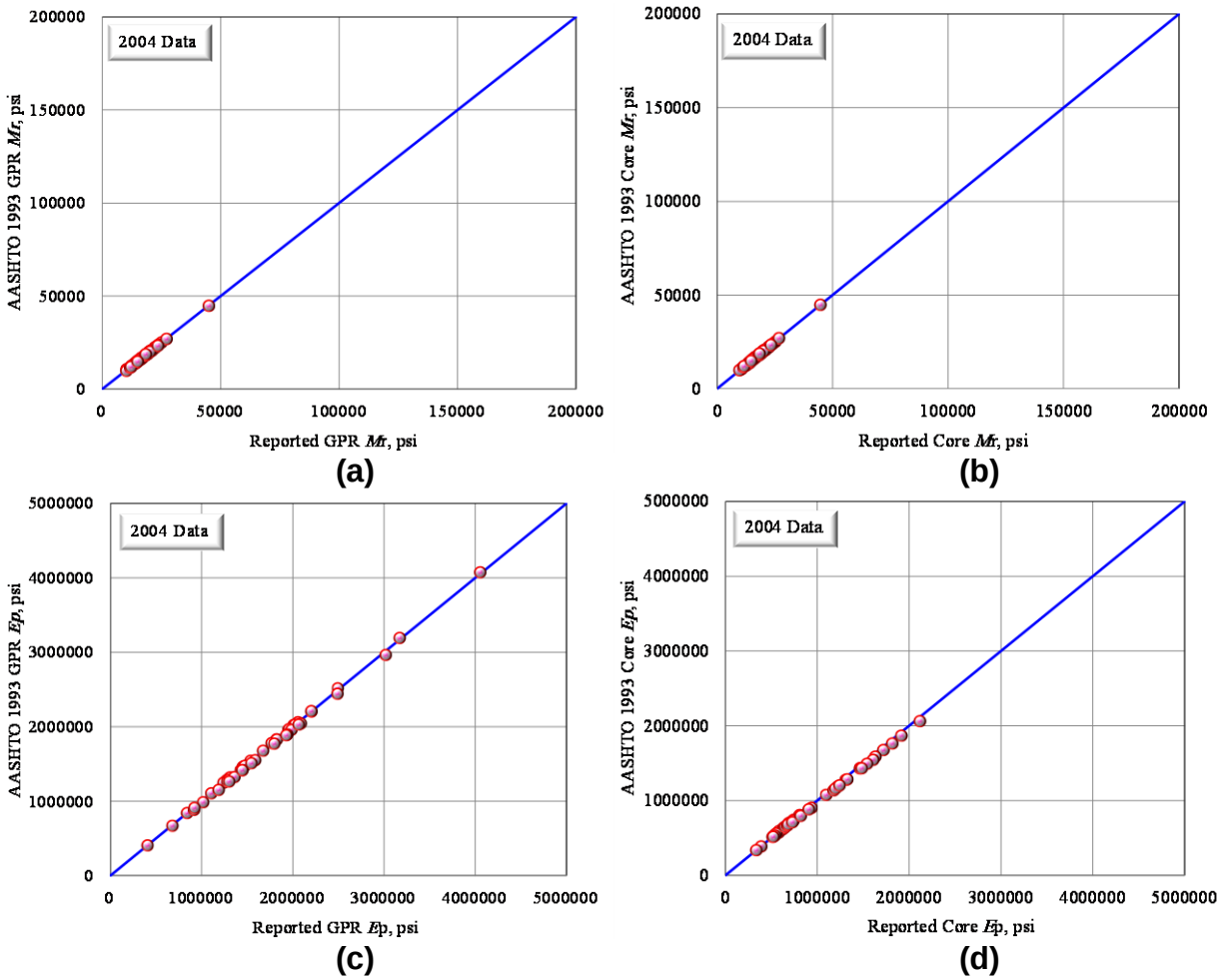

Figure 111 Comparison of 2004 reported and AASHTO 1993 Verified Values of (a) Mr Based on GPR and (b) Mr Based on Core, (c) Ep Based on GPR and (d) Ep Based on Core for Control Section 16-49.

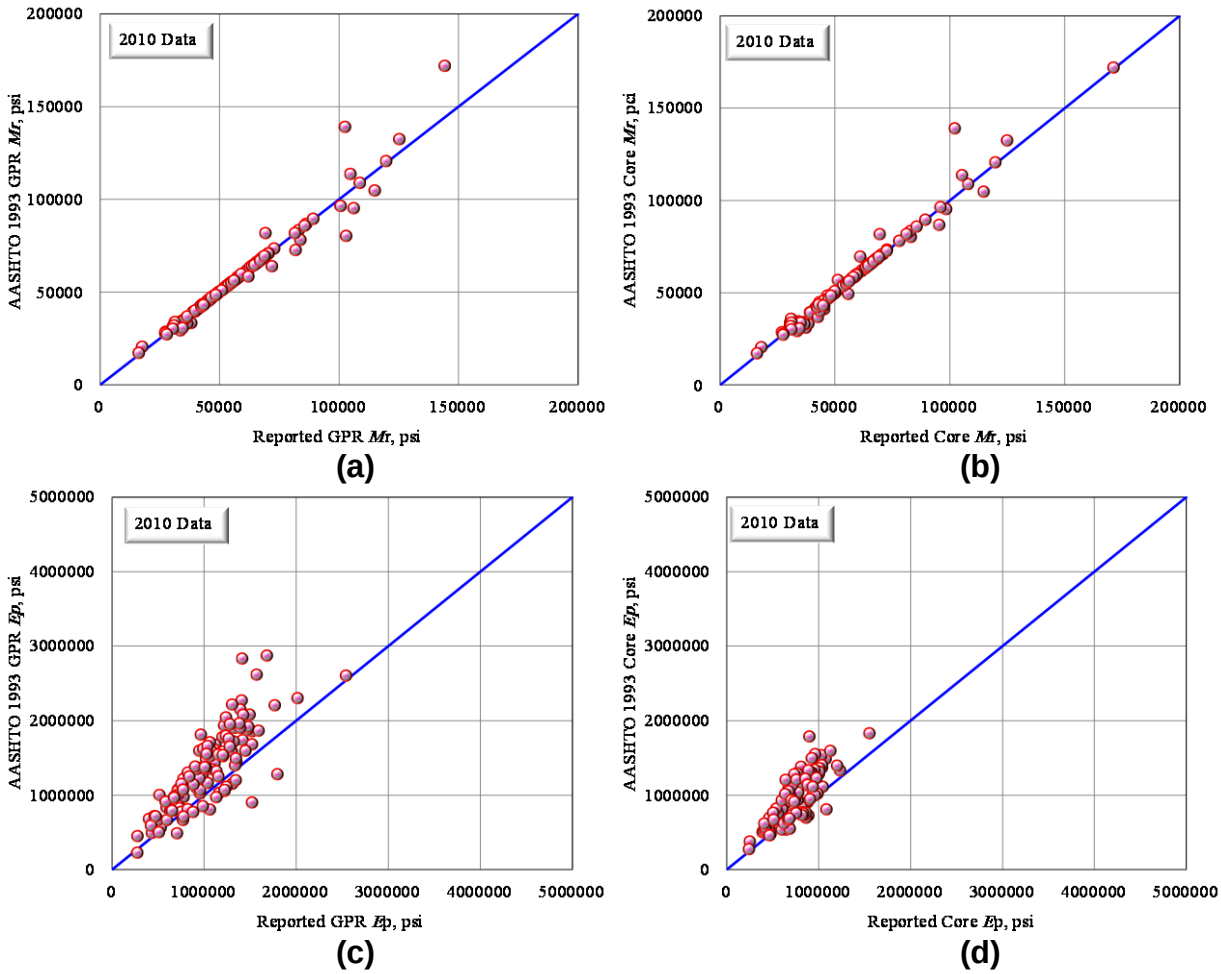

Figure 112 Comparison of 2010 reported and AASHTO 1993 Verified Values of (a) Mr Based on GPR and (b) Mr Based on Core, (c) Ep Based on GPR and (d) Ep Based on Core for Control Section 50-32.

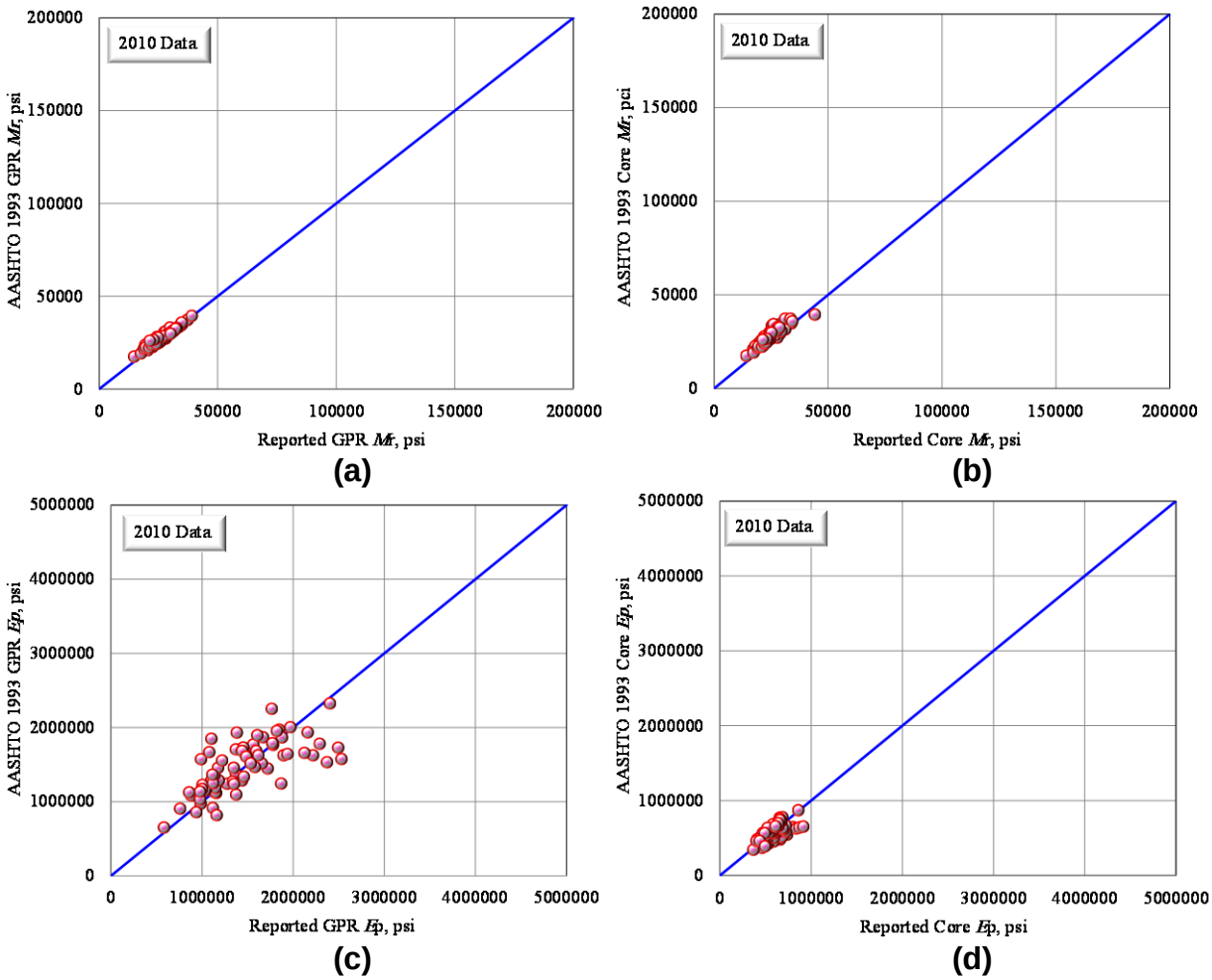

Figure 113 Comparison of 2010 reported and AASHTO 1993 Verified Values of (a) Mr Based on GPR and (b) Mr Based on Core, (c) Ep Based on GPR and (d) Ep Based on Core for Control Section 25-46.

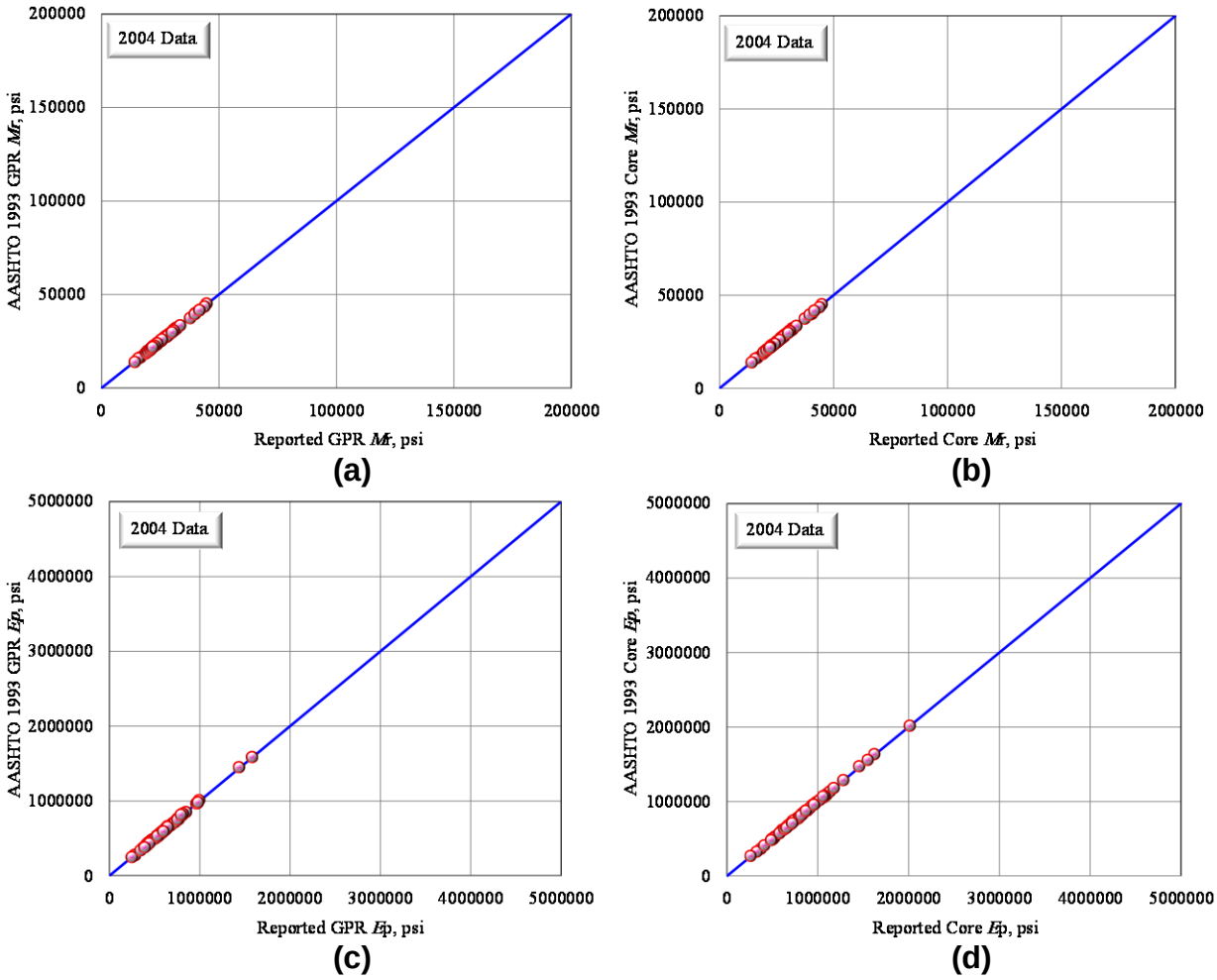

Figure 114 Comparison of 2004 reported and AASHTO 1993 Verified Values of (a) Mr Based on GPR and (b) Mr Based on Core, (c) Ep Based on GPR and (d) Ep Based on Core for Control Section 25-46.

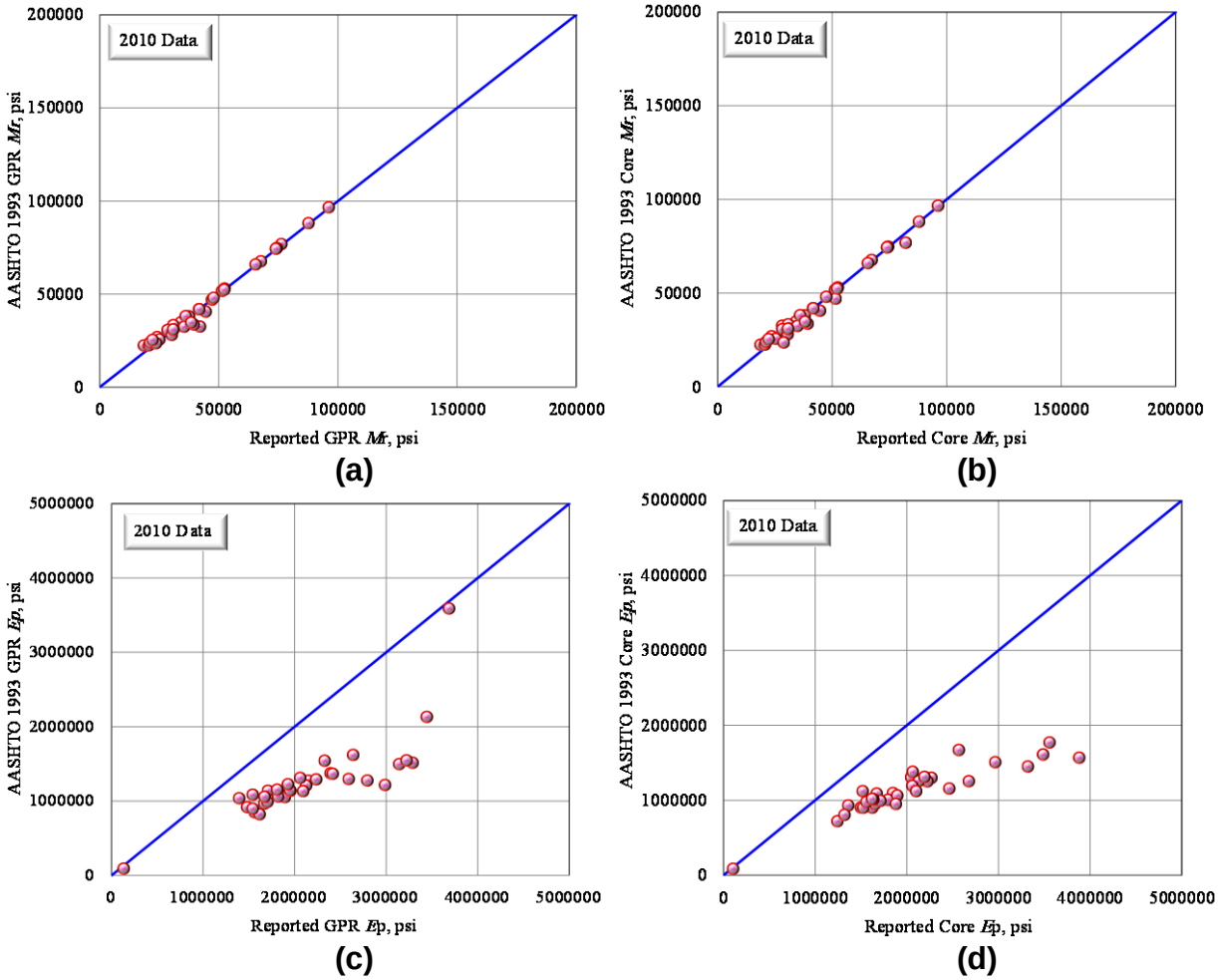

Figure 115 Comparison of 2010 reported and AASHTO 1993 Verified Values of (a) Mr Based on GPR and (b) Mr Based on Core, (c) Ep Based on GPR and (d) Ep Based on Core for Control Section 72-09.

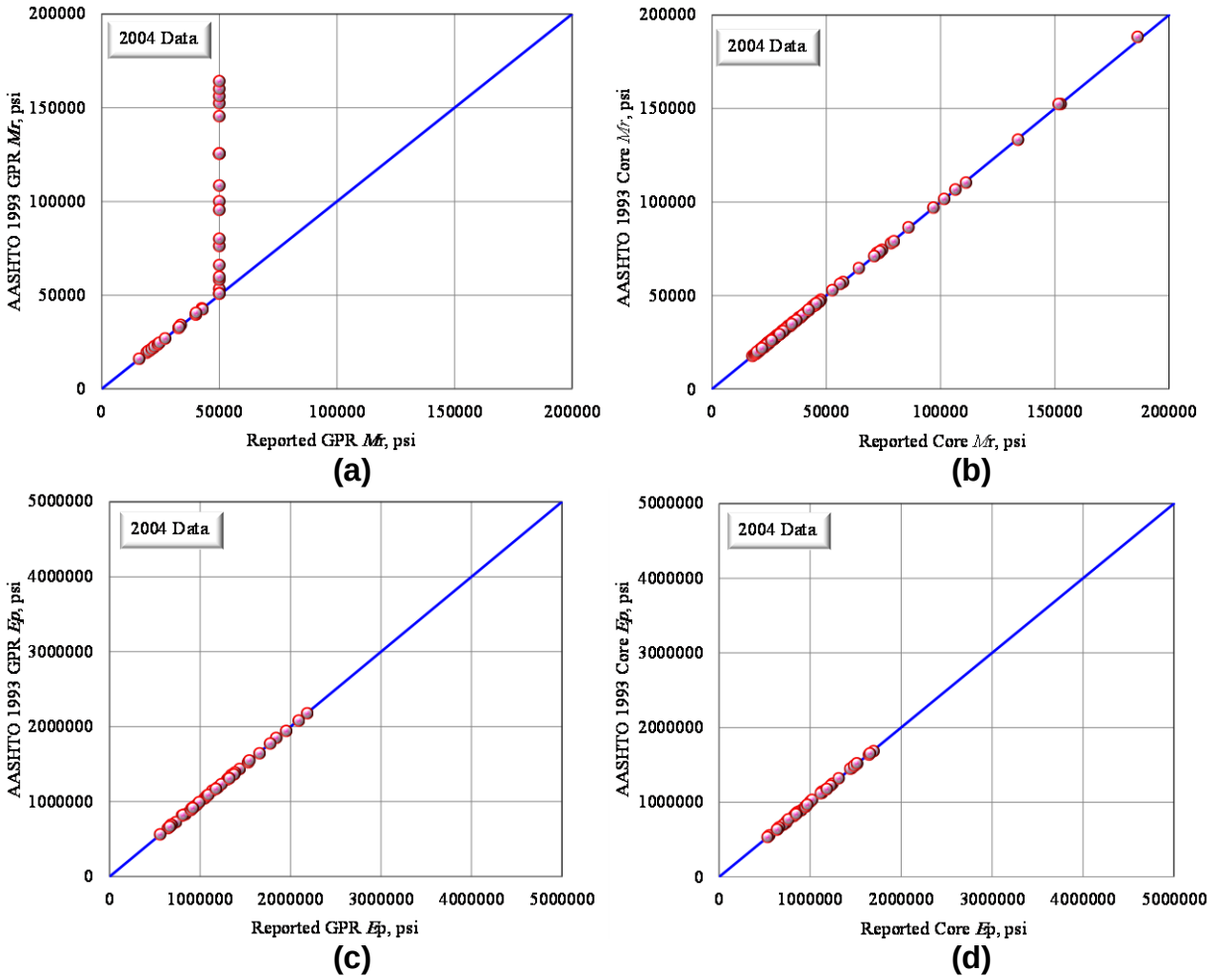

Figure 116 Comparison of 2004 reported and AASHTO 1993 Verified Values of (a) Mr Based on GPR and (b) Mr Based on Core, (c) Ep Based on GPR and (d) Ep Based on Core for Control Section 72-09.

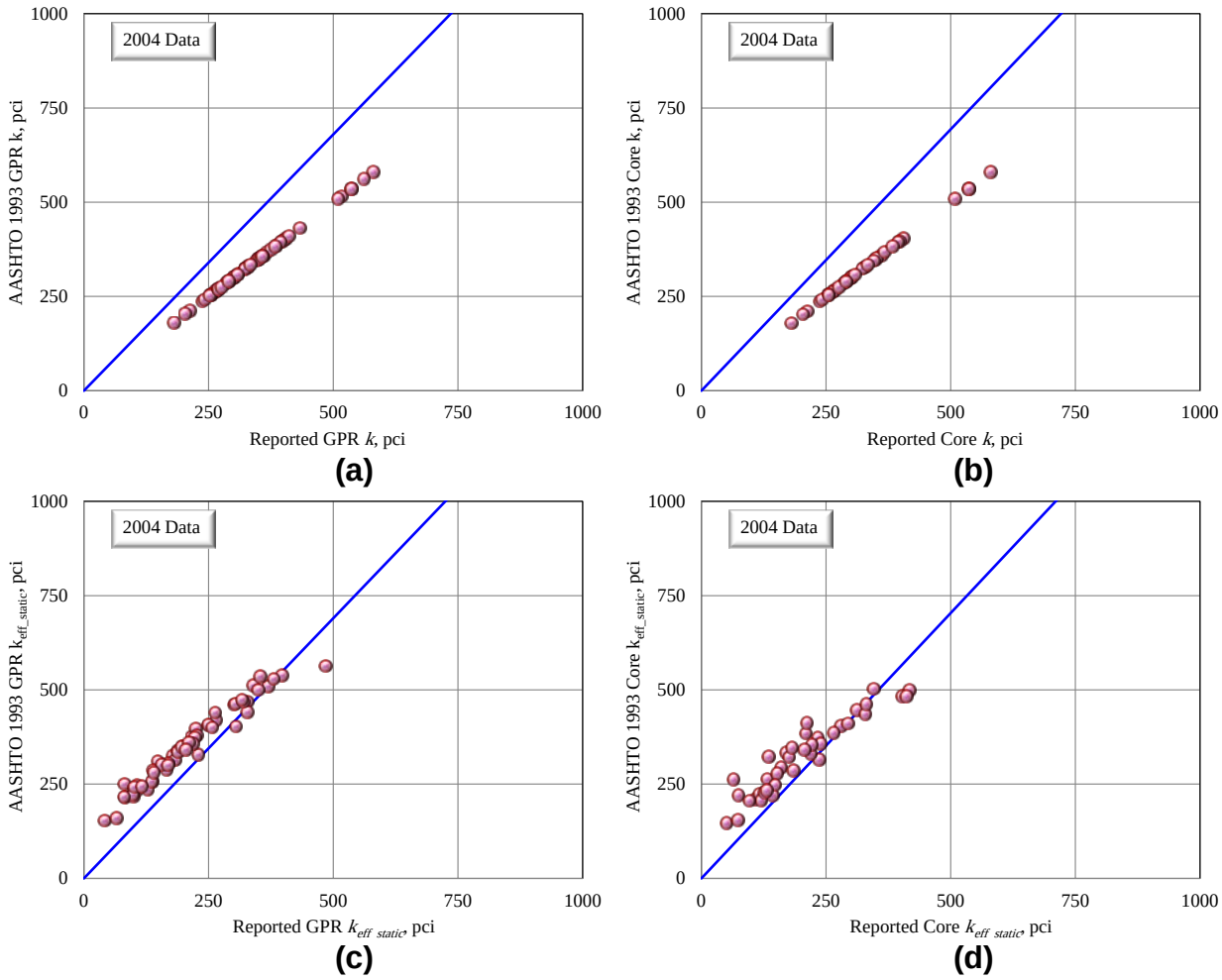

Figure 117 Comparison of 2004 reported and AASHTO 1993 Verified Values of (a) *k* Based on GPR and (b) *k* Based on Core, (c) k_{eff_static} Based on GPR and (d) k_{eff_static} Based on Core for Control Section 25-46.

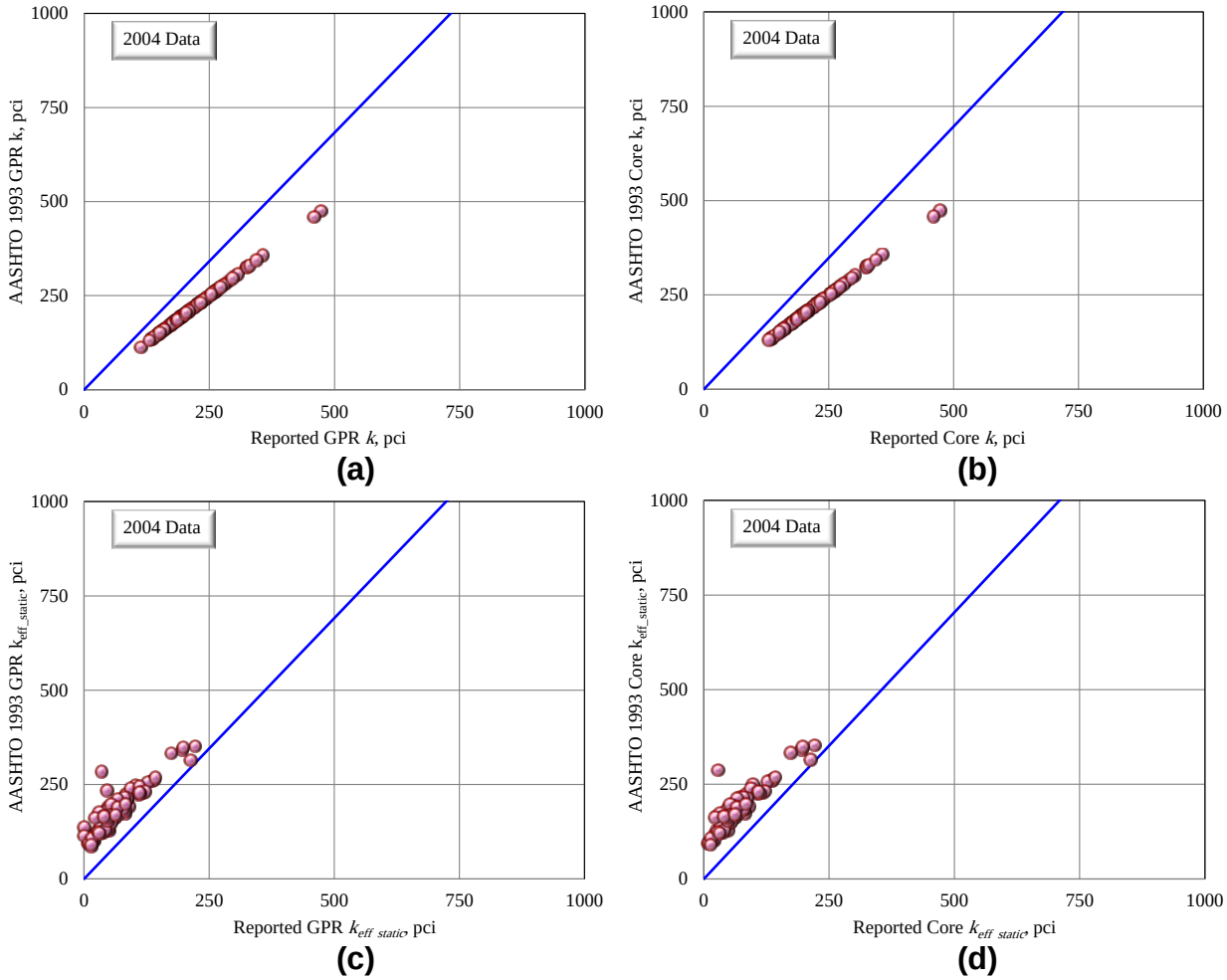

Figure 118 Comparison of 2004 reported and AASHTO 1993 Verified Values of (a) *k* Based on GPR and (b) *k* Based on Core, (c) k_{eff_static} Based on GPR and (d) k_{eff_static} Based on Core for Control Section 42-30.

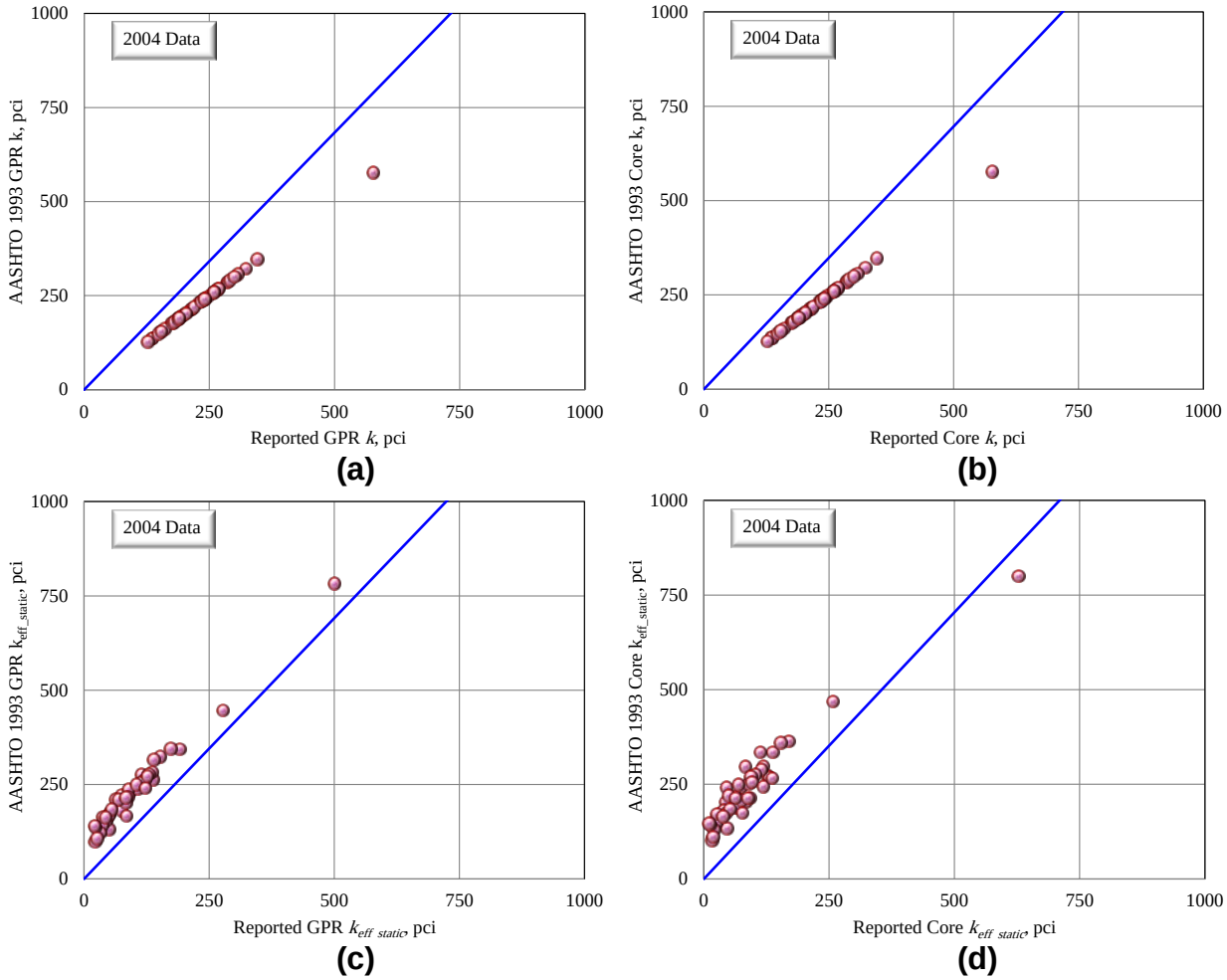

Figure 119 Comparison of 2004 reported and AASHTO 1993 Verified Values of (a) *k* Based on GPR and (b) *k* Based on Core, (c) k_{eff_static} Based on GPR and (d) k_{eff_static} Based on Core for Control Section 16-49.

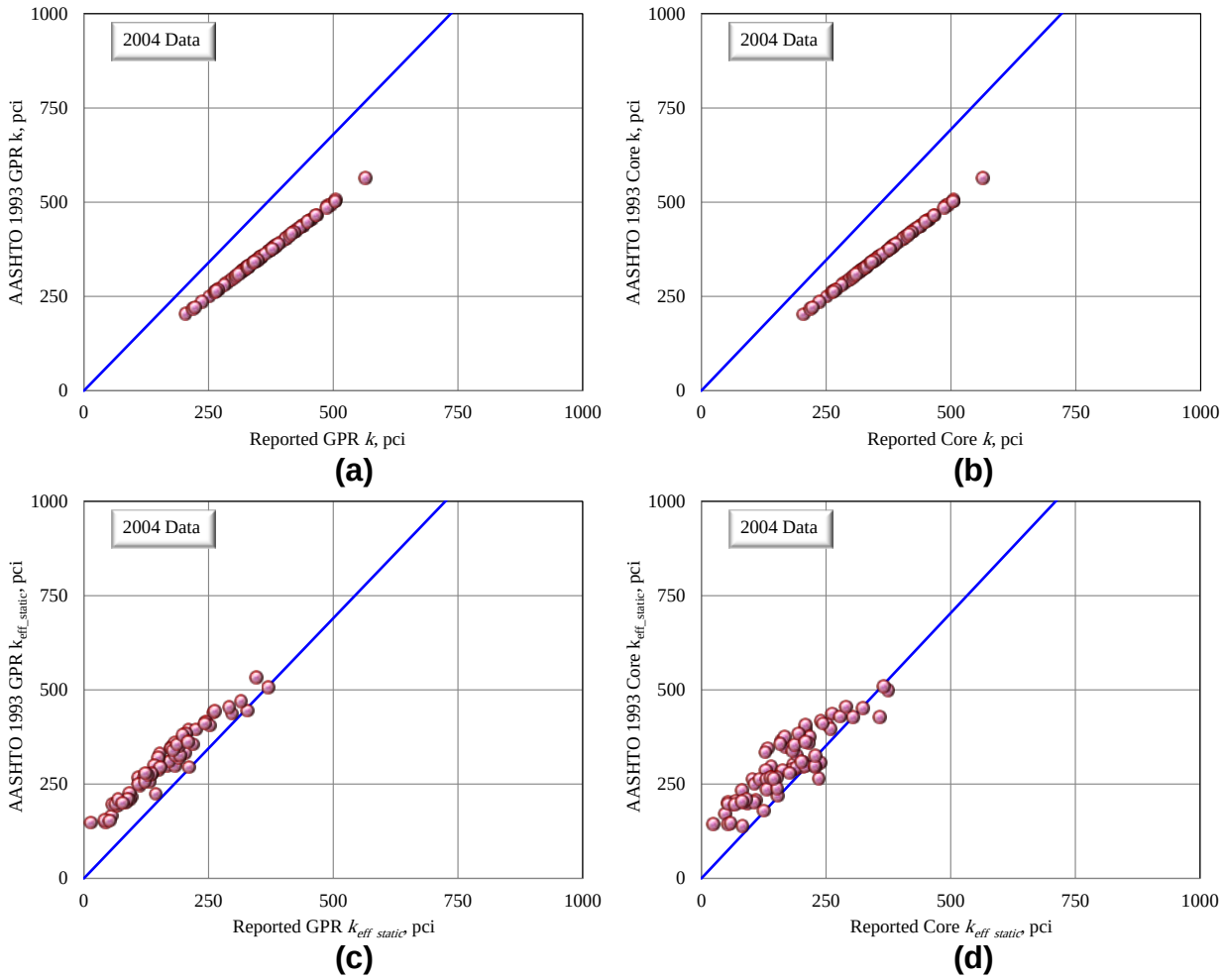

Figure 120 Comparison of 2004 Reported and AASHTO 1993 Verified Values of (a) *k* Based on GPR and (b) *k* Based on Core, (c) k_{eff_static} Based on GPR and (d) k_{eff_static} Based on Core for Control Section 25-46.

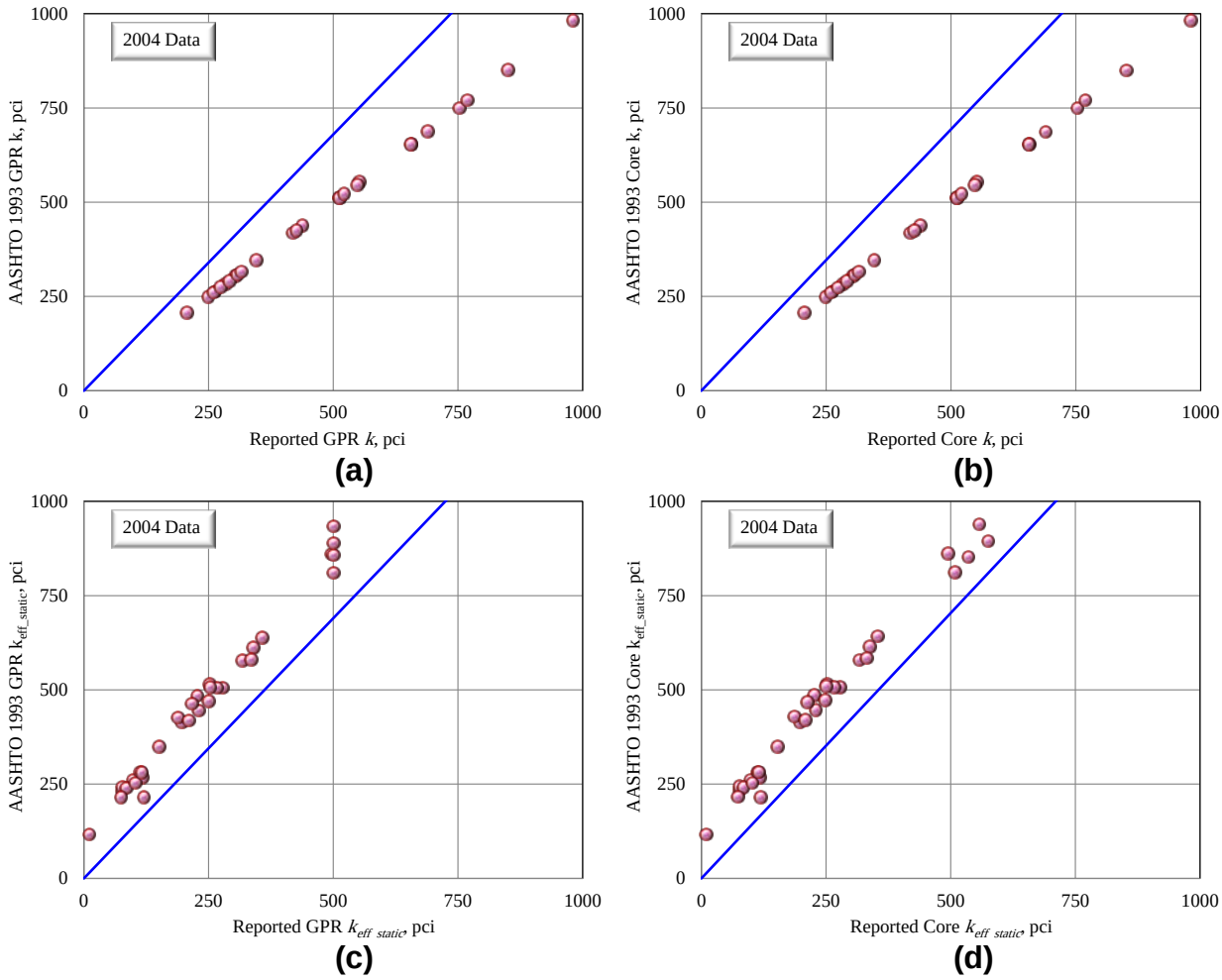

Figure 121 Comparison of 2004 reported and AASHTO 1993 Verified Values of (a) *k* Based on GPR and (b) *k* Based on Core, (c) k_{eff_static} Based on GPR and (d) k_{eff_static} Based on Core for Control Section 72-09.

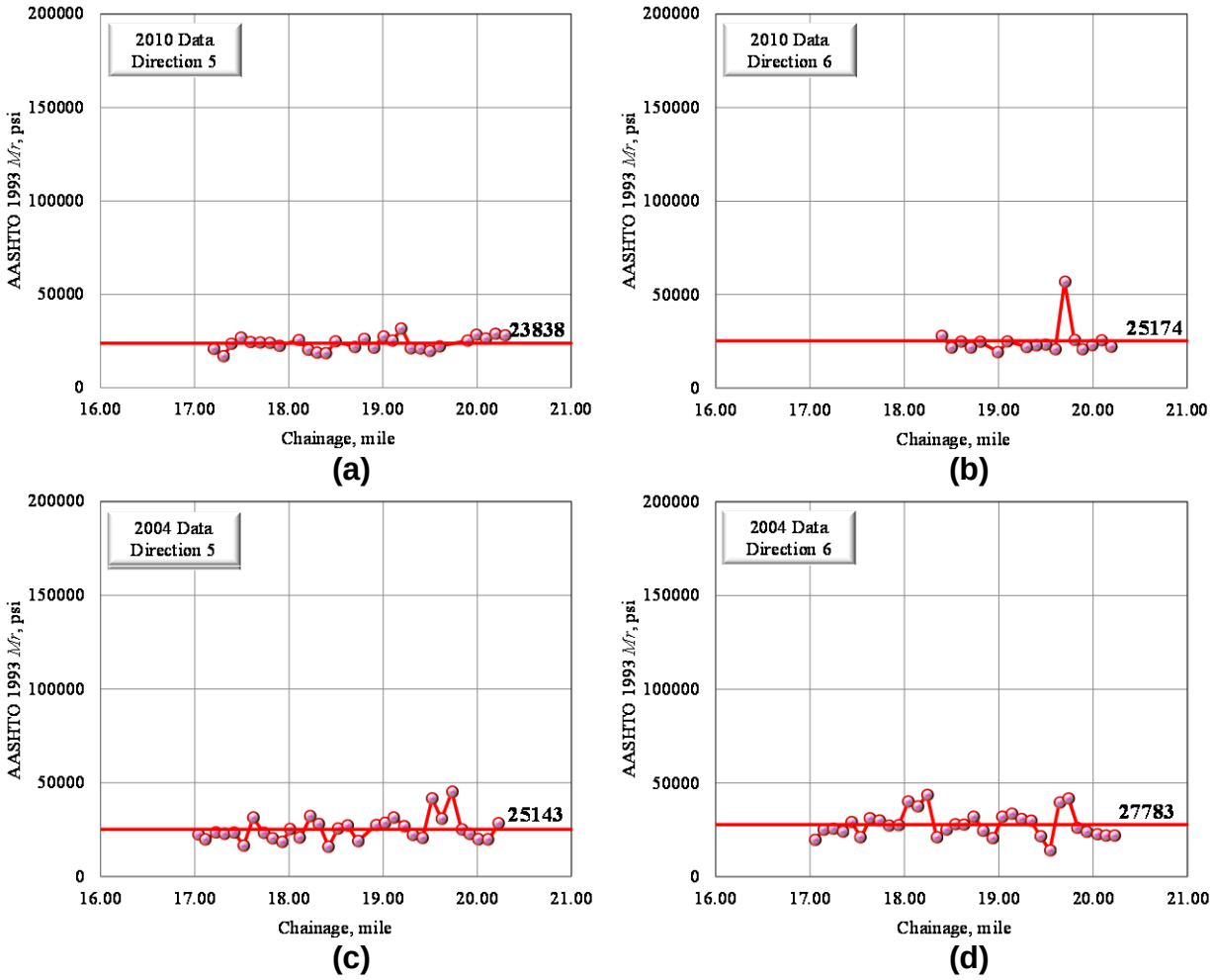

Figure 122 AASHTO 1993 Verified M_r Values Versus Distance for (a) 2010 Data in Direction 5, (b) 2010 Data in Direction 6, (c) 2004 Data in Direction 5, and (d) 2004 Data in Direction 6 for Control Section 25-46.

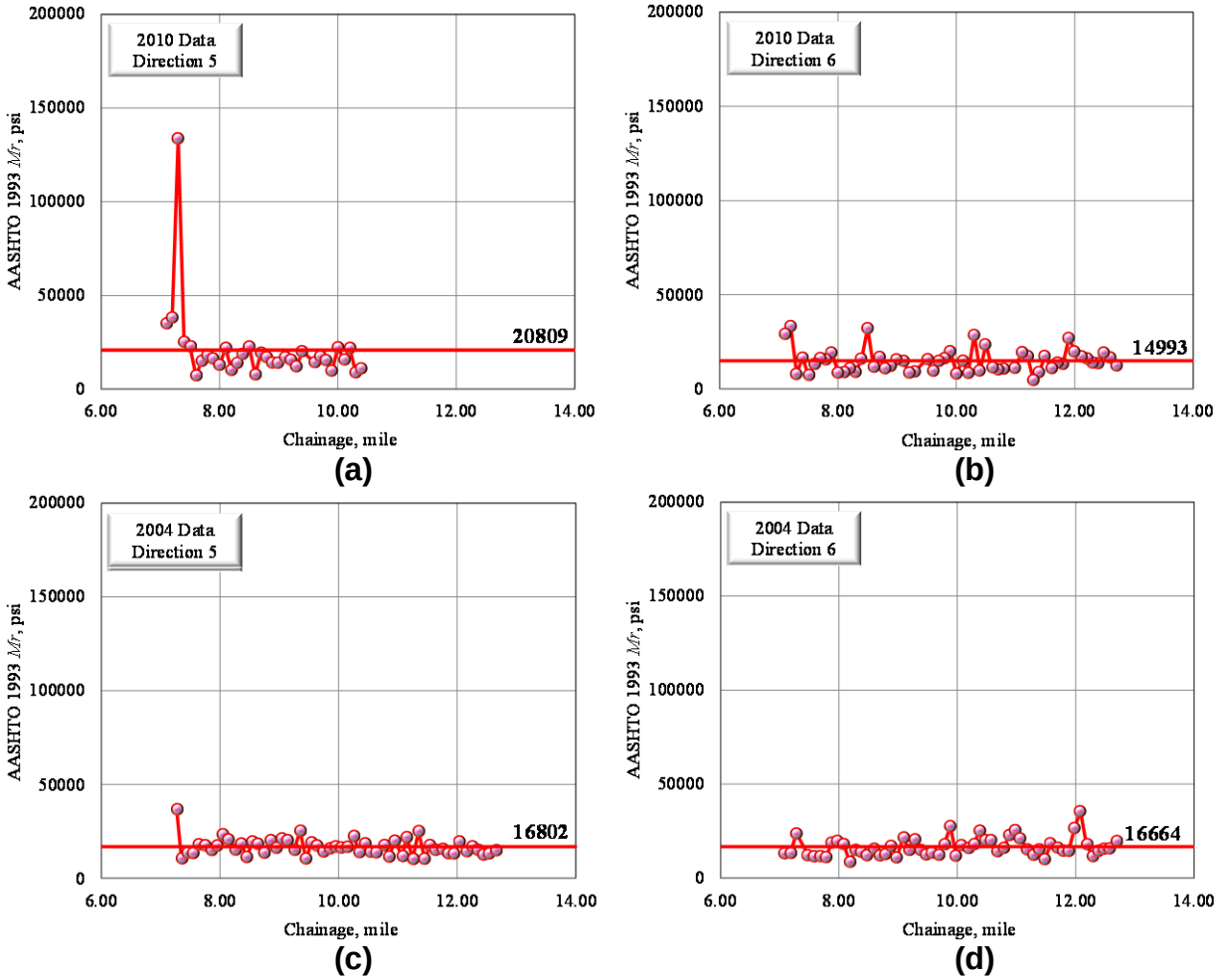

Figure 123 AASHTO 1993 Verified M_r Values Versus Distance for (a) 2010 Data in Direction 5, (b) 2010 Data in Direction 6, (c) 2004 Data in Direction 5, and (d) 2004 Data in Direction 6 for Control Section 42-30.

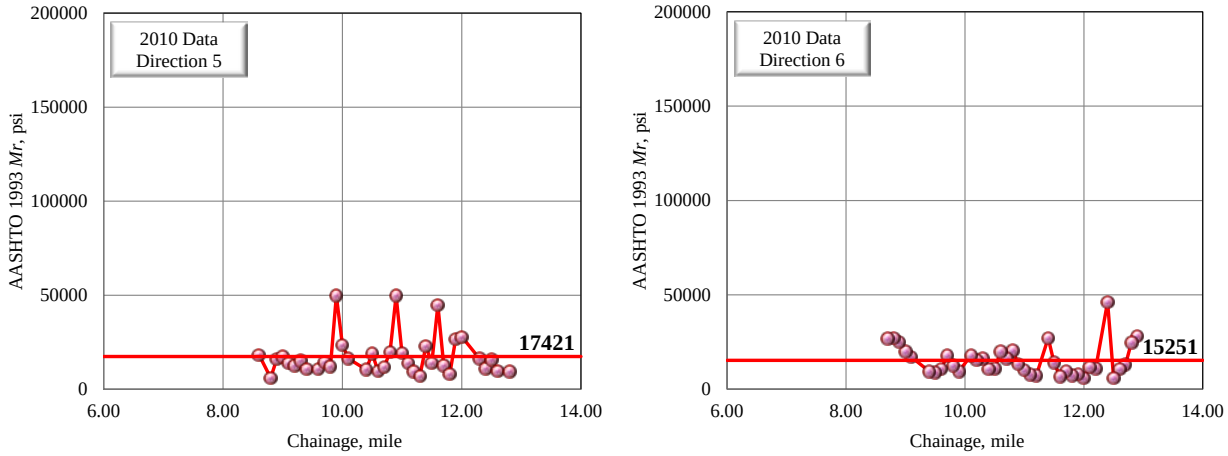

Figure 124 AASHTO 1993 Verified M_r Values Versus Distance for (a) 2010 Data in Direction 5, and (b) 2010 Data in Direction 6 for Control Section 65-09.

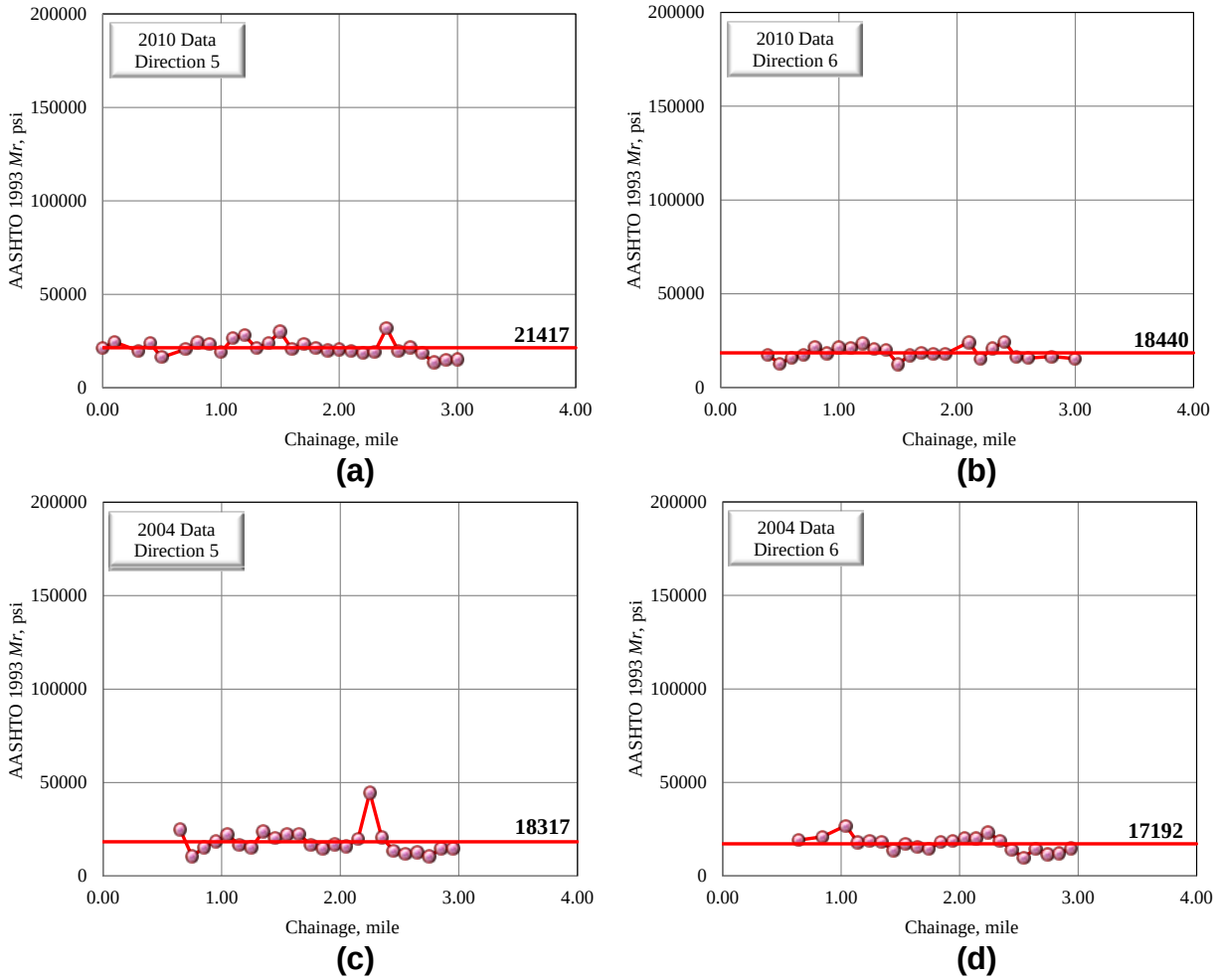

Figure 125 AASHTO 1993 Verified M_r Values Versus Distance for (a) 2010 Data in Direction 5, (b) 2010 Data in Direction 6, (c) 2004 Data in Direction 5, and (d) 2004 Data in Direction 6 for Control Section 16-49.

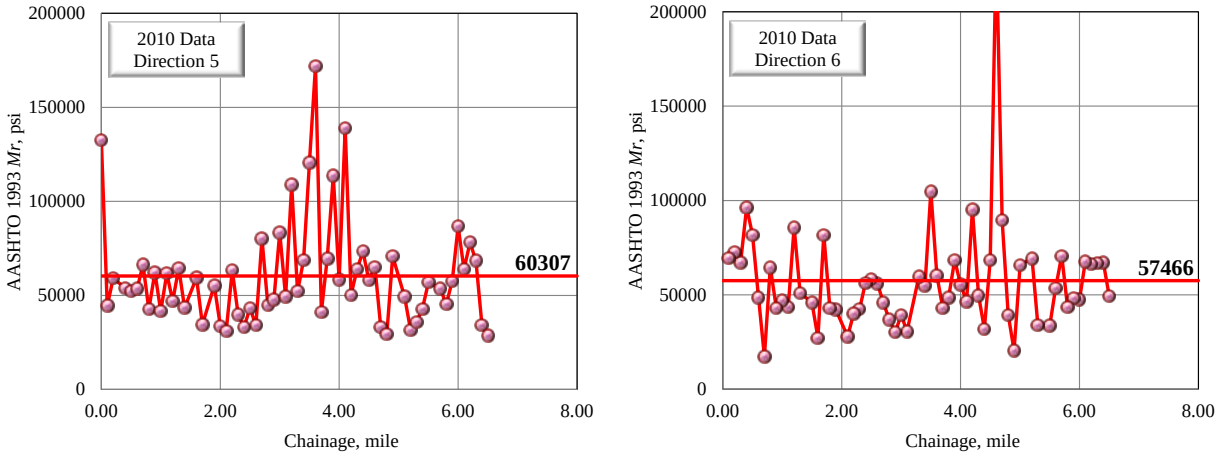

Figure 126 AASHTO 1993 Verified M_r Values Versus Distance for (a) 2010 Data in Direction 5, and (b) 2010 Data in Direction 6 for Control Section 50-32.

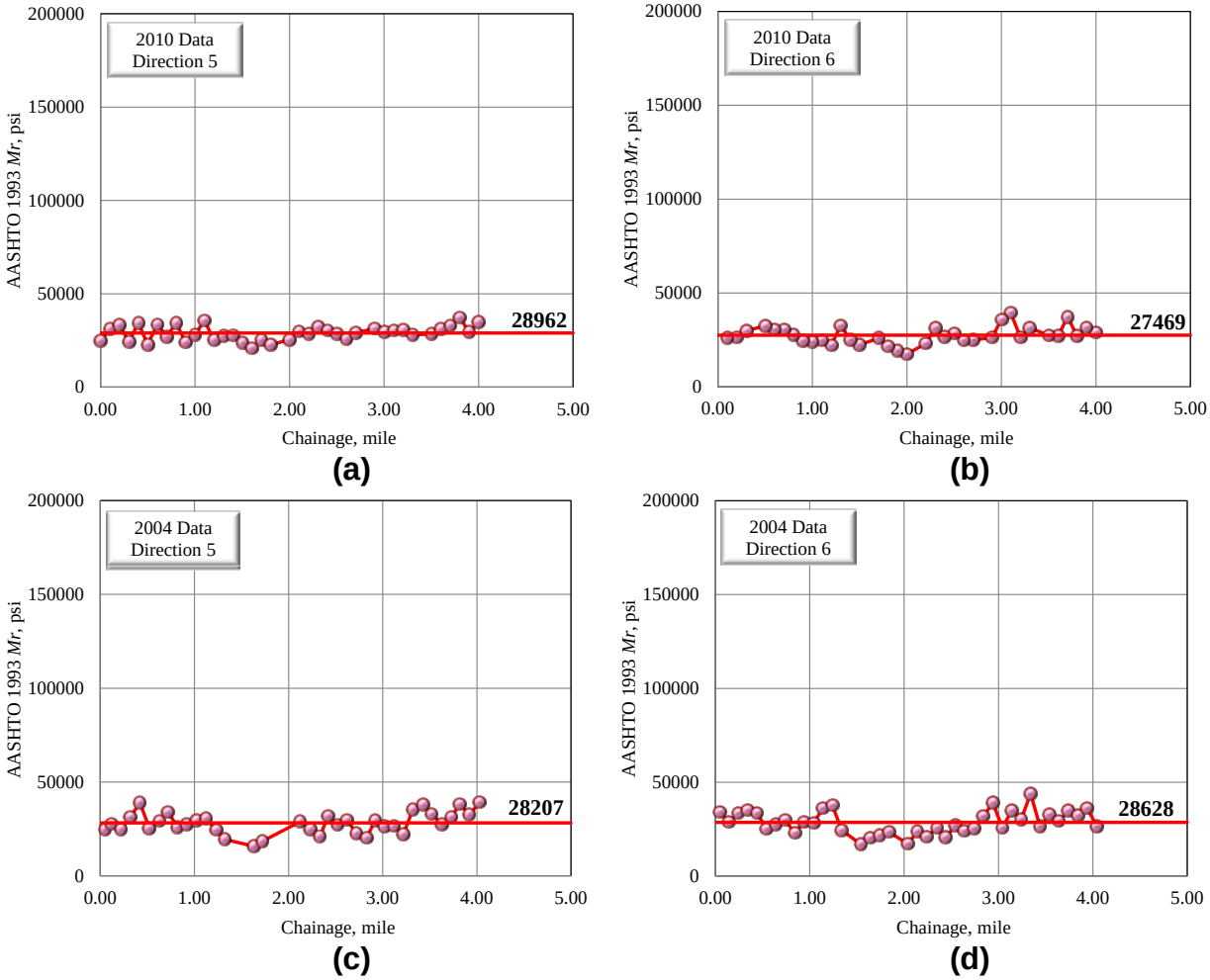

Figure 127 AASHTO 1993 Verified M_r Values Versus Distance for (a) 2010 Data in Direction 5, (b) 2010 Data in Direction 6, (c) 2004 Data in Direction 5 and (d) 2004 Data in Direction 6 for Control Section 25-46.

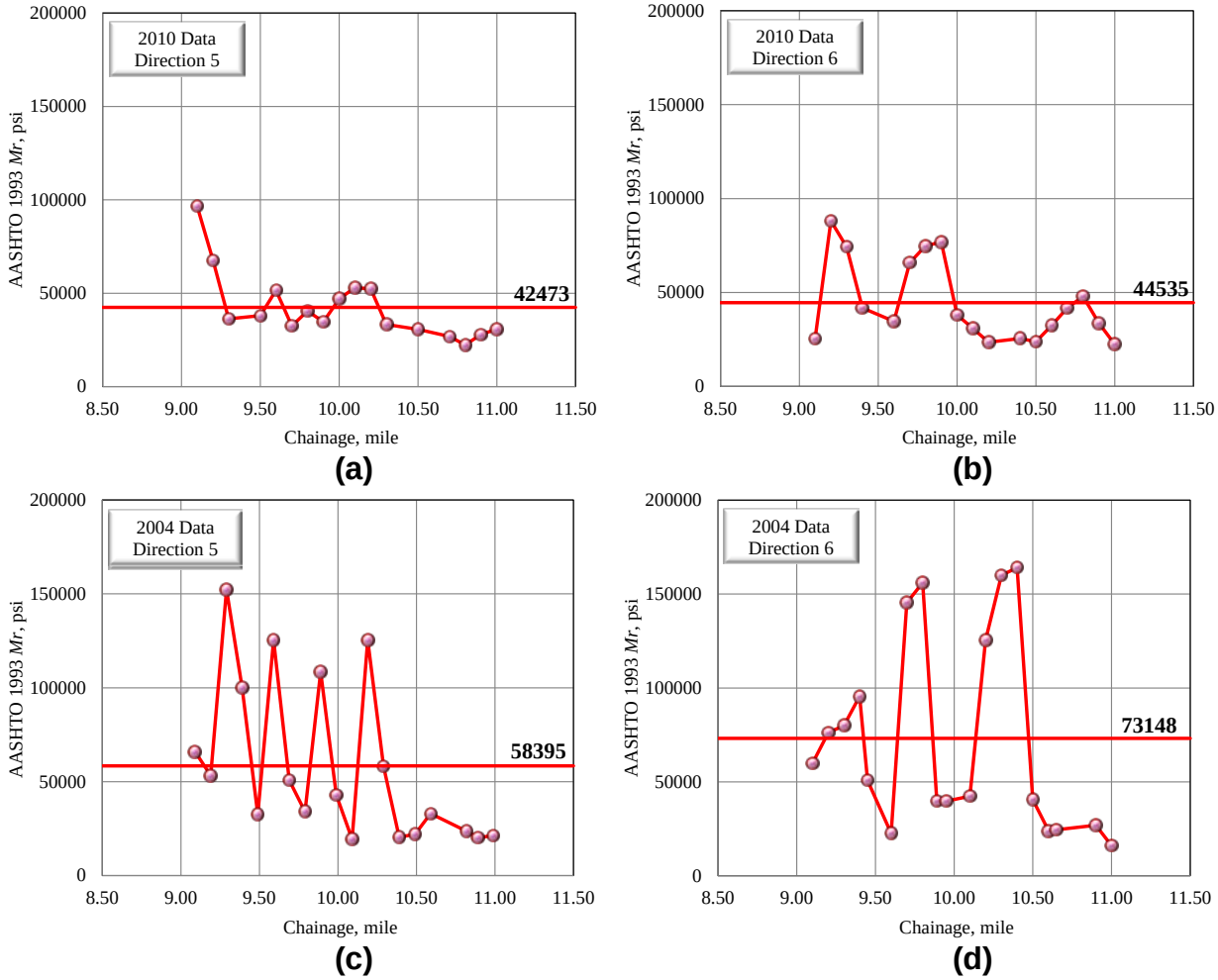

Figure 128 AASHTO 1993 Verified M_r Values Versus Distance for (a) 2010 Data in Direction 5, (b) 2010 Data in Direction 6, (c) 2004 Data in Direction 5, and (d) 2004 Data in Direction 6 for Control Section 72-09.

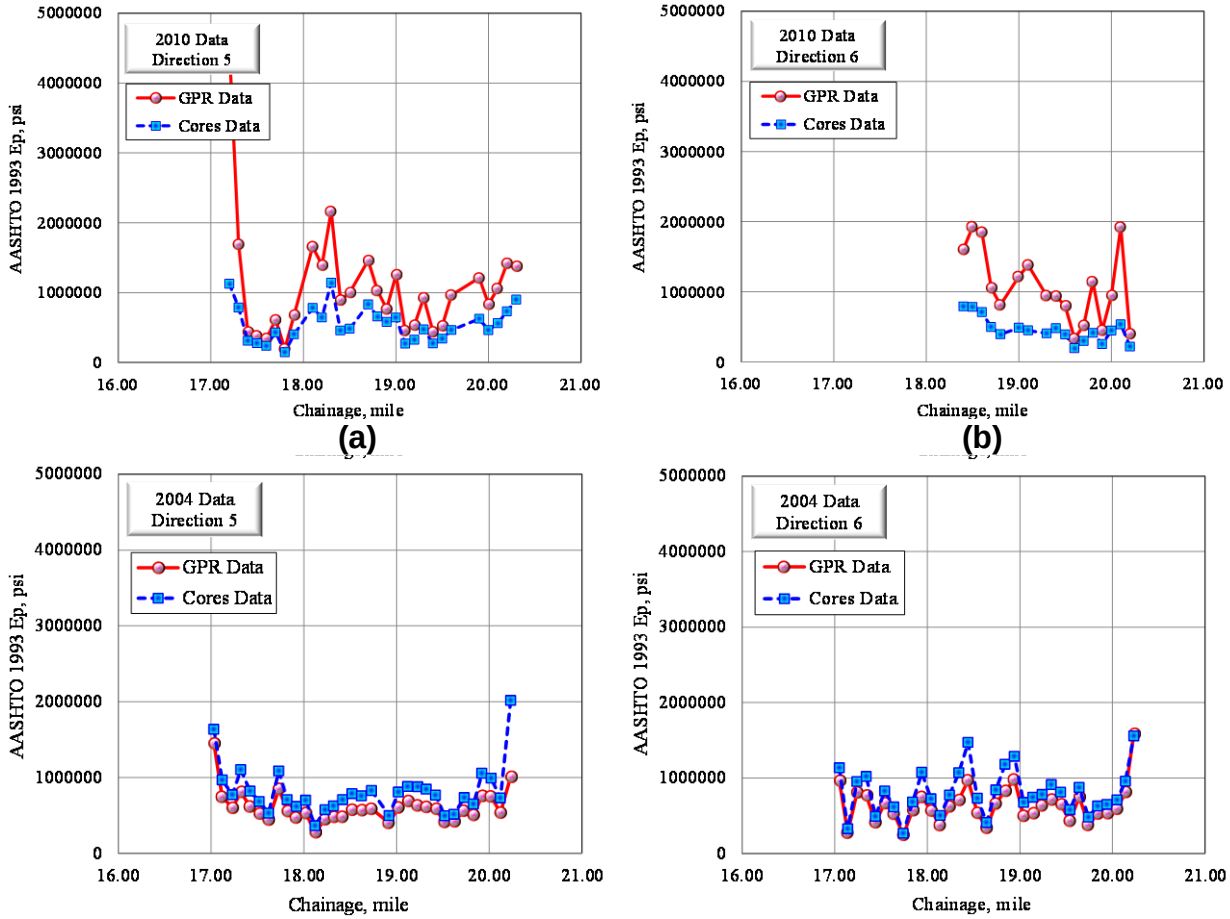

Figure 129 GPR and Core AASHTO 1993 Verified E_p Values Versus Distance for (a) 2010 Data in Direction 5, (b) 2010 Data in Direction 6, (c) 2004 Data in Direction 5, and (d) 2004 Data in Direction 6 for Control Section 25-46.

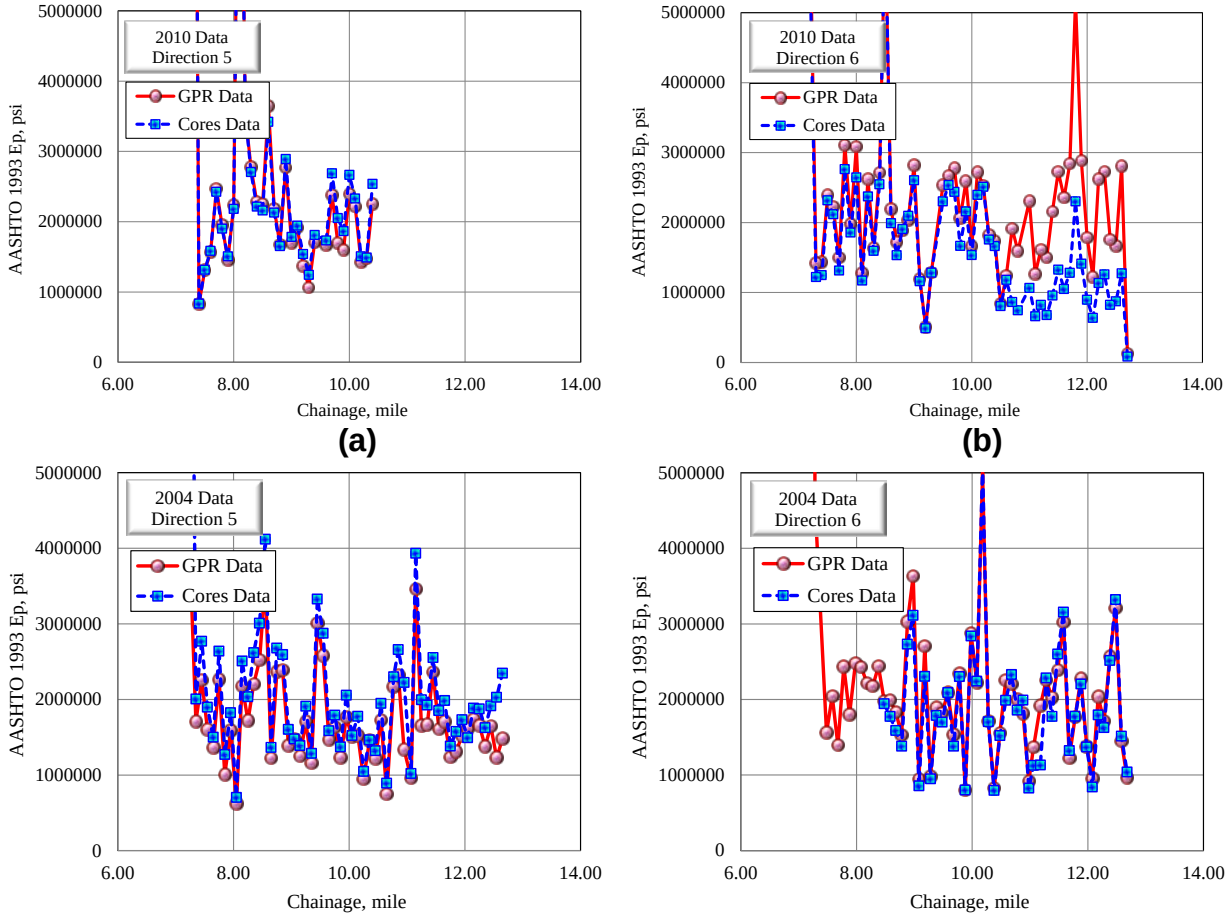

Figure 130 GPR and Core AASHTO 1993 Verified E_p Values Versus Distance for (a) 2010 Data in Direction 5, (b) 2010 Data in Direction 6, (c) 2004 Data in Direction 5, and (d) 2004 Data in Direction 6 for Control Section 42-30.

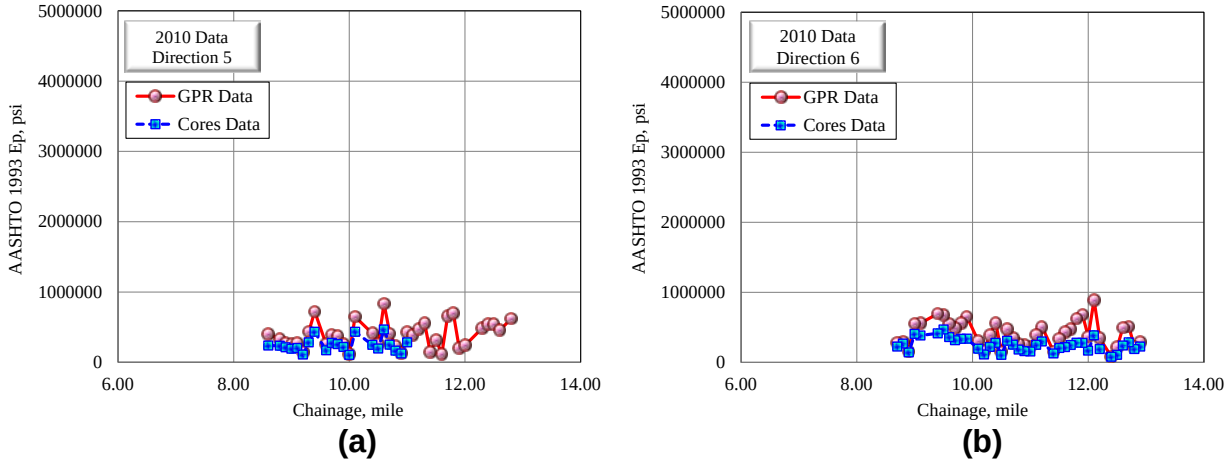

Figure 131 GPR and Core AASHTO 1993 Verified E_p Values Versus Distance for (a) 2010 Data in Direction 5 and (b) 2010 Data in Direction 6 for Control Section 65-09.

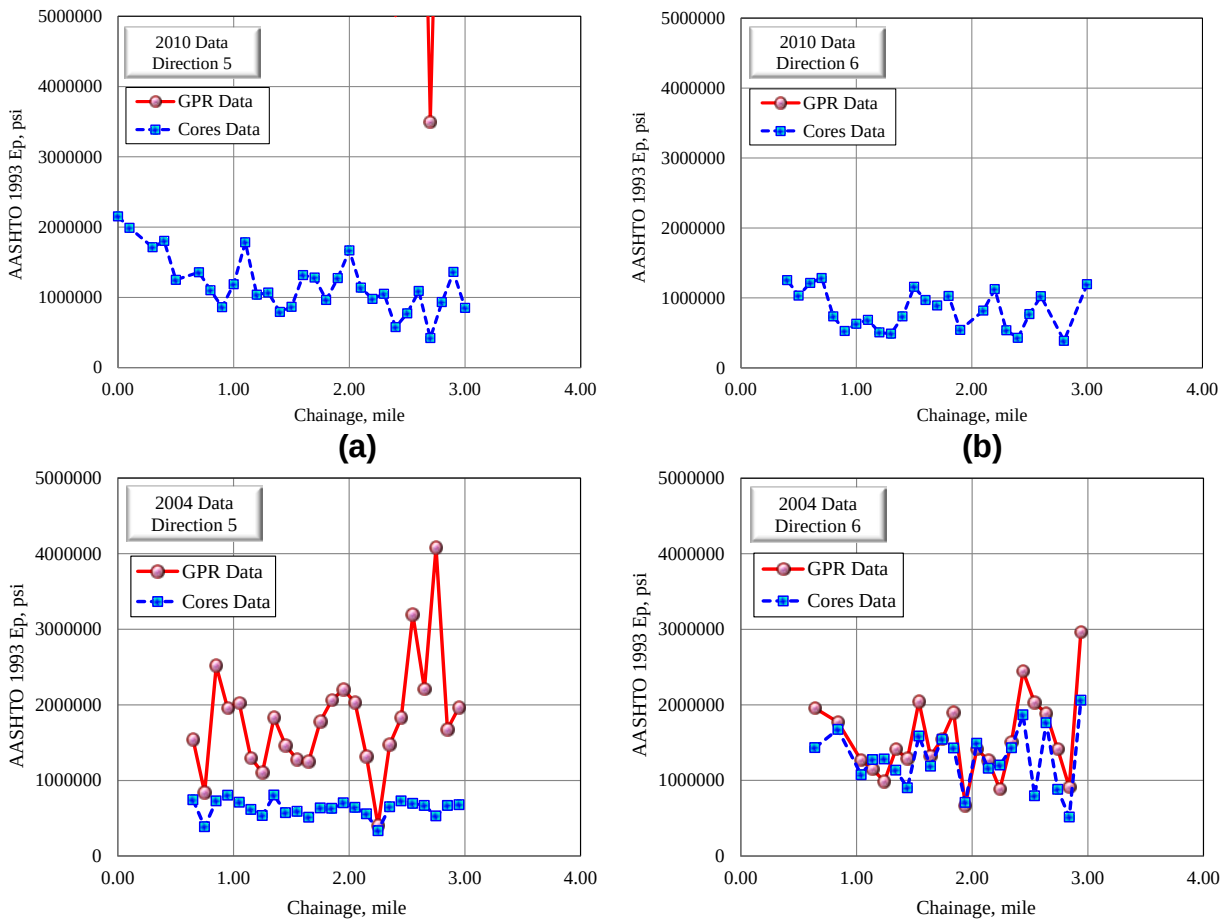

Figure 132 GPR and Core AASHTO 1993 Verified E_p Values Versus Distance for (a) 2010 Data in Direction 5, (b) 2010 Data in Direction 6, (c) 2004 Data in Direction 5, and (d) 2004 Data in Direction 6 for Control Section16-49.

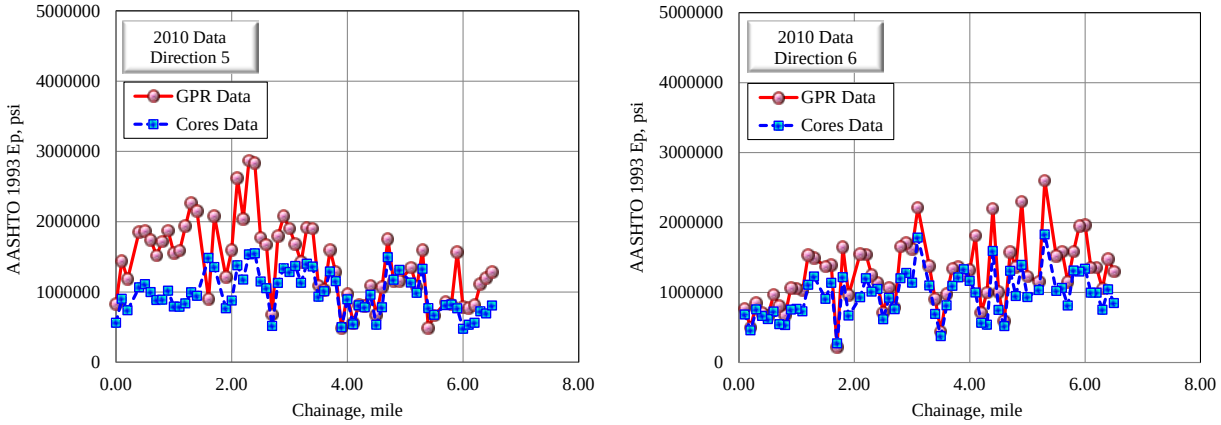

Figure 133 GPR and Core AASHTO 1993 Verified E_p Values Versus Distance for (a) 2010 Data in Direction 5, (b) 2010 Data in Direction 6 for Control Section 50-32.

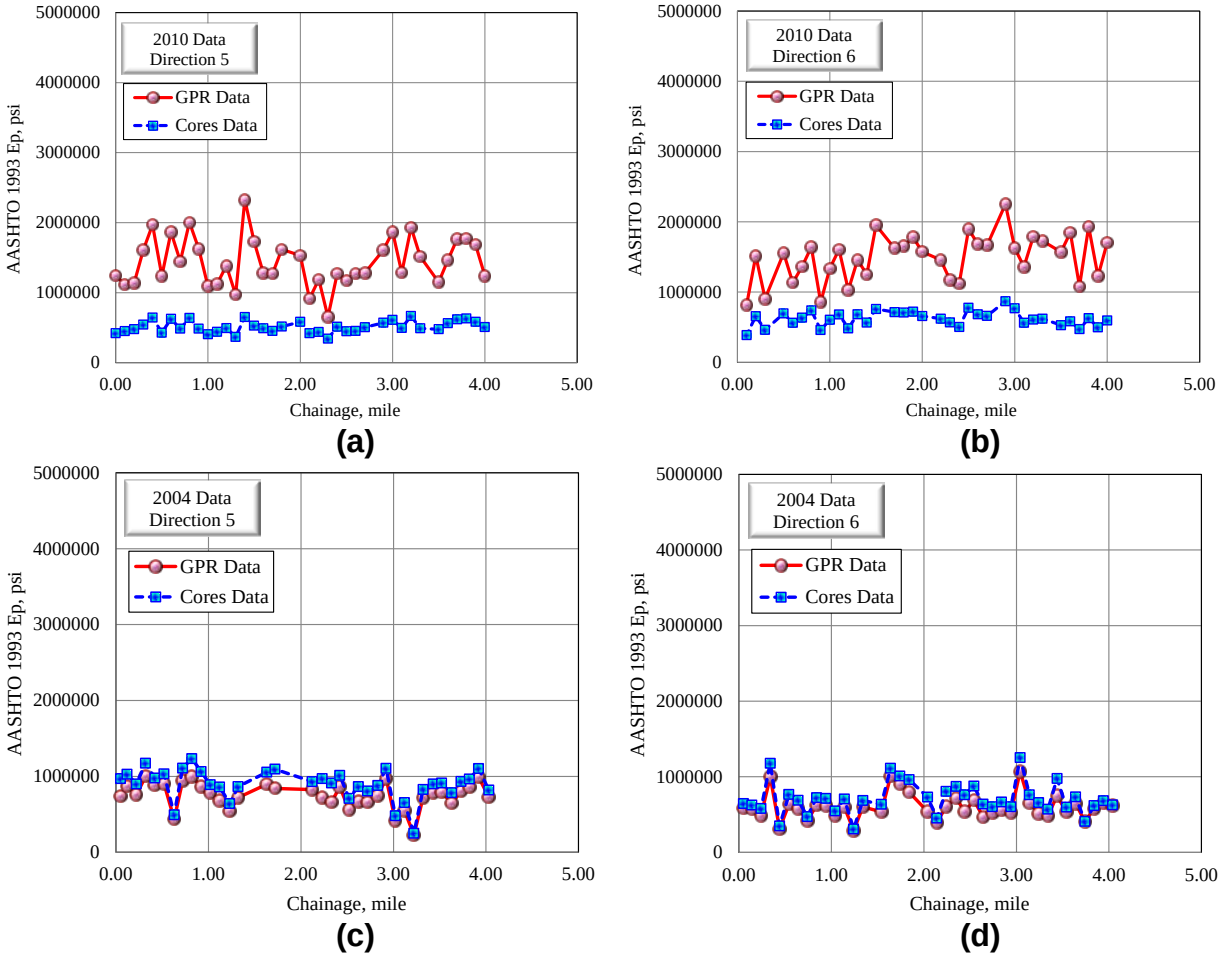

Figure 134 GPR and Core AASHTO 1993 Verified E_p Values Versus Distance for (a) 2010 Data in Direction 5, (b) 2010 Data in Direction 6, (c) 2004 Data in Direction 5, and (d) 2004 Data in Direction 6 for Control Section 25-46.

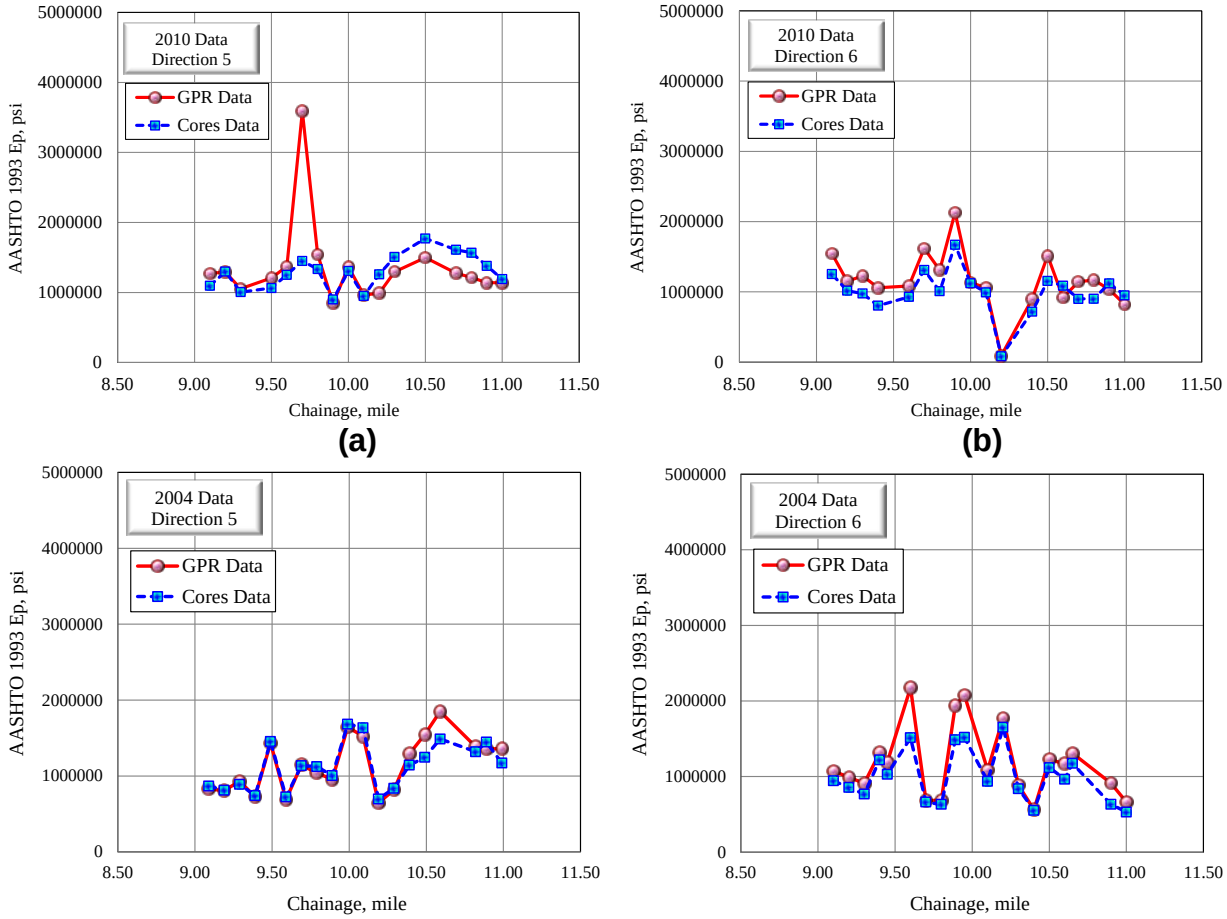

Figure 135 GPR and Core AASHTO 1993 Verified E_p Values Versus Distance for (a) 2010 Data in Direction 5, (b) 2010 Data in Direction 6, (c) 2004 Data in Direction 5, and (d) 2004 Data in Direction 6 for Control Section 72-09.

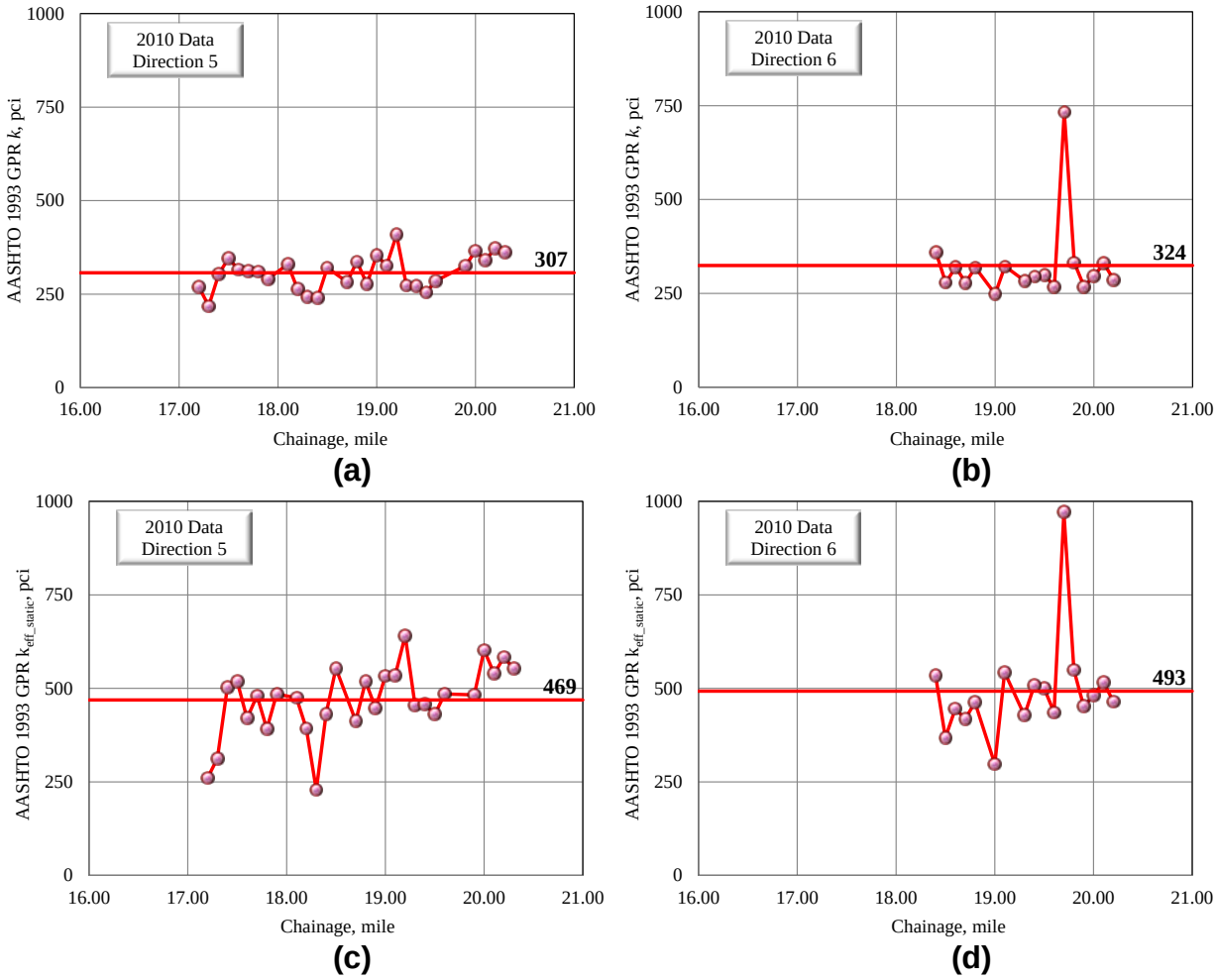

Figure 136 2010 GPR AASHTO 1993 Verified Values of (a) *k* in Direction 5, (b) *k* in Direction 6, (c) k_{eff_static} in Direction 5 and (d) k_{eff_static} in Direction 6 Versus Distance for Control Section 25-46.

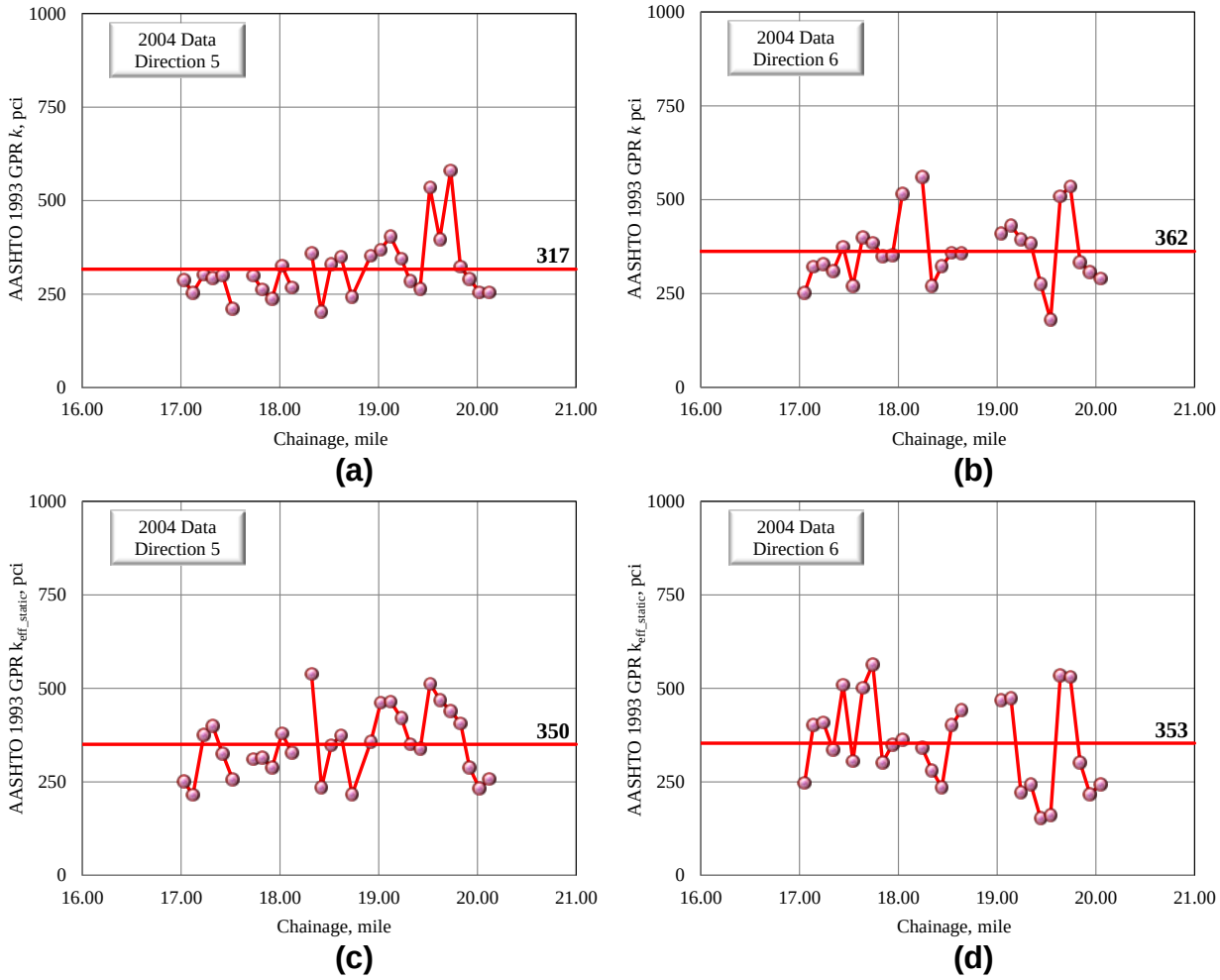

Figure 137 2004 GPR AASHTO 1993 Verified Values of (a) *k* in Direction 5, (b) *k* in Direction 6, (c) k_{eff_static} in Direction 5 and (d) k_{eff_static} in Direction 6 Versus Distance for Control Section 25-46.

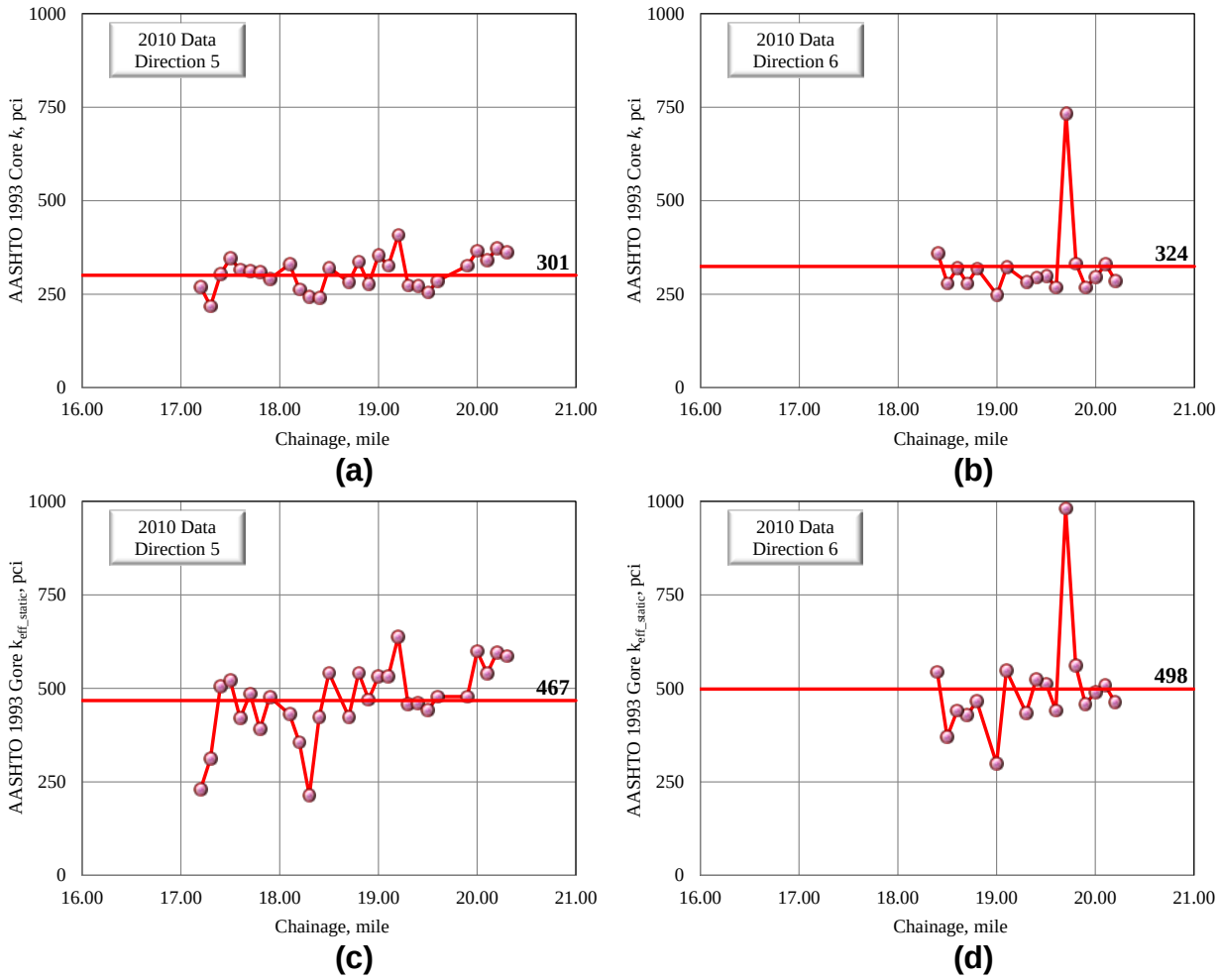

Figure 138 2010 core AASHTO 1993 Verified Values of (a) *k* in Direction 5, (b) *k* in Direction 6, (c) k_{eff_static} in Direction 5 and (d) k_{eff_static} in Direction 6 Versus Distance for Control Section 25-46.

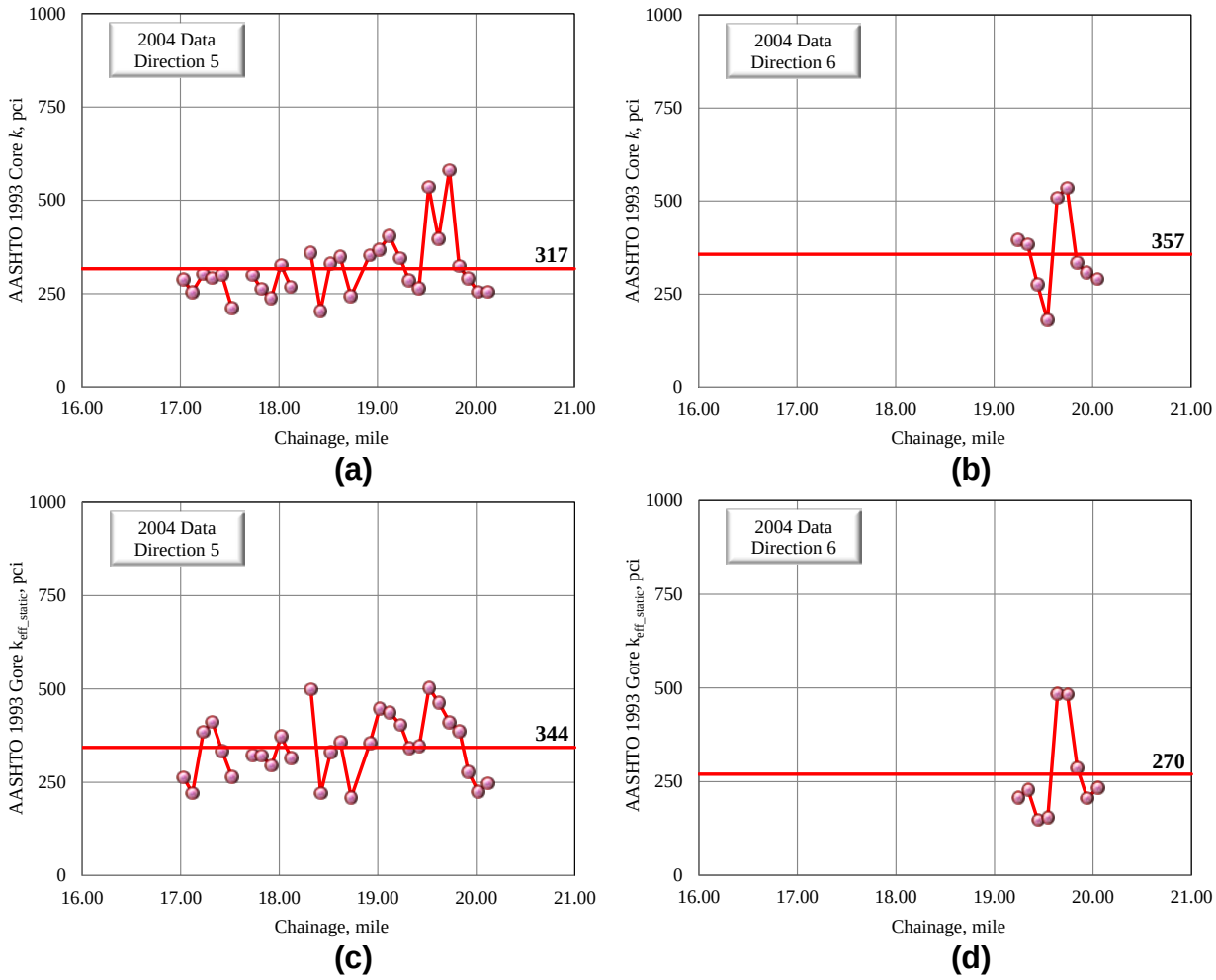

Figure 139 2004 core AASHTO 1993 Verified Values of (a) *k* in Direction 5, (b) *k* in Direction 6, (c) k_{eff_static} in Direction 5 and (d) k_{eff_static} in Direction 6 Versus Distance for Control Section 25-46.

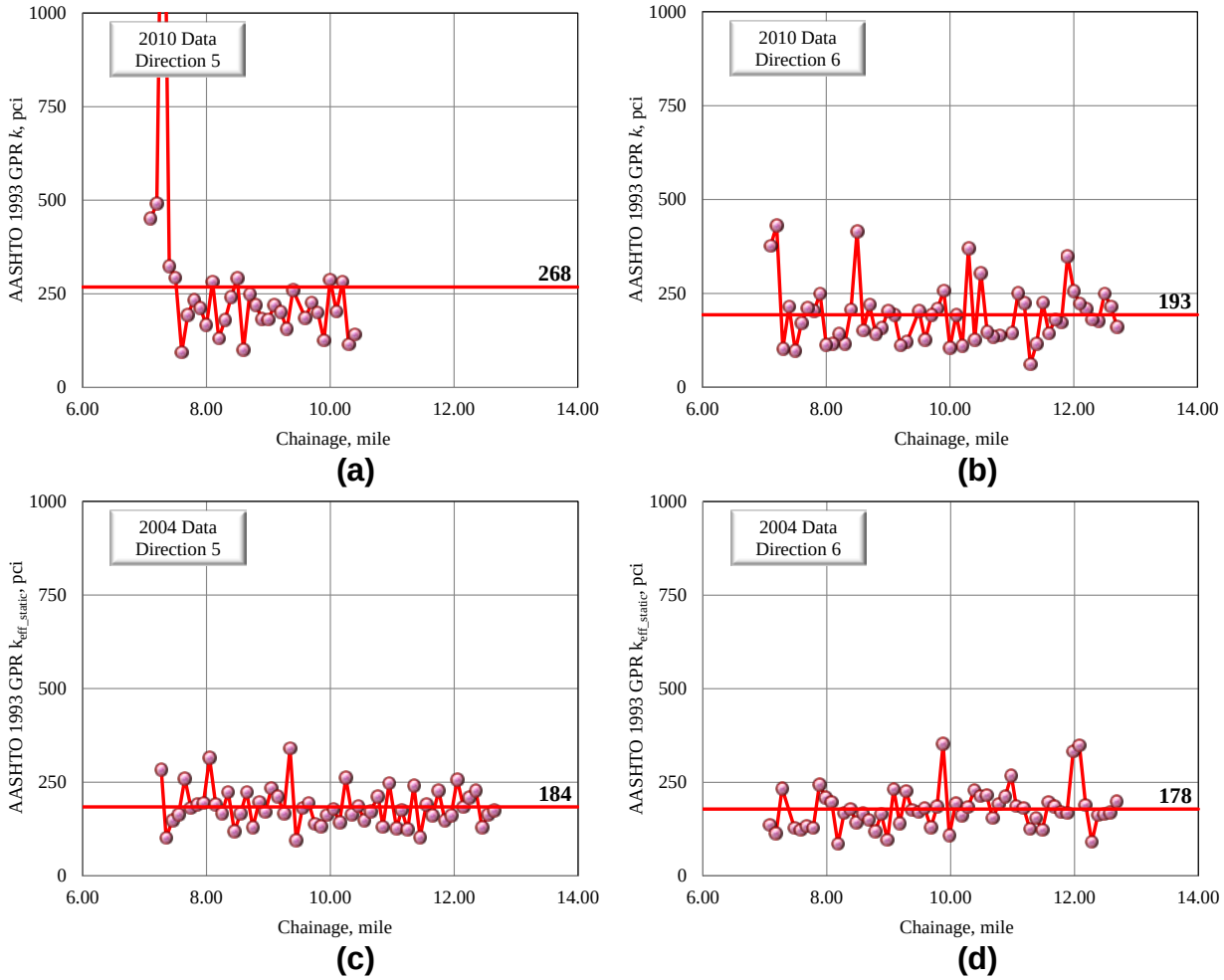

Figure 140 2010 GPR AASHTO 1993 Verified Values of (a) *k* in Direction 5, (b) *k* in Direction 6, (c) k_{eff_static} in Direction 5 and (d) k_{eff_static} in Direction 6 Versus Distance for Control Section 42-30.

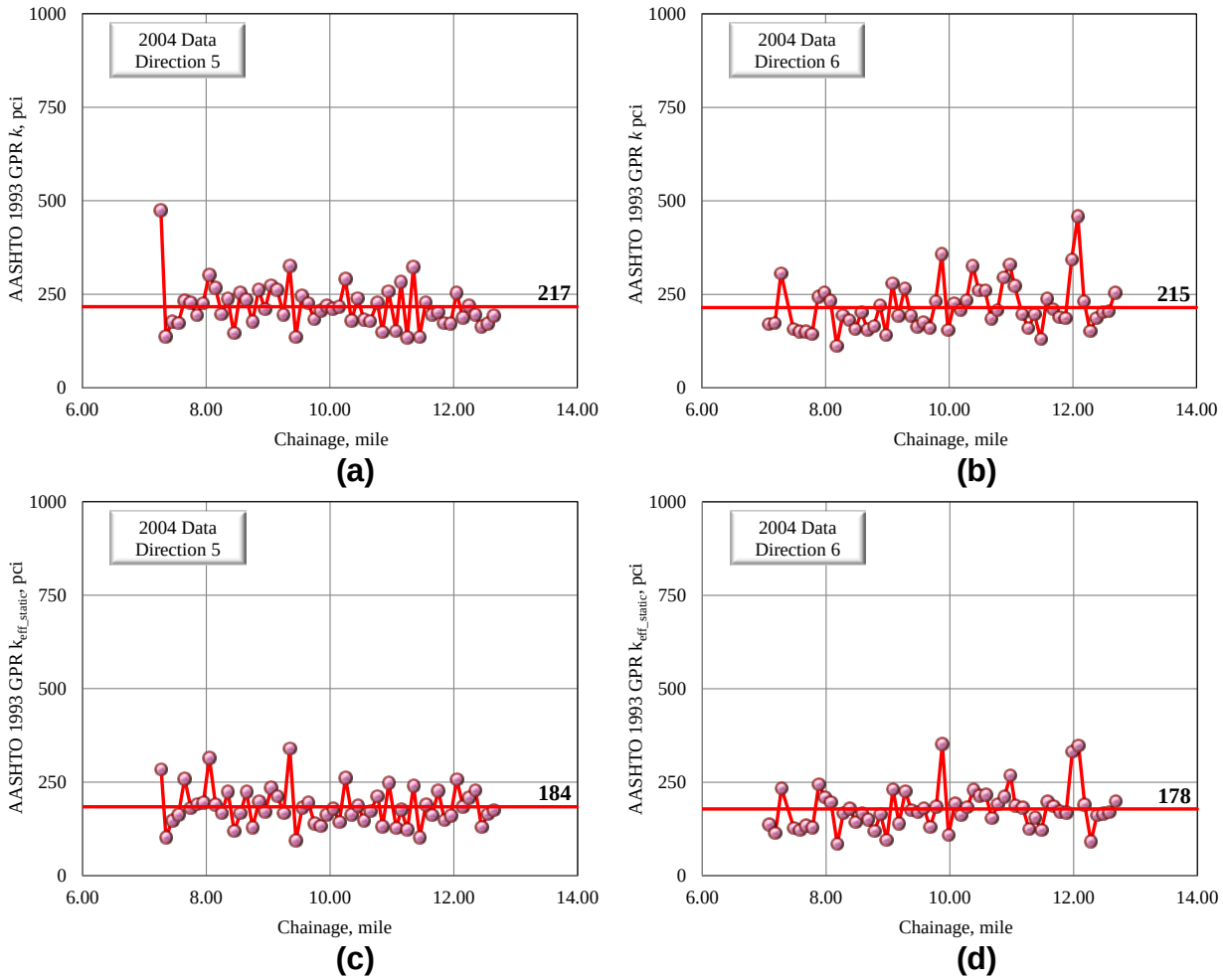

Figure 141 2004 GPR AASHTO 1993 Verified Values of (a) *k* in Direction 5, (b) *k* in Direction 6, (c) k_{eff_static} in Direction 5 and (d) k_{eff_static} in Direction 6 Versus Distance for Control Section 42-30.

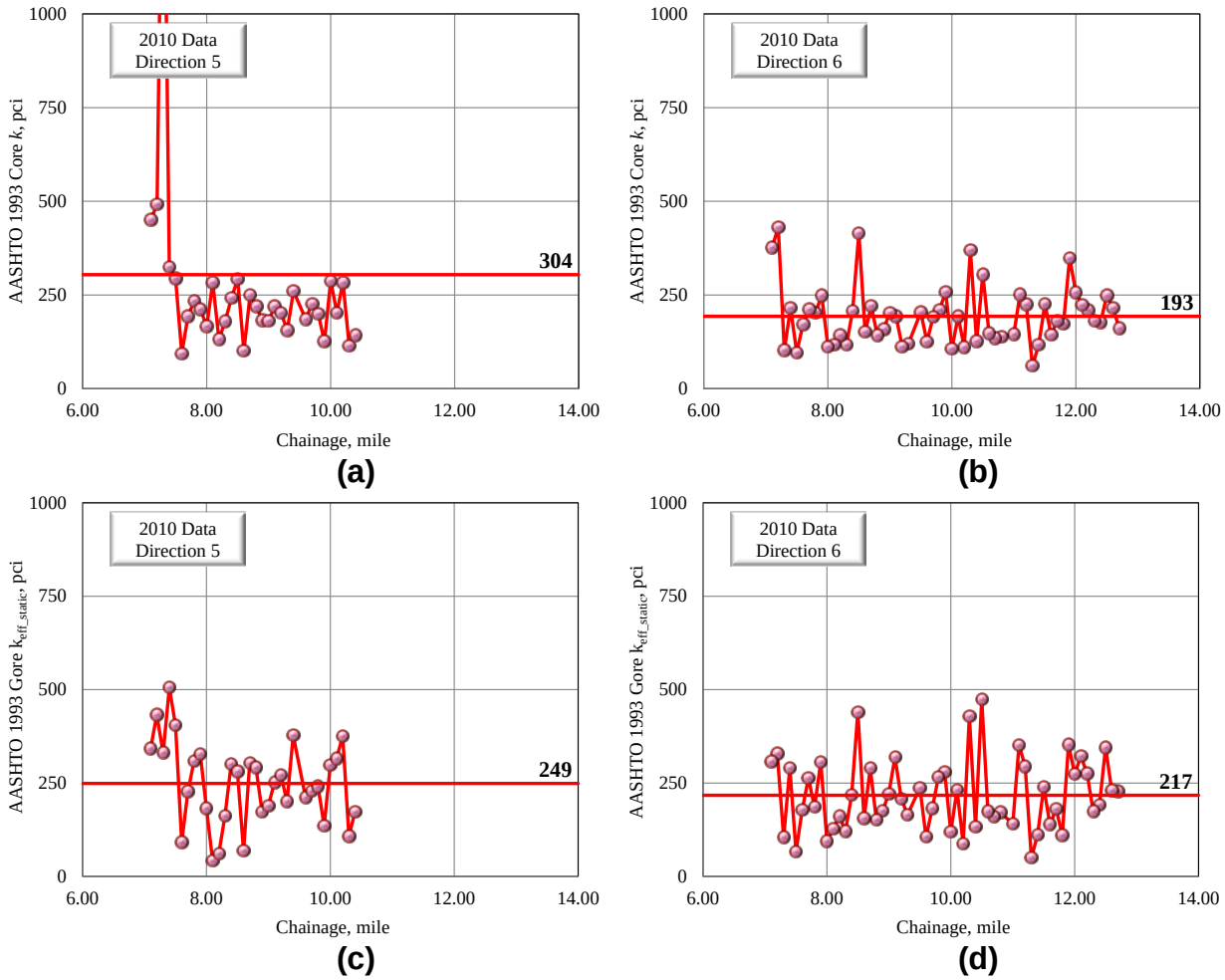

Figure 142 2010 Core AASHTO 1993 Verified Values of (a) *k* in Direction 5, (b) *k* in Direction 6, (c) k_{eff_static} in Direction 5 and (d) k_{eff_static} in Direction 6 Versus Distance for Control Section 42-30.

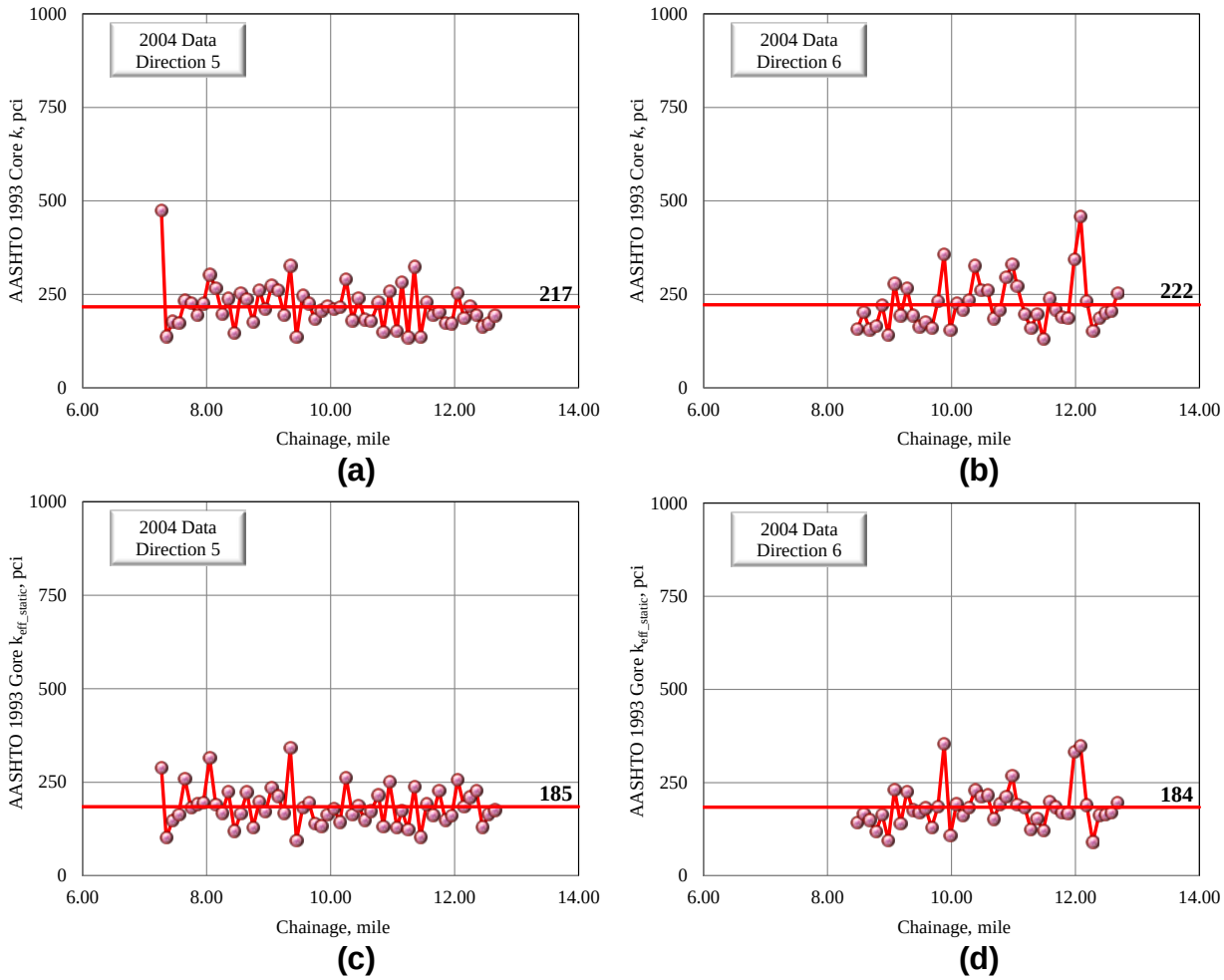

Figure 143 2004 Core AASHTO 1993 Verified Values of (a) *k* in Direction 5, (b) *k* in Direction 6, (c) k_{eff_static} in Direction 5 and (d) k_{eff_static} in Direction 6 Versus Distance for Control Section 42-30.

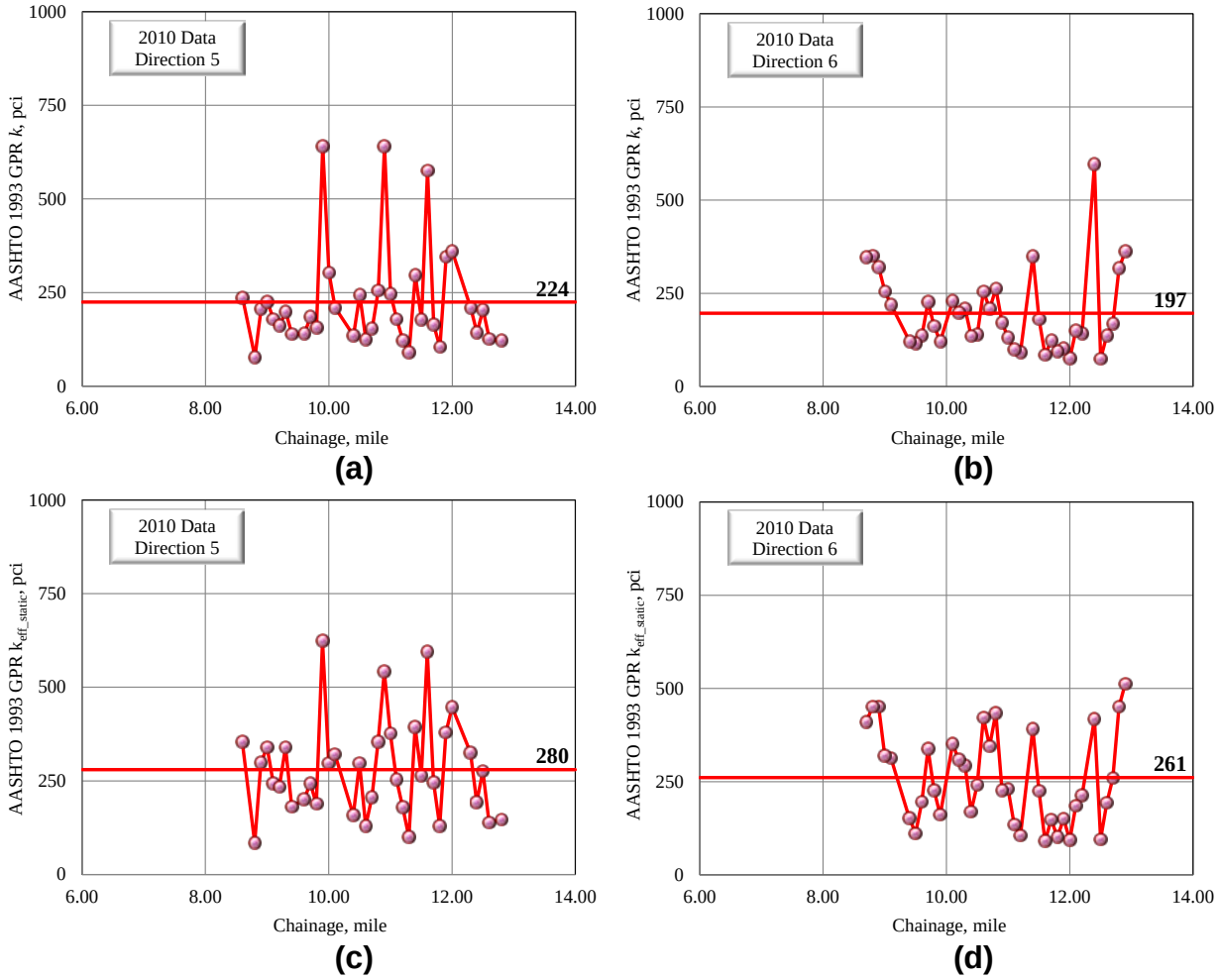

Figure 144 2010 GPR AASHTO 1993 Verified Values of (a) *k* in Direction 5, (b) *k* in Direction 6, (c) k_{eff_static} in Direction 5 and (d) k_{eff_static} in Direction 6 Versus Distance for Control Section 65-09.

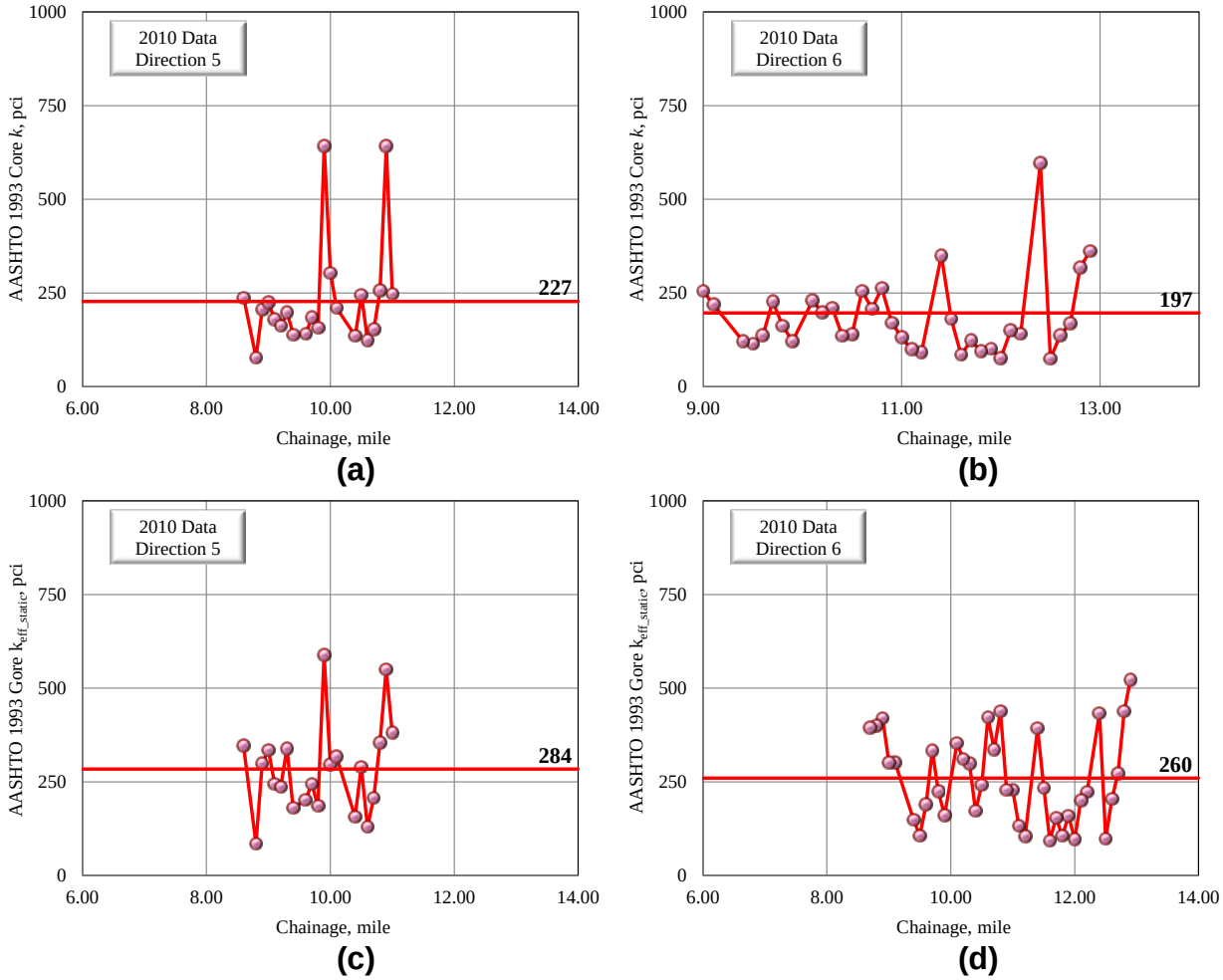

Figure 145 2010 Core AASHTO 1993 Verified Values of (a) *k* in Direction 5, (b) *k* in Direction 6, (c) k_{eff_static} in Direction 5 and (d) k_{eff_static} in Direction 6 Versus Distance for Control Section 65-09.

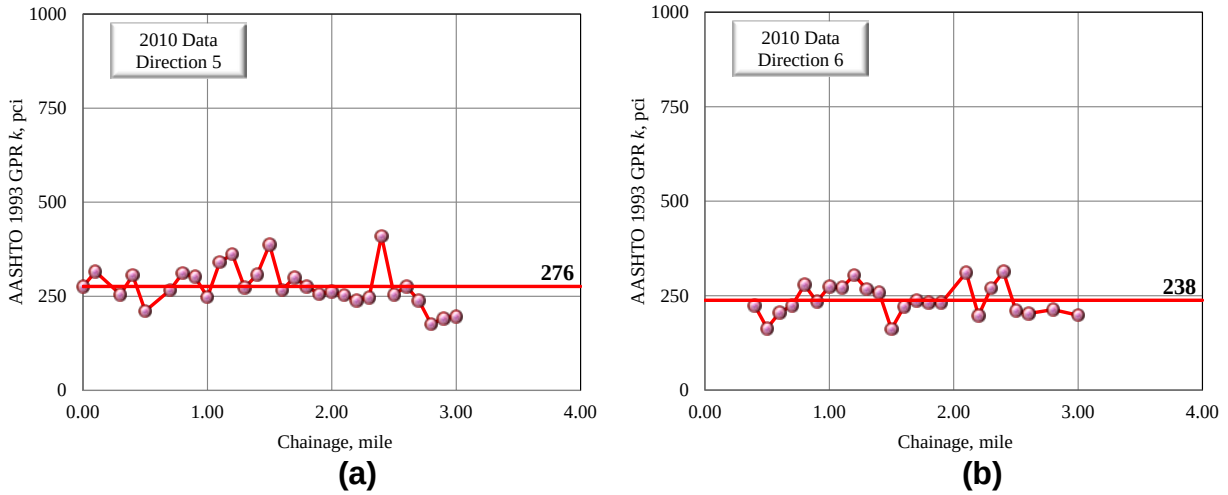

Figure 146 2010 GPR AASHTO 1993 Verified Values of (a) k in Direction 5, and (b) k in Direction 6 Versus Distance for Control Section 16-49.

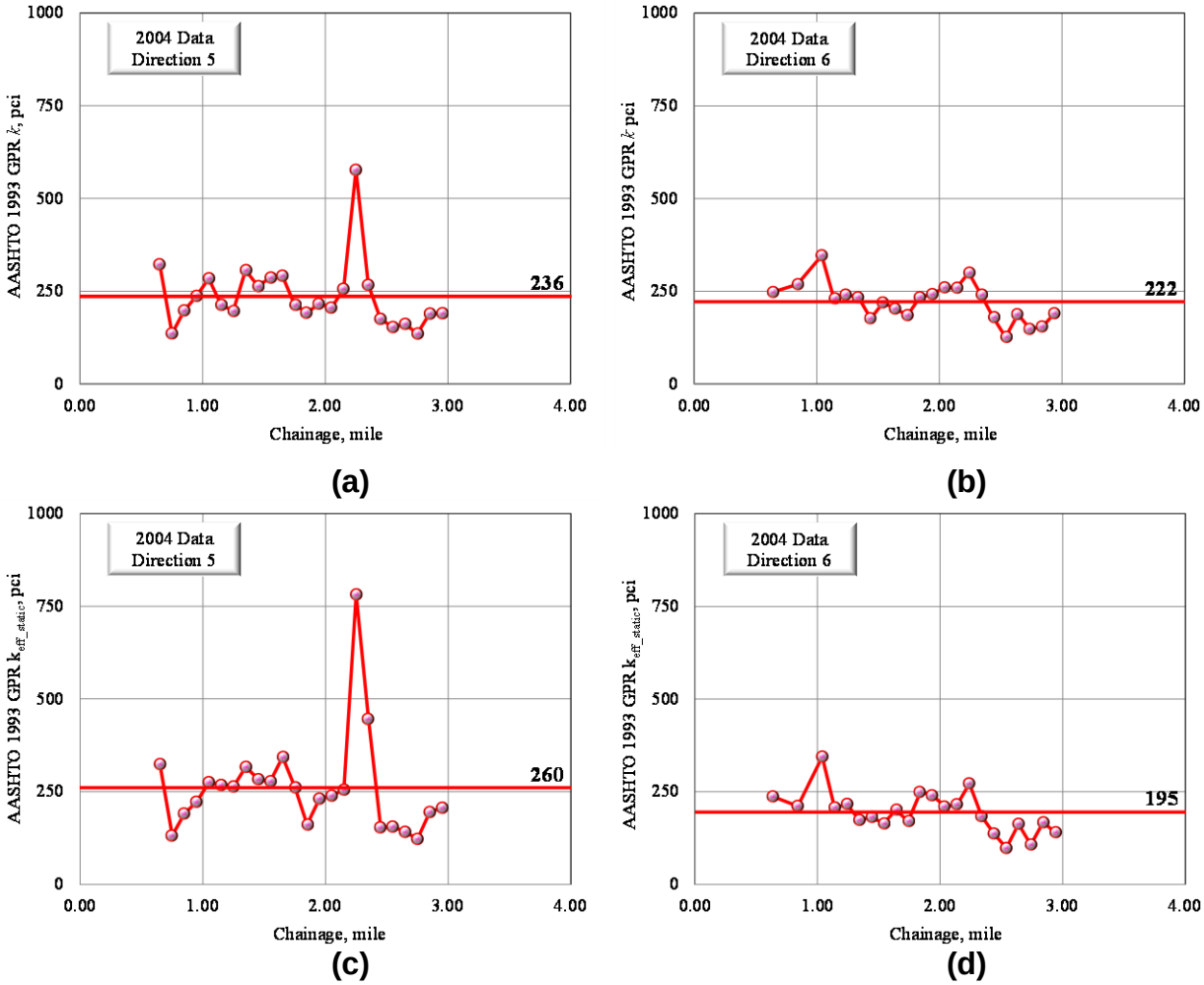

Figure 147 2004 GPR AASHTO 1993 Verified Values of (a) *k* in Direction 5, (b) *k* in Direction 6, (c) k_{eff_static} in Direction 5 and (d) k_{eff_static} in Direction 6 Versus Distance for Control Section 16-49.

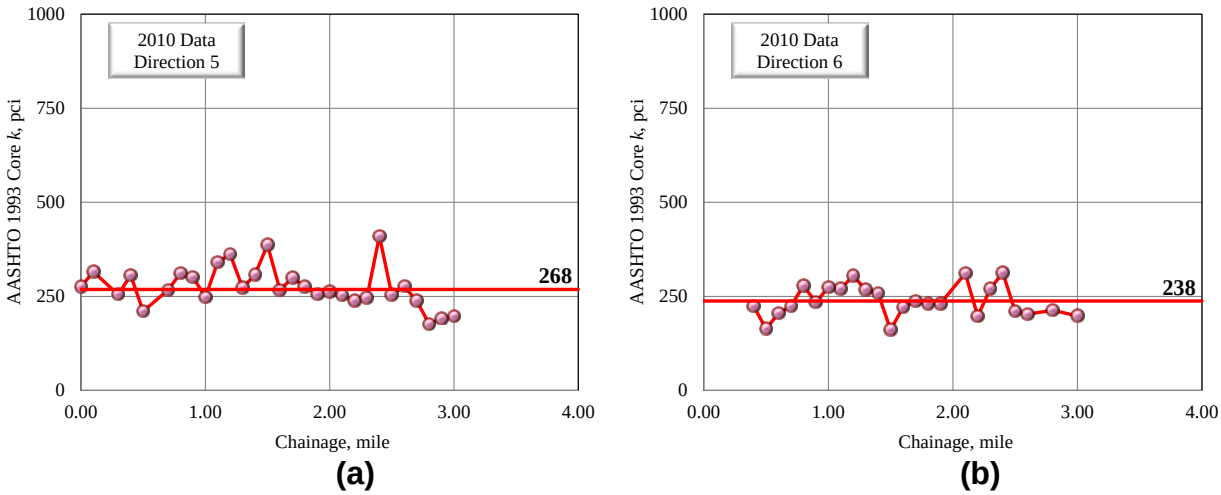

Figure 148 2010 Core AASHTO 1993 Verified Values of (a) *k* in Direction 5, (b) *k* in Direction 6 Versus Distance for Control Section 16-49

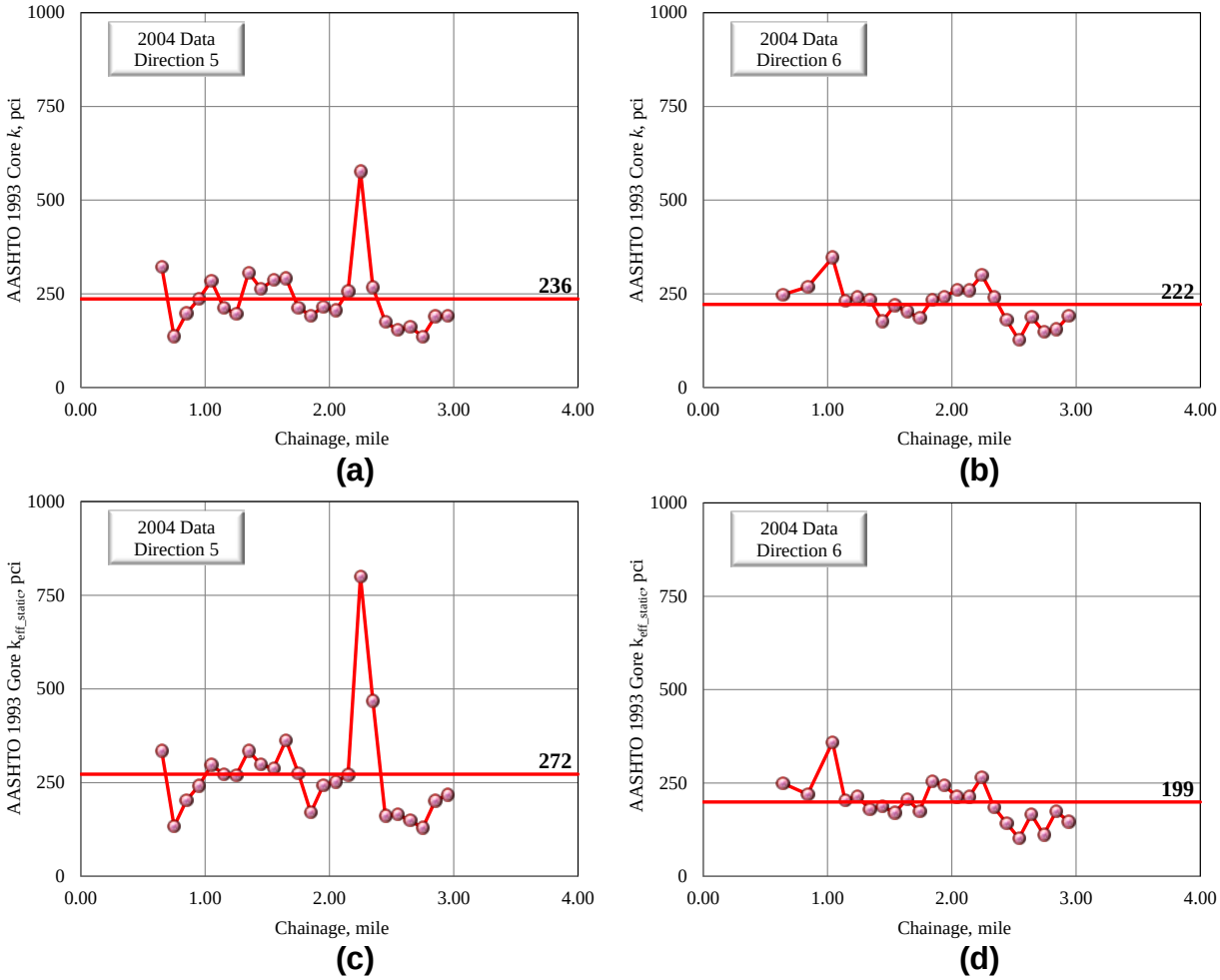

Figure 149 2010 Core AASHTO 1993 Verified Values of (a) *k* in Direction 5, (b) *k* in Direction 6, (c) k_{eff_static} in Direction 5 and (d) k_{eff_static} in Direction 6 Versus Distance for Control Section 16-49.

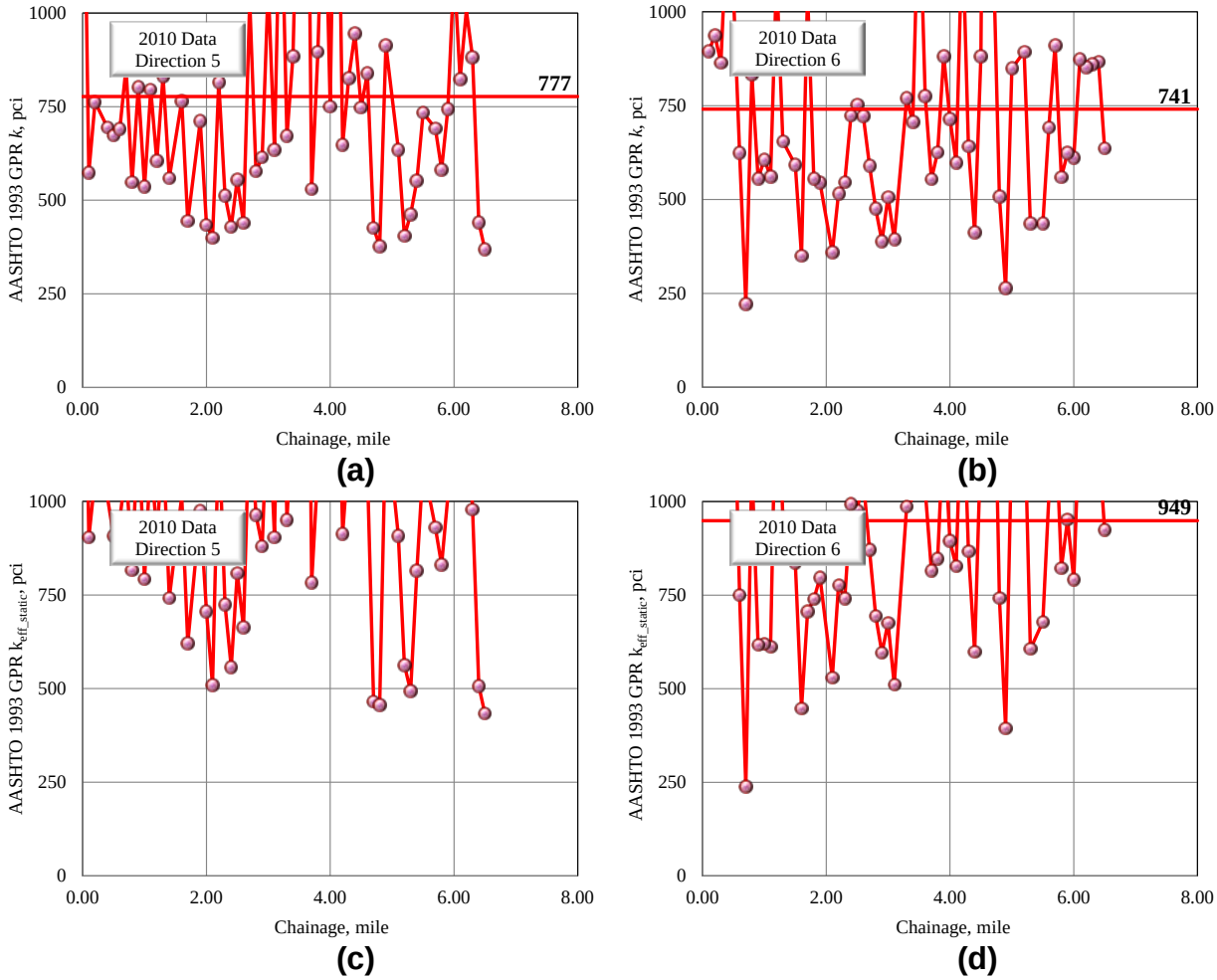

Figure 150 2010 GPR AASHTO 1993 Verified Values of (a) *k* in Direction 5, (b) *k* in Direction 6, (c) k_{eff_static} in Direction 5 and (d) k_{eff_static} in Direction 6 Versus Distance for Control Section 50-32.

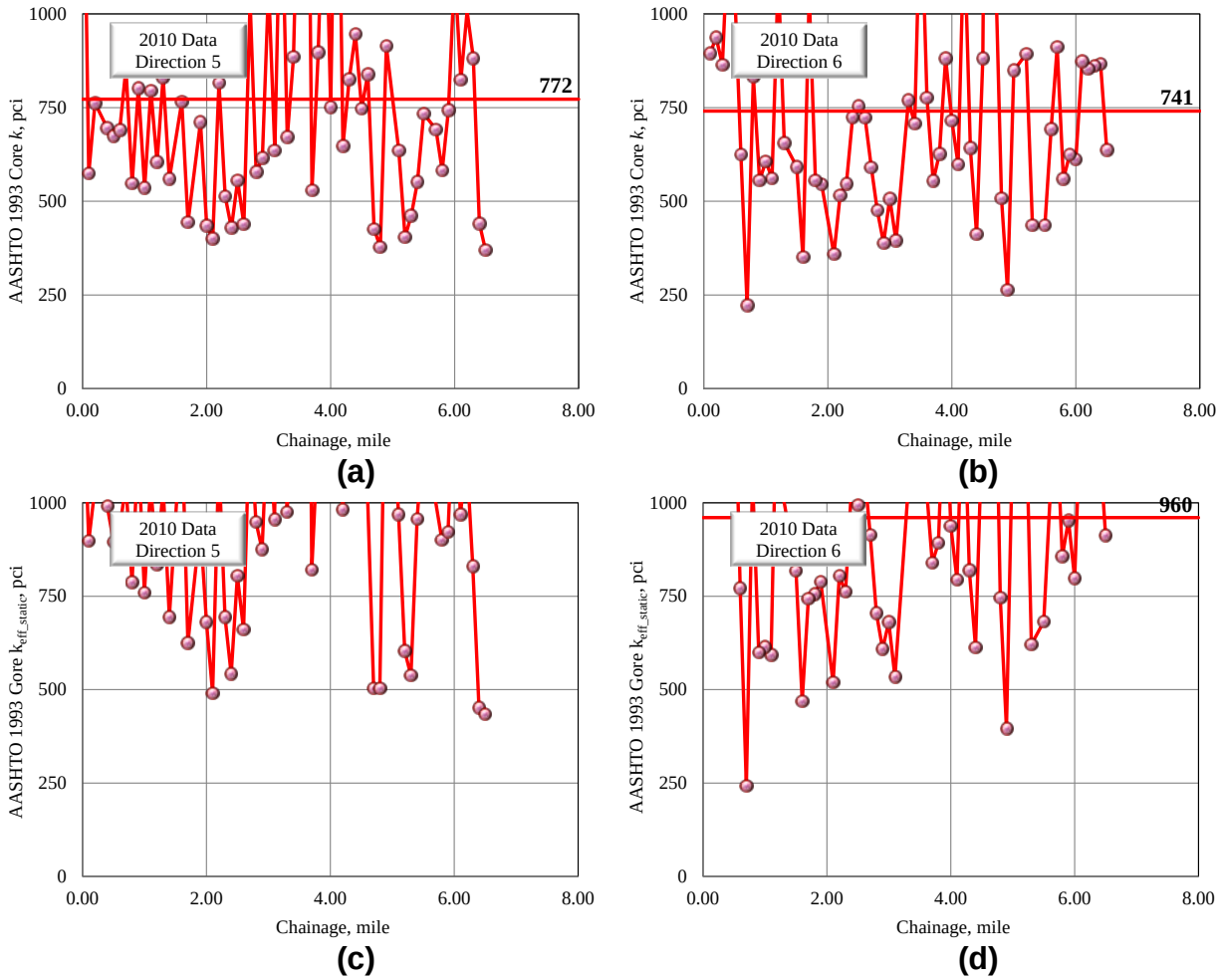

Figure 151 2010 Core AASHTO 1993 Verified Values of (a) *k* in Direction 5, (b) *k* in Direction 6, (c) k_{eff_static} in Direction 5 and (d) k_{eff_static} in Direction 6 Versus Distance for Control Section 50-32.

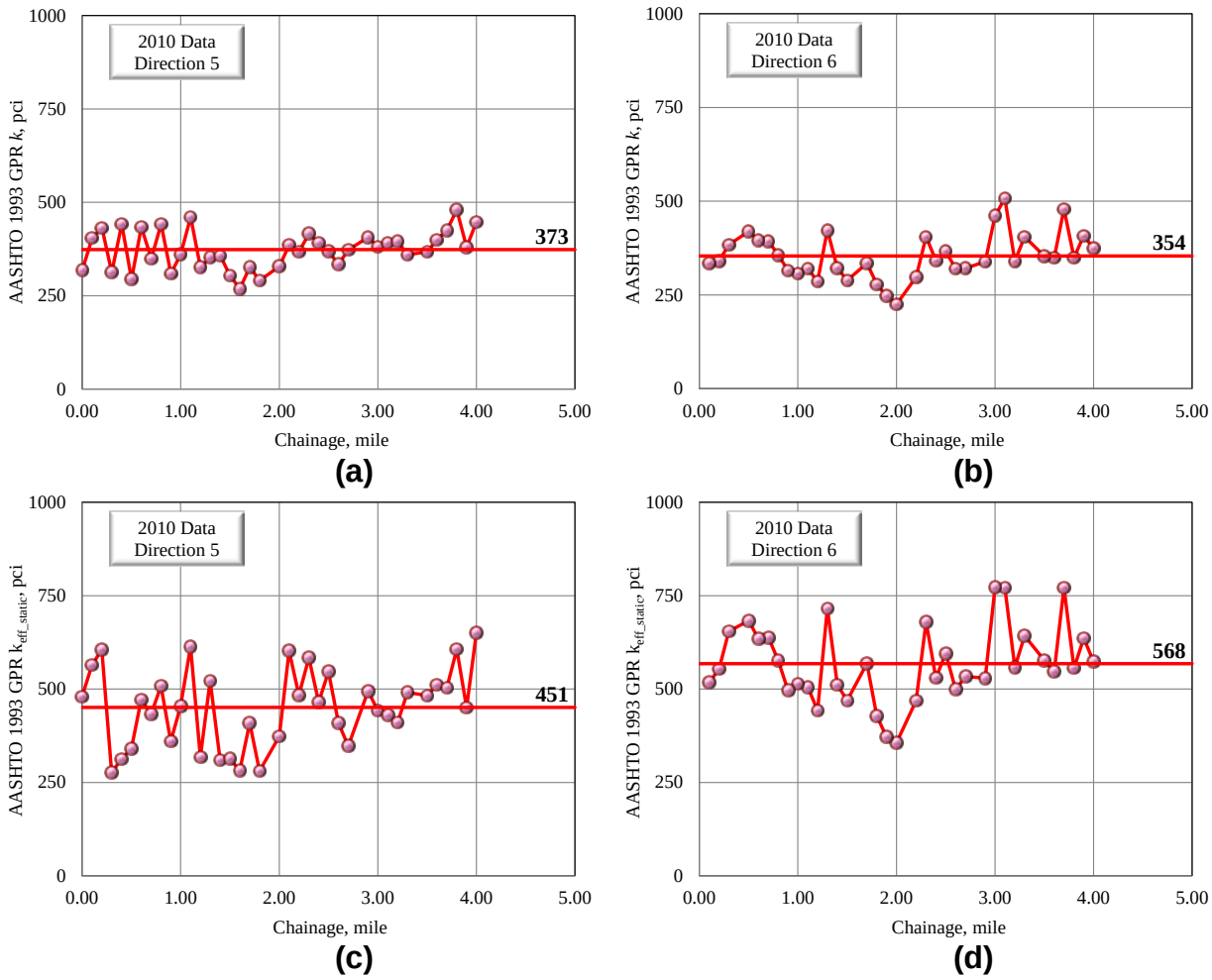

Figure 152 2010 GPR AASHTO 1993 Verified Values of (a) *k* in Direction 5, (b) *k* in Direction 6, (c) k_{eff_static} in Direction 5 and (d) k_{eff_static} in Direction 6 Versus Distance for Control Section 25-46.

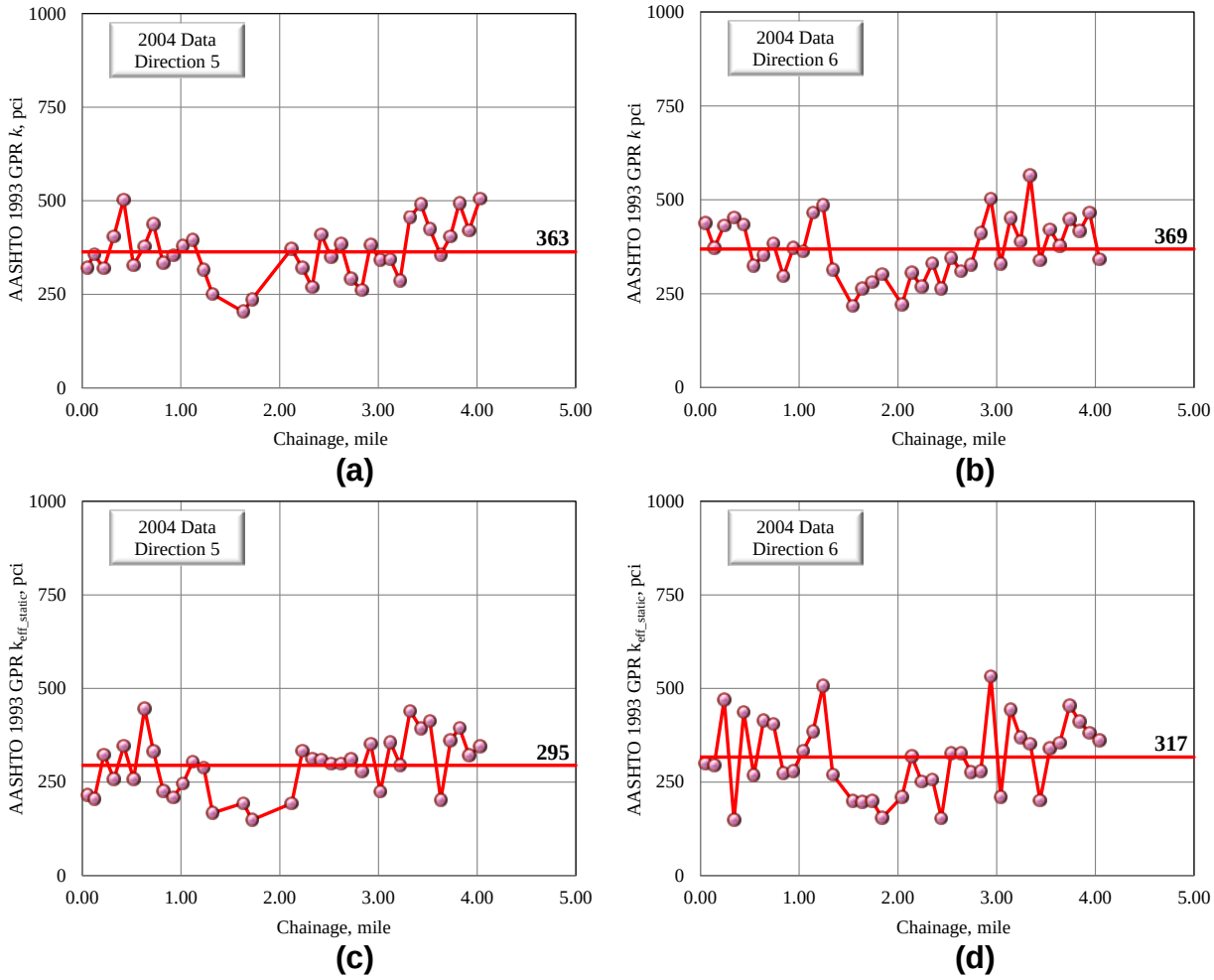

Figure 153 2004 GPR AASHTO 1993 Verified Values of (a) *k* in Direction 5, (b) *k* in Direction 6, (c) k_{eff_static} in Direction 5 and (d) k_{eff_static} in Direction 6 Versus Distance for Control Section 25-46.

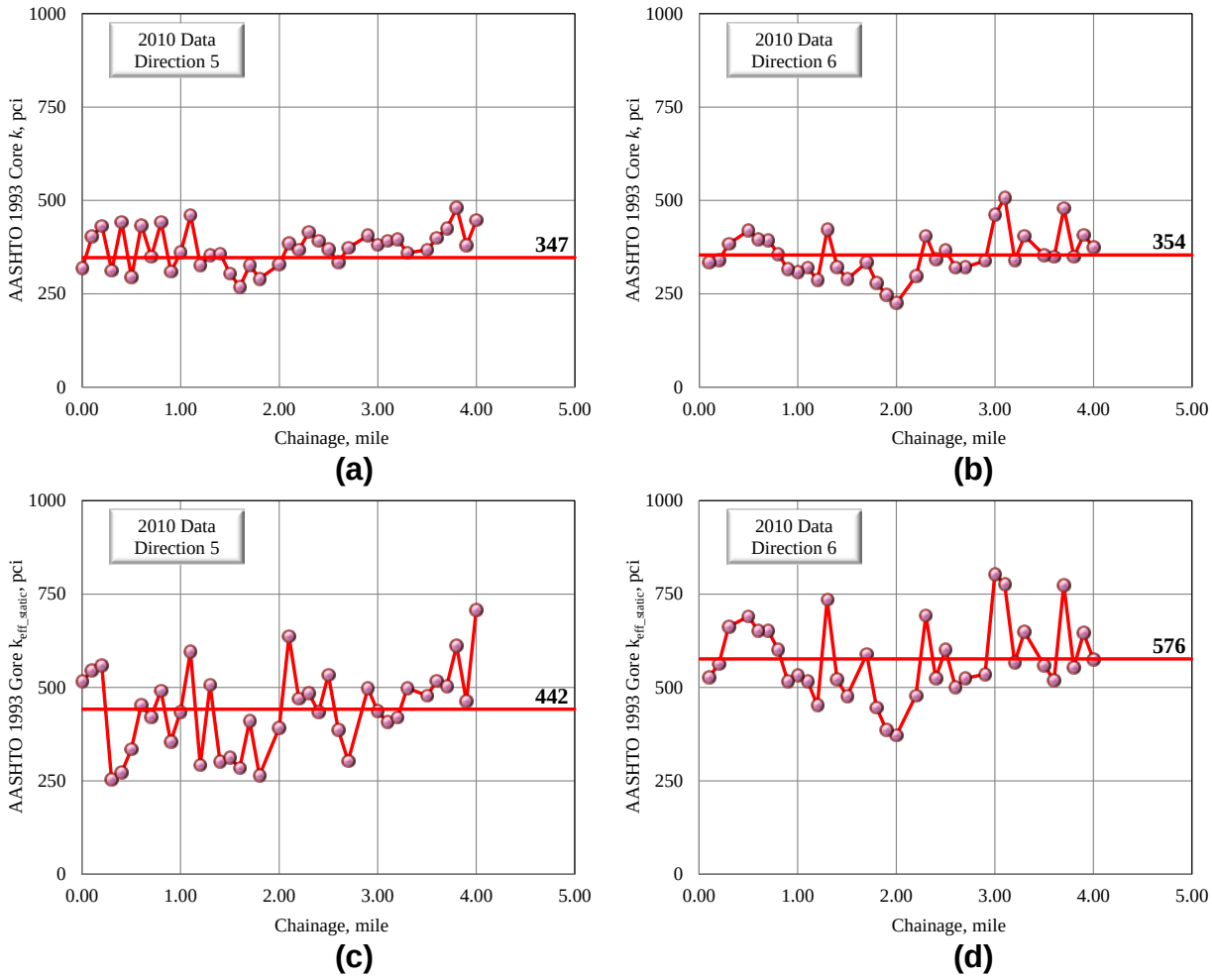

Figure 154 2010 Core AASHTO 1993 Verified Values of (a) *k* in Direction 5, (b) *k* in Direction 6, (c) k_{eff_static} in Direction 5 and (d) k_{eff_static} in Direction 6 Versus Distance for Control Section 25-46.

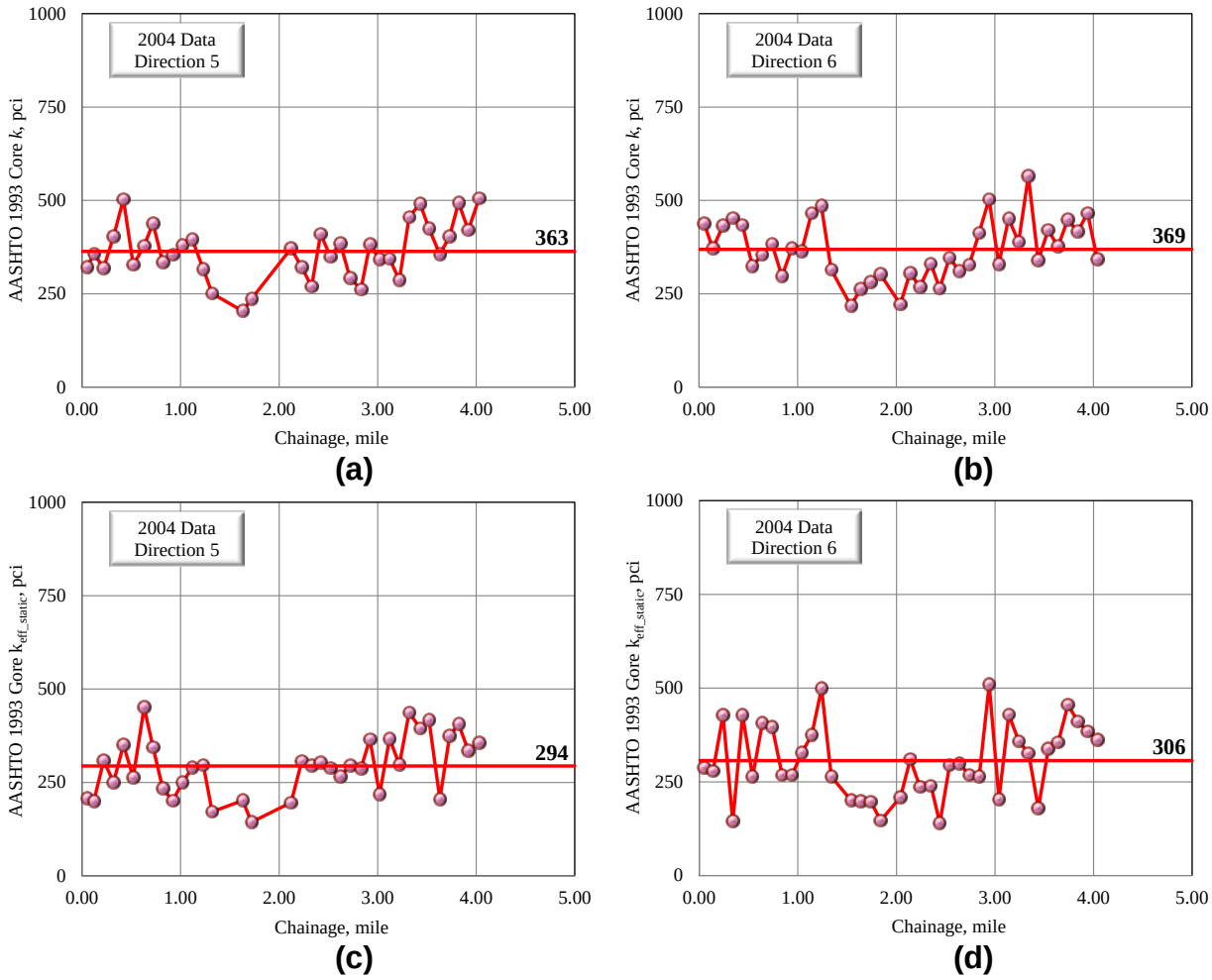

Figure 155 2004 Core AASHTO 1993 Verified Values of (a) *k* in Direction 5, (b) *k* in Direction 6, (c) k_{eff_static} in Direction 5 and (d) k_{eff_static} in Direction 6 Versus Distance for Control Section 25-46.

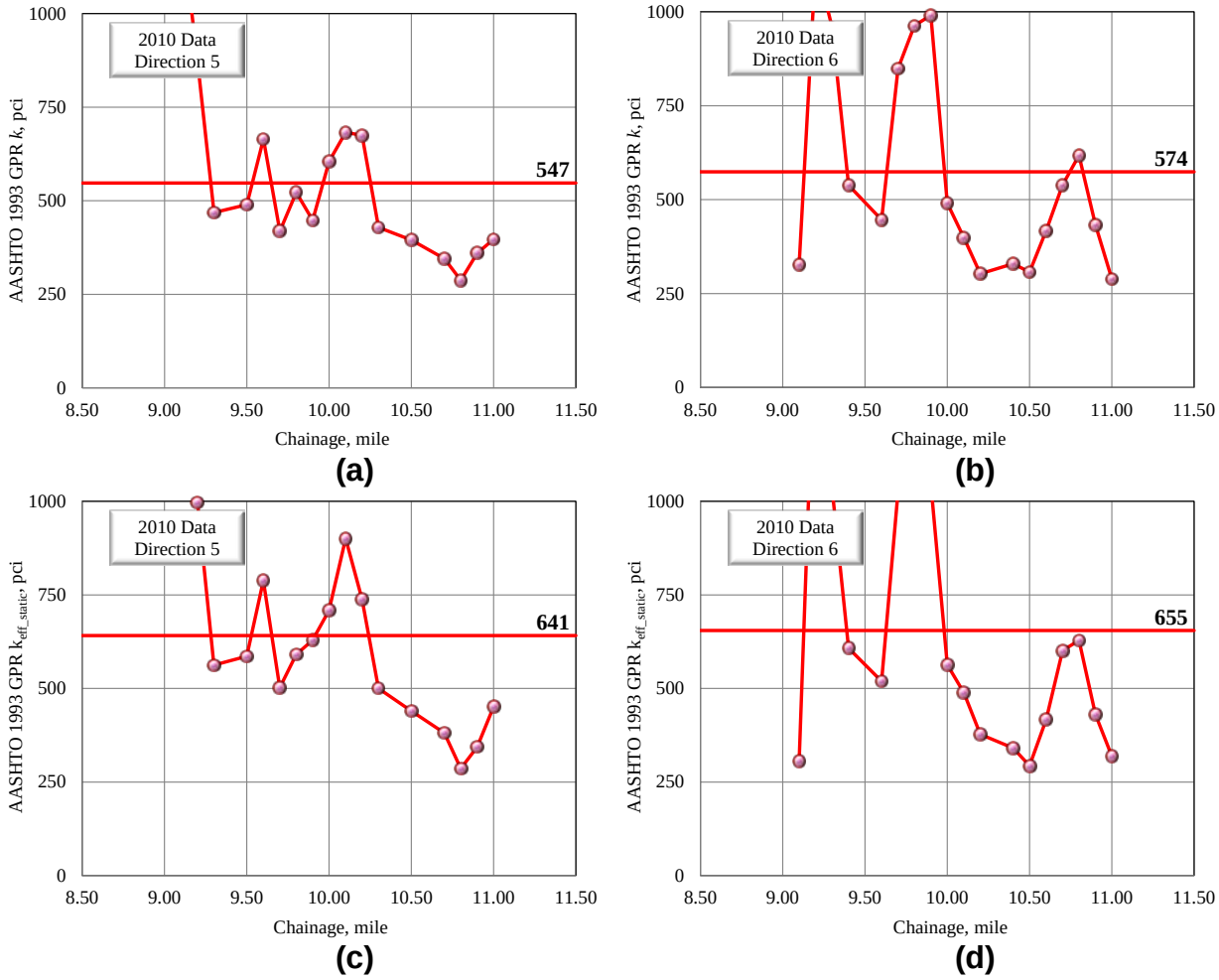

Figure 156 2010 GPR AASHTO 1993 Verified Values of (a) *k* in Direction 5, (b) *k* in Direction 6, (c) k_{eff_static} in Direction 5 and (d) k_{eff_static} in Direction 6 Versus Distance for Control Section 72-09.

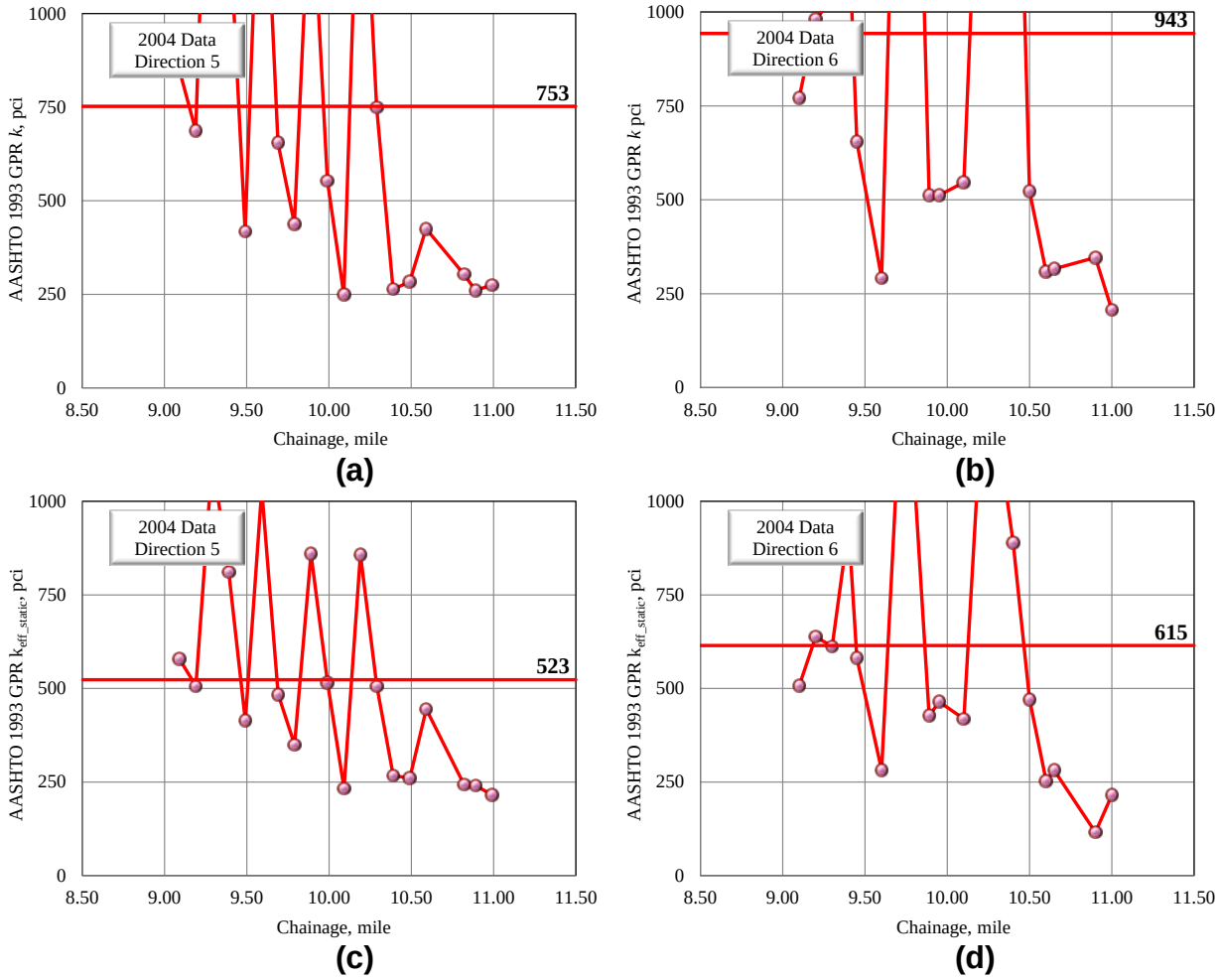

Figure 157 2004 GPR AASHTO 1993 Verified Values of (a) *k* in Direction 5, (b) *k* in Direction 6, (c) k_{eff_static} in Direction 5 and (d) k_{eff_static} in Direction 6 Versus Distance for Control Section 72-09.

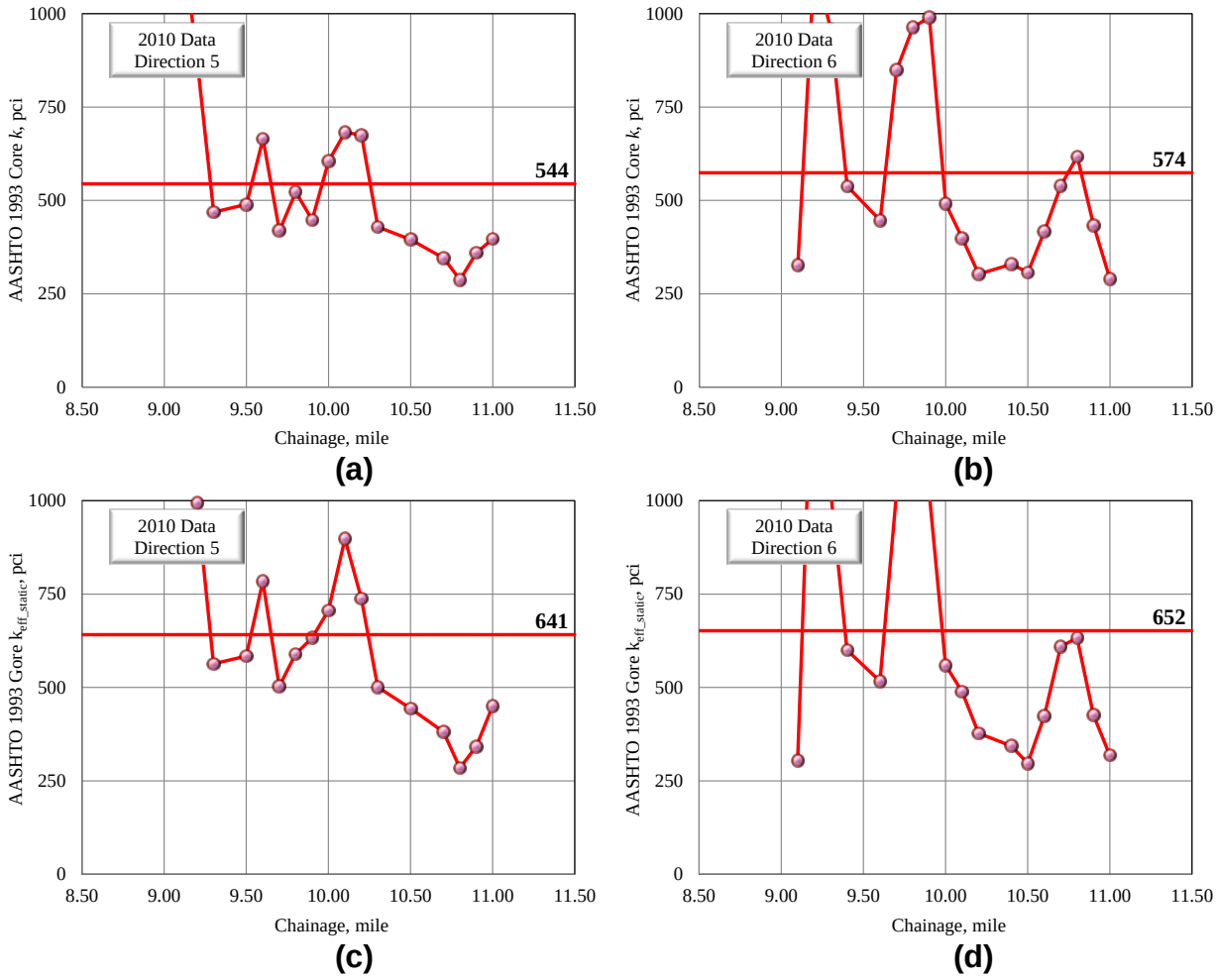

Figure 158 2010 Core AASHTO 1993 Verified Values of (a) *k* in Direction 5, (b) *k* in Direction 6, (c) k_{eff_static} in Direction 5 and (d) k_{eff_static} in Direction 6 Versus Distance for Control Section 72-09.

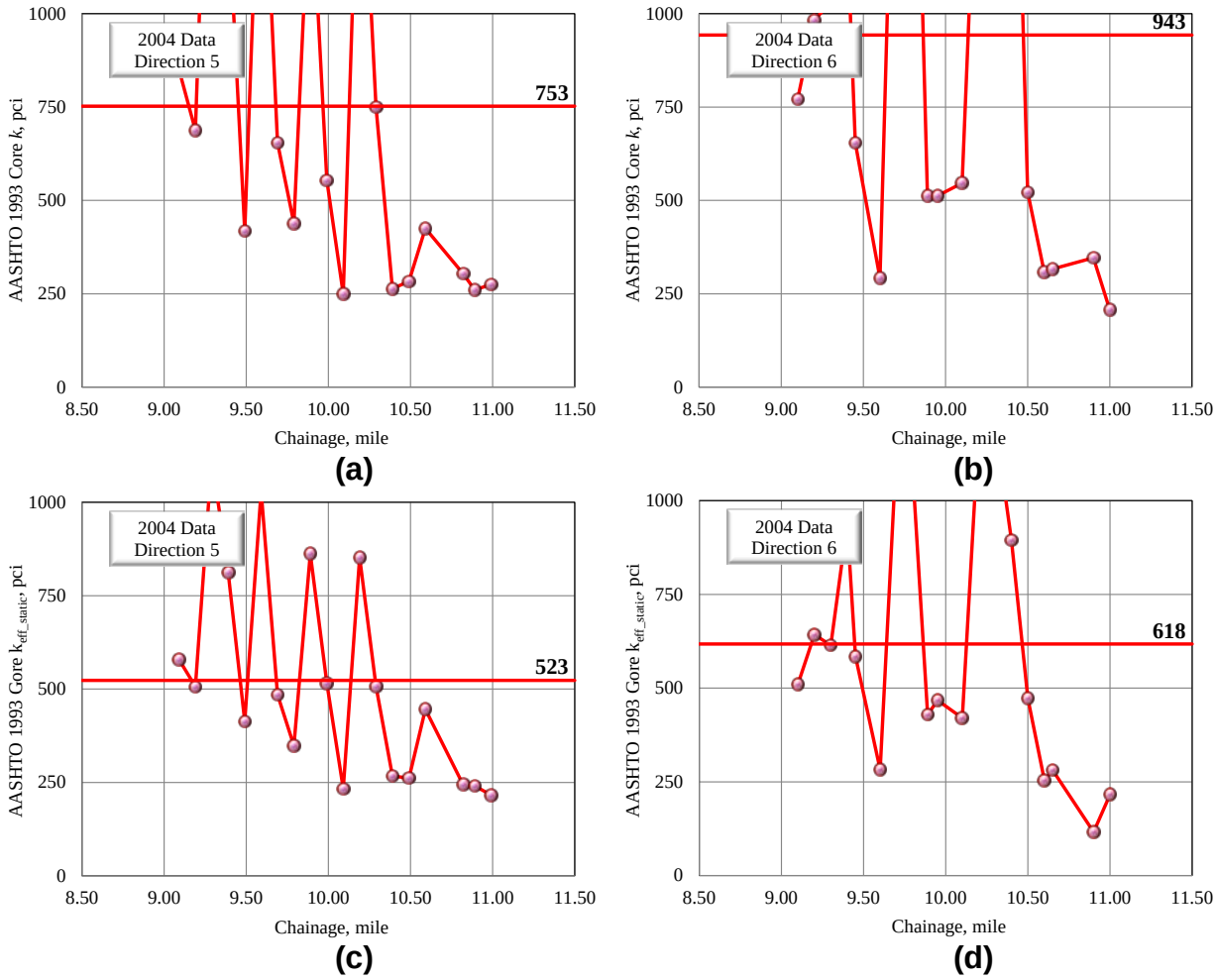

Figure 159 2004 Core AASHTO 1993 Verified Values of (a) *k* in Direction 5, (b) *k* in Direction 6, (c) k_{eff_static} in Direction 5 and (d) k_{eff_static} in Direction 6 Versus Distance for Control Section 72-09.

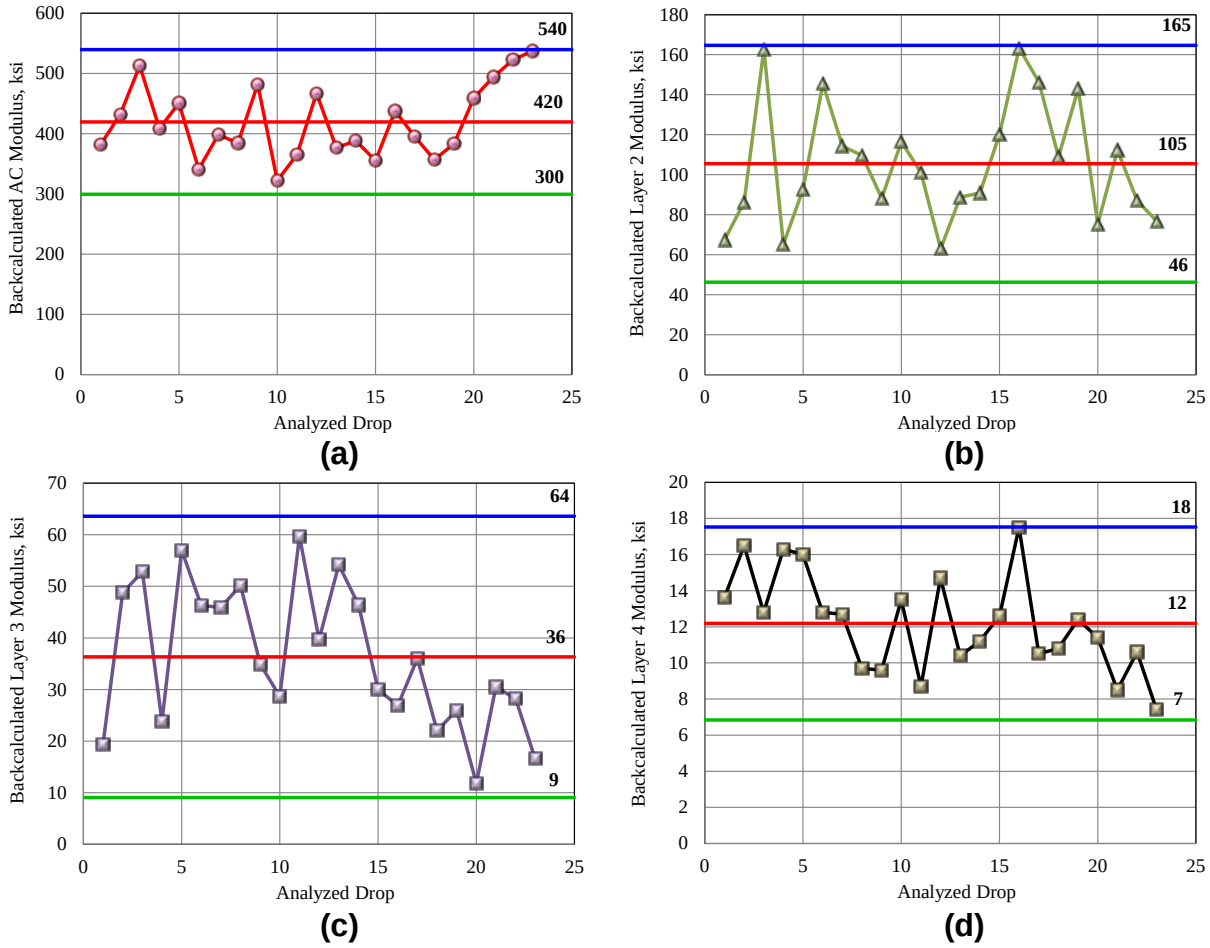

Figure 160 2010 Backcalculated (a) AC Layer, (b) Layer 2, (c) Layer 3 and (d) Layer 4 Moduli for Control Section 68-22, Direction 5.

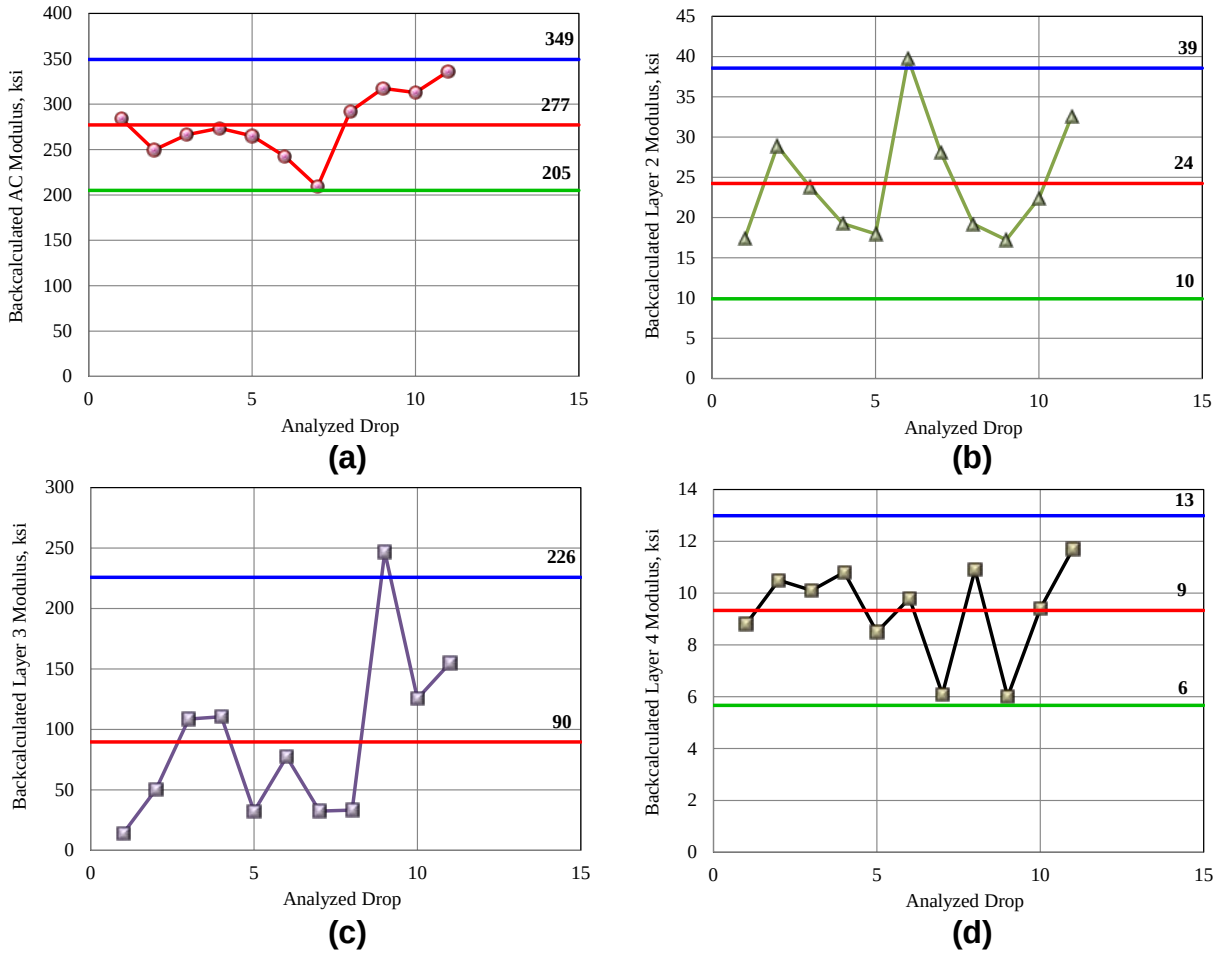

Figure 161 2010 Backcalculated (a) AC Layer, (b) Layer 2, (c) Layer 3 and (d) Layer 4 Moduli for Control Section 68-22, Direction 6.

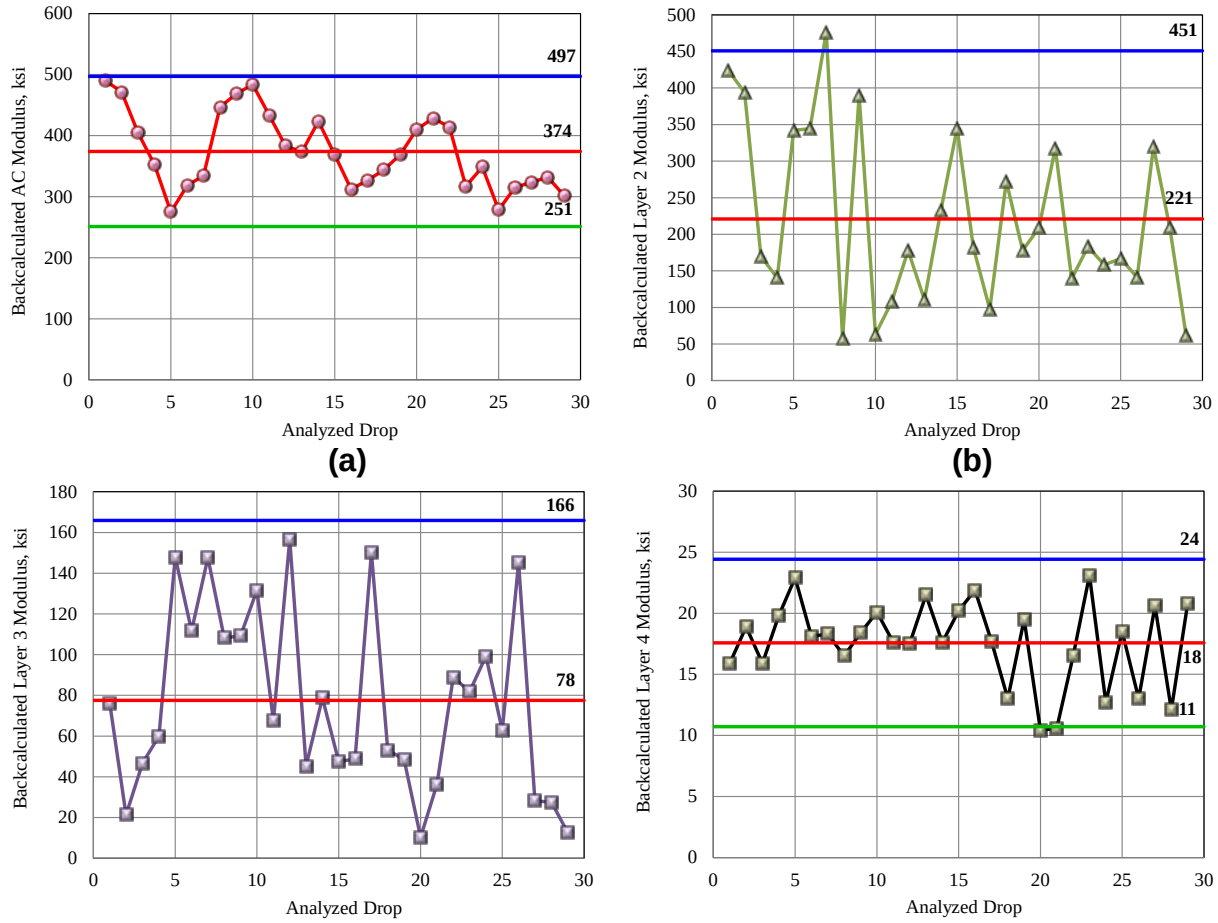

Figure 162 2010 Backcalculated (a) AC Layer, (b) Layer 2, (c) Layer 3 and (d) Layer 4 Moduli for Control Section 54-22, Direction 5.

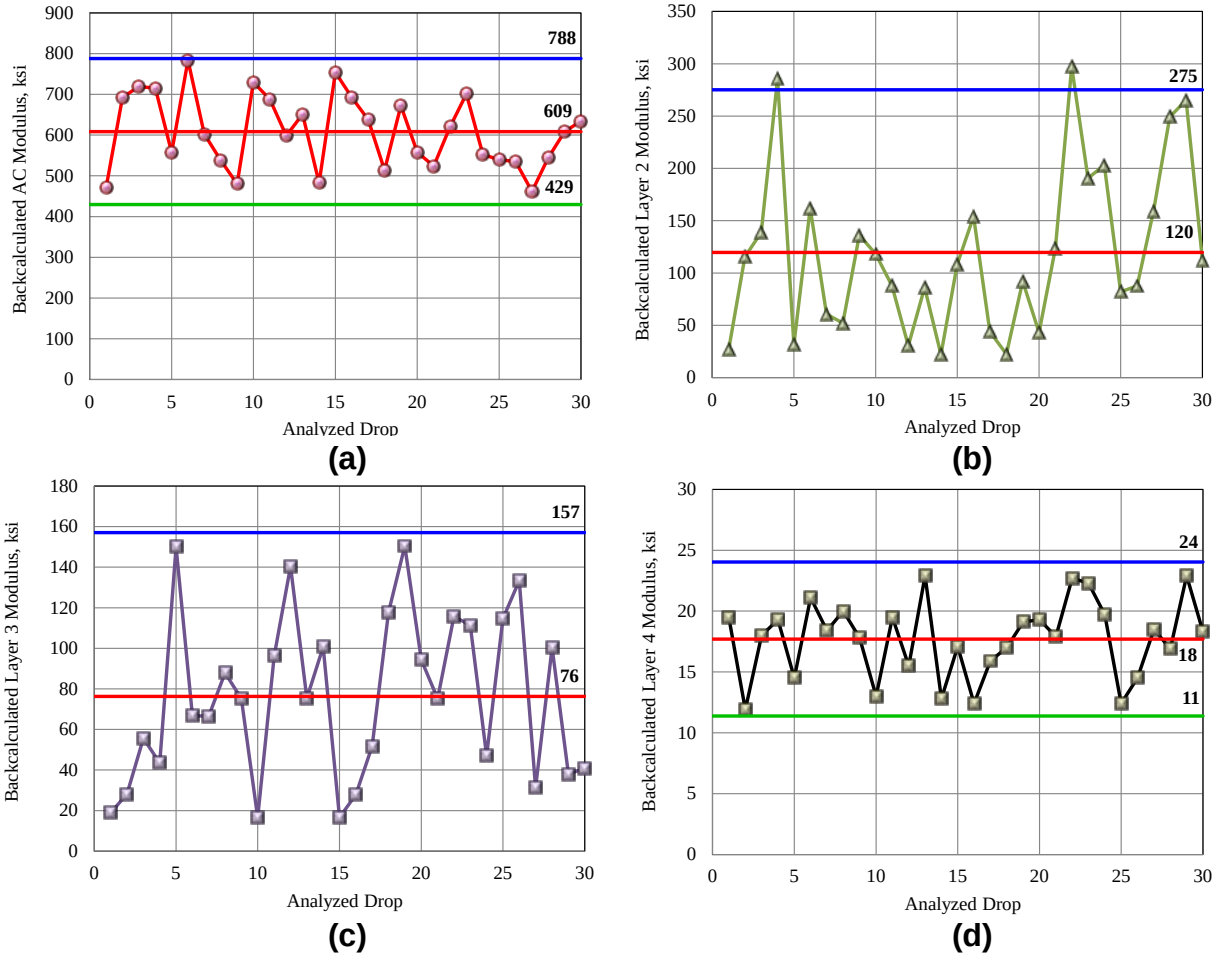

Figure 163 2010 Backcalculated (a) AC Layer, (b) Layer 2, (c) Layer 3 and (d) Layer 4 Moduli for Control Section 54-22, Direction 6.

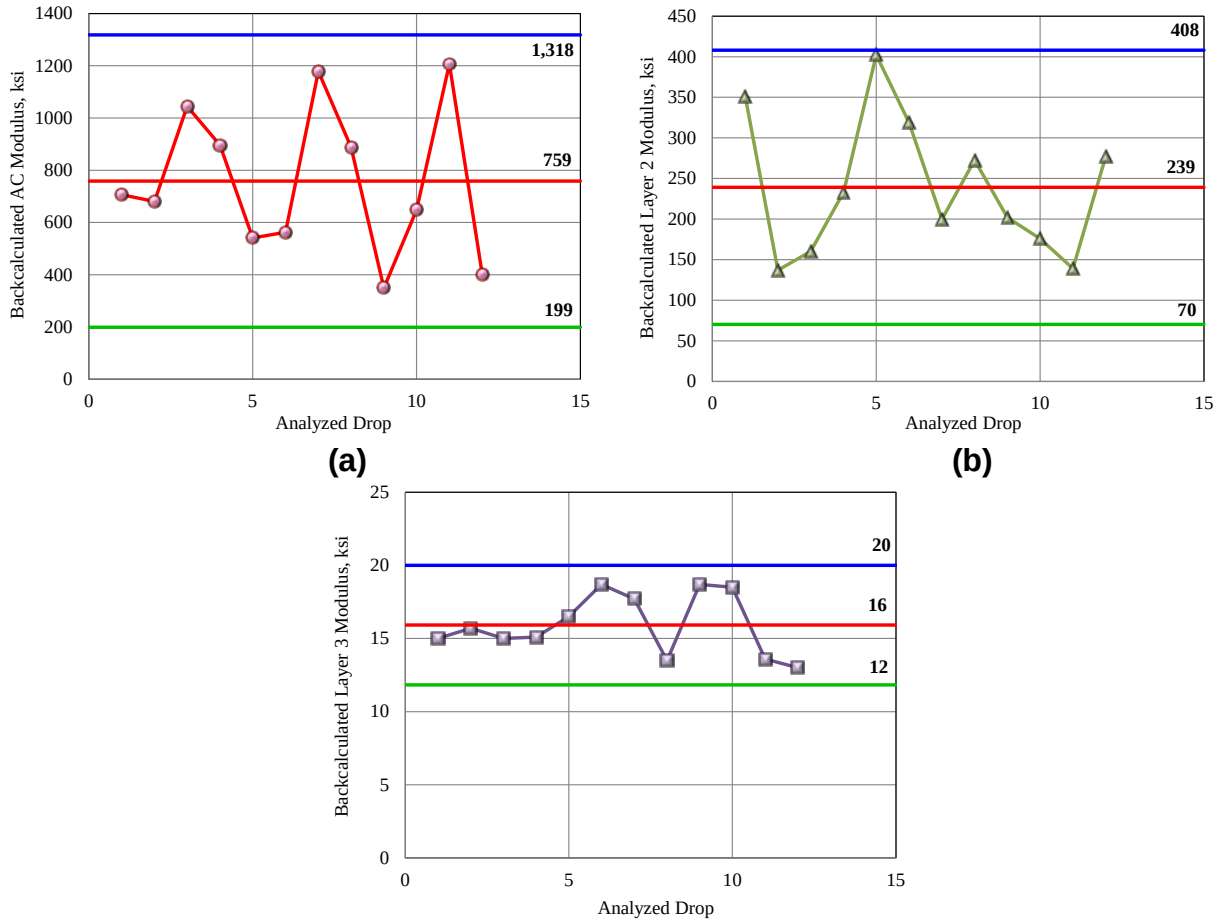

Figure 164 2010 Backcalculated (a) AC Layer, (b) Layer 2, and (c) Layer 3 Moduli for Control Section 44-05 MP 10.8, Direction 5.

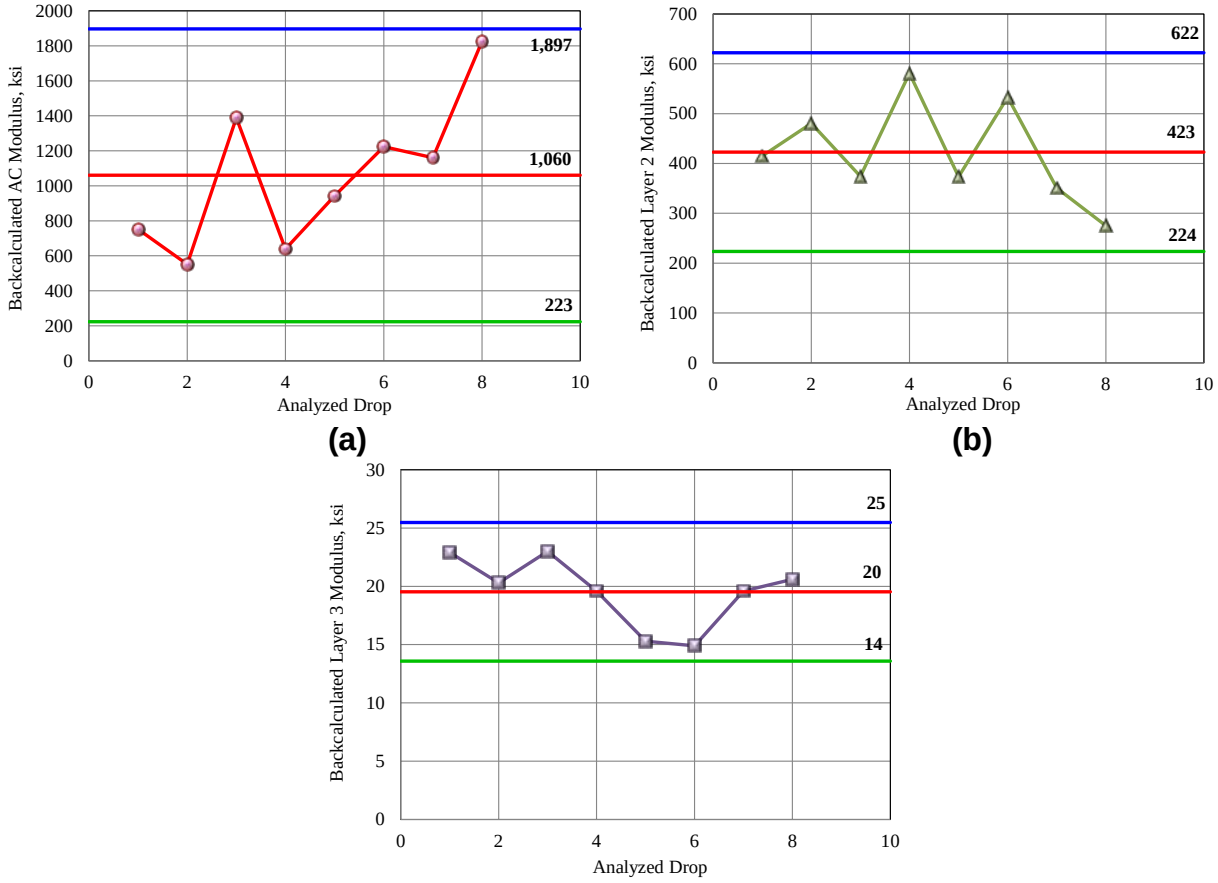

Figure 165 2010 Backcalculated (a) AC Layer, (b) Layer 2, and (c) Layer 3 Moduli for Control Section 44-05 MP 10.8, Direction 6.

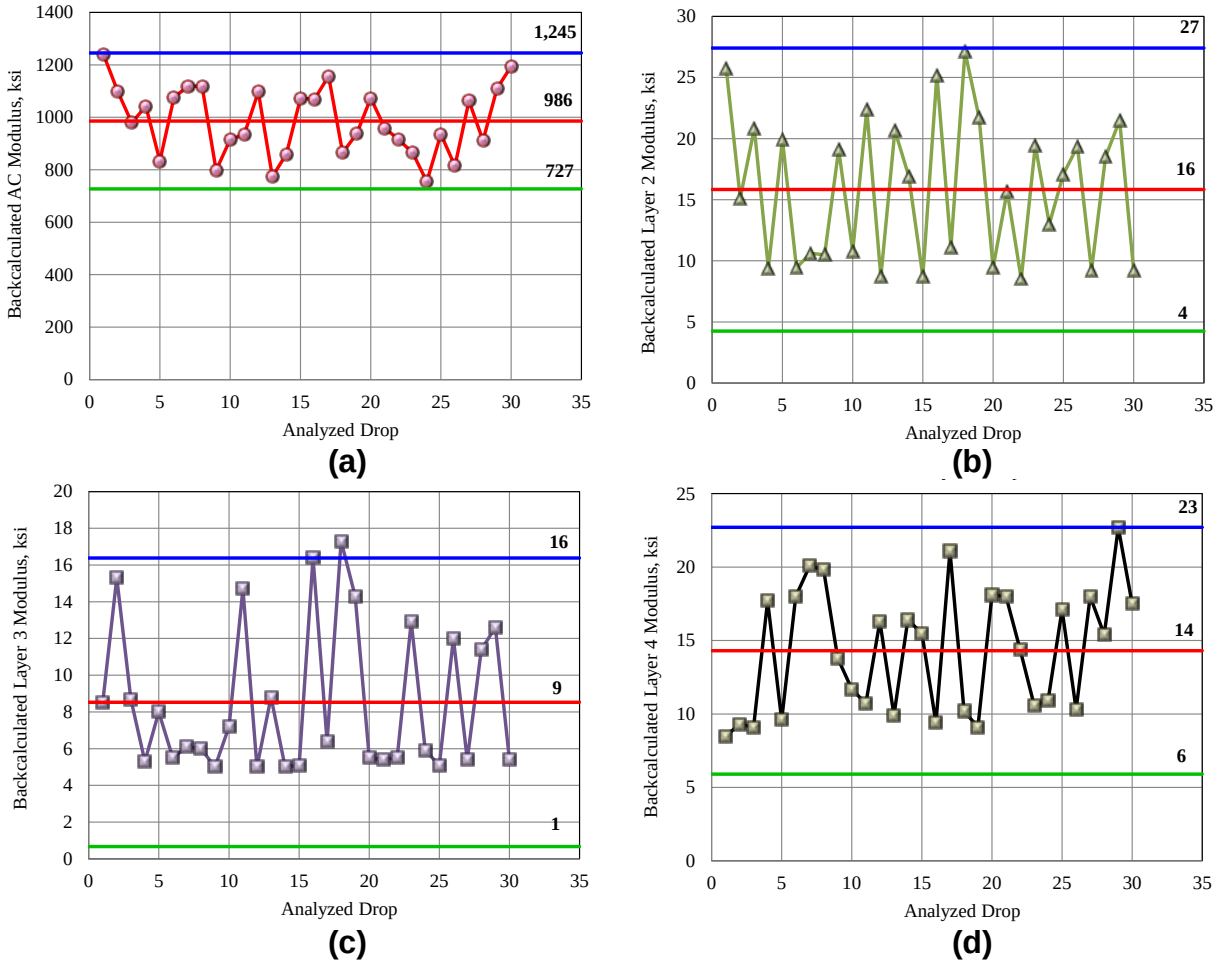

Figure 166 2010 Backcalculated (a) AC Layer, (b) Layer 2, (c) Layer 3 and (d) Layer 4 Moduli for Control Section 09-05, Direction 5.

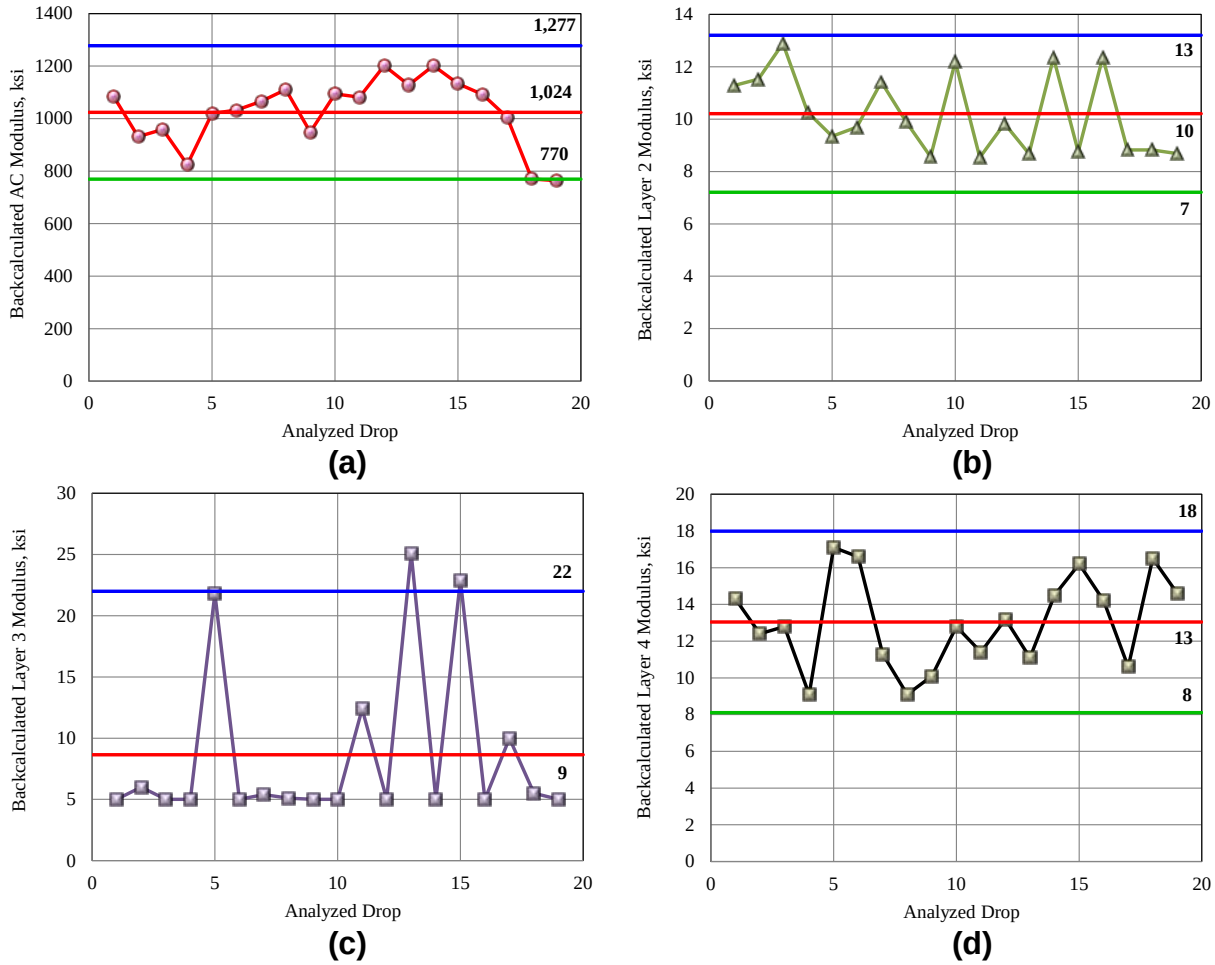

Figure 167 2010 Backcalculated (a) AC Layer, (b) Layer 2, (c) Layer 3 and (d) Layer 4 Moduli for Control Section 09-05, Direction 6.

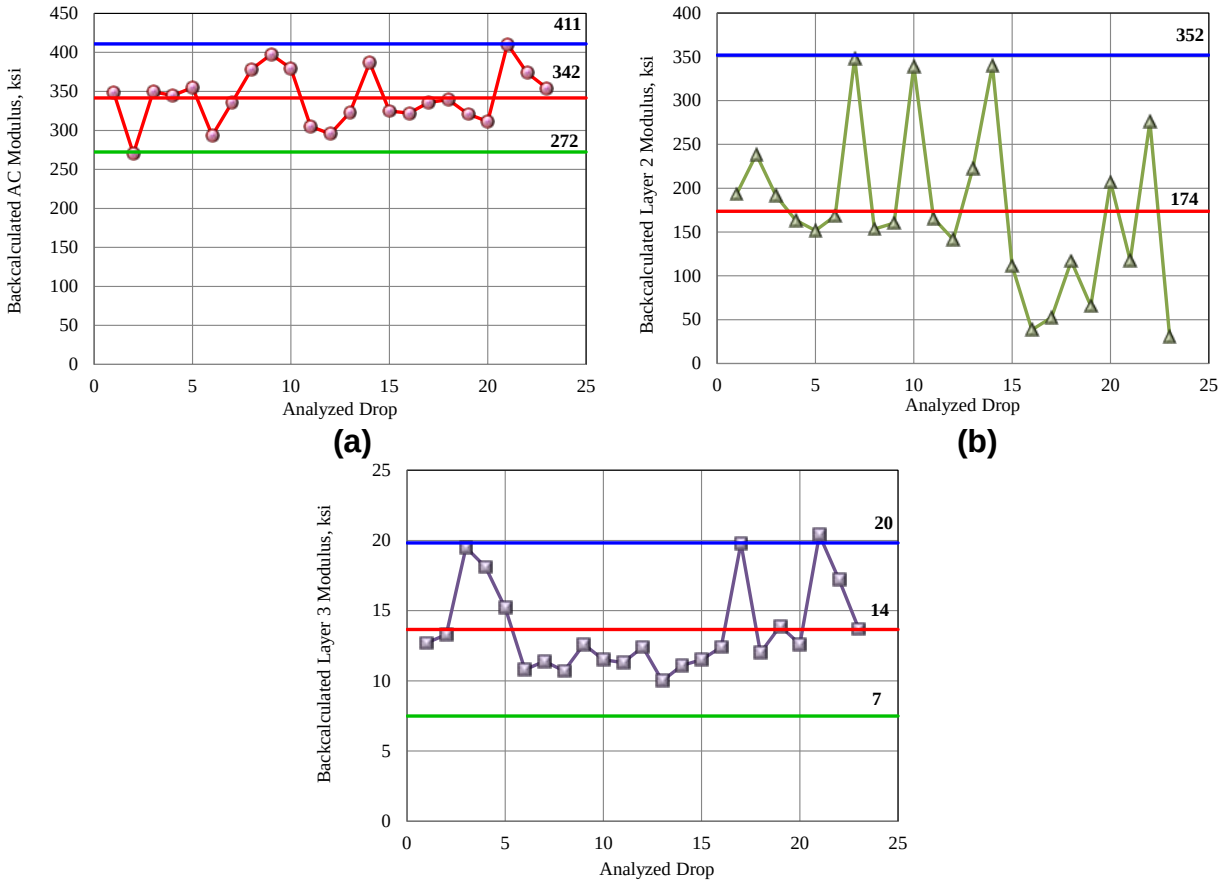

Figure 168 2010 Backcalculated (a) AC Layer, (b) Layer 2, and (c) Layer 3 Moduli for Control Section 55-68, Direction 5.

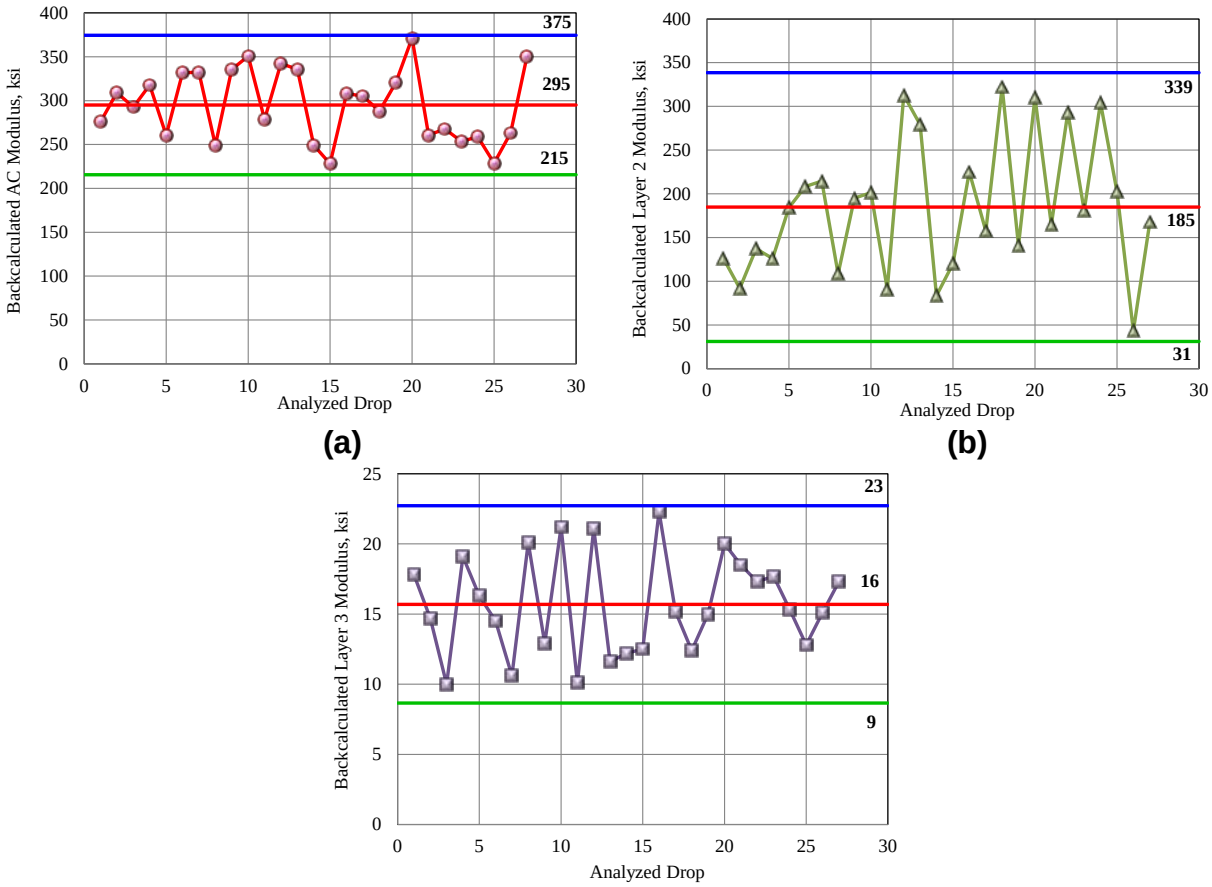

Figure 169 2010 Backcalculated (a) AC Layer, (b) Layer 2, and (c) Layer 3 Moduli for Control Section 55-68, Direction 6.

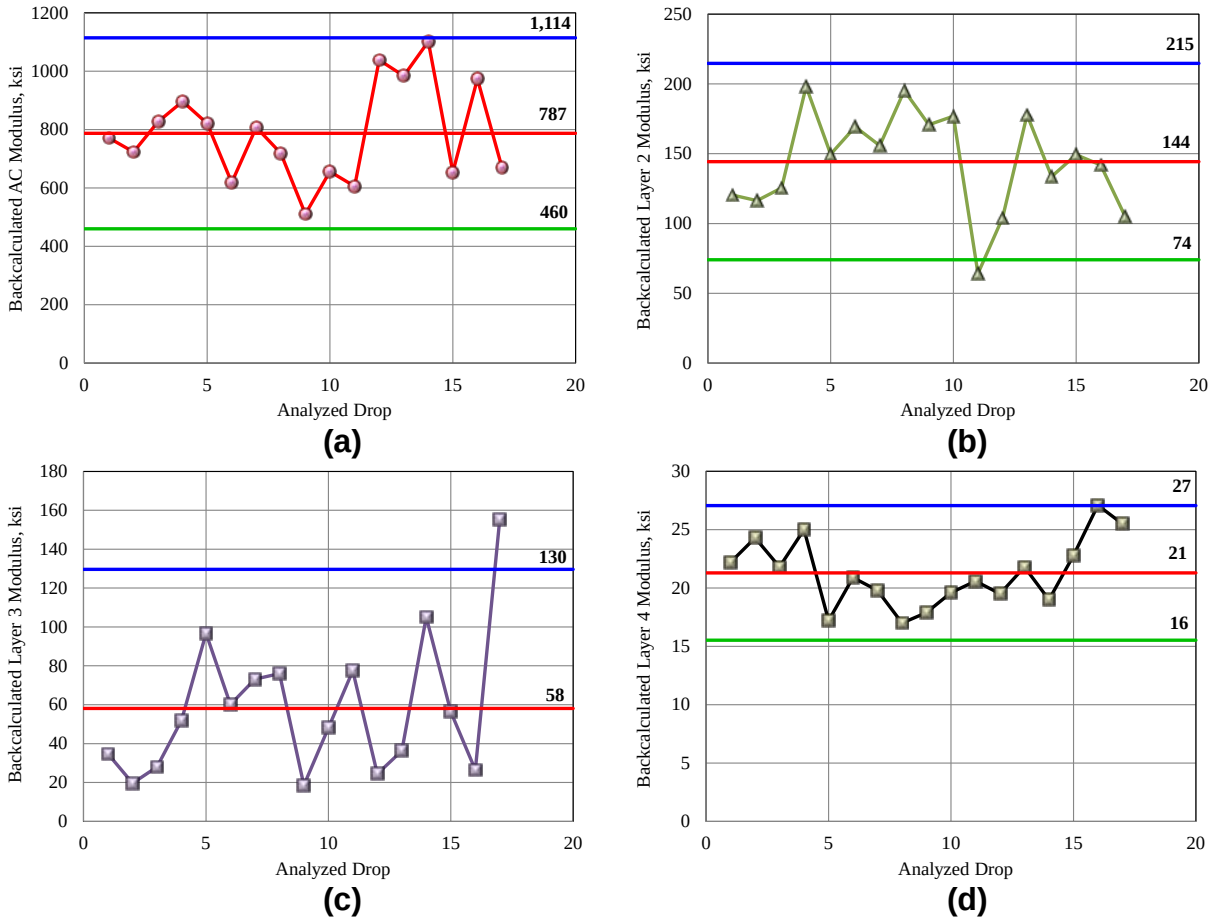

Figure 170 2004 Backcalculated (a) AC Layer, (b) Layer 2, (c) Layer 3 and (d) Layer 4 Moduli for Control Section 20-04, Direction 5.

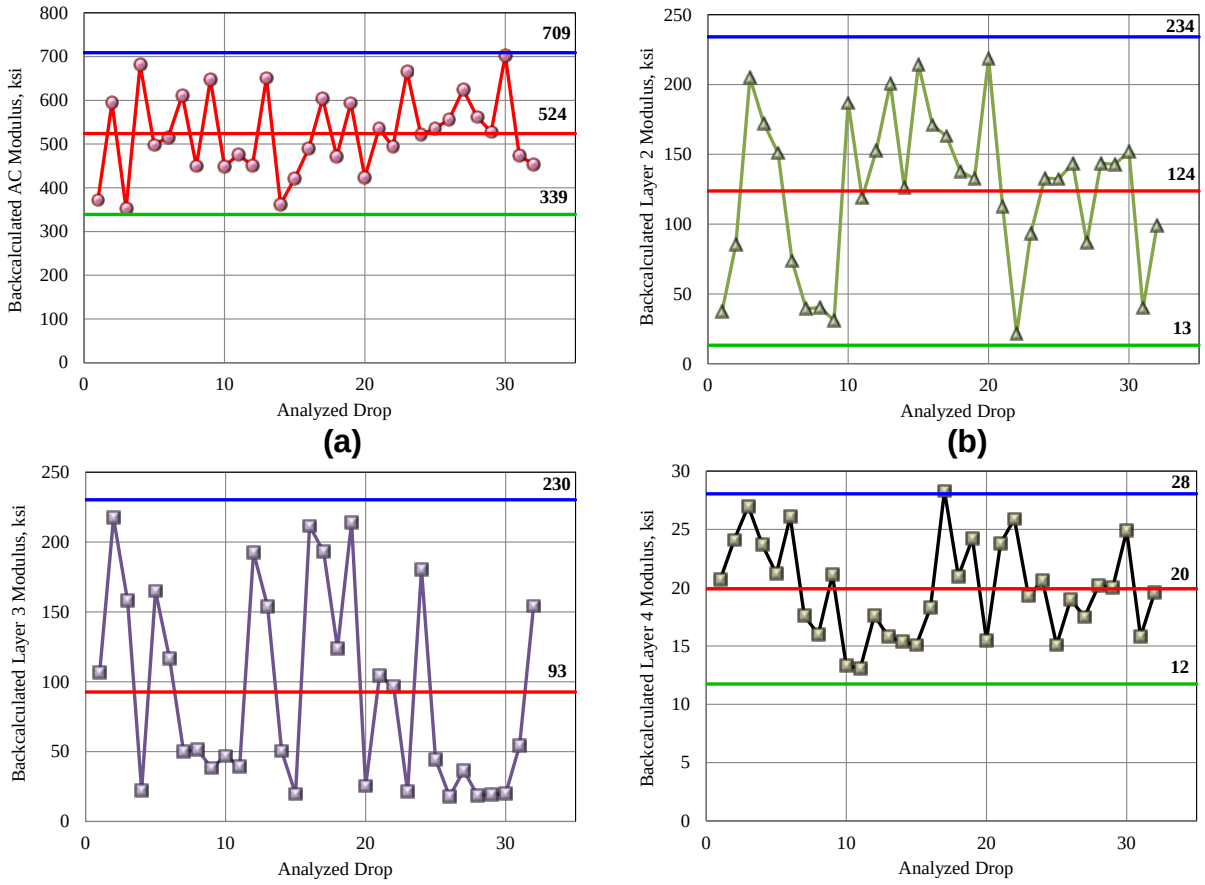

Figure 171 2004 Backcalculated (a) AC Layer, (b) Layer 2, (c) Layer 3 and (d) Layer 4 Moduli for Control Section 20-04, Direction 6.

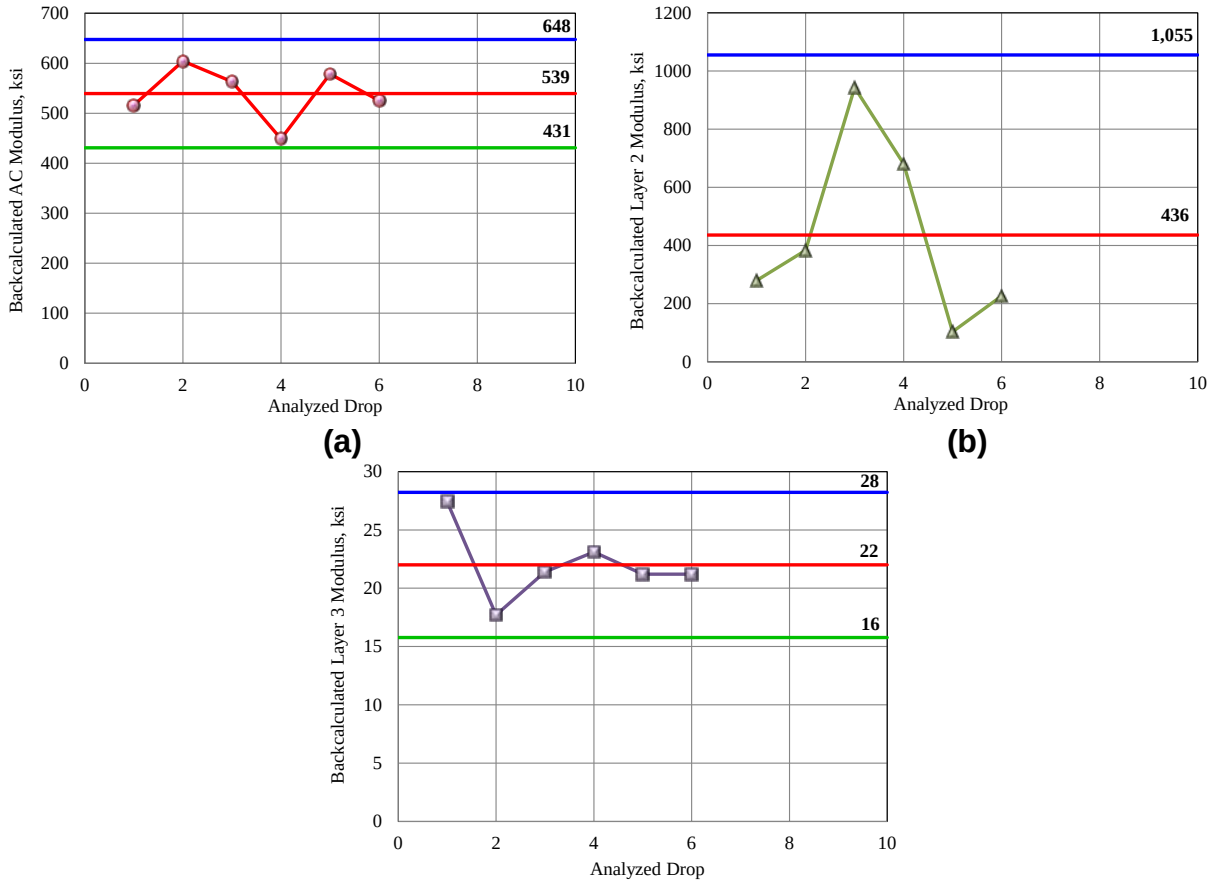

Figure 172 2010 Backcalculated (a) AC Layer, (b) Layer 2, and (c) Layer 3 Moduli for Control Section 44-05 MP 13.85, Direction 5.

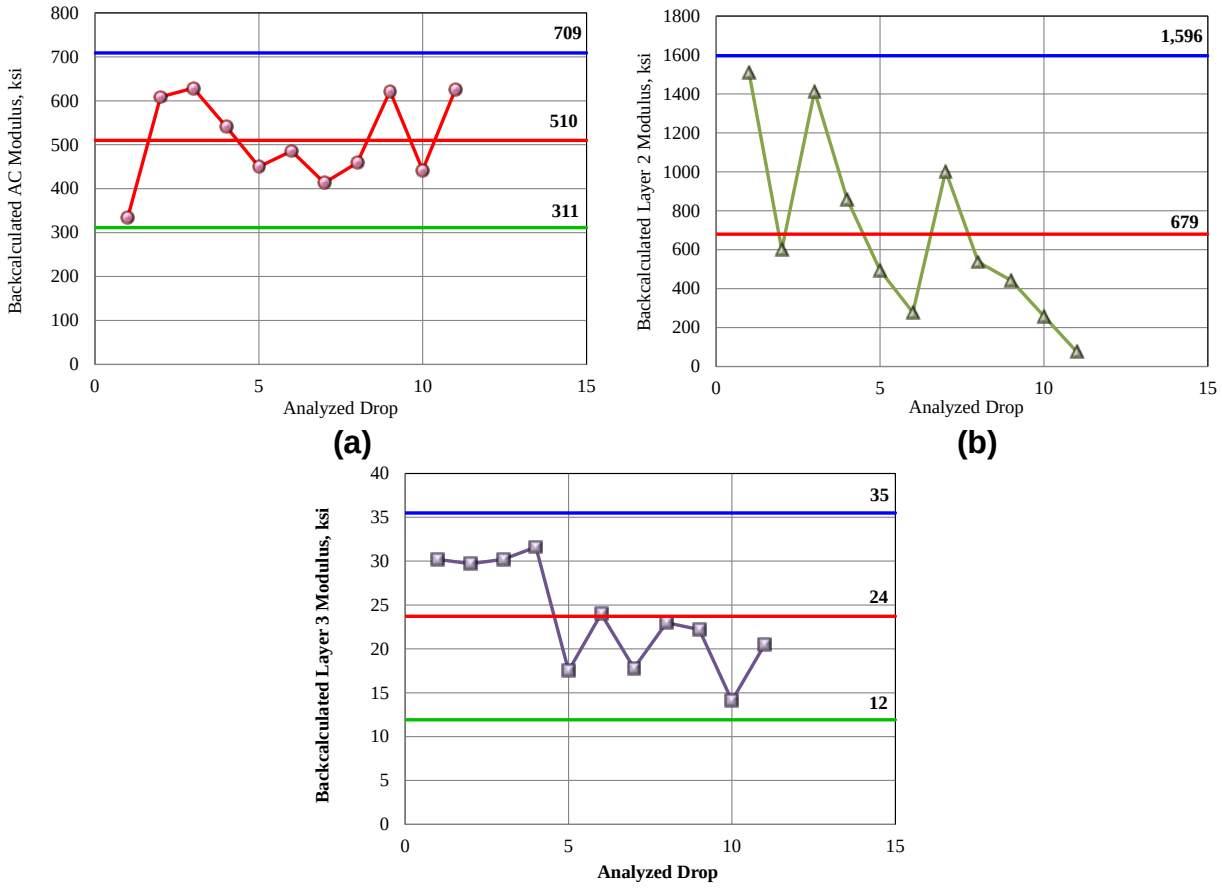

Figure 173 2010 Backcalculated (a) AC Layer, (b) Layer 2, and (c) Layer 3 Moduli for Control Section 44-05 MP 13.85, Direction 6.

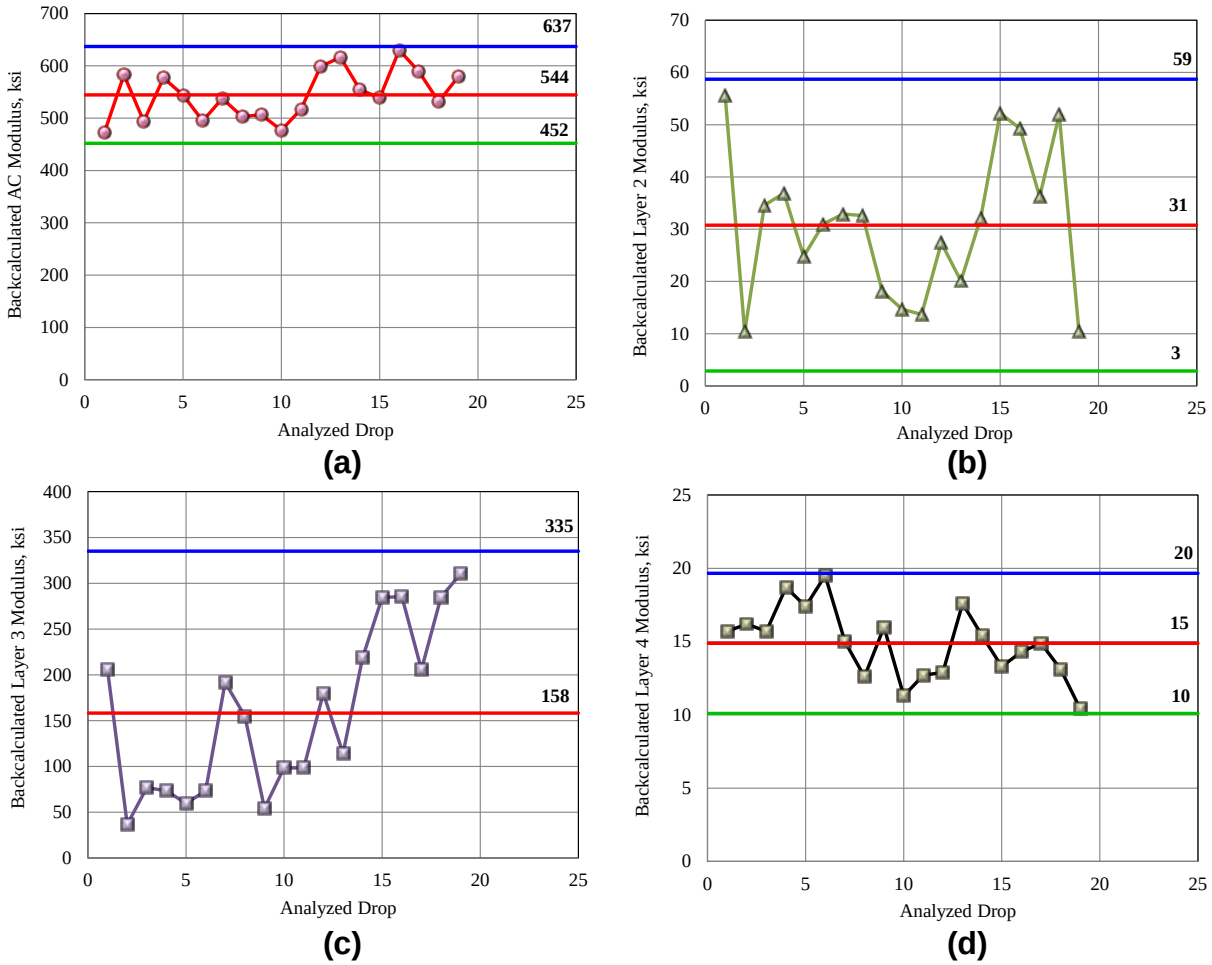

Figure 174 2010 Backcalculated (a) AC Layer, (b) Layer 2, (c) Layer 3 and (d) Layer 4 Moduli for Control Section 14-06, Direction 5.

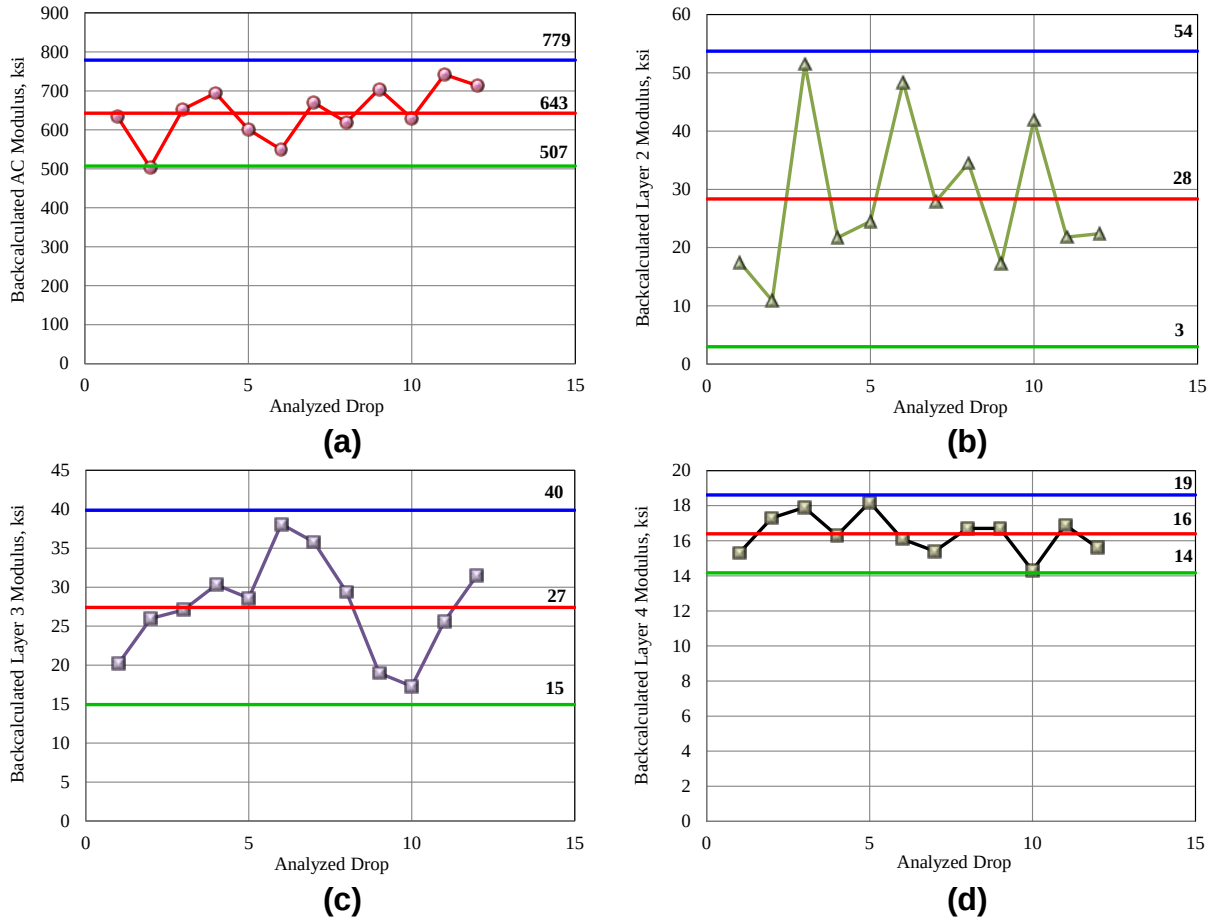

Figure 175 2010 Backcalculated (a) AC Layer, (b) Layer 2, (c) Layer 3 and (d) Layer 4 Moduli for Control Section 14-06, Direction 6.

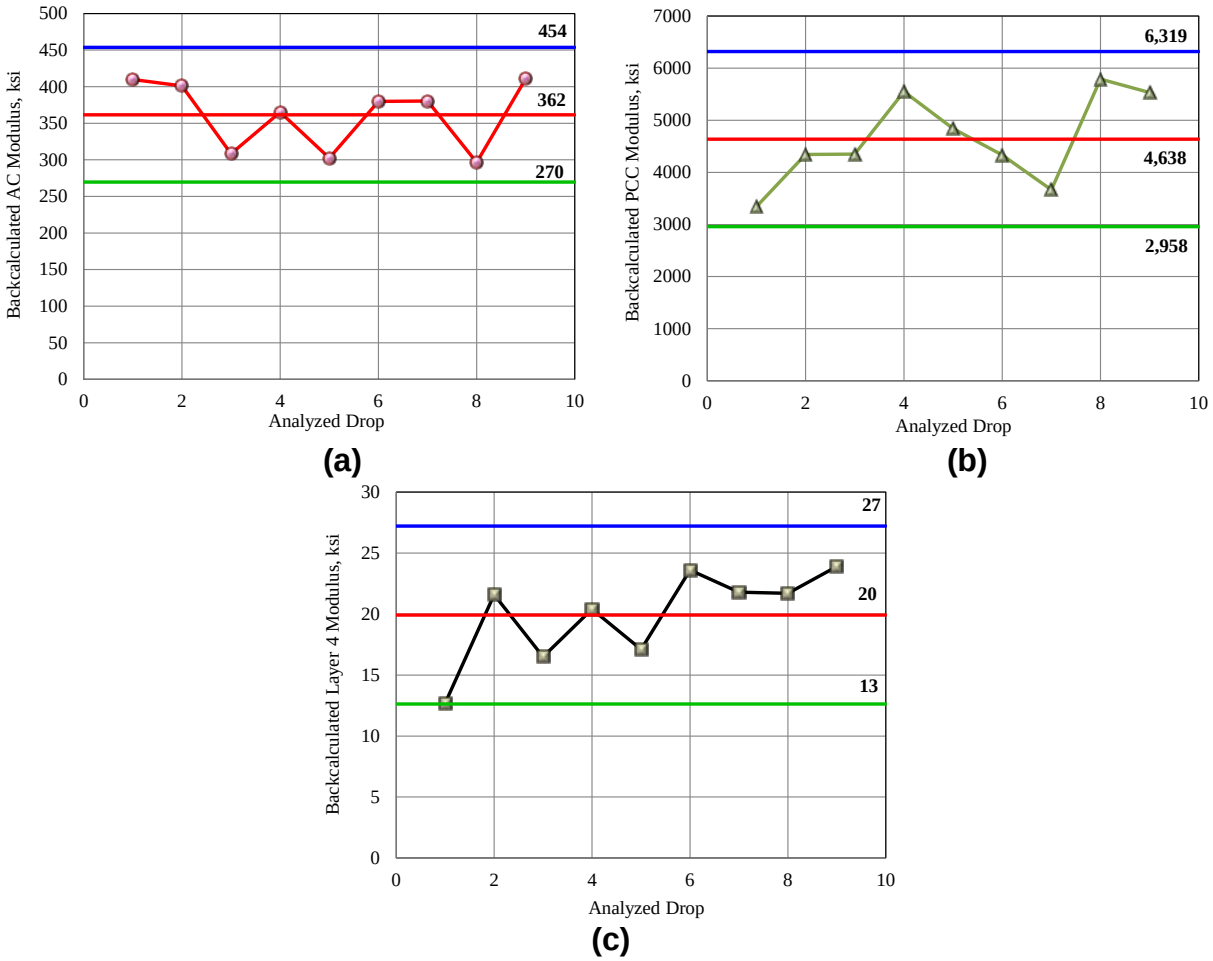

Figure 176 2010 Backcalculated (a) AC Layer, (b) Layer 2, and (c) Layer 3 Moduli for Control Section 25-46 MP 17, Direction 5.

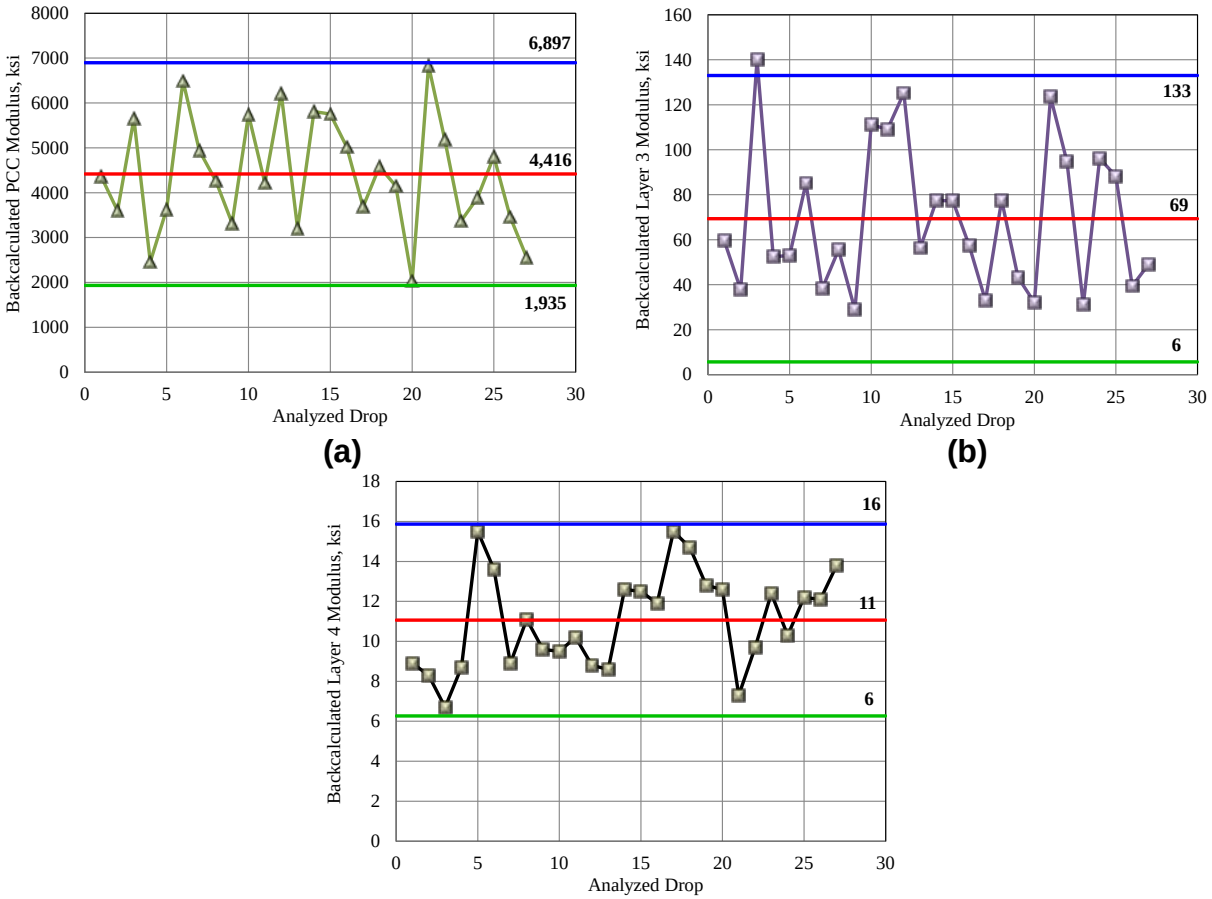

Figure 177 2004 Backcalculated (a) AC Layer, (b) Layer 2, and (c) Layer 3 Moduli for Control Section 42-30, Direction 6.

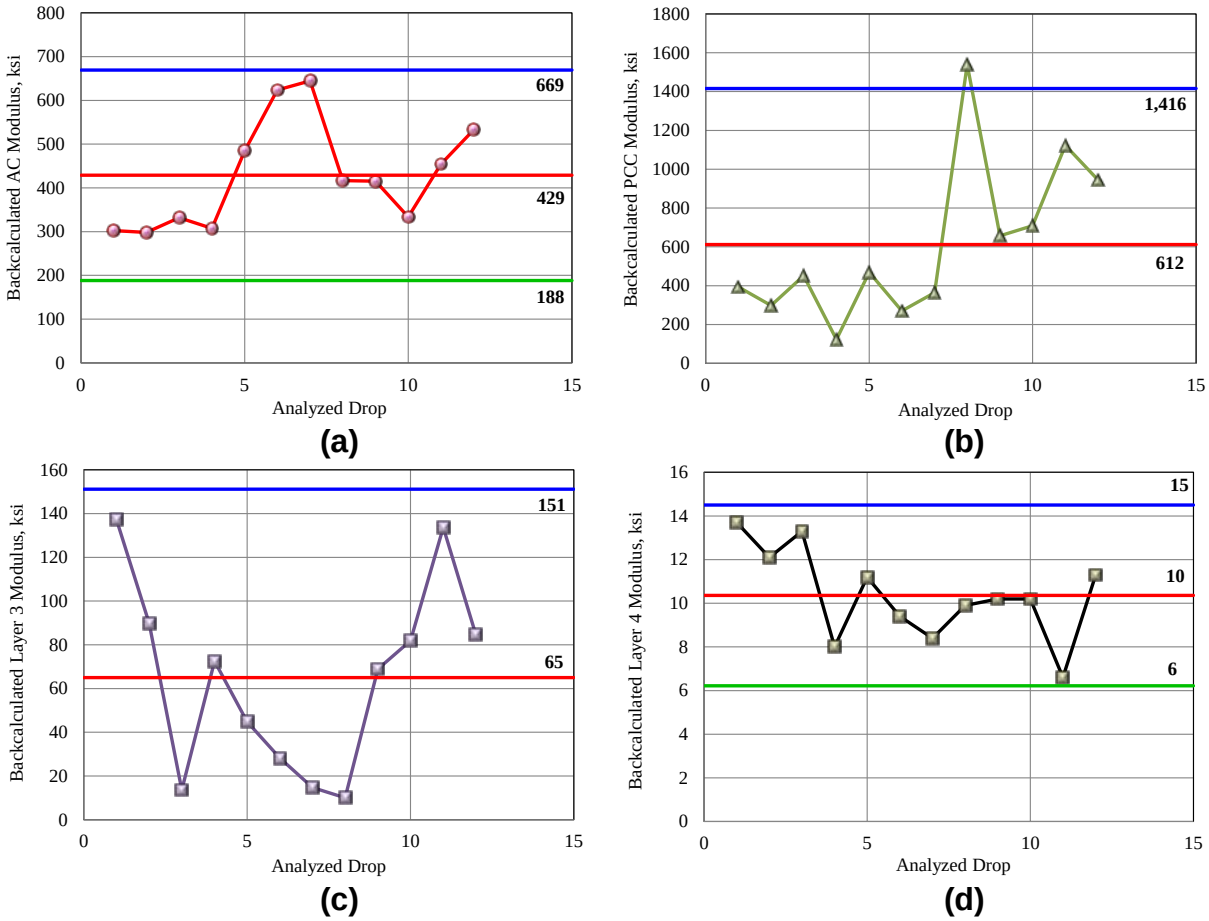

Figure 178 Backcalculated (a) AC Layer, (b) Layer 2, (c) Layer 3 and (d) Layer 4 Moduli for Control Section 55-09, Direction 5.

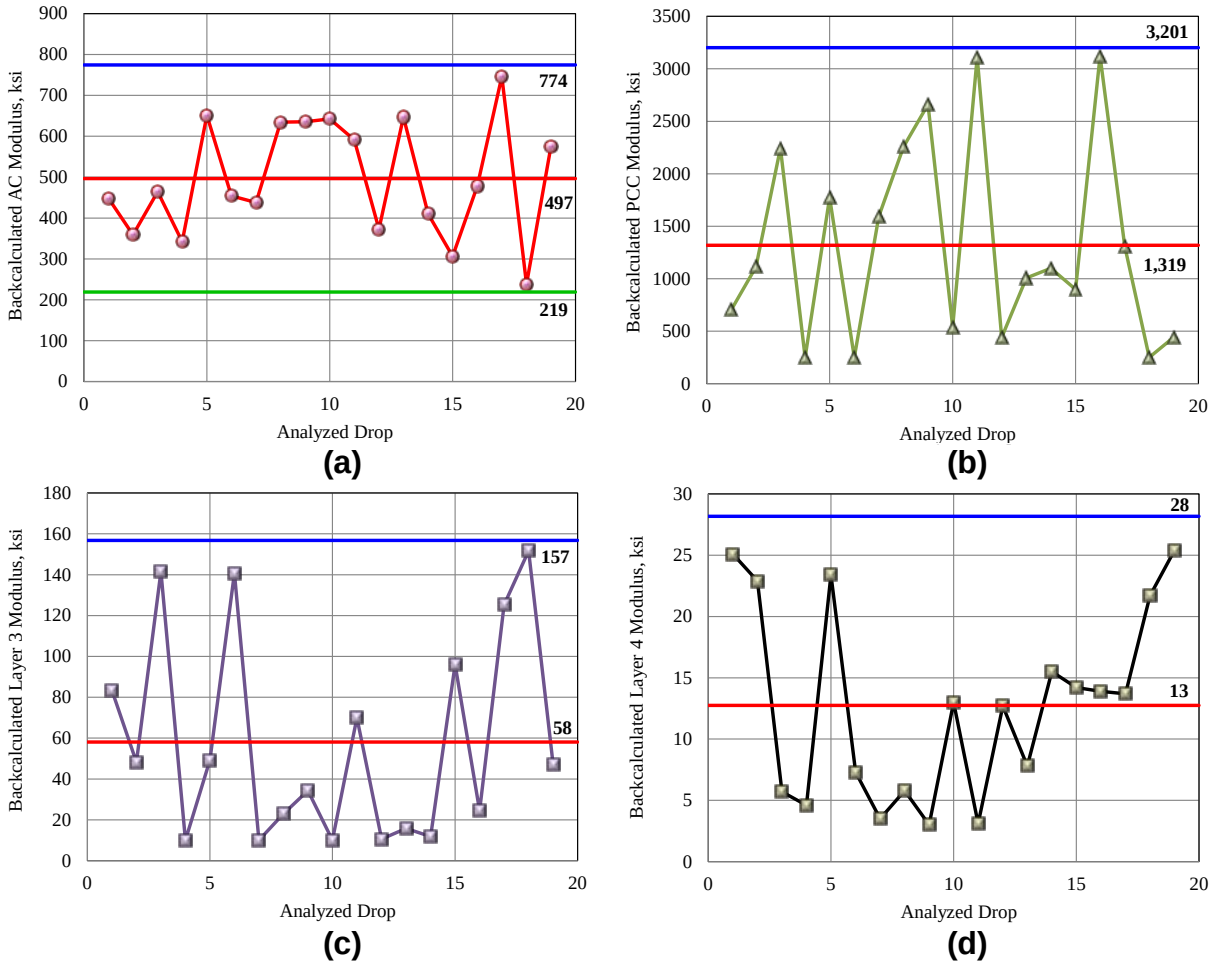

Figure 179 2010 Backcalculated (a) AC Layer, (b) Layer 2, (c) Layer 3 and (d) Layer 4 Moduli for Control Section 55-09, Direction 6.

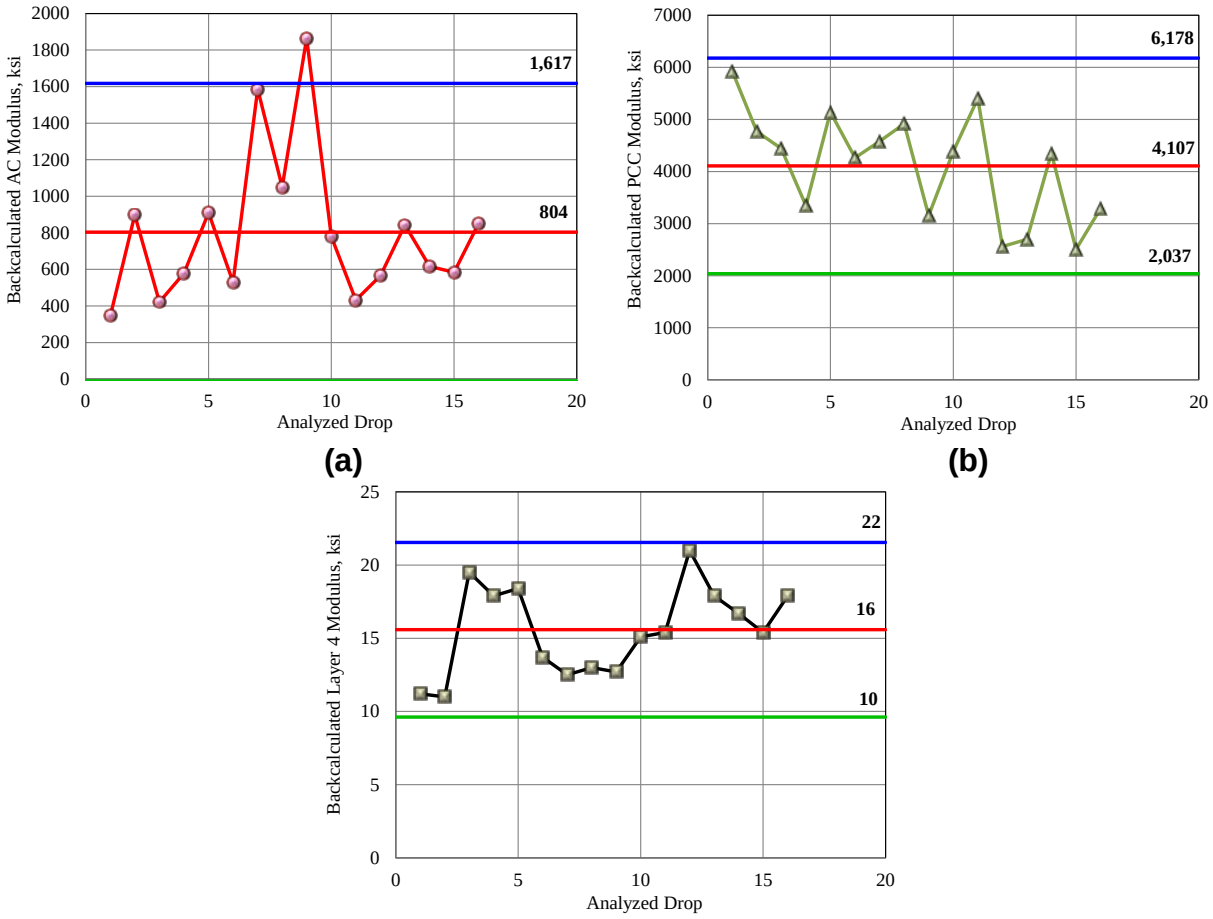

Figure 180 2010 Backcalculated (a) AC Layer, (b) Layer 2, and (c) Layer 3 Moduli for Control Section 16-49, Direction 6.

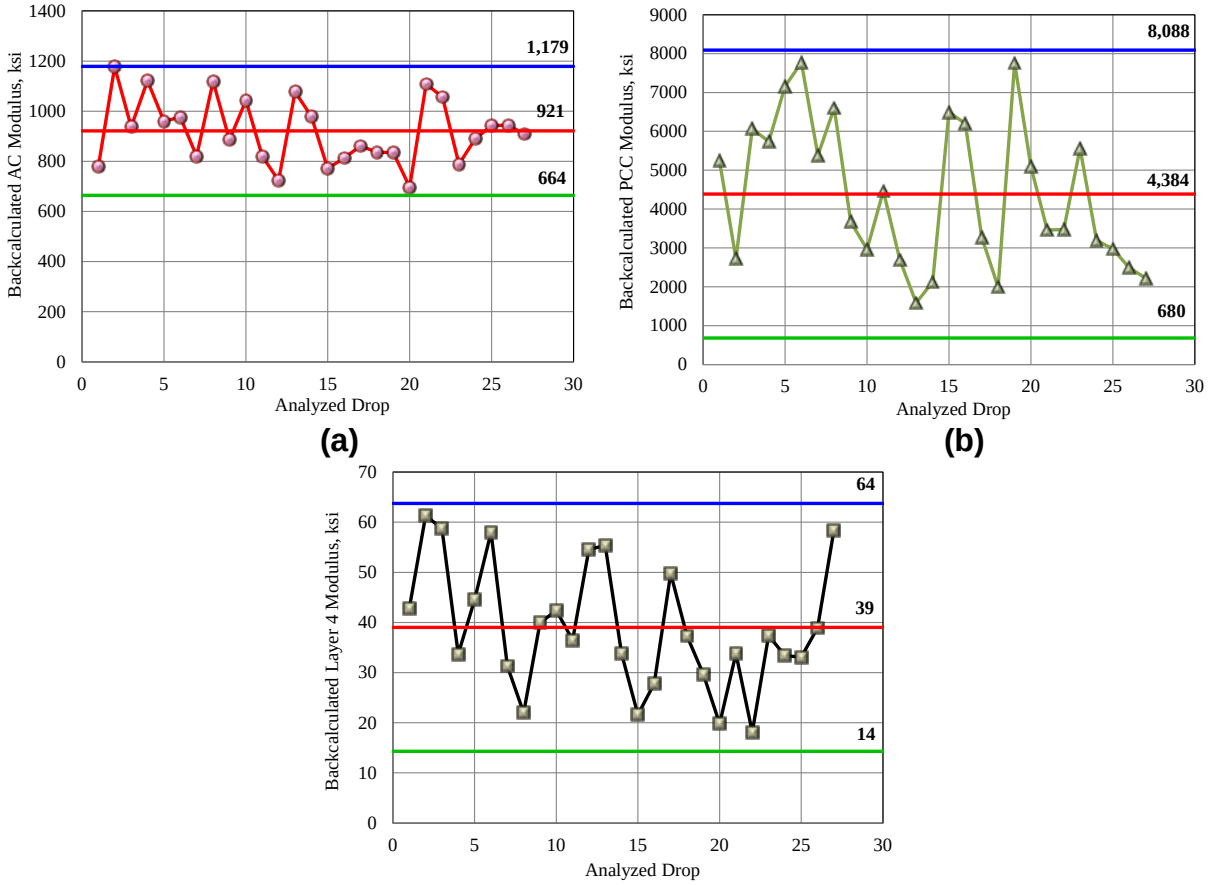

Figure 181 2010 Backcalculated (a) AC Layer, (b) Layer 2, and (c) Layer 3 Moduli for Control Section 50-32, Direction 6.

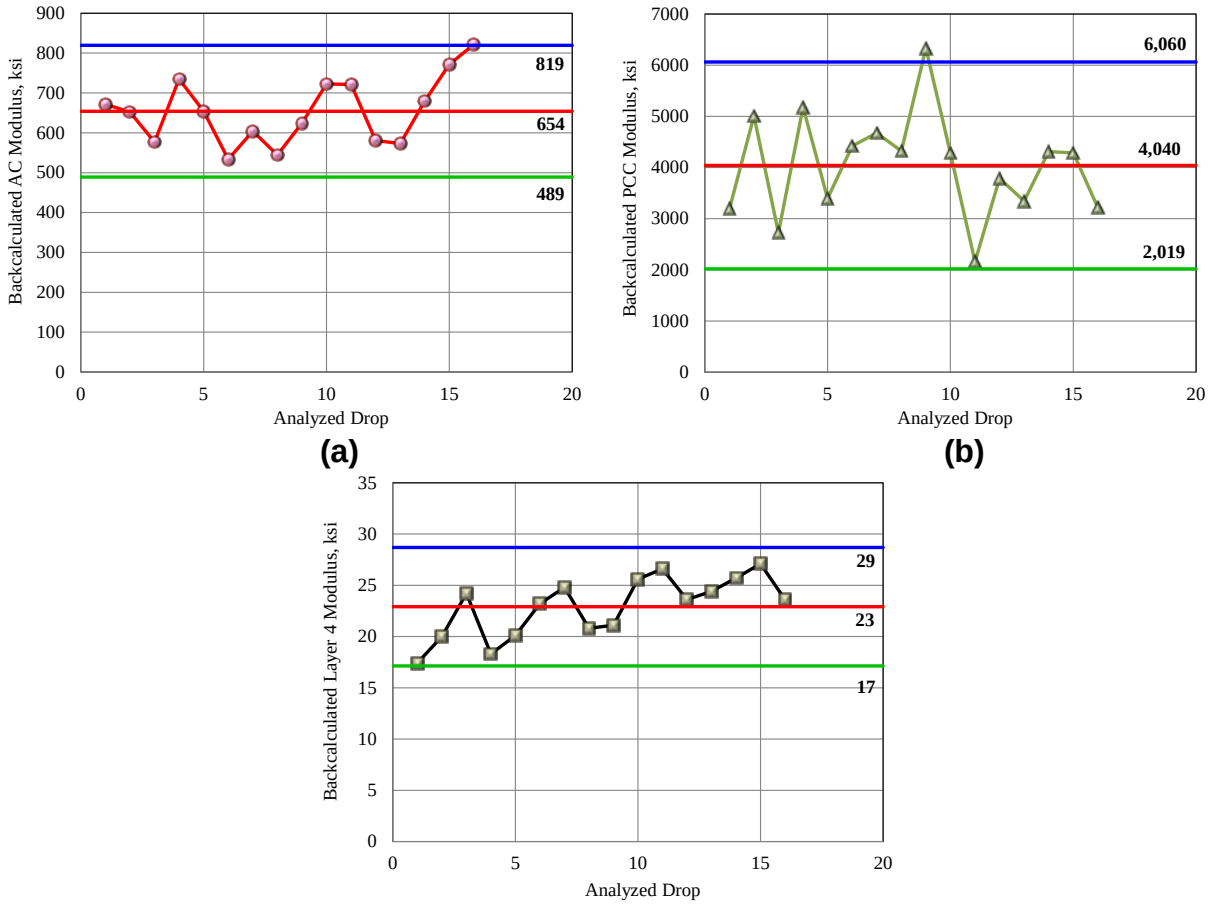

Figure 182 2010 Backcalculated (a) AC Layer, (b) Layer 2, and (c) Layer 3 Moduli for Control Section 25-46 MP 0, Direction 5.

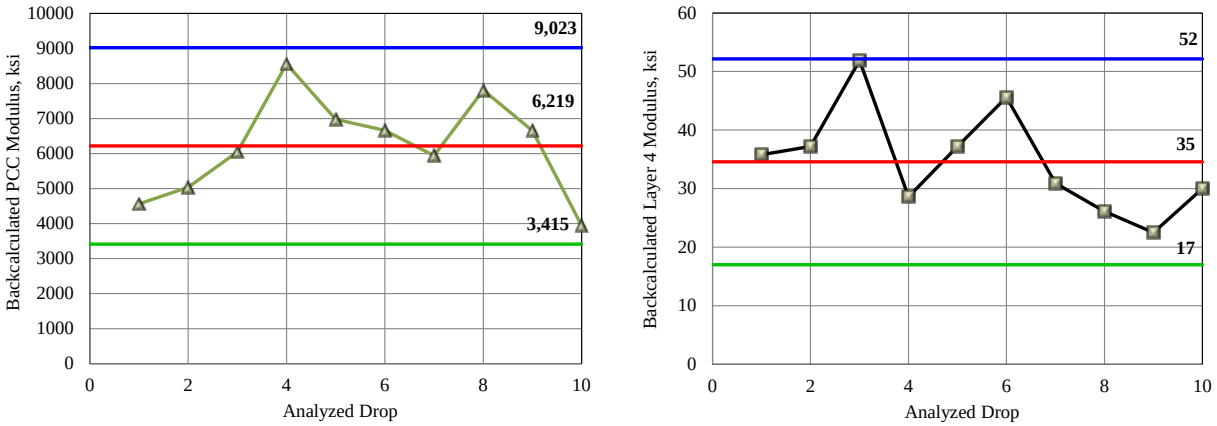

(a) (b)

Figure 183 2010 Backcalculated (a) PCC Layer, and (b) Layer 4 Moduli for Control Section 72-09, Direction 5.

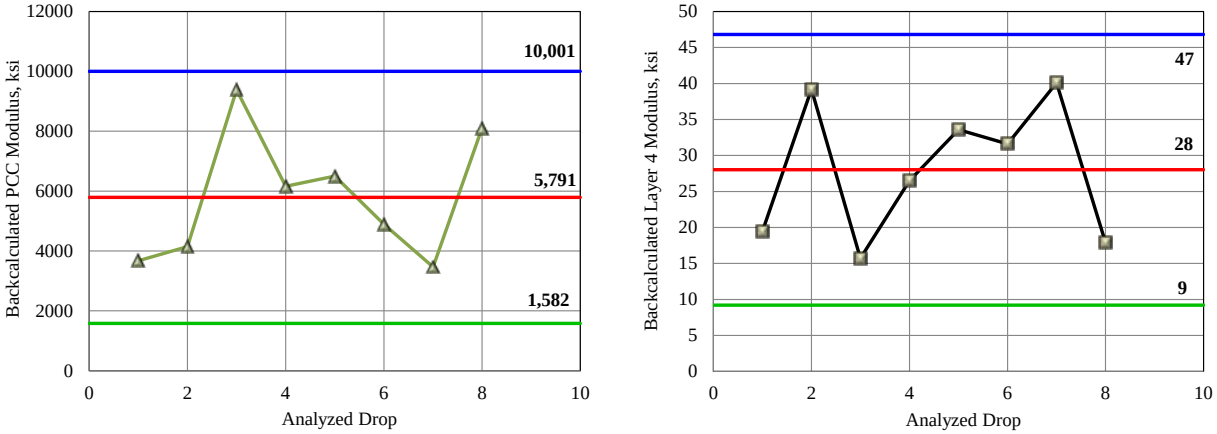

(a) (b)

Figure 184 2010 Backcalculated (a) PCC Layer, and (b) Layer 4 Moduli for Control Section 72-09, Direction 6.

APPENDIX G. PROJECT INFORMATION OF REPRESENTATIVE SECTIONS

Table 59 Project information of Control Section 68-22 Milepost 13

Control Section 68-22 Milepost 13	
Division	1
County	SEQUOYAH
Control Section	68-22
Route	I040
Original Construction Year	1969
Beg. Milepost	13
End Milepost	17.6
Direction	5
Length (Mile)	4.6
Number of lane	4
Pavement Type	AC
AADT2010	17,502
Total Truck %	27
Single Unit Truck %	4
Combination Trucks %	23
Annual Growth rate of Traffic	2.7
Percent of truck in design direction	50
Percent of truck in design lane	95
Beginning Latitute	35.45
Beginning Longitde	-94.88
Elevation (ft)(above sea level)	412
Depth of Water Table (ft)	11.59

Table 60 Project information of Control Section 44-05 Milepost 10.78

Control Section 44-05 Milepost 10.78	
Division	3
County	McCLAIN
Control Section	44-05
Route	I035
Original Construction Year	1970
Beg. Milepost	10.78
End Milepost	12.04
Direction	5
Length (Mile)	1.26
Number of lane	4
Pavement Type	AC
AADT2010	30,984
Total Truck %	29
Single Unit Truck %	8
Combination Trucks %	21
Annual Growth rate of Traffic	2.7
Percent of truck in design direction	50
Percent of truck in design lane	95
Beginning Latitute	35.00
Beginning Longitude	-97.38
Elevation (ft)(above sea level)	780
Depth of Water Table (ft)	21.09

Table 61 Project information of Control Section 09-05 Milepost 4.18

Control Section 09-05 Milepost 4.18	
Division	4
County	CANADIAN
Control Section	09-05
Route	I040
Original Construction Year	1962
Beg. Milepost	4.18
End Milepost	10.8
Direction	5
Length (Mile)	6.62
Number of lane	4
Pavement Type	AC
AADT2010	25,728
Total Truck %	29
Single Unit Truck %	7
Combination Trucks %	22
Annual Growth rate of Traffic	2.7
Percent of truck in design direction	50
Percent of truck in design lane	95
Beginning Latitute	35.53
Beginning Longitude	-98.24
Elevation (ft)(above sea level)	1270
Depth of Water Table (ft)	9.62

Table 62 Project information of Control Section 55-68 Milepost 6.55

Control Section 55-68 Milepost 6.55	
Division	4
County	OKLAHOMA
Control Section	55-68
Route	I040
Original Construction Year	1963
Beg. Milepost	6.55
End Milepost	11.9
Direction	5&6
Length (Mile)	5.35
Number of lane	4
Pavement Type	AC
AADT2010	39309
Total Truck %	14
Single Unit Truck %	6
Combination Trucks %	8
Annual Growth rate of Traffic	2.7
Percent of truck in design direction	50
Percent of truck in design lane	95
Beginning Latitute	35.43
Beginning Longitude	-97.37
Elevation (ft)(above sea level)	1215
Depth of Water Table (ft)	160.00

Table 63 Project information of Control Section 20-04 Milepost 0.0

Control Section 20-04 Milepost 0.0	
Division	5
County	CUSTER
Control Section	20-04
Route	I040
Original Construction Year	1962
Beg. Milepost	0
End Milepost	6
Direction	5&6
Length (Mile)	6
Number of lane	4
Pavement Type	AC
AADT2010	22,500
Total Truck %	37
Single Unit Truck %	9
Combination Trucks %	28
Annual Growth rate of Traffic	2.7
Percent of truck in design direction	50
Percent of truck in design lane	95
Beginning Latitute	35.51
Beginning Longitude	-98.92
Elevation (ft)(above sea level)	1500
Depth of Water Table (ft)	11.32

Table 64 Project information of Control Section 44-05 Milepost 13.85

Control Section 44-05 Milepost 13.85	
Division	3
County	McClain
Control Section	44-05
Route	I035
Original Construction Year	1959
Beg. Milepost	13.85
End Milepost	16.5
Direction	5&6
Length (Mile)	2.65
Number of lane	4
Pavement Type	AC
AADT2010	35,900
Total Truck %	25
Single Unit Truck %	7
Combination Trucks %	18
Annual Growth rate of Traffic	2.7
Percent of truck in design direction	50
Percent of truck in design lane	95.00
Beginning Latitute	35.05
Beginning Longitude	-97.38
Elevation (ft)(above sea level)	1099.87
Depth of Water Table (ft)	16.95

Table 65 Project information of Control Section 14-06 Milepost 3.35

Control Section 14-06 Milepost 3.35	
Division	3
County	CLEVELAND
Control Section	14-06
Route	I035
Original Construction Year	2010
Beg. Milepost	3.35
End Milepost	7
Direction	5&6
Length (Mile)	3.65
Number of lane	4
Pavement Type	AC
AADT2010	81,464
Total Truck %	13
Single Unit Truck %	5
Combination Trucks %	8
Annual Growth rate of Traffic	4.9
Percent of truck in design direction	50
Percent of truck in design lane	95
Beginning Latitute	35.23
Beginning Longitude	-97.49
Elevation (ft)(above sea level)	1200
Depth of Water Table (ft)	15.08

Table 66 Project information of Control Section 25-46 Milepost 17

Control Section 25-46 Milepost 17	
Division	3
County	GARVIN
Control Section	25-46
Route	I035
Original Construction Year	1970
Beg. Milepost	17
End Milepost	20.3
Direction	5
Length (Mile)	3.3
Number of lane	4
Pavement Type	Composite
AADT2010	30,951
Total Truck %	30
Single Unit Truck %	9
Combination Trucks %	21
Annual Growth rate of Traffic	1.4
Percent of truck in design direction	50
Percent of truck in design lane	95
Beginning Latitute	34.73
Beginning Longitde	-97.26
Elevation (ft)(above sea level)	860
Depth of Water Table (ft)	11.56

Table 67 Project information of Control Section 42-30 Milepost 7.09

Control Section 42-30 Milepost 7.09	
Division	4
County	LOGAN
Control Section	42-30
Route	I035
Original Construction Year	1960
Beg. Milepost	7.09
End Milepost	12.7
Direction	5
Length (Mile)	5.61
Number of lane	4
Pavement Type	Composite
AADT2010	23,627
Total Truck %	32
Single Unit Truck %	9
Combination Trucks %	23
Annual Growth rate of Traffic	3.1
Percent of truck in design direction	50
Percent of truck in design lane	95
Beginning Latitute	35.82
Beginning Longitde	-97.40
Elevation (ft)(above sea level)	1050
Depth of Water Table (ft)	31.4

Table 68 Project information of Control Section 55-09 Milepost 8.54

Control Section 55-09 Milepost 8.54	
Division	4
County	Oklahoma
Control Section	55-09
Route	I035
Original Construction Year	1959
Beg. Milepost	8.54
End Milepost	13
Direction	5
Length (Mile)	4.46
Number of lane	4
Pavement Type	Composite
AADT2010	48,100
Total Truck %	16
Single Unit Truck %	7
Combination Trucks %	9
Annual Growth rate of Traffic	1.36
Percent of truck in design direction	50
Percent of truck in design lane	95
Beginning Latitute	35.65
Beginning Longitde	-97.42
Elevation (ft)(above sea level)	1190
Depth of Water Table (ft)	150

Table 69 Project information of Control Section 16.49 Milepost 0.0

Control Section 16.49 Milepost 0.0	
Division	7
County	COMANCHE
Control Section	16-49
Route	I044
Original Construction Year	1964
Beg. Milepost	0
End Milepost	3
Direction	5
Length (Mile)	3
Number of lane	4
Pavement Type	Composite
AADT2010	6,800
Total Truck %	29
Single Unit Truck %	13
Combination Trucks %	16
Annual Growth rate of Traffic	3.6
Percent of truck in design direction	50
Percent of truck in design lane	95
Beginning Latitute	34.50
Beginning Longitde	-98.41
Elevation (ft)(above sea level)	1075
Depth of Water Table (ft)	11

Table 70 Project information of Control Section 50-32 Milepost 0.0

Control Section 50-32 Milepost 0.0	
Division	7
County	MURRAY
Control Section	50-32
Route	I035
Original Construction Year	1971
Beg. Milepost	0
End Milepost	6.54
Direction	5
Length (Mile)	6.54
Number of lane	4
Pavement Type	Comp.
AADT2010	29,631
Total Truck %	29
Single Unit Truck %	8
Combination Trucks %	21
Annual Growth rate of Traffic	3.19
Percent of truck in design direction	50
Percent of truck in design lane	95
Beginning Latitute	34.37
Beginning Longitde	-97.14
Elevation (ft)(above sea level)	750
Depth of Water Table (ft)	19.37

Table 71 Project information of Control Section 25-46 Milepost 0.0

Control Section 25-46 Milepost 0.0	
Division	7
County	MURRAY
Control Section	25-46
Route	I035
Original Construction Year	1971
Beg. Milepost	0
End Milepost	4.06
Direction	5
Length (Mile)	4.06
Number of lane	4
Pavement Type	Composite
AADT2010	29,631
Total Truck %	26
Single Unit Truck %	7
Combination Trucks %	19
Annual Growth rate of Traffic	2.26
Percent of truck in design direction	50
Percent of truck in design lane	95
Beginning Latitute	34.50
Beginning Longitde	-97.17
Elevation (ft)(above sea level)	952
Depth of Water Table (ft)	28

Table 72 Project information of Control Section 72-09 Milepost 9.0

Control Section 72-09 Milepost 9.0	
Division	8
County	TULSA
Control Section	72-09
Route	I244
Original Construction Year	1970
Beg. Milepost	9
End Milepost	11
Direction	5
Length (Mile)	2
Number of lane	8
Pavement Type	Composite
AADT2010	62,600
Total Truck %	7
Single Unit Truck %	4
Combination Trucks %	3
Annual Growth rate of Traffic	0.5
Percent of truck in design direction	50
Percent of truck in design lane	95
Beginning Latitute	36.15
Beginning Longitde	-95.92
Elevation (ft)(above sea level)	665
Depth of Water Table (ft)	15